Bioinspired Selective Surface Deposition of Fragrance Delivery Systems

PAR

Kemal Arda GÜNAY

EPFL

ÉCOLE POLYTECHNIQUE
FÉDÉRALE DE LAUSANNE

Suisse
2016

Acknowledgments

First of all, I would like to thank Prof. Harm-Anton Klok for giving me the opportunity to work on this exciting project. I am very grateful for his supervision, enthusiasm, support and for allowing me to express myself freely and pursue innovative ideas. Thank you HAK!

As a second, I would like to thank Firmenich SA, and particularly Dr. Andreas Herrmann for the excellent collaboration, supervision and support in this work and also for giving me the opportunity to work in their facilities as a research intern. I would like to thank Dr. Daniel Berczedi, Dr. Damien Berthier, Dr. Wolfgang Fieber and Dr. Lahoussine Ouali for the valuable discussions we have made in a regular basis. I would like to express my gratitude to Mr. Alain Trachsel and Mr. Serge Lamboley for helping me very kindly during my stay in Firmenich.

I am very grateful to Prof. Christian Heinis for giving me the opportunity to work in their group, Laboratory of Therapeutic Proteins and Peptides (LPPT) in EPFL, to carry the phage display experiments. I was a complete phage display noob in the beginning of this work, and I would like to thank all the members of LPPT, particularly Dr. Julia Morales Sanfrutos, Dr. Inmaculada Rentero Rebollo and Dr. Lisa Pollaro for their immense help during my stay in their group.

I would like to thank the Jury members, Prof. Esther Amstad, Dr. Andreas Herrmann and Prof. Sébastien Lecommandoux for the time they invest to read and evaluate this Thesis.

I have had a very entertaining time in Laboratoire des Polyméres (LP) in the last 5 years. Nariye, Maxime and Claudia, I am very happy to know you. You guys are my friends and I strongly believe that we will keep strong ties for much longer. Thank you Nicolas for your great company and supervision during my master's thesis. Thank you Ana for your kindness and helping me with a lot of things in the lab. Thank you Tugba for your help in the lab and for many outwork activities together. Thank you Solenne for tolerating me as an office mate for longer than 3 years. Thank you Ravey for the coffee (I am joking☺), thanks for your kindness and cheerfulness. Many thanks to the entire LP team, Caroline, Cindy Känel, Jacques, Raoul, Eloise, Dusko, Richard, Maarten, Fred, Thomas, Philippe, Sorin, Justin, Vitaly, Piotr and Tanja.

Good friends make a place livable. Eray, Emrah, Kerem, Zafer, Gökhan, Ali Galip, Meriç, Deniz, Başak, İsmail, Gözde and Özgün, I am very happy to get to know you.

Ve son olarak, her ne kadar burada iki satırda ifade edemeyecek olsam da, anneciğim, babacığım, sizlere her şey için çok teşekkür ediyorum ve gözlerinizden öpüyorum.

Table of contents

Summary

The perception of pleasantness in many of the consumer goods is provided by volatile chemical compounds called fragrances. While the volatility of fragrances is essential to provide a pleasant olfactory response, it presents at the same time a technological problem, such that their premature evaporation and degradation may occur prior to the application during the storage. This is also highly troublesome from a commercial standpoint; as fragrances are one of, if not the most, expensive ingredient of these consumer goods. The above mentioned problems have been relatively well addressed by using fragrance delivery systems that are mostly composed of polymers. In addition to the minimization of premature fragrance evaporation and degradation, polymeric fragrance delivery systems also aim to achieve a controlled fragrance release in order to provide a long lasting perception of these volatiles.

Apart from the storage and delivery of the fragrances, another crucial aspect that affects the performance of the consumer goods is the deposition of these delivery systems to the target of interest. The potential strategies to improve the deposition of fragrance delivery systems are much less explored compared to their preparation and predominantly based on the physiochemical optimization of the surface/interface properties, such as hydrophobicity and charge of the existing delivery systems. However, the extent of depositions achieved using these strategies are typically modest, for example, onto hair from a shampoo medium. In other words, the deposition of existing fragrance delivery systems relies on non-specific interactions; as these systems do not contain any "cues" that can selectively recognize, for example, textile and hair surfaces.

Phage display is an in vitro evolutionary selection technique that is widely used to identify substrate selective short peptide ligands. Although it has been predominantly used to isolate biomolecule binding ligands, its scope has been expanded in the last decade and it has also found use to identify "hard" and "soft" material binders. From this aspect, phage display may also provide short peptide ligands that can bind to *i. e.* cotton and hair surfaces under laundry and hair wash conditions. These ligands can be considered as a "tool" to improve the deposition of any fragrance delivery system upon their chemical incorporation via orthogonal functional groups.

This Thesis aims to explore the feasibility of phage display identified peptides to selectively deposit fragrance delivery systems on cotton fabric and human hair surfaces and it can be subdivided into 4 Chapters.

Summary

Chapter 1 provides a summary for the identification and characterization of "soft" matter binding peptides via phage display. Herein, soft matter will be subdivided into three general classes: synthetic polymers, small organic molecules and natural polymers.

Phage display can also be used the identification of peptide ligands having costrained conformations, such as cyclic peptide disulfides (CXC's). **Chapter 2** proposes a general synthetic method for the preparation of water soluble (CXC)-polymer conjugates that proceeds at mild conditions without the requirement of peptide protecting groups. The synthesized CXC-polymer conjugates will be later used as a model hair targeting polymeric profragrance system in Chapter 4.

Chapter 3 describes the preparation of fragrance delivery systems that can selectively deposit onto cotton fabric under laundry wash conditions. The Chapter will first show the identification of cotton fabric binding cyclic peptide disulfides (CXC)'s via phage display experiments. In the next steps, the strongest cotton binding peptide will be incorporated into two different model fragrance delivery systems that are based on linear polymers nanoparticles. The peptide-mediated enhanced deposition of these fragrance delivery systems will be detected by fluorescence intensity measurements and the increased fragrance release from the nanoparticles will be assessed using dynamic headspace measurements.

Chapter 4 applies the general strategy described in Chapter 3 to a more challenging task: Selectively depositing fragrance delivery systems onto hair under shampoo conditions. First, the feasibility of phage display to identify hair binding peptides under shampoo conditions will be demonstrated. Subsequently, two of the peptide-polymer conjugates described in Chapter 2 will be used as a model for hair targeting fragrance delivery systems. In the final section, the influence of the stringency of the shampoo conditions as well as the steric hindrance in the peptide terminal domains to the deposition of these peptides onto hair will be assessed.

Keywords: Fragrance delivery systems, phage display, peptide-polymer conjugates, bioconjugation, encapsulation.

Résumé

L'odeur agréable présente dans de nombreux biens de consommation est produite par des composés chimiques volatiles appelés fragrances. Bien que la propriété volatile de ces composés soit essentielle à leur perception par notre système olfactif, elle représente également un défi technologique important, dans la mesure où, il est indispensable de prévenir l'évaporation ou la dégradation de ces molécules odorantes durant le stockage des biens de consommation auxquels elles sont associées. A ceci s'ajoute également un défi commercial, étant donné que les fragrances sont souvent, l'un des ingrédients voir l'ingrédient le plus cher du bien de consommation en question. Ces problèmes ont été relativement bien résolus par l'utilisation de systèmes de libération de fragrances, consistant principalement en une matrice polymère. En plus de limiter l'évaporation et la dégradation des fragrances, ces systèmes polymériques visent également à libérer les molécules volatiles de manière contrôlée et prolongée dans le temps.

En dehors du stockage et de la libération contrôlée, un troisième aspect crucial et affectant la performance de ces biens de consommation doit être pris en compte. Il s'agit de la déposition sélective de ces systèmes de libération contrôlée vers un substrat cible. Les stratégies potentielles visant à améliorer la déposition sélective de ces systèmes sont largement moins développées que leur préparation et se limitent généralement à l'optimisation de paramètres physicochimique de surface tels que l'hydrophobicité ou la charge du système en question. L'étendue de la déposition sélective, en ayant recours à ce type de stratégies, restent relativement modeste, par exemple dans le cas de déposition sur les cheveux de fragrances issues d'un shampoing. En d'autres mots, la déposition sélective est essentiellement basée sur des interactions non-spécifiques, ces systèmes ne possédant pas d'attributs leur permettant de reconnaître de manière sélective des textiles ou la surface d'un cheveu par exemple.

L'exposition sur phage (ou phage display) est une technique in vitro de sélection évolutionnaire. Elle est aujourd'hui largement utilisée comme technique d'identification de séquences peptidiques sélectives pour un substrat donné. Bien que principalement utilisée en biologie moléculaire et cellulaire, sa portée a été étendue durant la dernière décennie et a aussi bien été appliquée afin d'identifier des ligands spécifiques aux corps durs ou corps mous (hard/soft materials). L'exposition sur phage (ou phage display) peut donc potentiellement fournir des peptides spécifique aux fibres de coton ou à la surface d'un cheveu dans des conditions respectivement de lavage des textiles ou des cheveux.

Ces ligands peuvent être considérés comme des outils permettant d'améliorer la déposition sélective de n'importe quel système de libération de fragrances par fonctionnalisation chimique orthogonale de ceux-ci avec les séquences peptidiques spécifiques en question.

Cette Thèse vise à explorer l'utilisation de séquences peptidiques spécifiques aux fibres textiles de coton et aux cheveux afin d'améliorer la déposition sélective de systèmes de libération de fragrances. Ce travail se divise en 4 chapitres.

Le **premier Chapitre** apporte un aperçu de la technique d'exposition sur phage (phage display) et la caractérisation des ligands peptidiques spécifiques aux corps mous (soft matter). Dans le présent chapitre, les corps mous seront divisés en trois classes générales : les polymères synthétiques, les molécules organiques et les polymères naturels.

L'exposition sur phage (ou phage dispaly) peut également être utilisée afin d'identifier des ligands peptidiques possédants une conformation restreinte, comme c'est le cas pour les peptides cycliques (CXC's pour cyclic peptide disulfides). Le **Chapitre 2** propose une méthode synthétique générale pour la préparation de conjugués (CXC)-polymère hydrosolubles qui fait appel à des conditions de réaction douces et évite l'utilisation de groupes protecteurs. Les conjugués CXC-polymère ainsi préparés seront utilisés plus tard (chapitre 4) comme systèmes de profragrance polymériques sélectifs aux cheveux.

Le **Chapitre 3** décrit la préparation de systèmes de libération de fragrances se déposant de manière sélective sur les fibres de coton dans des conditions de lavage des textiles. Tout d'abord ce chapitre discutera de l'identification de CXC's spécifiques aux fibres textiles de cotons par la méthode d'exposition sur phage (ou phage display). Ensuite, les meilleurs ligands seront incorporés dans deux modèles de systèmes de libération de fragrances, le premier basé sur un système utilisant un polymère linéaire et le second des nanoparticules. L'augmentation de la déposition sélective sera caractérisée par des mesures d'intensité de fluorescence. La libération de fragrance des nanoparticules sera elle évaluée en utilisant une méthode de mesure dynamique dite 'headspace analysis'.

Le **Chapitre 4** applique la stratégie générale décrite dans le chapitre 3 mais cette fois-ci pour la déposition sélective de systèmes de libération de fragrance sur les cheveux et ceci dans les conditions d'utilisation d'un shampoing. Premièrement, l'exposition sur phage (ou phage display) pour l'identification de peptides spécifiques aux cheveux dans les conditions de lavage sera discutée. Ensuite, deux des conjugués polymère-peptide décrits au chapitre 2 seront utilisés comme modèle de système de libération de fragrance

spécifique pour les cheveux. Finalement, l'influence des conditions drastiques liées à l'utilisation d'un shampoing ainsi que la gêne stérique lié aux domaines terminaux des peptides seront évalués dans le contexte de déposition sur les cheveux.

Mots clés : systèmes de libération de fragrances, exposition sur phage, conjugués peptide-polymère, bioconjugaison, encapsulation

1. Identification of Soft Matter Binding Peptide Ligands using Phage Display

Published as the following review article:

"Identification of Soft Matter Binding Peptide Ligands using Phage Display", Kemal Arda Günay, Harm-Anton Klok, *Bioconjugate Chemistry*, **2015**, *26*, 2002-2015.

1.1. Introduction

Inspired by the highly specific ligand-substrate interactions present in almost any of the biochemical processes in nature, phage display has been utilized for more than two decades for the identification of short peptide sequences that bind with high affinity and selectivity to the substrate of interest.[1-6] Following its first successful implementation by George P. Smith in 1985,[7] phage display has evolved into a powerful method for the identification of natural or novel ligands to a myriad of biological substrates including enzymes,[8-10] toxins,[11,12] receptors[13,14] and structural proteins.[15,16] Phage display has also proven to be a powerful method to identify binding sites of proteins via epitope mapping.[17-19] Nowadays, phage display is used for a variety of applications including drug discovery,[20-23] vaccine development,[24] analysis of the energetics at the binding interfaces of proteins[25] or to map the molecular diversity of receptors in the human vasculature.[26]

A typical phage display cycle consists of 4 steps (**Figure 1**). In the incubation step, a combinatorial phage library containing randomized inserts in one of the coat proteins is incubated with the substrate. Following the incubation, weakly bound phages are removed by washing the substrate several times with a buffer solution containing small amounts of a surfactant. In the next step, strongly bound phages are recovered by washing the substrate with an elution buffer and finally amplified using the *E. coli.* host strain to yield a phage mixture that is enriched towards the substrate. Repetition of this cycle eventually yields a phage mixture that is predominantly composed of substrate selective phage clones. Sequencing of the genome of the individual clones allows the identification of substrate selective, short peptides.
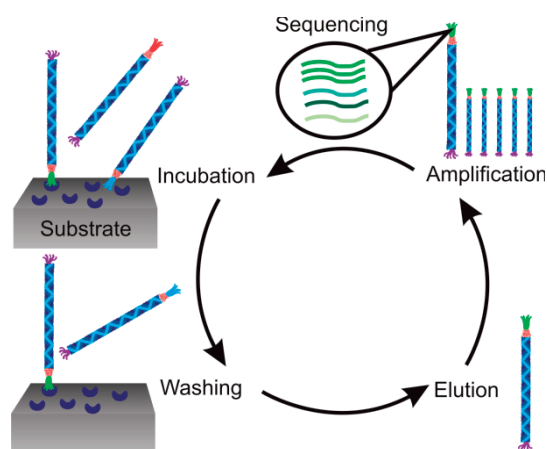
Figure 1. Schematic representation of the different steps involved in the phage display process.

While initially developed and used for biological substrates, over the past decade the scope of the phage display technique has been significantly expanded and this method is now also increasingly used for the identification of small peptide sequences that bind to solid substrates,[27,28] such as metals,[29,30] ceramics,[31-34] carbon based materials,[35,36] synthetic or natural polymers[37] as well as small organic molecules. These small peptides are attractive building blocks to functionalize or to modulate the properties of surfaces and interfaces. These peptides can be conjugated with biomolecules, synthetic polymers or nanoparticles to allow selective functionalization of the substrate of interest. This is attractive, for example, for the development of sensors,[38-40] templates for mineralization,[41-44] as well as electronic devices.[34,45-47]

The aim of this Chapter is to present the state-of-the-art and to highlight the potential of phage display to identify peptide sequences that are able to bind with high affinity and selectivity to "soft matter" surfaces. While the use of the phage display technique to identify peptide binders to "hard" inorganic substrates has been reviewed in several other articles,[27,28,41] this contribution specifically focuses on soft matter substrates. This Chapter consists of two main parts. The first part will summarize for three main classes of soft material substrates, viz. synthetic polymers, small organic molecules and natural polymers, the different peptide ligands identified by phage display that have been reported in the literature (**Figure 2**). The second part will discuss the various techniques that have been used to characterize the affinity of these peptide ligands.
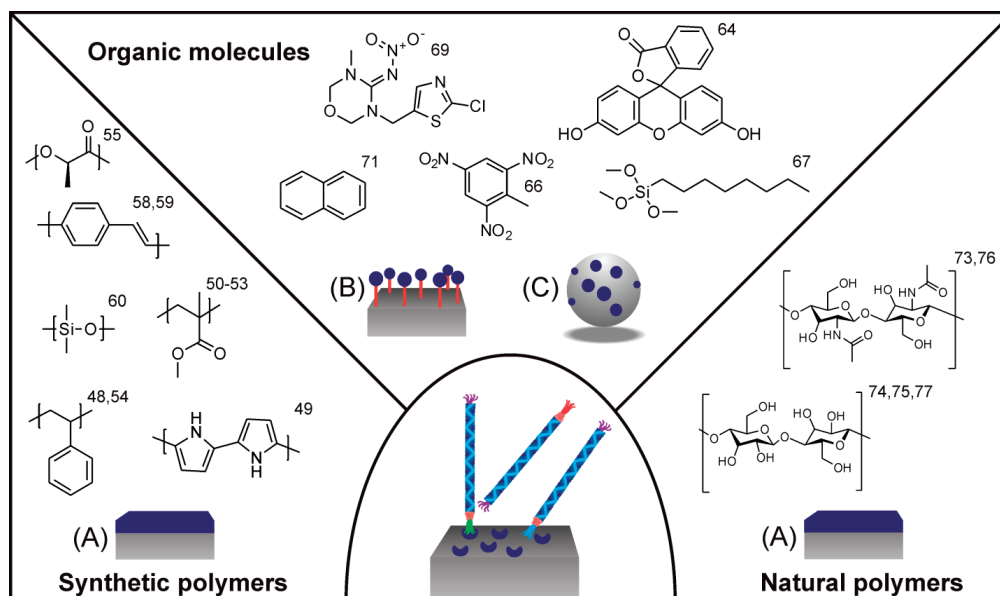
Figure 2. Phage display is a powerful tool allowing the identification of peptide ligands that are able to bind selectively to a myriad of substrates, including synthetic polymers, small organic molecules and natural polymers. While thin, spin coated films are most frequently used to carry out phage display on synthetic and natural polymer substrates (A), organic molecules are either covalently immobilized on flat surfaces (B) or on spherical beads (C). The numbers next to the chemical structures in this Figure refer to the references that have reported peptide binders to these substrates.

1.2. Identification of soft matter binding peptide ligands

This section will successively present and discuss peptide ligands that have been identified via phage display and which bind selectively to synthetic polymers, small organic molecules and natural polymer substrates. First, peptide ligands that bind to synthetic polymer substrates will be discussed, followed by small organic molecule binding peptides and peptides that bind to natural polymer substrates. The order in which these substrates are presented also reflects the historical evolution of the phage display technique. The first examples of the use of the phage display technique for synthetic polymer substrates go back to 1995.[48] Shortly after that, the first reports of the application of phage display to small organic molecule substrates were published and over the past decade this technique has also found application for the identification of small peptides that bind to natural polymer substrates.

Table 1. Overview of synthetic polymers that have been used as substrates in phage display affinity selection. For each substrate, the identified sequences as well as the selection conditions and characterization techniques that were used are listed.

Target(s)	Identified peptide(s) having strongest affinity	Selection conditions	Characterization technique(s) / K_a (M^{-1}) (if provided)	Comments
PS PVC	SSRLAYDHYFPSWRSYIF WMQSWYYHWGGGETFPIR	**Incubation:** 10^{11} phages in PBST 0.1% + 0.1% BSA (pH 7.4) to blocked PS or PVC microtiter plates. **Washing:** 5 x with PBS. **Elution:** 50 mM Glycine.HCl (pH 2.0). **Number of rounds:** 1	Phage ELISA	Enrichment of a particular sequence was not observed. Instead, a significant increase in the abundance of Tyr and Trp in the selected sequences was observed. [48]
PPyCl	THRTSTLDYFVI	**Incubation:** Phages in TBST 0.1% (pH 7.5) to thin films of PPyCl. **Washing:** 3 x with TBST 0.1%. **Elution:** Glycine.HCl (pH 2.2). **Number of rounds:** 5	Phage ELISA Peptide ELISA AFM (peptide) Fluorescamine assay (peptide)	Identified sequence conjugated with GRGDS was demonstrated to promote cell adhesion to PPyCl films. [49]
it-PMMA	ELWRPTR QLQKYPS ARPHLSF TLHLSPA	**Incubation:** 4 x 10^{11} phages/mL in TBST 0.1% spin-coated it-PMMA films. **Washing:** 5 x with TBST 0.1%. **Elution:** 500 mM Glycine.HCl (pH 2.2). **Number of rounds:** 5	Phage ELISA ($5.4 – 10 \times 10^{10}$) QCM (peptide) SPR (peptide) ($4.2 – 28.0 \times 10^5$)	A quantitative phage ELISA protocol allowing the determination of the apparent binding strengths of the phages to polymeric thin films was established. [50] The influence of the tacticity of the polymer substrate towards the binding of selected clones was demonstrated. [50-52]
st-PMMA	HKPDANR HPVHPHR LPPWQRQ HPRWHTP	**Incubation:** 4 x 10^{11} phages/mL in TBST 0.1% to spin-coated st-PMMA films. **Washing:** 5 x with TBST 0.1%. **Elution:** 500 mM Glycine.HCl (pH 2.2). **Number of rounds:** 5	Phage ELISA ($2.5 – 4.2 \times 10^{10}$)	The influence of the tacticity of the polymer substrate towards the binding of selected clones was demonstrated. [52,53]

Chapter 1: Identification of Soft Matter Binding Peptide Ligands using Phage Display

Table 1. (continued)

Target(s)	Identified peptide(s) having strongest affinity	Selection conditions	Characterization technique(s) / K_a (M^{-1}) (if provided)	Comments
st-PS	YLTMPTP FSWEAFA GETRAPL GETQCAA	**Incubation:** 3.3 x 10^{11} phages/mL in TBST 0.1% to st-PS films. **Washing:** 5 x with TBST 0.1%. **Elution:** 500 mM Glycine.HCl (pH 2.2). **Number of rounds:** 4	Phage ELISA (1.4 – 2.0 x 10^{11})	The influence of the tacticity of the polymer substrate towards the binding of selected clones was demonstrated.[54]
α-PLLA	QLMHDYR LSQSLTR RACSKDA ANTLRSP	**Incubation:** 4.0 x 10^{11} phages/mL in TBST 0.1% to α-PLLA films. **Washing:** 3 x with TBS. **Elution:** 100 mM Glycine.HCl (pH 2.2) + 1 mg/mL BSA. **Number of rounds:** 4	Phage ELISA (4.8 – 6.7 x 10^{9}) SPR (peptide) (6.1 x 10^{4})	Identified peptides were demonstrated to be able to distinguish different crystal polymorphs of PLLA.[55]
Azobenzene-containing poly(MA)'s	WPTPPNP SPSWLIQ WHTLPNA MHQGSNT	**Incubation:** 3.3 x 10^{11} phages/mL in TBST 0.1% to copolymer films. **Washing:** 5 x with TBST 0.1%(pH 7.5). **Elution:** 500 mM Glycine.HCl (pH 2.2). **Number of rounds:** 4	Phage ELISA (2.0 – 3.5 x 10^{10}) SPR (peptide) (1.4 x 10^{6}) QCM (peptide)	Identified peptides were able to more selectively bind to films having greater abundance of azobenzene groups having a *cis* conformation compared to the *trans* conformation.[56,57]
mpsPPV	HNAYWHWPPSMT HWDPFSLSAYFP	**Incubation:** 3.3 x 10^{11} phages/mL in TBST 0.1% to deposited polymer films. **Washing:** 1 x with TBST 0.1% and 4 x with PBS. **Elution:** 100 mM Glycine.HCl (pH 2.2). **Number of rounds:** 5	SPR (peptide) (1.3 x 10^{5})	The immobilization of the selected peptide enhanced the fluorescence intensity of the substrate.[58]

Table 1. (continued)

Target(s)	Identified peptide(s) having strongest affinity	Selection conditions	Characterization technique(s) / K_a (M^{-1}) (if provided)	Comments
PPV	HTDWRLGTWHHS (hyperbranched PPV binder) ELWSIDTSAHRK (linear PPV binder)	**Incubation:** 3.3 x 10^{11} phages/mL in TBST 0.1% to deposited polymer films. **Washing:** 1 x with TBST 0.1% and 4 x with PBS. **Elution:** 100 mM Glycine.HCl (pH 2.2) + 1 mg/mL BSA. **Number of rounds:** 5	SPR (peptide) (7.7 – 77.0 x 10^4)	The utilization of hyperbranched or linear PPV led to the identification of entirely different PPV-binding peptides, indicating that the influence of the architecture of the polymer substrate towards the binding of the selected clones were demonstrated.[59]
PDMS	LSNNNLR LQPRANF	**Incubation:** Phages in TBST 0.1 to 0.5% with PDMS slab. **Washing:** Several times with TBST. **Elution:** Glycine.HCl (pH 2.2). **Number of rounds:** 3	Fluorescence intentsity (phage -peptide)	The selected peptides selectively bounded to non-oxidized substrate, compared to plasma oxidized PDMS or PDMS containing microfluidic channels.[60]
Epoxy resin	TLHPAAD NERALTL SHSGYFS	**Incubation:** Phages in TBST 0.1 to 0.5% with epoxy slab. **Washing:** Several times with TBST. **Elution:** Glycine.HCl (pH 2.2). **Number of rounds:** 3	Fluorescence intentsity (phage -peptide)	[61]

1.2.1. Peptide binders to synthetic polymers

From the three classes of substrates considered in this section, most of the work that has been reported has involved the use of phage display to identify peptide ligands that bind to synthetic polymer substrates. **Table 1** presents a comprehensive list of the different substrates that have been investigated. For each substrate, **Table 1** includes the identified sequences, the selection conditions as well as the techniques that were used to assess the selectivity and affinity of the peptide ligands.

The first reports, which pointed out the potential of phage display to identify peptide sequences that can selectively bind to synthetic polymers, date back to 1995 when Adey and coworkers reported sequences that bind to polystyrene (PS) and polyvinyl chloride (PVC) surfaces.[48] In the same year, Caparon and coworkers, while searching to identify streptavidin binding ligands, reported a group of "nuisance peptides" of the consensus sequence WHWWXW, which were speculated to originate from phages that may have bound to the plastic substrates.[62] Since then, a number of other peptide sequences rich in tryptophan, such as WXW or WXXW as well as many others have been reported,[63] the selection of which was usually attributed to background binding to the plastic materials used in selection experiments.

Sanghvi *et al.* have used phage display to identify peptide binders to a conducting chlorine-doped polypyrrole (PPyCl) surface.[49] Fusion constructs of these affinity tags with the cell-adhesive GRGDS sequence were used to promote cell adhesion onto the PPyCl substrates (**Figure 3**).

Serizawa and coworkers have utilized phage display to identify peptide ligands for a broad variety of polymer substrates. Over the course of the last decade, they have identified peptide binders to poly(methyl methacrylate) (PMMA),[50-53] PS,[54] α-poly(L-lactide) (α-PLLA),[55] azobenzene-containing polymethacrylates,[56,57] poly(2-methoxy-5-propyloxysulfonate-1,4-phenylenevinylene) (mpsPPV)[58] and poly(phenylene vinylene) (PPV).[59] These experiments demonstrate that the tacticity, architecture or crystallinity of the polymer or even the conformation of polymer side chain functional groups can lead to the enrichment of different peptides and as a consequence the identification of selective peptide ligands. For instance, Serizawa and coworkers have shown that phage display carried out using atactic or syndiotactic PMMA led to the isolation of entirely different peptide sequences.[50-53] The apparent binding constants of the highest affinity peptides

towards one of these surfaces were reported to be 6 - 10 times higher as compared to the other surfaces. In another study, Serizawa *et al.* identified a crystalline α-PLLA binding peptide (QLMHDYR), which was demonstrated to have a lower affinity towards β-PLLA and amorphous PLLA as compared to α-PLLA.[55] The same group has also discovered peptides that can selectively recognize poly(methacrylates) containing cis-azobenzene groups over the ones having trans-azobenzenes.[56] In a final example, it was shown that phage display can be used to identify peptide binders that are selective to either linear or hyperbranched PPV derivatives.[59]

THRTSTLDYFVIGRGDS
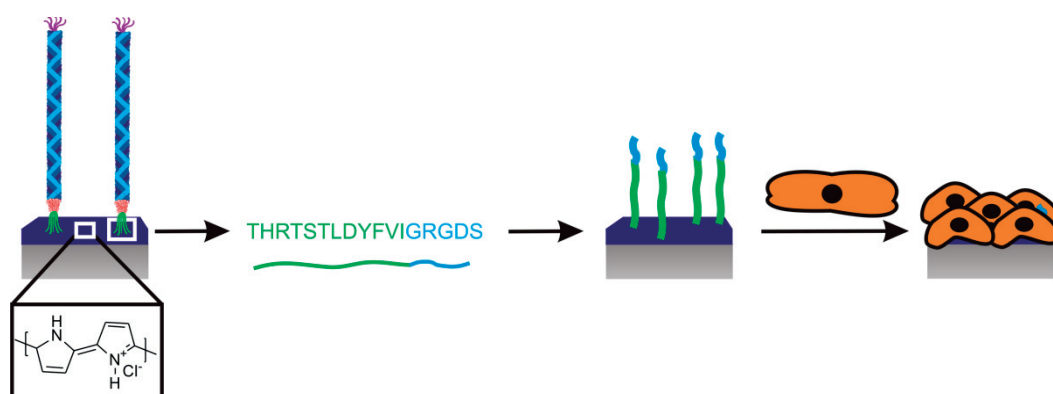
Figure 3. Incorporation of the RGD motif to the PPyCl binding peptide identified by phage display enhanced cell adhesion on PPyCl substrates as demonstrated by Sanghvi and coworkers.[49]

More recently, phage display has been used not just to identify peptide ligands that solely mediate surface immobilization, but which can also be used to generate surfaces with tunable properties. For instance, Ejima *et al.* have identified binders to water soluble poly(2-methoxy-5-propyloxysulfonate-1,4-phenylenevinylene) (mpsPPV).[58] Binding of these peptides to mpsPPV in aqueous solution was found to result in an increase in fluorescence intensity. The enhancement of the increase in fluorescence intensity could be modulated by tuning the amount of the peptide. Addition of thermolysin, an enzyme that degrades the peptide, was demonstrated to allow to "switch off" the fluorescence again. It was claimed that this modulation of the fluorescence intensity was due to the peptide-mediated dispersion/aggregation of the polymer in the aqueous solution. In another example, Chen and coworkers demonstrated that converting the conformation of azobenzene side chain functional groups from cis to trans by UV-irradiation resulted in

detachment of peptides that were identified by phage display to selectively bind to PMMA substrates that present the azobenzene groups in the cis conformation.[56,57] Swaminathan and coworkers have identified epoxy resin and poly(dimethylsiloxane) (PDMS) binding peptides in two different studies, and reported the increased localization of the bound peptides in specific regions on the respective microstructured substrates.[60,61]

1.2.2. Peptide binders to organic molecules

Phage display has also been used to identify peptides that can selectively bind to small organic molecules. These peptide ligands are of interest for a variety of purposes, including (i) the modulation of the fluorescence intensity of fluorophores, (ii) the selective detection of explosives and polycyclic hydrocarbons as well as for (iii) peptide-based patterning of substrates. **Table 2** summarizes the different small organic molecules that have been used as targets in phage display and lists the corresponding peptide ligands that have been identified. While the synthetic polymers that were discussed in the previous Section are very convenient as they can be directly used in the form of films as substrates for phage display, this can be more challenging for small organic molecules. In some cases small organic molecules can be used directly in form of solid crystals[66,69] as substrates for phage display. In many other cases, however, the molecules are immobilized on spherical beads[64,68,70] or on planar substrates.[67,71]

One of the first examples that reported the use of phage display to identify peptide-based binding ligands to small, organic molecules was the work by Rozinov and Nolan who used a variety of fluorophores such as Texas Red, Oregon Green 514 and fluorescein as substrates.[64] They demonstrated that site directed mutagenesis of the identified phage clones followed by their further selection towards the respective targets led to the isolation of new sequences having higher affinities than the originally selected ones. The highly affine interactions between these sequences and the fluorophores, particularly with Texas Red, were shown to be of use for the modulation of excitation and emission spectra of these molecules.

Table 2. Overview of organic molecules that have been used as substrates in phage display affinity selection. For each substrate, the identified sequences as well as the selection conditions and characterization techniques that were used are listed.

Target(s)	Identified peptide(s) having strongest affinity	Selection conditions	Characterization technique(s) / K_a (M^{-1}) (if provided)	Comments
Texas Red	KHVQYWTQMFYS KPVQYWTQMFYT (Texas red binders)	**Incubation:** 6.0 X 10^{10} phages/mL in TBST 0.1% (pH 7.4) to blocked fluorophore dye carrier beads. **Washing:** with TBST 0.1%. **Elution:** 200 mM Glycine.HCl (pH 2.2) + 1 mg/mL BSA. **Number of rounds:** 3 or 4 before the random mutagenesis. Another round was carried after the mutagenesis of the binding sequences were isolated.	Scatchard Plot based on phage titration (1.1 x 10^{10})	Random mutagenesis of the originally identified clones led to the isolation of newer clones having 2.7 to 6.5-fold greater affinity. The K_d values of the isolated clones were in low nanomolar range. [64]
Oregon Green 514	HGWDYYWDWTAW HEWEYYWDWTAW (Oregon Green 514 Binders)		Scatchard Plot based on fluorescence intensity (peptide) (6.0 x 10^5)	
Fluorescein	YPNDFEWWEYYF YPNEFDWWDYYY (Fluorescein Binders)			
2, 4, 6-Trinitrobenzene	WHRTPSTLWGVI NHRIWESFWPSA	**Incubation:** 4.0 x 10^{10} phages in artificial seawater to TNB coated wells. **Washing:** 10 x with artificial seawater containing 0.1% Tween 20. **Elution:** 100 mM Glycine.HCl (pH 2.2) + 1 mg/mL BSA. **Number of rounds:** 3	Phage ELISA Fluorescence intensity assay via a flow sensor.)	The identified clones showed significant selectivity towards the detection of TNB in seawater compared to PBS buffer. [65]
Trinitrotoluene	WHWQRPLMPVSI (TNT binder)	**Incubation:** 3.9 x 10^9 independent phages in TBST 0.1% to TNT and DNT crystals. **Washing:** 10 x with TBST 0.1%. **Elution:** 200 mM Glycine.HCl (pH 2.2) + 1 mg/mL BSA. **Number of rounds:** 3 or 4.	Fluorescence intensity (peptide)	Identified peptides immobilized onto a gold substrate via a oligoethylene glycol linker were demonstrated to act as a selective biosensor for the detection of volatile organic compounds. [66]
2, 4-Dinitrotoluene	HPNFSKYILHQR (DNT binder)		ITC (1.4 x 10^7)	

Chapter 1: Identification of Soft Matter Binding Peptide Ligands using Phage Display

Table 2. (continued)

Target(s)	Identified peptide(s) having strongest affinity	Selection conditions	Characterization technique(s) / K_a (M⁻¹) (if provided)	Comments
Octyltrimethoxy silane	SILPYPY HAIYPRH TTYSRFP QILAFNS	**Incubation:** 7.0×10^{11} phages in TBST with increasing amounts of Tween 20 with respect to number of rounds to OTMS-functionalized silicon substrate. **Elution:** 200 mM Glycine.HCl (pH 2.2). **Number of rounds:** 6	Fluorescence intensity	Patterned OTMS surfaces prepared via microcontact printing showed a patterned fluorescence signal upon selective immobilization of the binding clone.[67]
Polychlorinated biphenyls	DSNKLSPE LSFAADRT	**Incubation:** 1.7×10^{10} phages/mL in PBS + 5% milk powder to PCB-coated magnetic –COOH conjugated beads. **Washing:** 6 x with PBST 0.05%. **Elution:** 200 mM Glycine.HCl (pH 2.2) + 1 mg/mL BSA and 0.1 mg/mL phenol red. **Number of rounds:** 4	SPR ($1.4 – 1.7 \times 10^{4}$)	The identified phages selectivity recognized different PCB's.[68]
Thiamethoxam	ASTLPKA HTPPVTS ALTPTPP QPQVPDA	**Incubation:** 1×10^{10} phages/mL in TBST to blocked TMX crystals. **Washing:** Several times with TBST 0.1%. **Elution:** 200 mM Glycine.HCl (pH 2.2) + 1 M BSA. **Number of rounds:** 3	AFM	[69]
Naphthalene	HFTFPQQQPPRP TLTDPAYRPHRY KLHISKDHIYPT KNVDHMATFARG	**Incubation:** 8.0×10^{11} phages/mL in TBS to naphthalene immobilized SAM's. **Washing:** 5 x with TBST 0.1%. **Elution:** 200 mM Glycine.HCl (pH 2.2). **Number of rounds:** 5	SPR (peptide) (1.4×10^{5})	The peptide HFTFPQQQPPRP showed significant selectivity towards the recognition of naphthalene compared to benzene, anthracene and pyrene. This peptide was also demonstrated to show strong affinity towards free naphthalene in solution.[71]

Various groups have demonstrated the feasibility of peptides identified by phage display for the selective detection of molecules that are frequently used in explosives such as 1,3,5-trinitrobenzene (TNB), 2,4-dinitrotoluene (DNT) and 2,4,6-trinitrotoluene (TNT).[65,66,70] Goldman and coworkers have identified peptides that selectively recognize TNT in seawater, but not in a standard phosphate-buffered saline (PBS) buffer using phage display.[65] Furthermore, they have integrated phages that are labeled with a fluorescence dye into a continuous flow sensor, which allowed the detection of TNT. Jaworski *et al.* have identified sequences that selectively recognize TNT and DNT.[66] Covalent incorporation of the identified peptides to a gold chip via an oligo(ethylene glycol) linker allowed to selectively sense these explosives in the gas phase via headspace analysis (**Figure 4**). In another study, Na and coworkers used a library of single-chain variable fragments of antibodies (scFv) that were presented on a M13 bacteriophage to identify DNT binders.[70]
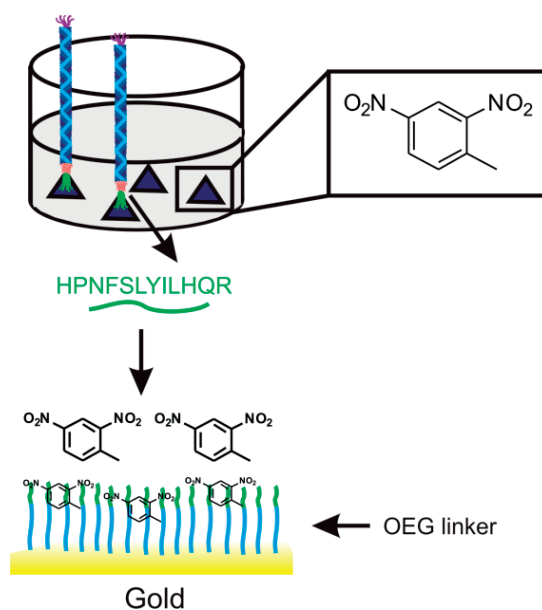
Figure 4. Detection of gaseous 2,4-dinitrotoluene (DNT) using a DNT-binding peptide coupled to a gold surface via a flexible oligoethylene glycol (OEG) linker.[66]

In addition to the detection of explosives, phage display has also been utilized for the identification of organic molecule binding peptides that can be of use for potential other sensing applications or surface patterning. Cui and coworkers have identified octyltrimethoxysilane (OTMS) binders and have prepared patterned OTMS-containing

silicon surfaces via microcontact printing or photolithography.[67] Fluorescence measurements demonstrated the localization of the OTMS binding phage in the microdomains that contains surface-immobilized OTMS. Van Dorst *et al.* have isolated two different sets of peptides that can selectively recognize two different polychlorinated biphenyl's (PCB's), which are known to be carcinogenic and can accumulate in tissue.[68,72] Cho *et al.* have identified binders to thiamethoxam (TMX) organic crystals and proposed that the surface manipulation of TMX crystals with the identified phages may prevent the sedimentation of their colloidal suspensions.[69] In a final example, Serizawa and coworkers have identified a naphthalene binding peptide (HFTFPQQQPPRP), which does not show any specificity towards other simple aromatic hydrocarbons, including anthracene and pyrene.[71]

1.2.3. Peptide binders to natural polymers

The last section of the first part of this Chapter summarizes the work that has been done using phage display for the identification of peptide ligands that selectively bind to natural polymers, especially to polysaccharides such as cellulose derivatives and chitin. These peptide binders are summarized in **Table 3**.

Fukusaki and coworkers have utilized a random phage library displaying cyclic peptides that are formed via disulfide bond formation of the flanking cysteine residues in order to identify chitin binders.[73] The identified peptide (CSRTTRTRC) was found to recognize chitin only in its cyclic conformation, whereas the linear derivative that was produced via reduction of the cyclic peptide did not show any affinity towards the target. Later, Khousab *et al.* identified linear chitin binders and reported the formation of porous chitin-peptide networks upon addition of the peptide to a mixture containing 0.5% colloidal chitin in water.[76] These biocompatible networks were proposed as possible scaffold materials for tissue engineering.

Table 3. Overview of natural polymers that have been used as substrates in phage display affinity selection. For each substrate, the identified sequences as well as the selection conditions and characterization techniques that were used are listed.

| Target(s)	Identified peptide(s) having strongest affinity	Selection conditions	Characterization technique(s) / K_a (M^{-1}) (if provided)	Comments
Chitin	CSRTTRTRC	**Incubation:** 10^{10} phages in PBS:EtOH 1:1 to a packed chitin column. **Washing:** 1 x PBS/EtOH 1:1. **Elution:** PBS/EtOH 1:1 + 50 mg/mL *N*-acetylglucosamine. **Number of rounds:** 5	SPR (Peptide) (9.1×10^3)	Identified clone bound to chitin only after intramolecular disulfide-bond formation *via* oxidation.[73]
Cellulose	HAIYPRH SHTLSAK TQMTSPR YAGPYQH	**Incubation:** 5×10^9 phages/mL in TBST 0.1% to dispersed cellulose microcrystals. **Washing:** 5 x with TBST 0.1%. **Elution:** 500 mM Glycine.HCl (pH 2.2). **Number of rounds:** 5	Phage ELISA ($4.6 – 5.2 \times 10^{10}$)	The isolated binding clones can be subdivided into two different groups, which were speculated to show affinity towards crystalline and amorphous domains, respectively.[74]
Cellulose	THKTSTQRRLLAA KCCYVNVGSVFS	**Incubation:** 2×10^{11} phages in TBST 0.1% containing 1 mg/mL BSA to cellulose samples. **Washing:** 6 x with TBST 0.1%. **Elution:** 200 mM Glycine.HCl (pH 2.2) + 1 mg/mL BSA. **Number of rounds:** 4	Phage ELISA GST activity assay Peptide ELISA	The preparation of a construct comprised of a carbon black and cellulose binder connected with a linking sequence was demonstrated to disperse the carbon black particles and subsequently attach them to paper surfaces.[75]
Chitin	EGKGVEAVGDGR GEVGEQEKARVG	**Incubation:** 10^{10} phages in PBST 0.1% to chitin-immobilized wells. **Washing:** 5 x with PBST 0.1%. **Elution:** 50 mM Glycine.HCl (pH 2.0). **Number of rounds:** 3	Phage ELISA Peptide ELISA	The specific interaction between the identified peptide and the clone allowed the assisted formation of a biomacromolecular network.[76]
CNW's	WHWRAWY WHWTYYW	**Incubation:** 2×10^{11} phages/mL in TBST 0.1% to cellulose-immobilized dishes. **Washing:** 10 x with TBST with increased concentration of Tween 20 w.r.t. number of rounds. **Number of rounds:** 3	Phage ELISA (1.0-10.0×10^{10}) ITC (Peptide) (1.1×10^5) Fluorescence quenching (Peptide) ($5.0 – 10.0 \times 10^4$) NMR (Peptide).	NMR and molecular modelling techniques allowed a more precise understanding of the interaction between the target and the substrate.[77]
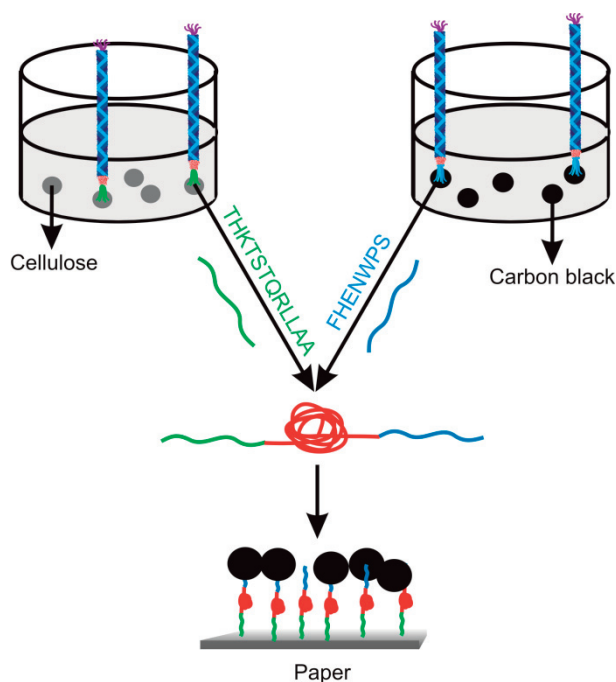
Figure 5. A triblock fusion construct composed of a central, rigid and hydrophilic interdomain linker (PTPTPTPTPTPTPTPTPTPTPT) flanked by cellulose and carbon black binding peptide ligands allows the deposition of carbon black particles onto paper surfaces.[75]

A variety of cellulose derivatives has also been used as target substrates for the identification of peptide binding ligands. Serizawa and coworkers have identified a variety of heptapeptides using microcrystalline cellulose as the substrate. These ligands were subdivided in two different groups. The first group was characterized by the presence of an –OH containing amino acid (S, T, Y) in the 1st and 5th position and a cationic amino acid (H, R, K) in the 7th position, while the second group of peptides was primarily composed of aliphatic residues.[74] The origin of this difference between the two groups was proposed to arise either from the affinity of different groups separately to crystalline and amorphous domains, or from different modes of peptide-crystalline cellulose interactions. Later, Guo and coworkers identified a crystalline cellulose nanowhisker binding peptide that was predominantly composed of aromatic residues (WHWTYYW).[77] The binding of this peptide to cellulose nanowhiskers (CNW) was studied using a variety of techniques, such as phage ELISA, isothermal titration calorimetry (ITC) and fluorescence quenching as well as nuclear magnetic resonance (NMR) and molecular modelling, which allowed a better understanding of the role of the

individual amino acids. These studies indicated that the peptide ligand adopts a bent conformation, which allows the tyrosine residue in the 5th position to form CH/π stacking interactions and a hydrogen bond with the cellulose glucose ring. In a final example, Qi and coworkers have identified binders to fibrous cellulose as well as to carbon black by using phage display.[75] A fusion construct that incorporated both the cellulose and carbon black binding sequence was able to disperse carbon black particles and allowed to subsequently attach these to paper surfaces, which are primarily composed of fibrous cellulose (**Figure 5**).

1.3. Characterization of soft matter binding peptides identified by phage display

The second part of this Chapter will present and discuss the techniques that are most commonly used to characterize the affinity of peptide ligands, which have been identified via phage display, towards soft matter surfaces. This part is organized in five sections, which will successively discuss ELISA and fluorescent based techniques, surface plasmon resonance (SPR), isothermal titration calorimetry (ITC), atomic force microscopy (AFM) and quartz crystal microbalance (QCM). These techniques are illustrated in **Figure 6**. Following a brief introduction to each technique, examples describing the use of these techniques for the determination of the binding strengths of soft matter binding peptide ligands will be presented.

1.3.1. ELISA and fluorescent based techniques

Phage ELISA is a robust technique that is frequently used to obtain insight into the binding affinity of phage clones (**Figure 6A**). A typical direct phage ELISA experiment consists of 3 steps. First, a phage solution is incubated with the substrate of interest and the unbound phages are washed with a buffer that usually contains small amounts of surfactant. In the next step, a primary antibody - enzyme conjugate, such as for example antiM13 - horseradish peroxidase (HRP), which binds with the substrate bound phages, is added. Following the removal of the excess primary antibody – enzyme conjugate by repeating the washing step several times, a HRP substrate that yields a colorimetric response upon reaction with HRP is introduced and the intensity of this signal is measured. As it does not require the isolation of individual phage clones, phage ELISA

can even be used as a monitoring step between successive affinity selection cycles. However, to calculate absolute binding affinities of the identified clones, a substrate concentration is required, which is ambiguous for solid substrates. As a consequence, phage ELISA is predominantly used to obtain qualitative information by comparing the ELISA readout from an experiment with a selected phage clone with that from an experiment with the starting, random phage library at a specific concentration with a predetermined amount (mass) of the substate.[49,65,75,76] This simple experiment provides the relative ratio of the deposition of different phage clones at a particular phage concentration, however, it does not yield absolute quantitative information about the affinity of the phage.

In order to circumvent the uncertainty in the substrate concentration, Serizawa and coworkers have developed a method that allows the determination of the apparent binding affinities of phages to solid surfaces by phage ELISA.[50] Their method is based on the assumption that the surface deposition of the phages follows a Langmuir-type adsorption and the ratio of the ELISA signals obtained from the assay with the individual phage clones and that with the library on an identical substrate as a function of phage concentration would yield an adsorption isotherm. This isotherm, then, can be utilized to calculate the apparent affinities of individual phage clones. This method is based on the assumption that in a given set of experiments at each phage concentration, both for the selected clone as well as for the random library, all the substrates (at an equivalent surface area), present the same surface concentration of binding sites, which may not be applicable to substrates having high surface roughness, which is a general limitation of a Langmuir-type adsorption model. Serizawa and coworkers have successfully used this approach to calculate the apparent affinities of selected phages to thin, spin coated films of a broad range of synthetic and natural polymers, including PMMA, PS, PLLA, PPV's and cellulose, amongst others.[50,52,54-56,74]

The calculated binding affinities obtained by phage ELISA are typically in the range of 10^{10}-10^{11} M^{-1}, which is ~ 2 - 5 orders of magnitude greater than the calculated binding constants of the corresponding peptides to solid surfaces. This apparent discrepancy between the phage and peptide affinities is due to multivalency effects. Whereas each peptide can only act as a single binder, the most frequently used M13 phage displays multiple copies of each peptide, which allows for multivalent interactions. From experiments that have compared single peptides with multivalent constructs, it is known that multivalency can significantly increase the binding strength.[16,78,79] From this point, it

can be speculated that the binding strengths obtained from phage ELISA experiments are an overestimate. It is also worth noting that the calculated binding affinities of identified phage clones using phage ELISA experiments depend on the extent of non-specific interactions between the random phage library and the surfaces, and therefore, are apparent values. This is because the affinity of an individual phage clone is calculated from the ratio between the adsorption isotherm of that particular phage clone to the random phage library in phage ELISA.

The binding of phages and peptides has also been assessed using fluorescently labeled primary or secondary antibodies. These allow the direct observation and analysis of the substrate bound phages/peptides by fluorescence microscopy techniques.[60,61,65-67] Sanghvi and coworkers have used streptavidin-fluorescein isothiocyanate (FITC) either as a primary or secondary antibody, respectively, to compare the extent of binding of different phage clones or biotinylated variants of the peptide that was previously isolated as the strongest binder to PPyCl.[49] Similarly, Jaworski and coworkers have used Atto-425-streptavidin to detect the extent of binding of biotinylated DNT-binding peptide and its alanine-substituted derivatives.[66] These fluorometric assays were not performed to determine the binding-strengths of the individual clones, but rather used to qualitatively assess the amount of phage/peptide that was bound to the desired substrate. Sanghvi and coworkers directly determined the amount of bound peptide to PPyCl surfaces with fluorescamine, which can rapidly react with N–terminal amine groups to yield a strong fluorescent signal.[49] Guo *et al.* used a method previously designed by Yoon and coworkers[80] to calculate the binding strength of the CNW-binding peptide sequence WHWTYYW to cello-oligosaccharides. This method was based on the quenching of the intrinsic fluorescence of the tryptophan and tyrosine residues upon binding of the peptide ligands to the substrates. The binding affinity of this peptide was found to be on the order of 10^5 M^{-1}, which was approximately 5 orders of magnitude smaller than the affinity of the phage-containing this peptide.
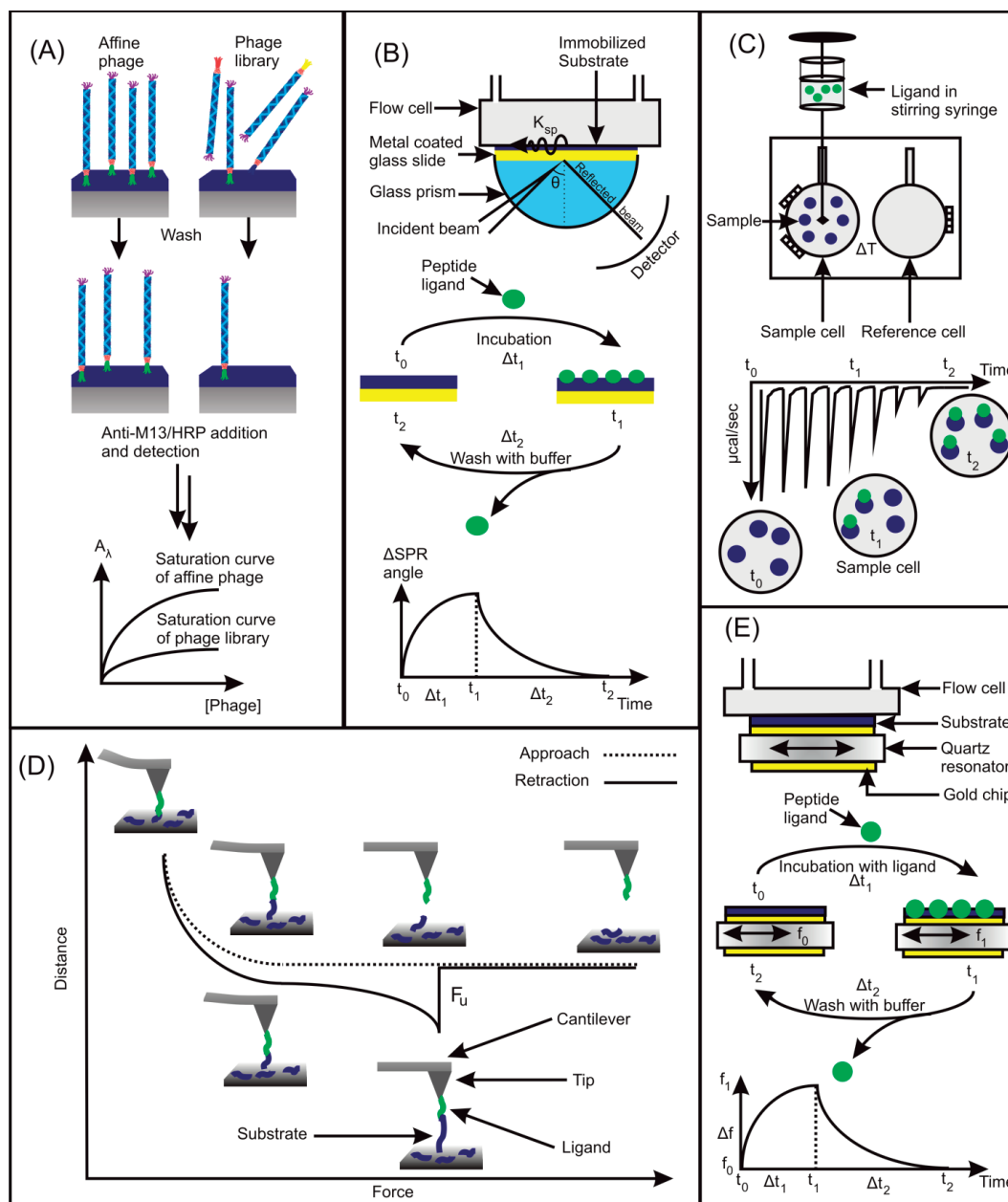
Figure 6. Schematic overview of the most frequently utilized techniques to assess the strength of phage - soft matter interactions. (A) Phage ELISA, (B) surface plasmon resonance (SPR), (C) isothermal titration calorimetry (ITC), (D) atomic force microscopy (AFM) and (E) quartz crystal microbalance (QCM). In a typical SPR experiment (B), the substrate is incubated in a solution containing the ligand at t_0 until all of the substrate binding sites are populated with the ligand (t_1). At this point, the SPR angle does no longer changes as a function of time. Next, the ligand bound substrate is washed with a buffer until the SPR angle returns back its original value (t_2). In a typical ITC experiment (C), the concentration of the ligand in the sample cell is zero at t_0. Titration of the sample

with the ligand leads to the release or absorption of heat with each titration, the amount of heat gradually decreases due to the decrease in the number of possible ligand sample interactions (t_1) and eventually reaches to zero (t_2), which indicates the saturation of substrate binding sites. Similar to the SPR experiment, in QCM (E), the substrate immobilized on the QCM chip is incubated with the ligand at t_0 until saturation of the substrate binding sites (t_1). At this point, the resonance frequency of the QCM chip stays constant as a function of time. Next, incubation of the chip with the buffer solution leads to the detachment of the ligand from the substrate, and complete detachment occurs at the point that the resonance frequency of the QCM chip returns back to its initial value (t_2).

1.3.2. Surface plasmon resonance

Surface plasmon resonance (SPR) is a powerful optical technique that is frequently utilized for the real-time determination of the affinities of ligands in solution to surface-immobilized substrates. As it allows the analysis of thin, polymer coatings deposited onto silver or gold metallic films, it is a very valuable tool for the investigation of degradation,[81] adsorption[82] or hydration[83] processes of synthetic or natural polymeric films, as well as for the characterization of ligands that selectively bind to these substrates.[84] A major advantage of SPR is that it does not require chemical modification of the ligand or the substrate. As the measurement does not rely on the signal of a reporting molecule (*i.e.* primary or secondary antibody) it represents a direct method for the determination of binding affinities.

Figure 6B schematically outlines the SPR analysis of surface binding peptides and phages. Briefly, in the Kretschmann configuration, which is based on the principle of attenuated total reflectance (ATR), the instrument is composed of a glass/metal/dielectric interface, where the thickness of the metal layer is less than the wavelength of the incident light. While gold and silver are the most suitable thin metallic films, the dielectric medium can be *e.g.* a thin polymer film in an aqueous solution. When a p-polarized incident beam in the near-IR range undergoes total internal reflection (TIR) at the glass/metal interface, it generates an evanescent wave parallel to the metal/dielectric interface that can resonantly excite a surface plasmon at a specific angle of incidence of the incoming beam.[85,86] Since the excitation of the surface plasmon depends on the refractive index of the medium in close proximity of the metal/dielectric interface, any event that results in a change in the refractive index of this medium, such as ligand-

binding or dissociation, leads to a change in the angle of incidence required to excite the surface plasmons.[87] Therefore, an SPR coupled with a flow cell can first allow the determination of the rate constant of association (k_{ass}) by using a constant flow of a solution containing a predetermined concentration of the ligand until the change in the SPR angle becomes zero over time, which is an indication of the surface saturation. Next, the rate constant of dissociation (k_{diss}) can be calculated by passing a blank solution over the saturated substrate until the SPR angle reaches the initial value, which indicates complete dissociation. From the determined k_{ass} and k_{diss} values, the binding constant can be calculated ($K_a = k_{ass}/k_{diss}$).[84,88]

In an early example, Fukusaki *et al.* have immobilized a chitin-binding peptide onto a gold chip and determined a binding affinity of 9×10^3 M^{-1} to a soluble derivative of chitin, chitotriose, which was passed through the flow cell.[73] It is important to note that while the affinity selection was carried out using chito-oligoagarose as the substrate, chitotriose was utilized in the SPR measurements, which may result in lower binding affinities measured via SPR as slight differences in the properties of polymeric substrates were reported to significantly affect the strength of the phage/peptide-substrate interactions.[50,52,55,59] Matsuno and coworkers have prepared thin films of α, β and atactic (at) PLLA on gold substrates and compared the binding affinity of a β-PLLA-binding peptide (QLMHDYR) to these substrates.[55] A K_a of 6.1×10^4 M^{-1} was found for α-PLLA, which was approximately ten-fold higher than the affinity of this peptide towards β and at-PLLA, illustrating the selective binding of this peptide to α-PLLA. It is worth noting that a K_a value of 6.7×10^9 M^{-1} was obtained when phage ELISA was performed using the phage clone displaying this sequence and α-PLLA as the substrate. Possible reasons for this discrepancy were discussed in the previous section. Ejima *et al.* found K_a values of 7.7×10^5 M^{-1} and 7.7×10^4 M^{-1} for two different peptides towards hyperbranched (hyp) and linear PPV's, respectively.[59] Furthermore, SPR analysis of the hypPPV-binding peptide variants prepared via alanine scanning provided important insights into the binding mechanism of this peptide to these polymeric surfaces. The same authors also used SPR to identify the binding affinity of a peptide recognizing poly-(2-methoxy-5-propyloxysulfonate-1,4-phenylenevinylene) (mpsPPV) surfaces ($K_a = 1.3 \times 10^5$ M^{-1}).[58]

SPR has also been used to determine the binding affinity of small peptide ligands towards organic molecule targets. For example, Van Dorst and coworkers have chemically immobilized polychlorinated bisphenyl (PCB)-binding phages onto an SPR chip and monitored the rate of change of SPR angle as a function of PCB concentration in

the aqueous phase.[68] The resulting saturation curves allowed the calculation of K_a in the range of 1.4 to 2 x 10^4 M^{-1}. Sawada and coworkers have immobilized 2-naphthylamine on gold substrates and determined a K_a value of 1.4 x 10^5 M^{-1} for a naphthalene-binding peptide identified by phage display and demonstrated its selectivity towards naphthalene over other aromatic hydrocarbons such as benzene, anthracene and pyrene using SPR.[71]

1.3.3. Isothermal titration calorimetry

Isothermal titration calorimetry (ITC) is a powerful technique that allows the determination of the thermodynamic interaction parameters between two or possibly more components in solution.[89-91] An isothermal titration calorimeter consists of two cells. The reference cell only contains a buffer solution. The sample cell is loaded with the substrate of interest at a defined concentration in the same buffer solution. The method relies on the measurement of the temperature difference between these two cells upon gradual titration of the substrate with the corresponding ligand until saturation is reached. Each addition results in heat that is released or absorbed as a result of the reaction or interaction between the species that are added together. The heat is measured by the isothermal titration calorimeter and appears as spikes in the titration curves, as shown in **Figure 6C**. Integration of these spikes does not only provide information about the binding affinity but can also allow calculating the changes in the enthalpy and entropy associated with the ligand substrate interactions.[90,91]

ITC is often not a very convenient technique to determine the binding affinities of ligands to solid substrates since the concentration of the binding sites that are available for the phage or the peptide, which is a required parameter for the calculation of the binding affinities, is ambiguous when solid surfaces are used. Several groups, however, have successfully utilized ITC for the determination of binding affinities of peptide ligands to small organic molecules having a known concentration. Jaworski and coworkers, for example, have calculated a binding constant of 1.4 x 10^7 M^{-1} of a trinitrotoluene (TNT) binding peptide to TNT in pure acetonitrile.[66] Guo and coworkers have titrated homogenous suspensions of CNWs with the corresponding CNWs-binding peptide and have calculated a binding constant of ~ 10^5 M^{-1}, which was in the same range obtained from fluorescence quenching measurements.[77]

1.3.4. Atomic force microscopy

Due to its ability to accurately measure forces in the piconewton range, atomic force microscopy can be used to determine the strength of non-covalent ligand-substrate interactions. The determination of the unbinding force between the ligand and the substrate is usually carried out using AFM tips and substrates that are functionalized with the respective molecules.[92-94] Briefly, a typical AFM force measurement cycle reveals a hysteresis between the force-distance curves that are recorded during approach and retraction of the AFM tip (**Figure 6D**). This hysteresis reflects the unbinding force that is required to separate an interacting pair immobilized to the tip and the substrate at a given loading rate. The loading rate is defined as the time derivative of the force applied to a bound pair and depends on the retraction velocity and the spring constant of the cantilever.[94] As a consequence, the unbinding force is an "apparent" value that allows to compare ligand-substrate interactions at a particular loading rate. It is also worth noting that although AFM force measurements in theory can allow the calculation of binding affinities, the determination of the rate of association may not be feasible or require laborious scans and a careful interpretation of the data for many of the ligand-substrate interactions.[95] As a consequence, binding affinities ($K_a = k_{ass}/k_{diss}$) are not frequently reported. A detailed theoretical and practical framework for the utilization of AFM for the determination of the strength of ligand-substrate interactions is provided in several excellent reviews.[96,97]

While AFM force measurements potentially are a powerful complementary technique to study the interaction between phages or peptide ligands and surfaces, this technique has been used less as compared to, for example, SPR or QCM, which is presumably due to the relative difficulties in the optimization of the experiments and the interpretation of the results. Sanghvi and coworkers have determined an unbinding force of 112 pN between a PPyCl-binding peptide selected via phage display and thin films of PPyCl.[49] Experiments with biotin-avidin (as a positive control) and GRGDS non-specifically adsorbed on the PPyCl films as a negative control afforded forces of 309 and 43 pN. In another interesting experiment, Cho *et al.* covalently immobilized a thiamethoxam (TMX) – binding phage as well as a random phage library onto Si_3N_4 tips and assessed the unbinding forces between these tips and TMX immobilized to a glass substrate via an epoxy resin at a constant loading rate.[69] The experiments revealed an approximately 8-fold greater unbinding force for the phage displaying TMX-binding peptide (~ 147 pN) as

compared to the random phage library ($\sim$ 18 pN), highlighting its specificity towards TMX surfaces.

1.3.5. Quartz crystal microbalance

The quartz crystal microbalance (QCM) technique allows to determine the mass of material that is adsorbed or deposited on a surface from the change in resonance frequency of an oscillating quartz crystal (**Figure 6E**).[98-101] The QCM technique can also be used in liquid solutions, which makes this approach an attractive tool to study (bio)interfacial phenomena. The QCM technique has been utilized to assess the interaction between antibody presenting phages and the complementary antigens.[33,102] In principle, the QCM technique could represent an alternative method to obtain (semi-)quantitative insight into the binding affinities of soft matter binding peptides. QCM can be used in two ways to (semi-)quantitatively characterize binding affinities. The first approach involves measuring in real time the adsorption and desorption of molecules by monitoring the changes in the frequency of the QCM sensor upon successively exposing the chip to a solution containing the ligand and a washing buffer similar to a SPR measurement highlighted above.[103] The second method is based on the measurement of the resonance frequency at different concentrations of the ligand subjected to a fixed amount of substrate until the frequency no longer changes as a function of ligand concentration. The resulting saturation curves can be treated as a Langmuir adsorption isotherm, which can eventually provide K_a values.[104]

In spite of the potential opportunities to also provide (semi-)quantitative information, so far the QCM technique has been mainly used to qualitatively monitor the interactions between soft matter binding ligands and their target substrates. In one example, Serizawa and coworkers have exposed QCM chips, which were coated either with isotactic (it) or syndiotactic (sn)-PMMA films, to a solution containing the peptide selected via phage display.[50] The QCM experiment confirmed the ability of the peptide to selectively recognize the it-PMMA surface. In another example, Chen *et al.* prepared spin coated films of poly(methacrylates) containing cis or trans-azobenzene side chain functional groups on a QCM chip, which were then subjected to a solution containing a biotinylated derivative of the peptide recognizing cis-azobenzene groups.[57] Next, the QCM chip was exposed to a solution containing streptavidin and the QCM frequency changes were used to assess the extent of deposition of streptavidin on the surfaces and provided further

evidence for the selectivity of this sequence towards cis-azobenzene over its trans conformer.

1.4.   Challenges and Opportunities

The examples presented in this Chapter demonstrate the feasibility of phage display to identify soft matter binding peptide ligands for a variety of substrates. These peptide ligands can be used to promote cell adhesion to polymer surfaces,[49] to modulate the fluorescence of organic molecules or polymers,[58,64] to direct scaffold formation,[76] to selectively detect explosives[65,66] and in printing applications.[75] However, the applicability of the phage display technique and the utilization of the identified soft matter binding peptide ligands may present some limitations. In this section, some of these limitations will be discussed and potential solutions or alternatives that may allow to overcome these challenges will be presented.

First of all, unlike biological substrates such as enzymes and proteins, synthetic polymer films or organic crystals generally do not have well-defined binding pockets that can be occupied with the corresponding ligands with very high affinity. As a consequence, the binding constants of soft matter binding peptides are typically relatively low in the range of $10^4 - 10^6$ M^{-1}. For practical applications, it may be desirable to enhance the binding strengths of these ligands. One possibility to enhance the affinities of the selected peptides is the use of mutagenesis.[64] Another approach is to explore multivalency, since multivalent ligands have been shown to have few orders of magnitude higher binding constants as compared to monovalent ligands.[105,106] This can be achieved, for example, by using scaffolds (polymers, particles, ….), which present multiple copies of the peptide ligand of interest.[16,78,79] These multivalent constructs may also allow to diminish the discrepancy between the reported phage and peptide binding constants as the most frequently used M13 phage contains five copies of each peptide. Another way to overcome the discrepancy between phage and peptide affinities would be to use phage platforms that only display a single copy of the peptides can also be used in affinity selection experiments.[107]

Most of the examples presented in this Chapter have used commercially available, linear 7- or 12-mer M13 phage libraries. There is a number of other phage display formats, however, which can also be used to screen and identify binding ligands to soft

matter substrates. In addition, the use of phage libraries displaying conformationally constrained cyclic sequences may allow the isolation of cyclic peptide binders with higher affinities as compared to flexible linear sequences.[108-111] When comparing phage display formats that generate peptide ligands of different lengths, it is worth mentioning that the diversity of phage libraries is typically in the range of 10^8 - 10^9 clones, indicating that any insert having more than 7 amino acids ($20^7 = 1.28 \times 10^9$) would only cover only a small fraction of all possible sequences.

In addition to peptide phage display, there are several other combinational techniques that can be used to identify soft matter binding ligands. Antibody phage display[112-114] and bacterial cell surface display,[115,116] for example, have been used to identify either short peptide sequences or large antibodies that bind to soft matter substrates. Particularly, single-chain variable fragment (scFv) antibody phage display may yield soft matter binding proteins having higher binding strengths as compared to short, flexible peptides. For instance, calculated binding constants of strongest DNT-binding antibody was an order magnitude (10^8 M^{-1}) higher than previously identified DNT-binding peptides (10^7 M^{-1}), which were identified via peptide phage display.[66,113] However, the use of antibodies in hybrid conjugates may present some challenges due to their lower stability and higher costs compared to short peptides.[23] Another technique that is of potential interest for the identification of small ligands that bind to soft matter substrates is systematic evolution of ligands by exponential enrichment (SELEX).[117-119] SELEX generates nucleic acid ligands, so-called aptamers, and is particularly advantageous to identify small molecule binding ligands owing to the small size of nucleotides compared to phages. An interesting aspect of SELEX is the diversity of the initial random library. SELEX typically starts from a chemically synthesized random oligonucleotide library composed of ~ 10^{15} molecules[119] whereas phage display typically involves 10^{10} different clones.[3] Aptamer selection has been reported to be facilitated by the presence of positively charged groups as well as groups that can act as hydrogen bond donors and acceptors and be more difficult on substrates that are hydrophobic or present negatively charged groups.[119] Nevertheless, this technique has been very successfully used to identify highly affine binders to a broad range of substrates including e.g. sugars, drugs as well as polysaccharides such as chitin.[119,120,121]

A final challenge is the elucidation of the binding mechanisms of peptides identified via phage display. Few recent works have used NMR techniques combined with computational modelling to understand the molecular structures of peptides/proteins

bound onto well-defined solid surfaces.[122-124] However, the applicability of these techniques to more complex targets, such as structurally heterogeneous polymer films yet needs to be demonstrated. Furthermore, it is important to highlight that most of the phage display experiments cited in this review did not yield consensus sequences or motifs, but rather compositionally diverse peptides that do not necessarily share similar properties, *i.e.* hydrophobicity or charge. As a consequence, the role of each amino acid in each of the identified sequences towards the binding onto these substrates should be analyzed separately, for example, using alanine scan variants of each sequence,[59] which is a time consuming task. The lack of consensus may also require the sequencing of a greater number of clones following the affinity selection to identify otherwise undetected binders, which can be carried using high-throughput, next generation sequencing.[125-127] Furthermore, polymeric substrates often are structurally heterogeneous, such that they for example simultaneously present crystalline and amorphous domains, have different tacticities, architectures and side chain functional groups. Each of these features can lead to the selection of entirely different peptide binders, as shown by Serizawa and coworkers,[37] which can make establishing unambiguous sequence – property relationships daunting task.

1.5. Conclusions

With its rapidly expanding scope, it is evident that the phage display technique is a powerful tool that allows the identification of specific peptide binders to a myriad of artificial or natural substrates including synthetic polymers, small organic molecules as well as natural macromolecules. These peptide ligands open new avenues to functionalize and interface both man-made and biological materials. While a number of experimental techniques can be used to (semi-) quantitatively assess binding of phages and peptides to soft matter substrates, an accurate, molecular level characterization remains a challenge. Possibly the use of advanced molecular modelling and simulations combined with experimental techniques such as NMR and next generation sequencing, may pave the way for a better understanding of the interactions between phages/peptides and their substrates.

1.6. References

(1)   Smith, G. P.; Petrenko, V. A. *Chem. Rev.* **1997**, *97*, 391-410.

(2)   Rodi, D. J.; Makowski, L. *Curr. Opin. Biotechnol.* **1999**, *10*, 87-93.

(3)   Azzazy, H. M. E.; Highsmith Jr, W. E. *Clin. Biochem.* **2002**, *35*, 425-445.

(4)   Cortese, R.; Monaci, P.; Nicosia, A.; Luzzago, A.; Felici, F.; Galfré, G.; Pessi, A.; Tramontano, A.; Sollazzo, M. *Curr. Opin. Biotechnol.* **1999**, *6*, 73-80.

(5)   Winter, G.; Griffiths, A. D.; Hawkins, R. E.; Hoogenboom, H. R. *Annu. Rev. Immunol.* **1994**, *12*, 433-455.

(6)   Pande, J.; Szewczyk, M. M.; Grover, A. K. *Biotechnol. Adv.* **2010**, *28*, 849-858.

(7)   Smith, G. *Science* **1995**, *228*, 1315-1317.

(8)   Sparks, A. B.; Quilliam, L. A.; Thorn, J. M.; Der, C. J.; Kay, B. K. *J. Biol. Chem.* **1994**, *269*, 23853-23856.

(9)   Hyde-DeRuyscher, R.; Paige, L. A.; Christensen, D. J.; Hyde-DeRuyscher, N.; Lim, A.; Fredericks, Z. L.; Kranz, J.; Gallant, P.; Zhang, J.; *et al. Chem. Biol.* **2000**, *7*, 17-25.

(10)   Dennis, M. S.; Eigenbrot, C.; Skelton, N. J.; Ultsch, M. H.; Santell, L.; Dwyer, M. A.; O'Connell, M. P.; Lazarus, R. A. *Nature* **2000**, *404*, 465-470.

(11)   Petrenko, V. A.; Vodyanoy, V. J. *J. Microbiol. Methods* **2003**, *53*, 253-262.

(12)   Mourez, M.; Kane, R. S.; Mogridge, J.; Metallo, S.; Deschatelets, P.; Sellman, B. R.; Whitesides, G. M.; Collier, R. J. *Nat. Biotech.* **2001**, *19*, 958-961.

(13)   Deshayes, K.; Schaffer, M. L.; Skelton, N. J.; Nakamura, G. R.; Kadkhodayan, S.; Sidhu, S. S. *Chem. Biol.* **2002**, *9*, 495-505.

(14)   Koolpe, M.; Burgess, R.; Dail, M.; Pasquale, E. B. *J. Biol. Chem.* **2005**, *280*, 17301-17311.

(15)   Grosso, L. E.; Scott, M. *Biochemistry* **1993**, *32*, 13369-13374.

(16)   Helms, B. A.; Reulen, S. W. A.; Nijhuis, S.; Graaf-Heuvelmans, P. T. H. M. D.; Merkx, M.; Meijer, E. W. *J. Am. Chem. Soc.* **2009**, *131*, 11683-11685.

(17)   Scott, J.; Smith, G. *Science* **1990**, *249*, 386-390.

(18)   Luzzago, A.; Felici, F.; Tramontano, A.; Pessi, A.; Cortese, R. *Gene* **1993**, *128*, 51-57.

(19)   Fack, F.; Hügle-Dörr, B.; Song, D.; Queitsch, I.; Petersen, G.; Bautz, E. K. F. *J. Immunol. Methods* **1997**, *206*, 43-52.

(20)   Gallop, M. A.; Barrett, R. W.; Dower, W. J.; Fodor, S. P. A.; Gordon, E. M. *J. Med. Chem.* **1994**, *37*, 1233-1251.

(21)   Gordon, E. M.; Barrett, R. W.; Dower, W. J.; Fodor, S. P. A.; Gallop, M. A; *J. Med. Chem.* **1994**, *37*, 1385-1401.

(22)   Sidhu, S. S. *Curr. Opin. Biotechnol.* **2000**, *11*, 610-616.

(23)   Ladner, R. C.; Sato, A. K.; Gorzelany, J.; de Souza, M. *Drug Discov. Today* **2004**, *9*, 525-529.

(24)   Wang, L.-F.; Yu, M. *Curr. Drug Targets* **2004**, *5*, 1-15.

(25)   Sidhu, S. S.; Koide, S. *Curr. Opin. Struct. Biol.* **2007**, *17*, 481-487.

(26)   Arap, W.; Kolonin, M. G.; Trepel, M.; Lahdenranta, J.; Cardo-Vila, M.; Giordano, R. J.; Mintz, P. J.; Ardelt, P. U.; Yao, V. J.; Vidal, C. I.; *et al. Nat. Med.* **2002**, *8*, 121-127.

(27)   Sarikaya, M.; Tamerler, C.; Jen, A. K. Y.; Schulten, K.; Baneyx, F. *Nat. Mater.* **2003**, *2*, 577-585.

(28)   Baneyx, F.; Schwartz, D. T. *Curr. Opin. Biotechnol.* **2007**, *18*, 312-317.

(29)   Naik, R. R.; Stringer, S. J.; Agarwal, G.; Jones, S. E.; Stone, M. O. *Nat. Mater.* **2002**, *1*, 169-172.

(30)   Sano, K.-I.; Shiba, K. *J. Am. Chem. Soc.* **2003**, *125*, 14234-14235.

(31)   Whaley, S. R.; English, D. S.; Hu, E. L.; Barbara, P. F.; Belcher, A. M. *Nature* **2000**, *405*, 665-668.

(32)   Artzy Schnirman, A.; Zahavi, E.; Yeger, H.; Rosenfeld, R.; Benhar, I.; Reiter, Y.; Sivan, U. *Nano Lett.* **2006**, *6*, 1870-1874.

(33)   Chen, H.; Su, X.; Neoh, K.-G.; Choe, W.-S. *Anal. Chem.* **2006**, *78*, 4872-4879.

(34)   Nam, K. T.; Kim, D.-W.; Yoo, P. J.; Chiang, C.-Y.; Meethong, N.; Hammond, P. T.; Chiang, Y.-M.; Belcher, A. M. *Science* **2006**, *312*, 885-888.

(35)   Wang, S.; Humphreys, E. S.; Chung, S.-Y.; Delduco, D. F.; Lustig, S. R.; Wang, H.; Parker, K. N.; Rizzo, N. W.; Subramoney, S.; Chiang, Y.-M.; *et al. Nat. Mater.* **2003**, *2*, 196-200.

(36)   Cui, Y.; Kim, S. N.; Jones, S. E.; Wissler, L. L.; Naik, R. R.; McAlpine, M. C. *Nano Lett.* **2010**, *10*, 4559-4565.

(37)   Serizawa, T.; Matsuno, H.; Sawada, T. *J. Mater. Chem.* **2011**, *21*, 10252-10260.

(38)   Cui, Y.; Kim, S. N.; Naik, R. R.; McAlpine, M. C. *Acc. Chem. Res.* **2012**, *45*, 696-704.

(39)   Goldman, E. R.; Medintz, I. L.; Whitley, J. L.; Hayhurst, A.; Clapp, A. R.; Uyeda, H. T.; Deschamps, J. R.; Lassman, M. E.; Mattoussi, H. *J. Am. Chem. Soc.* **2005**, *127*, 6744-6751.

(40)   Souza, G. R.; Christianson, D. R.; Staquicini, F. I.; Ozawa, M. G.;Snyder, E. Y.; Sidman, R. L.; Miller, J. H.; Arap, W.; Pasqualini, R. *Proc. Natl. Acad. Sci. U.S.A.* **2006**, *103*, 1215-1220.

(41)   Merzlyak, A.; Lee, S.-W. *Curr. Opin. Chem. Biol.* **2006**, *10*, 246-252.

(42)   Naik, R. R.; Jones, S. E.; Murray, C. J.; McAuliffe, J. C.; Vaia, R. A.; Stone, M. O. *Adv. Funct. Mater.* **2004**, *14*, 25-30.

(43)   Sano, K.-I.; Sasaki, H.; Shiba, K. *Langmuir* **2005**, *21*, 3090-3095.

(44)   Lee, S.-W.; Mao, C.; Flynn, C. E.; Belcher, A. M. *Science* **2002**, *296*, 892-895.

(45)   Demir, H. V.; Seker, U. O. S.; Zengin, G.; Mutlugun, E.; Sari, E.; Tamerler, C.; Sarikaya, M. *ACS Nano* **2011**, *5*, 2735-2741.

(46)   Kim, T. H.; Lee, B. Y.; Jaworski, J.; Yokoyama, K.; Chung, W.-J.; Wang, E.; Hong, S.; Majumdar, A.; Lee, S.-W. *ACS Nano* **2011**, *5*, 2824-2830.

(47)   Lee, B. Y.; Zhang, J.; Zueger, C.; Chung, W.-J.; Yoo, S. Y.; Wang, E.; Meyer, J.; Ramesh, R.; Lee, S.-W. *Nat. Nanotechnol.* **2012**, *7*, 351-356.

(48)   Adey, N. B.; Mataragnon, A. H.; Rider, J. E.; Carter, J. M.; Kay, B. K. *Gene* **1995**, *156*, 27-31.

(49)   Sanghvi, A. B.; Miller, K. P. H.; Belcher, A. M.; Schmidt, C. E. *Nat. Mater.* **2005**, *4*, 496-502.

(50)   Serizawa, T.; Sawada, T.; Matsuno, H.; Matsubara, T.; Sato, T. *J. Am. Chem. Soc.* **2005**, *127*, 13780-13781.

(51)   Serizawa, T.; Sawada, T.; Matsuno, H. *Langmuir* **2007**, *23*, 11127-11133.

(52)   Date, T.; Yoshino, S.; Matsuno, H.; Serizawa, T. *Polym. J.* **2012**, *44*, 366-369.

(53)   Serizawa, T.; Sawada, T.; Kitayama, T. *Angew. Chem. Int. Edit.* **2007**, *46*, 723-726.

(54)   Serizawa, T.; Techawanitchai, P.; Matsuno, H. *ChemBioChem* **2007**, *8*, 989-993.

(55)   Matsuno, H.; Sekine, J.; Yajima, H.; Serizawa, T. *Langmuir* **2008**, *24*, 6399-6403.

(56)   Chen, J.; Serizawa, T.; Komiyama, M. *Angew. Chem. Int. Edit.* **2009**, *48*, 2917-2920.

(57)   Chen, J.; Serizawa, T.; Komiyama, M. *J. Pept. Sci.* **2011**, *17*, 163-168.

(58)   Ejima, H.; Kikuchi, H.; Matsuno, H.; Yajima, H.; Serizawa, T. *Chem. Mater.* **2010**, *22*, 6032-6034.

(59)   Ejima, H.; Matsuno, H.; Serizawa, T. *Langmuir* **2010**, *26*, 17278-17285.

(60)   Swaminathan, S.; Cui, Y. *Mater. Sci. Eng., C.* **2013**, *33*, 3082-3084.

(61)   Swaminathan, S.; Cui, Y. *RSC Adv.* **2012**, *2*, 12724-12727.

(62)   Caparon, M.; De Ciechi, P.; Devine, C.; Olins, P.; Lee, S. *Mol. Divers.* **1995**, *1*, 241-246.

(63)   Vodnik, M.; Zager, U.; Strukelj, B.; Lunder, M. *Molecules* **2011**, *16*, 790-817.

(64)   Rozinov, M. N.; Nolan, G. P. *Chem. Biol.* **1998**, *5*, 713-728.

(65)   Goldman, E. R.; Pazirandeh, M. P.; Charles, P. T.; Balighian, E. D.; Anderson, G. P. A*nal. Chim. Acta* **2002**, *457*, 13-19.

(66)   Jaworski, J. W.; Raorane, D.; Huh, J. H.; Majumdar, A.; Lee, S. W. *Langmuir* **2008**, *24*, 4938-4943.

(67)   Cui, Y.; Pattabiraman, A.; Lisko, B.; Collins, S. C.; McAlpine, M. C. *J. Am. Chem. Soc.* **2010**, *132*, 1204-1205.

(68)   Van Dorst, B.; Mehta, J.; Rouah-Martin, E.; De Coen, W.; Petrenko, V.; Blust, R.; Robbens, J. *Anal. Methods* **2011**, *3*, 1865-1871.

(69)   Cho, W.; Fowler, J. D.; Furst, E. M. *Langmuir* **2012**, *28*, 6013-6020.

(70)   Na, J. H.; Joo, M. S.; Lee, W. K.; Shim, H; Lim, S. H.; Jung, S. T.; Yu, Y. G. *Bull. Korean Chem. Soc.* **2013**, *34*, 460-464.

(71)   Sawada, T.; Okeya, Y.; Hashizume, M.; Serizawa, T. *Chem. Commun.* **2013**, *49*, 5088-5090.

(72)   Safe, S. *Crit. Rev. Toxicol.* **1990**, *21*, 51-88.

(73)   Fukusaki, E.; Ogawa, K.; Okazawa, A.; Kajiyama, S. I.; Kobayashi, A. *J. Mol. Catal. B. Enzym.* **2004**, *28*, 181-184.

(74)   Serizawa, T.; Iida, K.; Matsuno, H.; Kurita, K. *Chem. Lett.* **2007**, *36*, 988-989.

(75)   Qi, M.; O'Brien, J. P.; and Yang, J. J. *Biopolymers* **2008**, *90*, 28-36.

(76)   Khoushab, F.; Jaruseranee, N.; Tanthanuch, W.; Yamabhai, M. *Int. J. Biol. Macromol.* **2012**, *50*, 1267-1274.

(77)   Guo, J.; Catchmark, J. M.; Mohamed, M. N. A.; Benesi, A. J.; Tien, M.; Kao, T. H.; Watts, H. D.; Kubicki, J. D. *Biomacromolecules* **2013**, *14*, 1795-1805.

(78)   Gray, B. P.; Li, S.; Brown, K. C. *Bioconjugate Chem.* **2012**, *24*, 85-96.

(79)   Bastings, M. M. C.; Helms, B. A.; van Baal, I.; Hackeng, T. M.; Merkx, M.; Meijer, E. W. *J. Am. Chem. Soc.* **2011**, *133*, 6636-6641.

(80)   Yoon, T.; Cowan, J. A. *J. Am. Chem. Soc.* **2003**, *125*, 6078-6084.

(81)   Chen, X.; Shakesheff, K. M.; Davies, M. C.; Heller, J.; Roberts, C. J.; Tendler, S. J. B.; Williams, P. M. *J. Phys. Chem.* **1995**, *99*, 11537-11542.

(82)   Green, R. J.; Tasker, S.; Davies, J.; Davies, M. C.; Roberts, C. J.; Tendler, S. J. B. *Langmuir* **1997**, *13*, 6510-6515.

(83)   Green, R. J.; Corneillie, S.; Davies, J.; Davies, M. C.; Roberts, C. J.; Schacht, E.; Tendler, S. J. B.; Williams, P. M. *Langmuir* **2000**, *16*, 2744-2750.

(84)   Green, R. J.; Frazier, R. A.; Shakesheff, K. M.; Davies, M. C.; Roberts, C. J.; Tendler, S. J. B. *Biomaterial*s **2000**, *21*, 1823-1835.

(85)   Kretschmann, E.; Raether, H. *Z. Naturforsch A Phys. Sci.* **1968**, *23*, 2135.

(86)   Matsubara, K.; Kawata, S.; Minami, S. *Appl. Opt.* **1988**, *27*, 1160-1163.

(87)   Liedberg, B.; Nylander, C.; Lunström, I; *Sensor. Actuator.* **1983**, *4*, 299-304.

(88)   Fägerstam, L. G.; Frostell-Karlsson, Å.; Karlsson, R.; Persson, B.; Rönnberg, I; *J. Chromatogr. A* **1992**, *597*, 397-410.

(89)   Wiseman, T.; Williston, S.; Brandts, J. F.; Lin, L.-N. *Anal. Biochem.* **1989**, *179*, 131-137.

(90)   Freire, E.; Mayorga, O. L.; Straume, M. *Anal. Chem.* **1990**, *62*, 950A-959A.

(91)   Leavitt, S.; Freire, E. *Curr. Opin. Struct. Biol.* **2001**, *11*, 560-566.

(92)   Florin, E.; Moy, V.; Gaub, H. *Science* **1994**, *264*, 415-417.

(93)   Lee, G. U.; Kidwell, D. A.; Colton, R. J. *Langmuir* **1994**, *10*, 354-357.

(94)   Moy, V.; Florin, E.; Gaub, H. *Science* **1994**, *266*, 257-259.

(95)   Hinterdorfer, P.; Baumgartner, W.; Gruber, H. J.; Schilcher, K.; Schindler, H. *Proc. Natl. Acad. Sci. U.S.A.* **1996**, *93*, 3477-3481.

(96)   Hinterdorfer, P.; Dufrene, Y. F. *Nat. Methods.* **2006**, *3*, 347-355.

(97)   Lee, C.-K.; Wang, Y.-M.; Huang, L.-S.; Lin, S. *Micron* **2007**, *38*, 446-461.

(98)   Sauerbrey, G; *J. Physik* **1959**, *155*, 206-212.

(99)   Alder, J. F.; McCallum, J. J. *Analyst* **1983**, *108*, 1169-1189.

(100)   Bruckenstein, S.; Shay, M. *Electrochim. Acta* **1985**, *30*, 1295-1300.

(101)   Rodahl. M.; Höök, F.; Krozer, A.; Brzezinski, P.; Kasemo, B. *Rev. Sci. Instrum.* **1995**, *66*, 3924-3930.

(102)   Hengerer, A.; Decker, J.; Prohaska, E.; Hauck, S.; Kößlinger, C.; Wolf, H. *Biosens. Bioelectron.* **1999**, *14*, 139-144.

(103)   Hengerer, A.; Kösslinger, C.; Decker, J.; Hauck, S.; Queitsch, I.; Wolf, H.; Dübel, S. *Biotechniques* **1999**, *26*, 956-965.

(104)   Karpovich, D. S.; Blanchard, G. J. *Langmuir* **1994**, *10*, 3315-3322.

(105)   Mammen, M.; Choi, S.-K.; Whitesides, G. M. *Angew. Chem. Int. Edit.* **1998**, *37*, 2754-2794.

(106)   Kiessling, L. L.; Gestwicki, J. E.; Strong, L. E. *Angew. Chem. Int. Edit.* **2006**, *45*, 2348-2368.

(107)   Matthews, D. J.; Wells, J. A. *Science* **1993**, *260*, 1113-1117.

(108)   Koivunen, E.; Wang, B.; Ruoslahti, E. *Nat. Biotech.* **1995**, 13, 265-270.

(109)   Giebel, L. B.; Cass, R.; Milligan, D. L.; Young, D.; Arze, R.; Johnson, C. *Biochemistry* **1995**, *34*, 15430-15435.

(110)   Seker, U. O. S.; Wilson, B.; Dincer, S.; Kim, I. W.; Oren, E. E.; Evans, J. S.; Tamerler, C.; Sarikaya, M. *Langmuir* **2007**, *23*, 7895-7900.

(111)   Heinis, C.; Rutherford, T.; Freund, S.; Winter, G. *Nat. Chem. Biol.* **2009**, *5*, 502-507.

(112)   Goldman, E. R.; Hayhurst, A.; Lingerfelt, B. M.; Iverson, B. L.; Georgiou, G.; Anderson, G. P. *J. Environ. Monit.* **2003**, *5*, 380-383.

(113)   Nagatomo, K.; Kawaguchi, T.; Miura, N.; Toko, K.; Matsumoto, K. *Talanta* **2009**, *79*, 1142-1148.

(114)   Na, J. H.; Joo, M. S.; Lee, W. K.; Shim, H.; Lim, S. H.; Jung, S. T.; Yu, Y. G. *B. Korean Chem. Soc.* **2013**, *34*, 460-464.

(115)   Sakiyama, T.; Ueno, S.; Imamura, K.; Nakanishi, K. *J. Mol. Catal. B: Enzym.* **2004**, *28*, 207-214.

(116)   Kumada, Y.; Tokunaga, Y.; Imanaka, H.; Imamura, K.; Sakiyama, T.; Katoh, S.; Nakanishi, K. *Biotechnol. Progr*. **2006**, *22*, 401-405.

(117)   Ellington, A. D.; Szostak, J. W. *Nature* **1990**, *346*, 818-822.

(118)   Tuerk, C.; Gold, L. *Science* **1990**, *249*, 505-510.

(119)   Stoltenburg, R.; Reinemann, C.; Strehlitz, B. *Biomol. Eng.* **2007**, *24*, 381-403.

(120)   Famulok, M; *Curr. Opin. Struct. Biol.* **1999**, *9*, 324-329.

(121)   Arnaud, J.; Audfray, A.; Imberty, A. *Chem. Soc. Rev.* **2013**, *42*, 4798-4813.

(122)   Masica, D. L.; Gray, J. J. *Biophys. J.* **2009**, *96*, 3082-3091.

(123)   Mirau, P. A.; Naik, R. R., Gehring, P. *J. Am. Chem. Soc.* **2011**, *133*, 18243-18248.

(124)   Shaw, W. J. *Solid State Nuc. Mag. Reson.* **2014**.

(125)   Dias-Neto, E.; Nunes, D. N.; Giordano, R. J.; Sun, J., Botz, G. H.; Yang, K.; Setubal, J. C.; Pasqualini, R.; Arap, W. *PLoS ONE* **2009**, *4*, e8338.

(126)   Matochko, W. L.; Chu, K.; Jin, B.; Lee, S. W.; Whitesides, G. M.; Derda, R. *Methods* **2012**, *58*, 47-55.

(127)   Liu, G. W.; Livesay, B. R.; Kacherovsky, N. A.; Cieslewicz, M.; Lutz, E.; Waalkes, A.; Jensen, M. C.; Salipante, S. J.; Pun, S. H. sequencing. *Bioconjugate Chem.* **2015**, *26*, 1811-1817.

2. Synthesis of Cyclic Peptide Disulfide-PHPMA Conjugates via Sequential Active Ester Aminolysis and CuAAC Coupling

Submitted as the following article:

"Synthesis of Cyclic Peptide Disulfide-PHPMA Conjugates via Sequential Active Ester Aminolysis and CuAAC Coupling", Kemal Arda Günay, Harm-Anton Klok, *Polymer Chemistry*, Accepted.

2.1. Introduction

There are a large number of cyclic peptides that are formed by the formation of an intramolecular disulfide bond. Examples of these cyclic peptide disulfides (CXC) include natural peptides such as i.e. somatostatin, conotoxins, apamin and defensins[1-4] as well as a large number of cyclic sequences that have been identified via phage display.[5-7] These CXC's are an important class of biomolecules that function as toxins,[2,8] antimicrobial agents[9,10] and can also be used to engineer materials interfaces.[11,12]

It is well known that the covalent conjugation of peptides to synthetic polymers allows circumventing many limitations associated with the use of free peptides. These so called "peptide-polymer conjugates" often have enhanced solubility and stability, reduced toxicity/immunogenicity as well as longer circulation times compared to the free peptides.[13,14] The advent and refinement of various controlled/"living" radical polymerization techniques combined with the availability of a rapidly increasing toolbox of highly efficient conjugation strategies have greatly facilitated the preparation of peptide-polymer conjugates.[15-17]

There have been a number of literature reports that describe polymer conjugates, which incorporate cyclic peptides that do not contain disulfide bonds.[18-22] The conjugation of a CXC to a polymer, however, may present some challenges. For instance, the use of many of the highly efficient thiol-based conjugation strategies, such as thiol-maleimide Michael addition, thiol-ene/thiol-yne addition and native chemical ligation reactions would either

require the incorporation of a third cysteine or a thiol reactive group into the peptide sequence, which can result in side reactions due to the dynamic exchange between the free thiols and the disulfides.[23,24] Alternatively, the N-terminal amine of the CXC or the side chain amine group present in a lysine residue may be used to prepare CXC-polymer conjugates. Ma *et al.* for instance, successfully used this approach to conjugate a cyclic peptide that binds to *Clostridium Botulinum* neurotoxin serotype A (Ac-A**C**VPVSQLGVY**C**-aminohexanoic acid-K) to a poly(ethylene-*co*-maleic anhydride) copolymer.[25] If multiple amine groups are present in the peptide sequence, however, conjugation to a polymer containing the complementary reactive group such as an active ester, carboxylic acid, aldehyde, ketone, epoxide, isocyanate and others would potentially yield cross-linked and insoluble products, and may lead to a loss of peptide activity. These difficulties may be overcome by the use of bioorthogonal reactions that proceed in mild conditions without the requirement of protective groups.

Following the initial reports by Sharpless and Meldal,[26,27] the copper catalyzed azide-alkyne cycloaddition (CuAAC) reaction has found widespread use for the preparation of bioconjugates owing to its orthogonality with many of the side chain amino acid functional groups.[28,29] The use of the traditional CuAAC protocols, however, has some limitations because the reactive oxygen species formed during the reaction was shown to cause depolymerization of polysaccharides[30] as well as oxidize the imidazole groups of the histidine present in peptides/proteins.[31,32] To overcome these problems, the Finn group developed a CuAAC strategy that employs μM concentrations of CuSO$_4$, few fold excess of a water soluble ligand, tris(3-hydroxypropyltriazolylmethyl)amine (THPTA) with respect to copper, mM concentrations of ascorbate (Na$_{asc}$) as well as aminoguanidine at room temperature in aqueous media.[32] In this protocol, the use of 5 equivalents of THPTA with respect to CuSO$_4$ in aqueous media was found to minimize the H$_2$O$_2$ concentration in the reaction mixture without significantly hindering the CuAAC reaction rate. This decreased concentration of H$_2$O$_2$ was demonstrated to almost completely prevent the oxidation of histidine imidazole groups. Furthermore, the introduction of aminoguanidine was shown to mitigate the reactions between ascorbate oxidation byproducts and the proteins. Therefore, this protocol allows CuAAC bioconjugation reactions that are not accompanied by oxidative side reactions or crosslinked products and has been also successfully used to label live cells.[33]
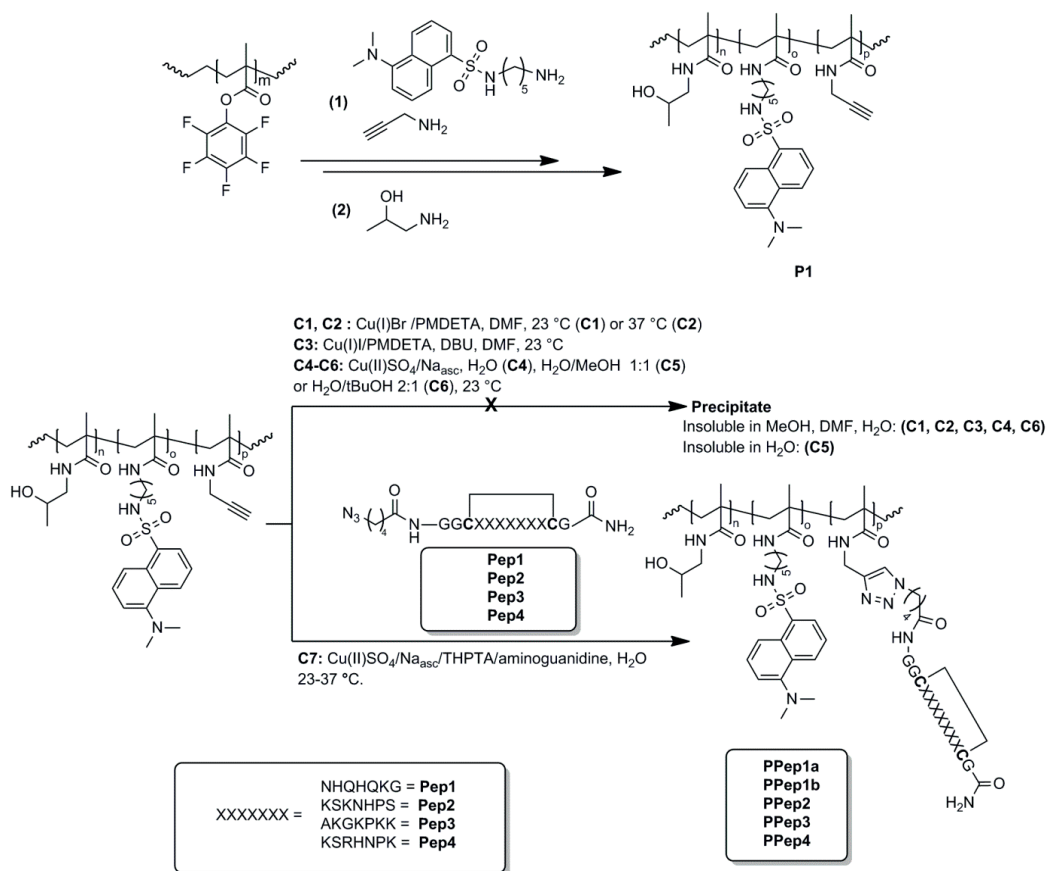
Scheme 1. Synthesis of cyclic peptide disulfide (CXC)-PHPMA conjugates via sequential active ester aminolysis and CuAAC coupling.

This Chapter presents a novel strategy for the preparation of CXC-polymer conjugates that does not require the use of peptide protecting groups. The approach presented here is outlined in **Scheme 1** and involves a three-step post-polymerization modification of poly(pentafluorophenyl methacrylate) (PPFMA) to afford CXC-poly(*N*-(2-hydroxypropyl) methacrylamide) (PHPMA) conjugates. PPFMA is a very versatile amine reactive polymer scaffold for post-polymerization modification reactions[34-37] and PHPMA is widely used as a water-soluble and biocompatible carrier for the conjugation of both chemotherapeutics as well as biomolecular species.[38-42] The introduction of CXC starts with the post-polymerization modification of the PPFMA precursor with a small amount of propargylamine. By incorporating a second functional amine in this step such as dansyl cadaverine, dual functional conjugates can be prepared. In a subsequent step, the remaining unreacted pentafluorophenyl groups are quantitatively converted with 1-amino-2-propanol, which results in a water-soluble PHPMA copolymer. In a final step,

the CXC is conjugated to the polymer precursor via CuAAC coupling. To this end, a number of CuAAC procedures were screened using model CXC's, which incorporated side chain functional groups that are known to either interfere with traditional active ester based conjugation strategies or that have been reported to be involved in side reactions during CuAAC reactions. These experiments allowed to identify CuAAC conditions that were devoid of side reactions and which also allows access to water-soluble well-defined CXC-polymer conjugates. These conjugates will be used as model polymeric profragrances that can selectively target human hair under shampoo conditions in Chapter 4.

2.2.   Experimental Section

Materials. All chemicals were used as received unless described otherwise. Pentafluorophenol ($\geq$ 99%) was purchased from MatrixScientific. Methacryoyl chloride (97%) was purchased from Alfa-Aesar. 2,6-Lutidine ($\geq$ 99%), 1-amino-2-propanol (95%), dansyl cadaverine (> 97%),   N,N,N′,N″,N″-pentamethyldiethylenetriamine (PMDETA) (99%), N,N-diisopropylethylamine (DIEA) (98.0%), N-methyl-2-pyrrolidone (NMP) ($\geq$ 98.0%), trifluoroacetic acid (TFA) ($\geq$ 99.0%), 4,4-azobis(4-cyanopentanoic acid) (97%), (4-cyanopentanoic acid)-4-dithiobenzoate (CTA) (95%), triethylamine (TEA), tris(3-hydroxypropyltriazolylmethyl)amine   (THPTA)   (95%),   propargylamine   (97%), triisopropylsilane (TIS) (99%), ethylenediaminetetraaceticacid (EDTA) (98%), 1,8-diazabicyclo[5.4.0]undec-7-ene (DBU) (98%), aminoguanidine hydrochloride (99%), $CuSO_4 \cdot 5H_2O$ (97%), sodium ascorbate (Na_{Asc}) (98%), Cu(I)Br (99.999%) and Cu(I)I (99.5%) were obtained from Sigma-Aldrich. TEA was freshly distilled prior to use. 2,2′-Azobis(2-methylpropionitrile) (98%) (AIBN) and piperidine (99%) were purchased from Acros. *O*-Benzotriazole-N,N,N',N'-tetramethyl-uronium-hexafluoro-phosphate (HBTU) was obtained from Fluorochem. All Fmoc-amino acids except S-acetaminomethyl protected cysteine (Fmoc-Cys(Acm)) and Oxyma-Pure were received from Iris Biotech. Fmoc-Cys(Acm) (99%) and 5-azidopentanoic acid (5-AzPOH) (97%) were obtained from Bachem. Thallium trifluoroacetate ($Tl(CF_3COO)_3$) (97%) was obtained from TCI. Acetonitrile (AcN) (HPLC grade) was obtained from VWR international. Pentafluorophenyl methacrylate (PFMA) was prepared according to the protocol described by Eberhardt *et al.*[43] The poly(pentafluorophenyl methacrylate) (PPFMA) polymer used in this study was prepared via reversible addition-fragmentation chain

transfer (RAFT) polymerization as described by Gibson *et al.*[35] The ^{1}H-NMR spectrum of the as synthesized PPFMA is provided in **Figure S1**. Subsequent removal of dithiobenzoate end groups of PPFMA was achieved using the method reported by Perrier and coworkers.[44] The number average molecular weight of the PPFMA polymer was determined by ^{1}H-NMR as 42000 g/mol ($M_{n,NMR}$) and size exclusion chromatography revealed a polydispersity (M_w/M_n) of 1.20.

Methods. Peptides were synthesized via Fmoc solid phase peptide synthesis using a CEM Liberty automated microwave synthesizer. HPLC was performed using a Shimadzu Prominence system containing LC-20AP pumps, a FRC-10A fraction collector, a CTD-20AC column oven and an SPD-M20A diode array detector coupled to a LCMS-2020 liquid chromatography mass spectrometer. The peptides were characterized using an analytical Grace Vydac 218TP54 C18 column and purified using a Grace Vydac 218TP15 preparative column. ^{1}H-NMR spectra were recorded on a Bruker (ARX-400) 400 MHz spectrometer at room temperature using a relaxation time (t_1) of 10 seconds. Chemical shifts are reported relative to the residual proton signal of the solvent. Size exclusion chromatography (SEC) was performed on a Waters Alliance GPCV 2000 system equipped with refractive index (RI) detector. Separation was carried out at 60 °C with TSK-Gel Alpha 3000 + 4000 columns using DMF + 1gL^{-1} LiBr as eluent and a flow rate of 0.6 mL min^{-1}. Molecular weights were determined relative to narrow polydispersity poly(methyl methacrylate) (PMMA) standards or for PHPMA, where indicated, using the RI detector. Results were calculated with the Empower Pro multidetection GPC software (V. 5.00).

Procedures.

Synthesis of N-terminal azide functionalized cyclic peptide disulfides (CXC). Solid phase peptide synthesis (SPPS) was carried out on a 0.25 mmol scale using a Rink-amide resin with a loading capacity of 0.71 mmol/g. Deprotection of Fmoc groups, coupling with the amino acid and washing was performed before and after the incorporation of each amino acid. A two-step Fmoc deprotection was performed at 75 °C using 40 W microwave power for 30 seconds and 54 W microwave power for 6 minutes, respectively, with a 5 mL DMF/piperidine = 4 : 1 solution containing 0.1 M Oxyma pure. Coupling of the amino acids was carried out with the subsequent addition of 0.2 M of amino acids in 5

mL DMF, 0.5 M of HBTU and Oxyma-Pure in 2 mL DMF (activator) and 2 M DIEA in 1 mL NMP (activator base) for 6 minutes using a microwave power of 24 W (T = 60 °C). Washing of the resin before and after the addition of each amino acid was performed using 10 mL DMF. Following SPPS, the resin was transferred to a reaction vessel, washed with 50 mL DMF, DCM, MeOH and DCM and dried under a flow of N_2.

The subsequent cyclization and N-terminal azide incorporation was performed similar to the protocol described by Feldborg and coworkers.[45] Briefly, cyclization was carried out by first swelling the resin (352 mg, 0.25 mmol) in 2.5 mL anhydrous DMF under N_2. In parallel, 272 mg (2 equiv. with respect to the resin bound peptide) of $Tl(CF_3COO)_3$ was dissolved in 2.5 mL anhydrous DMF under a flow of N_2 and this solution was transferred to the reaction vessel with a cannula. The reaction mixture was left to react for 2 hours at room temperature with gentle agitation. After that, the resin was washed extensively with DMF to remove residual thallium ions and dried under a flow of N_2.

Finally, the N-terminal amine group of the cyclic peptides was modified with 5-azidopentanoic acid (5-AzPOH). To this end, 379 mg HBTU (1.00 mmol, 4 equiv. with respect to the resin bound peptide) was dissolved in 5 mL DMF in a round bottom flask under N_2. After that, 348 μL DIEA (2.00 mmol, 8 equiv. with respect to the resin load) and 143 mg 5-AzPOH (1.00 mmol, 4 equiv. with respect to the resin bound peptide) was added under a flow of N_2. In parallel, the resin was swollen in 5 mL anhydrous DMF and the mixture containing the 5-AzPOH was transferred to the reaction vessel via a cannula under a flow of N_2. The reaction was left to react for 2 hours at room temperature under gentle agitation. After that, the resin was washed 3 times with 50 mL DMF and once more with 50 mL DCM and dried. Cleavage of the peptide from the resin was achieved by treating the resin with a 5 mL solution of TFA/TIS/H_2O = 95:2.5:2.5 for 2 hours at room temperature under gentle agitation. The cleaved peptide was precipitated in Et_2O 4 times, dissolved in 20 mL H_2O and lyophilized. Following lyophilization, the peptides were purified via preparative HPLC using a gradient from 95% H_2O / 5% AcN (0.05% TFA) to 65% H_2O / 35% AcN (0.05% TFA) in 30 minutes and the pure fractions were collected and lyophilized. White powders were obtained. The yields were between 18-25% and the peptide purities were greater than 95%. Analytical HPLC elution profiles as well as the corresponding ESI-MS spectra of the pure peptides are provided in **Figure S2** and **S3.**

Synthesis of alkyne functionalized PHPMA (P1). A typical procedure is as follows: 300 mg PPFMA (1.188 mmol PFMA groups) with $M_{n,NMR}$ = 42000 g/mol and $M_w/M_{n,SEC}$ = 1.20 was dissolved in a round bottom flask at room temperature under N_2 in a mixture of 12.5 mL anhydrous DMF and 1.5 mL freshly distilled TEA. Subsequently, 4.00 mg (0.0188 mmol, 1 mol% with respect to PFMA groups) dansyl cadaverine and 3.28 mg (0.0593 mmol, 5 mol% with respect to PFMA groups) propargylamine was dissolved in 1 mL anhydrous DMF under N_2. This solution was transferred to the PPFMA solution and the reaction allowed to proceed at room temperature for 24 hours under stirring and N_2. After that, 336.8 μL (4.752 mmol, 4 equiv. with respect to the starting PFMA groups) of 1-amino-2-propanol, 9 mL anhydrous DMF and 3 mL of TEA were added to the mixture under a flow of N_2 and the reaction was allowed to continue at room temperature under stirring and N_2. After 4 days, the polymer was precipitated in Et_2O and redissolved in DMF for 3 times and subsequently dialyzed extensively against MilliQ water using a Spectra/Por dialysis membrane having a MWCO of 3500 g/mol. Finally, the conjugates were lyophilized. A white, water soluble solid is obtained. Yield = 63%. $M_{w,SEC}$ = 44000 g/mol, $M_{n,SEC}$ = 33000 g/mol, M_w/M_n = 1.34. The ^{1}H-NMR spectrum and SEC chromatogram of P1 are provided in **Figure S4** and **Figure 2**, respectively.

CuAAC cyclic peptide disulfide coupling reactions.

C1, C2. To a Schlenk tube, 40 mg **P1** (12.6 μmol alkyne groups), 17 mg **Pep1** (12.6 μmol) and 9.30 μL (45.0 μmol) PMDETA in 2 mL anhydrous DMF was added and the reaction mixture degassed by performing 3 freeze-thaw cycles. Next, 6.30 mg (45.0 μmol) Cu(I)Br was added under a flow of N_2 and the reaction was carried out either at 23°C (**C1**) or at 37 °C (**C2**) for 16 hours with stirring. The procedure yielded in both conditions a precipitate that could not be dissolved in H_2O, MeOH and DMF.

C3. To a Schlenk tube, 40 mg **P1** (12.6 μmol alkyne groups), 17 mg **Pep1** (12.6 μmol), 5.2 μL PMDETA (25.2 μmol) and 1.9 μL DBU (12.6 μmol) in 2 mL anhydrous DMF was added and the reaction mixture was degassed by performing 3 freeze-pump-thaw cycles. Next, 2.4 mg Cu(I)I (12.6 μmol) was added under a flow of N_2 and the reaction was carried out at 23 °C for 16 hours with stirring. At the end of the reaction, a precipitate was obtained which could not be dissolved in in H_2O, MeOH and DMF.

C4-C6. To a Schlenk tube, 20 mg **P1** (6.3 μmol alkyne groups), 8.5 mg **Pep1** (6.3 μmol) and 6.2 mg sodium ascorbate (31.5 μmol) either in 0.8 mL H_2O (**C4**), H_2O/MeOH

= 1:1 (**C5**) or H_2O/tBuOH = 2:1 (**C6**) were added and the reaction mixture was degassed by 3 freeze-pump-thaw cycles. Next, 0.2 mL of a solution containing 5.0 mg $CuSO_4 \cdot 5H_2O$ (31.5 μmol) was added under a flow of N_2 and the reaction was carried out at 23 °C for 16 hours with stirring. At the end of the reaction, precipitates were observed in C4 and C6, whereas the reaction mixture **C5** was homogenous. The resulting polymer was named as **PC5**. Following the reaction, **PC5** was passed through a basic alumina column using an eluent of H_2O/MeOH = 1:1 and attempts were made to dialyze the material using a Spectra/Por membrane having a MWCO of 8000 g/mol against MilliQ water. Precipitates were started to be observed after 15 minutes of dialysis and their quantity increased as a function of dialysis time. After one day, the dialysate containing the precipitates was recovered via resuspension and lyophilized. The lyophilized conjugate was insoluble in water, but soluble in MeOD and DMF so that ^{1}H-NMR (**Figure 1** and **Figure S5**) and SEC analysis (**Figure 2**) could be performed.

C7. The protocol was adapted from the method reported by Hong and coworkers.[32] To a round bottom flask, 20 mg **P1** (6.3 μmol alkyne groups) and 6.3 μmol of the peptide in H_2O were added under N_2. Next, 0.4 mL of an aqueous solution containing 6.5 mg THPTA (15.0 μmol) and 0.75 mg $CuSO_4 \cdot 5H_2O$ (2.5 μmol) was added to reaction mixture under N_2. Then, 0.1 mL of an aqueous solution containing 3.3 mg aminoguanidine hydrochloride (30.0 μmol) and 0.5 mL of a solution containing 5.9 mg sodium ascorbate (30.0 μmol) were subsequently added under N_2. The reaction proceeded for 16 hours under stirring either at 23 °C or 37 °C. The reaction mixture was directly transferred into a Spectra/Por dialysis membrane having a MWCO of 8000 gr/mol and subsequently dialyzed against solutions of (i) 0.1 M PBS buffer containing 0.05 M EDTA, pH 7.4, for 2 days (ii) 0.1 M PBS buffer, pH 7.4 for 1 day and (iii) MilliQ water for 2 more days and finally removed from the membrane and lyophilized. White, water soluble peptide-polymer conjugates were obtained. Yields: 82-90%. Complete ^{1}H-NMR spectra and the corresponding peak assignment of the conjugates (**PPep1a**, **PPep1b**, **PPep2, PPep3** and **PPep4**, respectively) are provided in **Figure S6-S10.** SEC chromatogram of **PPep1b** is provided in **Figure 2**.

2.3. Results and Discussion

The preparation of the cyclic peptide disulfide (CXC)-PHPMA conjugates as outlined in Scheme 1 involves three steps, viz. (i) the synthesis of the cyclic peptides, (ii) the preparation of the side chain reactive polymer precursor and (iii) the post-polymerization CuAAC of the CXC's. The following sections will first briefly describe the preparation of the CXC's and the reactive polymer precursor and then in more depth discuss the various conjugation approaches that have been explored to couple the CXC to the polymer backbone.
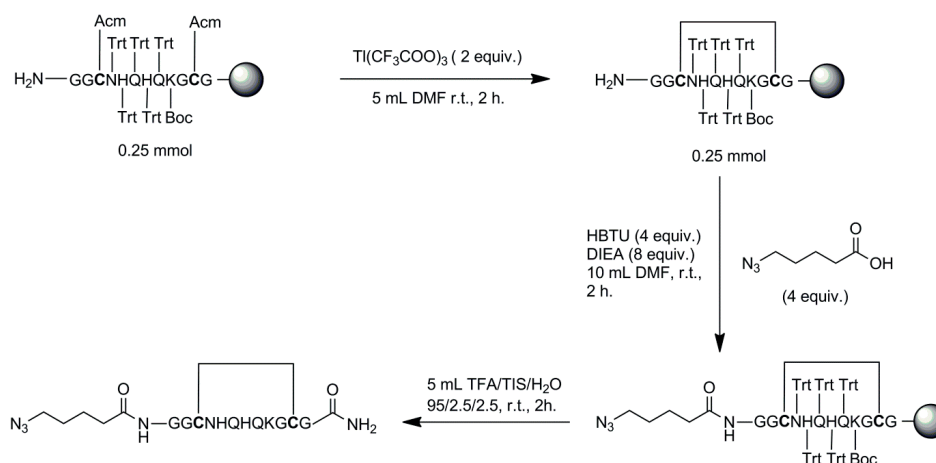
Scheme 2. Synthesis of N-terminal azide functionalized cyclic peptide disulfides (CXC). Acm, Trt and Boc denote acetamidomethyl, trityl and *tert*-butyloxycarbonyl protecting groups, respectively.

2.3.1. Synthesis of N-terminal azide functionalized cyclic peptide disulfides.

As an example, the synthesis of the N-terminal azide functionalized **Pep1** will be briefly discussed. For this CXC, the different intermediates in the synthetic process were analyzed by ESI-MS. Cyclic peptides **Pep2-Pep4** were subsequently prepared using the same procedures that were also used for the synthesis of **Pep1**. After assembly of the linear precursor peptide by Fmoc SPPS, the resin bound peptides were treated with 2 equiv. of Tl(CF$_3$COO)$_3$ in anhydrous DMF. This leads to the removal of the acetamidomethyl (Acm) protecting groups of cysteine and the subsequent formation of an intramolecular disulfide bond.[46] Although the ESI mass spectrum of the reaction mixture

after 2 hours (and resin cleavage) shows incomplete removal of Acm protecting groups, the most abundant peak was associated with the intramolecularly cyclized peptide (**Figure S2A**). Next, the resin bound peptides were treated with 4 equiv. of 5-AzPOH and HBTU as well as with 8 equiv. of DIEA for 2 hours in anhydrous DMF in order to introduce N_3 groups and subsequently cleaved from the resin to yield the desired cyclic, N-terminal azide functionalized peptides. ESI-MS analysis confirmed quantitative functionalization of the N-terminal amine group with 5-AzPOH but also revealed partial reduction of some of the azide groups into amines (**Figure S2B**). The latter has been previously reported as a side reaction that can accompany resin cleavage of peptide azides in the presence of free thiols.[47] The amine end-functionalized cyclic peptides, the linear peptide containing residual Acm protective groups as well as other impurities could be removed by HPLC purification of the crude product. Typical yields of the isolated peptides were between 18-25% and their purities were at least 95%. Analytical HPLC elution profiles and ESI-MS spectra of **Pep1-Pep4** are provided in **Figure S2** and **S3**, respectively.

2.3.2. Synthesis of alkyne functionalized PHPMA (P1).

The alkyne side chain functional PHPMA copolymer **P1** that was used for the conjugation of the azide modified CXC's was obtained in a two-step post-polymerization modification protocol as outlined in **Scheme 1**. First, PPFMA ($DP_{n,NMR}$ = 166, $M_{n,NMR}$ = 42000 g/mol) was prepared via RAFT polymerization following a previously reported protocol (**Figure S1**).[35] Since reaction between the dithiobenzoate end-group of the PPFMA polymer and amines yields free thiols,[48] which could undergo thiol-disulfide exchange reactions with the CXC's, these end-groups were removed according to the protocol described by Perrier *et al.*[44]

Next, a PHPMA conjugate bearing side chain alkyne groups (**P1**) was synthesized via a two-step, room temperature post-polymerization modification process. First, a solution of the PPFMA polymer in DMF/TEA 9:1 v/v was reacted at room temperature with 0.01 equiv. propargylamine and 0.05 equiv. dansyl cadaverine with respect to pentafluorophenyl groups. The fluorescent dansyl group will be used to determine the extent of deposition of the synthesized peptide-PHPMA conjugates onto human hair via fluorescence intensity measurements in Chapter 4. Furthermore, its presence also facilitates ^{1}H-NMR analysis owing to its three distinctive aromatic 1H signals (*vide*

infra). Subsequently, the remaining PPFMA groups were converted into HPMA units by the addition of 4 equivalents of 1-amino-2-propanol in DMF/TEA 5:1 at room temperature, which afforded a water soluble PHPMA copolymer (**P1**). Attempts to incorporate 0.07 equiv. of alkyne and 0.07 equiv. of dansyl cadaverine resulted in a PHPMA copolymer that was only partially soluble in water (data not shown). As a consequence, the relative amounts of dansyl cadaverine and propargylamine to pentafluorophenyl groups in the first post-polymerization modification step were kept at 1 and 5 mol%. ^{1}H-NMR spectrum of **P1** in methanol-d_4, which is shown in **Figure 1** and **Figure S4**, revealed the incorporation of dansyl groups owing to its three aromatic signals at 8.19, 8.37 and 8.56 ppm. Second, the conversion of the pentafluorophenyl ester groups into HPMA units is evidenced from the characteristic signal associated with CH_3-**CH**(OH)-CH$_2$- hydrogen of HPMA at 3.87 ppm. On the other hand, the signal of the -C≡**CH** group of propargylamine was overlapping both with the methylene proton signals of the polymer backbone (–**CH$_2$**-C(CH$_3$)-) and the (-**CH$_2$**) signal of the dansyl group linker, and therefore could not be detected directly. The composition of **P1** was determined from the ^{1}H-NMR spectrum assuming (i) quantitative conversion of dansyl groups and (ii) quantitative conversion of PFMA units, which have not reacted with propargylamine/dansyl cadaverine in the first post-polymerization modification step with 1-amino-2-propanol (i.e. the absence of pentafluorophenyl group hydrolysis during post-polymerization modification). This calculation revealed an alkyne content of 4.8 mol% for **P1**. SEC analysis indicated a monomodal distribution with a M_n of 33000 g/mol and a PDI of 1.34, (**Figure 2**) indicating the absence of any detectable side reactions that may lead to crosslinking during post-polymerization modification.

2.3.3. CuAAC conjugation experiments.

For the preparation of the cyclic peptide disulfide-PHPMA conjugates, a variety of CuAAC reaction conditions were screened (**C1** - **C7** in **Scheme 1**). First, CuAAC modification of **P1** with **Pep1** (5-AzPOH-GG**C**NHQHQKG**C**G) was attempted in the presence of either Cu(I)Br/PMDETA (**C1**, **C2**) or Cu(I)/DBU/PMDETA (**C3**) in DMF. Among these three protocols, particularly the Cu(I)Br/PDMETA catalyst system in DMF has been frequently used for the CuAAC post-polymerization modification of polymers.[49-51] All of these 3 reaction conditions, however, resulted in the formation of precipitates, which could not be redissolved in H$_2$O, MeOH or DMF, and therefore the

reaction products could not be analyzed. Next, the coupling of **Pep1** to **P1** was attempted using a catalyst system of $CuSO_4/Na_{asc}$ either in H_2O (**C4**), $H_2O/MeOH = 1 : 1$ (**C5**) or $H_2O/tBuOH = 2 : 1$ (**C6**), which has been explored before for the preparation of peptide-polymer conjugates.[52-54] After 16 hours, only **C5** resulted in a homogenous reaction mixture. Dialysis of the resulting polymer (**PC5**) against H_2O, however, led to the formation of precipitates, which were not water soluble, but could be dissolved in MeOH and DMF. The ^{1}H-NMR spectrum of this polymer (**Figure 1** and **Fig S5**) reveals small signals at 6.98 ppm and 7.85 ppm, which could be attributed to the imidazole groups of the histidine residue in the cyclic peptide and the triazole ring that forms upon CuAAC coupling, respectively. The signals due to the CH_2 group that is neighboring the triazole ring, which should appear around 4.40-4.51 ppm (*vide supra*) as well as another signal due to the histidine imidazole group that would be expected around 8.55 ppm, however, were not clearly visible in the ^{1}H-NMR spectrum of **PC5**. Assuming that **PC5** contains 1 mol% dansyl residues and comparing the ratios of the integral at 6.98 ppm to the ones between 8.19 to 8.55 ppm, which were associated with the dansyl groups, indicates that **PC5** contains less than 0.2 mol% **Pep1**. Since the alkyne content of the **P1** was calculated as 4.8 mol%, the conversion of the alkyne groups was found to be 4% in this CuAAC post-polymerization modification protocol. SEC analysis of **PC5** (**Figure 2**) revealed a multimodal distribution, which could indicate the presence of side reactions leading to partial cross-linking and explains the limited water solubility of this material. The nature of these side reactions, however, could not be verified via ^{1}H-NMR analysis. As a conclusion, the CuAAC protocols **C1** - **C6** were found to be not suitable for the preparation of well-defined cyclic peptide disulfide-polymer conjugates.

Following the unsuccessful attempts to prepare well-defined cyclic peptide disulfide-PHPMA conjugates using protocols **C1** - **C6**, the reaction conditions developed by Finn and coworkers were explored.[32] In a first example, the CuAAC reaction between **P1**, which contains ~ 5.0 mol% of alkyne groups, and **Pep1** was performed at room temperature in H_2O using alkyne/azide/Cu(II)SO_4/THPTA/Na_{asc}/aminoguanidine 2.5 : 2.5 : 1 : 6 : 15 : 15 for a period of 16 hours. This protocol yielded a water soluble conjugate (**PPep1a**, **Table 1**). The ^{1}H-NMR spectrum of the conjugate (**Fig S6**) revealed a signal associated with the triazole group at 7.91 ppm, 2H peaks of two –CH$_2$- groups flanking the triazole at 4.40 and 4.51 ppm as well as 2 1H peaks of the imidazole group of histidine at 6.97-7.01 and 8.54 ppm, reflecting the coupling of the azide modified peptide to the alkyne functional polymer. Assuming that a dansyl content of 1% and by

comparing the signals at 6.97-7.01 ppm with those at 8.20-8.36 ppm revealed 0.3 mol% of **Pep1** incorporation to **P1**, which indicates 7 % conversion of alkyne groups.
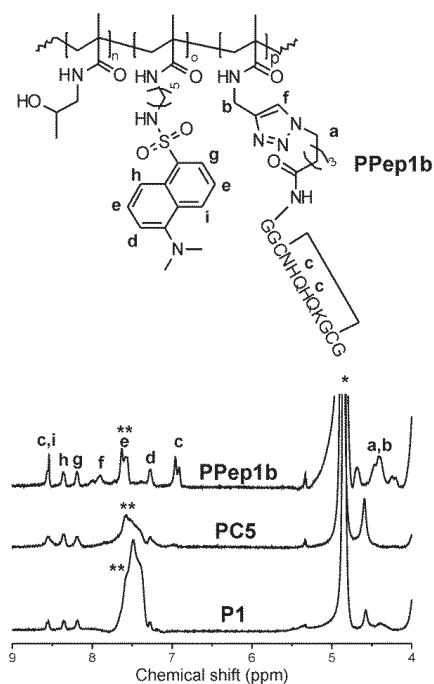

Figure 1. ^{1}H-NMR spectra of conjugates **P1**, **PC5** and **PPep1b** between 4 to 9 ppm in methanol-d_4. **P1** is the alkyne and dansyl functionalized PHPMA intermediate, **PC5** is the conjugate obtained via the CuAAC reaction in the presence of Cu(II)SO$_4$ and sodium ascorbate in H$_2$O/MeOH 1:1 (**C5**) and **PPep1b** is the CXC-polymer conjugate prepared using Cu(II)SO$_4$, THPTA, Na$_{asc}$ and aminoguanidine in H$_2$O at 37 °C (**C7**). * = Methanol-d_4 solvent peak. ** = 1H signals associated with the hydrogen of the amide groups.
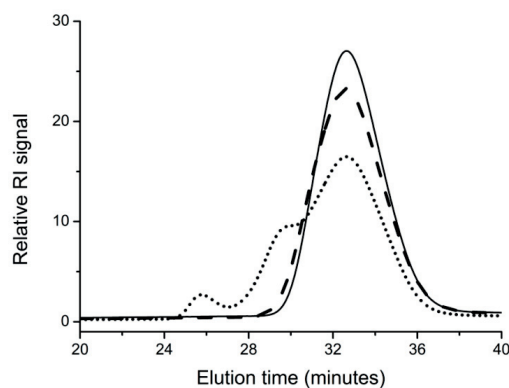
Figure 2. SEC chromatograms of **P1** (—), **PC5** (···) and **PPep1b** (– –).

To increase the **Pep1** content in the conjugate, another experiment was performed using the exact same CuAAC protocol but at 37 °C instead of at room temperature. The **Pep1** content of the resulting polymer conjugate (**PPep1b**) was increased to 1.6 mol% as evidenced by ^{1}H-NMR (**Figure 1** and **Fig S7**) indicating 34 % conversion of the alkyne groups. The extent of peptide incorporation was calculated from the ratio of the ^{1}H-NMR signal of the 1H of the triazole group at 7.91 ppm and the average of 2 aromatic 1H dansyl group signals at 8.20 and 8.36 ppm. SEC analysis of **PPep1b** revealed a monomodal distribution that was slightly shifted to higher molecular weight compared to **P1**, with a M_n of 33900 g/mol and a M_w/M_n of 1.42 (**Figure 2**). In summary, the results of the ^{1}H-NMR and SEC analysis demonstrate the feasibility of CuAAC protocol **C7** to generate cyclic peptide disulfide-PHPMA conjugates.

Table 1. Overview of the prepared cyclic peptide disulfide (CXC)-PHPMA conjugates. The Table indicates for each of the conjugates (**PPep1a** – **PPep4**), the peptide incorporation as well as the alkyne conversion following the reaction with **P1**, which contains 1 and 5 mol% of dansyl and alkyne groups, respectively. Results of SEC analysis of the conjugates in DMF using PMMA standards, if available, are also reported. * = The discrepancy between the theoretical molecular weight of PPFMA ($M_{n\ NMR}$ = 42000 g/mol) and the values obtained from SEC analysis in DMF using PMMA standards has already been reported by Gibson *et al.*[35]

Polymer name	Peptide sequence	Feed w.r.t. monomer units (mol%)	Incorporation w.r.t. monomer units (mol%)	Alkyne conversion	M_w (g/mol)	M_n (g/mol)	PDI
PPFMA	-	-	-		18000*	15000*	1.20*
P1	-	-	-		44100	33000	1.34
PC5	**C**NHQHQKG**C**	5.0	< 0.2	< 4%	N.A.	N.A.	N.A.
PPep1a	**C**NHQHQKG**C**	5.0	0.3	7%	N.A.	N.A.	N.A.
PPep1b	**C**NHQHQKG**C**	5.0	1.6	34%	48100	33900	1.42
PPep2	**C**KSKNHPS**C**	5.0	1.6	34%	N.A.	N.A.	N.A.
PPep3	**C**AKGKPKK**C**	5.0	2.2	46%	N.A.	N.A.	N.A.
PPep4	**C**KSRHNPK**C**	5.0	1.4	29%	N.A.	N.A.	N.A.

To further explore the versatility of the CuAAC protocol **C7**, the PHPMA intermediate **P1** was reacted at 37 °C with three other cyclic peptide disulfides (**Pep2** - **Pep4**) that also contain unprotected lysine and/or histidine groups. After 16 hours, all of the resulting conjugates (**PPep2**, **PPep3** and **PPep4**) were water soluble and the extent of peptide incorporation into **P1** was found to be 1.6, 2.2 and 1.4 mol% for **Pep2**, **Pep3** and **Pep4** by comparing the signals at 7.87-7.91 ppm with those at 8.20-8.36 ppm. **Table 1** summarizes the peptide incorporation and alkyne conversion as well as SEC analysis, if available, for all of the synthesized polymers. These results suggest that the aqueous CuAAC protocol **C7** provides a general method for the incorporation of cyclic peptide disulfides to the polymers independent of the peptide sequence and without the requirement of protecting groups for potentially side chain reactive amino acids, such as lysine and histidine.

2.4. Conclusions

This Chapter has presented a new, general strategy for the preparation of cyclic peptide disulfide-PHPMA conjugates, which does not require the use of peptide protecting groups. Cyclic peptide disulfide-PHPMA conjugates are obtained via a three step post-polymerization modification strategy from a PPFMA precursor. First, via a sequence of two consecutive post-polymerization aminolysis reactions, a PHPMA copolymer that contains both dansyl and alkyne side chain functional groups is prepared. The alkyne functional groups, finally, are used to allow CuAAC coupling of azide modified cyclic peptide disulfides. To this end, a number of CuAAC protocols was screened using a small library of cyclic peptide disulfides, which incorporated amino acids with side chain functional groups that were known to interfere with active ester based conjugation strategies or susceptible to oxidation side reactions. It was found that conjugation via a CuAAC protocol using Cu(II)SO4, THPTA, sodium ascorbate and aminoguanidine yielded well-defined cyclic peptide disulfide-polymer conjugates. In Chapter 4, three of these synthesized conjugates, **PPep1a**, **PPep1b** and **PPep2** will be used as model polymeric profragrances that can selectively target human hair under shampoo conditions.

2.5.   References

(1)   Patel, Y. C. *Front. Neuroendocrinol.* **1999**, *20*, 157-198.

(2)   Myers, R. A.; Zafaralla, G. C.; Gray, W. R.; Abbott, J.; Cruz L. J.; Olivera, B. M. *Biochemistry* **1991**, *30*, 9370-9377.

(3)   Callewaert, G. L.; Shipolini, R.; and Vernon, C. A. *FEBS Lett.* **1968**, *1*, 111-113.

(4)   Selsted, M. E.; Ouellette, A. J. *Nat. Immunol.* **2005**, *6*, 551-557.

(5)   McLafferty, M. A.; Kent, R. B.; Ladner, R. C.; Markland, W. *Gene* **1993**, *128*, 29-36.

(6)   Giebel, L. B.; Cass, R.; Milligan, D. L.; Young, D.; Arze, R.; Johnson, C. *Biochemistry* **1995**, *34*, 15430-15435.

(7)   Koivunen, E.; Wang, B.; Ruoslahti, E. *Nat. Biotech.* **1995**, *13*, 265-270.

(8)   Craik, D. J.; Daly N. L.; Waine, C. *Toxicon* **2001**, *39*, 43-60.

(9)   Tam, J. P.; Lu, Y.-A.; Yang, J.-L.; Chiu, K.-W. *Proc. Natl. Acad. Sci. U. S. A.* **1999**, *96*, 8913-8918.

(10)   Hancock, R. E. W.; Sahl, H.-G. *Nat. Biotech.* **2006**, *24*, 1551-1557.

(11)   Flynn, C. E.; Mao, C.; Hayhurst, A.; Williams, J. L.; Georgiou, G.; Iverson, B.; Belcher, A. M. *J. Mater. Chem.* **2003**, *13*, 2414-2421.

(12)   Seker, U. O. S.; Wilson, B.; Dincer, S.; I. Kim, I. W.; Oren, E. E.; Evans, J. S.; Tamerler, C.; Sarikaya, M. *Langmuir* **2007**, *23*, 7895-7900.

(13)   Pasut, G.; Veronese, F. M. *Prog. Polym. Sci.* **2007**, *32*, 933-961.

(14)   Qi, Y.; Chilkoti, A. *Curr. Opin. Chem Biol.* **2015**, *28*, 181-193.

(15)   Gauthier, M. A.; Klok, H.-A. *Chem. Commun.* **2008**, 2591-2611.

(16)   Lutz, J.-F. Börner, H. G. *Prog. Polym. Sci.* **2008**, *33*, 1-39.

(17)   Nicolas, J.; Mantovani, G.; Haddleton, D. M. *Macromol. Rapid Commun.* **2007**, *28*, 1083-1111.

(18)   Markó, K.; Ligeti, M.; Mező, G.; Mihala, N.; Kutnyánszky, E.; Kiss, É.; Hudecz, F.; Madarász, E.; *Bioconjugate Chem.* **2008**, *19*, 1757-1766.

(19)   Loschonsky, S.; Couet, J.; Biesalski, M.; *Macromol. Rapid Commun.* **2008**, *29*, 309-315.

(20)   Aimetti, A. A.; Feaver, K. R.; Anseth, K. S. *Chem. Commun.* **2010**, *46*, 5781-5783.

(21)   Chapman, R. ; Warr, G. G.; Perrier, S.; K. A. Jolliffe, K. A. *Chem. Eur J.* **2013**, *19*, 1955-1961.

(22)   Danial, M.; Tran, C. M. N.; Jolliffe, K. A.; Perrier, S. *J. Am. Chem. Soc.* **2014**, *136*, 8018-8026.

(23)   Fava, A.; Iliceto, A.; Camera, E. *J. Am. Chem. Soc.* **1957**, *79*, 833-838.

(24)   Fernandes, P. A.; Ramos, M. J. *Chem. Eur. J.* **2004**, *10*, 257-266.

(25)   Ma, M.; Zhou, B.; Kim, Y.; Janda, K. D. *Toxicon* **2006**, *47*, 901-908.

(26)   Rostovtsev, V. V.; Green, L. G.; Fokin, V. V.; Sharpless, K. B. *Angew. Chem.* **2002**, *114*, 2708-2711.

(27)   Tornøe, C. W.; Christensen, C.; Meldal, M. *J. Org. Chem.* **2002**, *67*, 3057-3064.

(28)   Wang, Q.; Chan, T. R.; Hilgraf, R.; Fokin, V. V.; Sharpless, K. B.; Finn, M. G. *J. Am. Chem. Soc.* **2003**, *125*, 3192-3193.

(29)   Lutz, J.-F.; Zarafshani, Z. *Adv. Drug. Del. Rev.* **2008**, *60*, 958-970.

(30)   Lallana, E.; Fernandez-Megia, E.; Riguera, R. *J. Am. Chem. Soc.* **2009**, *131*, 5748-5750.

(31)   Liu, Y.; Sun, G.; David, A.; Sayre, L. M. *Chem. Res. Toxicol.* **2004**, *17*, 110-118.

(32)   Hong, V.; Presolski, S. I.; Ma, C.; Finn, M. G. *Angew. Chem. Int. Edit.* **2009**, *48*, 9879-9883.

(33)   Hong, V.; Steinmetz, N. F.; Manchester, M.; Finn, M. G. *Bioconjugate Chem.* **2010**, *21*, 1912-1916.

(34)   Eberhardt, M.; Mruk, R.; Zentel, R.; Théato, P. *Eur. Polym. J.* **2005**, *41*, 1569-1575.

(35)   Gibson, M. I.; Fröhlich, E.; Klok, H.-A. *J. Polym. Sci. Polym. Chem.* **2009**, *47*, 4332-4345.

(36)   Singha, N. K.; Gibson, M. I.; Koiry, B. P.; Danial, M.; Klok, H.-A. *Biomacromolecules* **2011**, *12*, 2908-2913.

(37)   Richards, S.-J.; Jones, M. W.; Hunaban, M.; Haddleton, D. M.; Gibson, M. I. *Angew. Chem. Int. Edit.* **2012**, *51*, 7812-7816.

(38)   Říhová, B.; Kovář, M. *Adv. Drug Del. Rev.* **2010**, *62*, 184-191.

(39)   Duncan, R.; Vicent, M. J. *Adv. Drug Del. Rev.* **2010**, *62*, 272-282.

(40)   Danial, M.; Root, M. J.; Klok, H.-A. *Biomacromolecules* **2012**, *13*, 1438-1447.

(41)   Nuhn, L.; Hartmann, S.; Palitzsch, B.; Gerlitzki, B.; Schmitt, E.; Zentel, R.; Kunz, H. *Angew. Chem. Int. Edit.* **2013**, *52*, 10652-10656.

(42)   Mohr, N.; Barz, M.; Forst, R.; Zentel, R. *Macromol. Rapid Commun.* **2014**, *35*, 1522-1527.

(43)   Eberhardt, M.; Théato, P. *Macromol. Rapid. Commun.* **2005**, *26*, 1488-1493.

(44)   Perrier, S.; Takolpuckdee, P.; Mars, C. A. *Macromolecules* **2005**, *38*, 2033-2036.

(45)   Feldborg, L. N.; Jølck, R. I.; Andresen, T. L. *Bioconjugate Chem.* **2012**, *23*, 2444-2450.

(46)   Fujii, N.; Otaka, A.; Funakoshi, S.; Bessho, K.; Watanabe, T.; Akaji, K.; Yajima, H. *Chem. Pharm. Bull.* **1987**, *35*, 2339-2347.

(47)   Schneggenburger, P. E.; Worbs, B.; Diederichsen, U. *J. Pep. Sci.* **2010**, *16*, 10-14.

(48)   Deletre, M.; Levesque, G. *Macromolecules* **1990**, *23*, 4733-4741.

(49)   Zhang, X.; Lian, X.; Liu, L.; Zhang, J.; Zhao, H. *Macromolecules* **2008**, *41*, 7863-7869.

(50)   Engler, A. C.; Lee, H.-I.; Hammond, P. T. *Angew. Chem. Int. Edit.* **2009**, *48*, 9334-9338.

(51)   Yu, Y.; Zou, J.; Yu, L.; Ji, W.; Li, Y.; Law, W.-C.; Cheng, C. *Macromolecules* **2011**, *44*, 4793-4800.

(52)   Pechar, M.; Pola, R.; Laga, R.; Ulbrich, K.; Bednárová, L.; Maloň, P.; Sieglová, I.; Král, V.; Fábry, M.; Vaněk, O. *Biomacromolecules*, **2011**, *12*, 3645-3655.

(53)   Carberry, T. P.; Tarallo, R.; Falanga, A.; Finamore, E.; Galdiero, M.; Weck, M.; Galdiero, S. *Chem. Eur. J.* **2012**, *18*, 13678-13685.

(54)   O'Connor, A.; Marsat, J.-N.; Mitrugno, A.; Flahive, T.; Moran, N.; D. Brayden, D.; Devocelle, M. *Molecules* **2014**, *19*, 17559-17577.
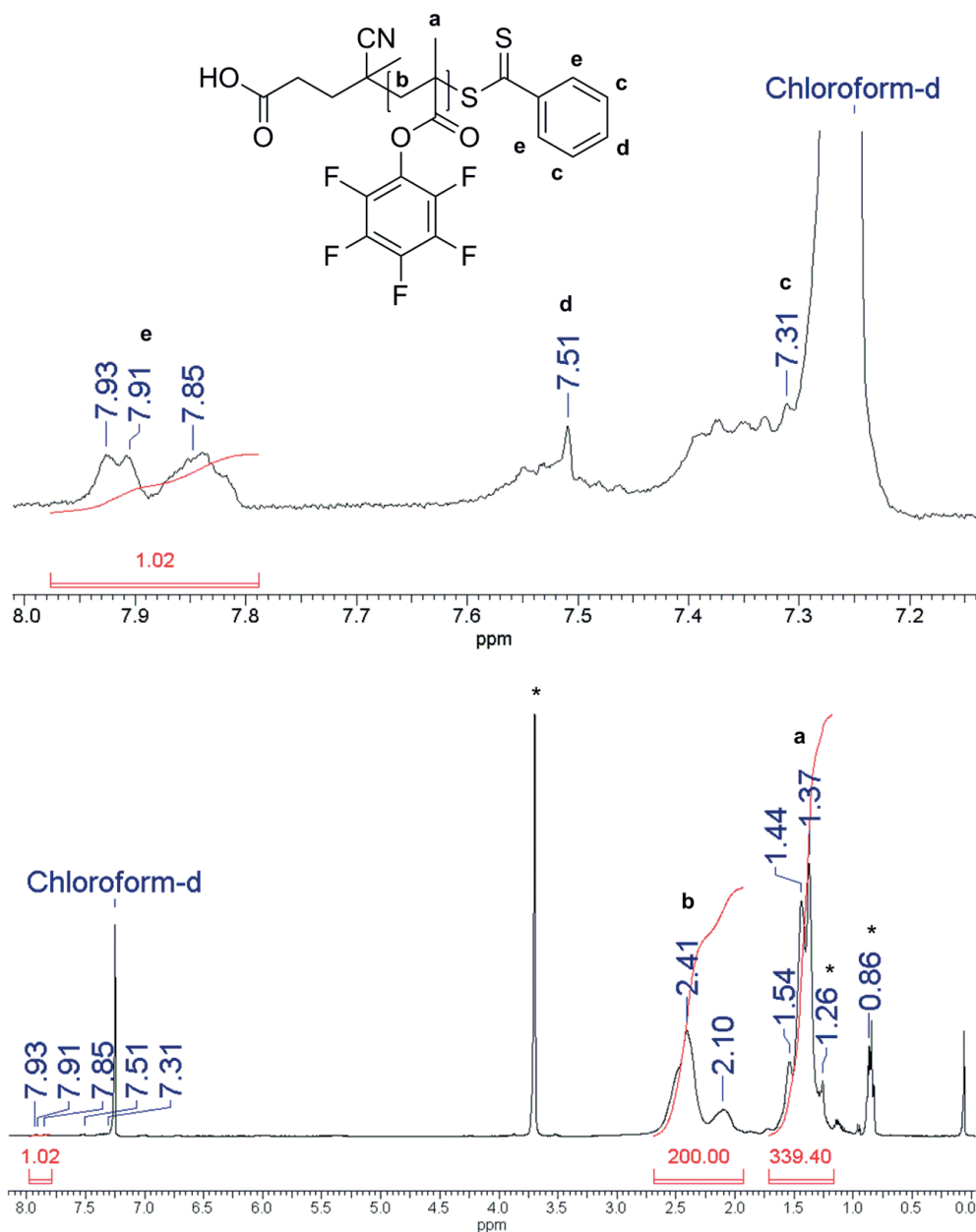
2.6.   Supporting Information

Figure S1. ^{1}H-NMR spectrum of PPFMA polymer used in this study prior to removal of dithiobenzoate end-groups. **Top:** Enlarged region between 7.15-8.00 ppm highlighting the signals associated to the dithiobenzoate end-groups; **Bottom:** Complete ^{1}H-NMR spectrum of PPFMA in CDCl₃. * = Residual solvent peaks.
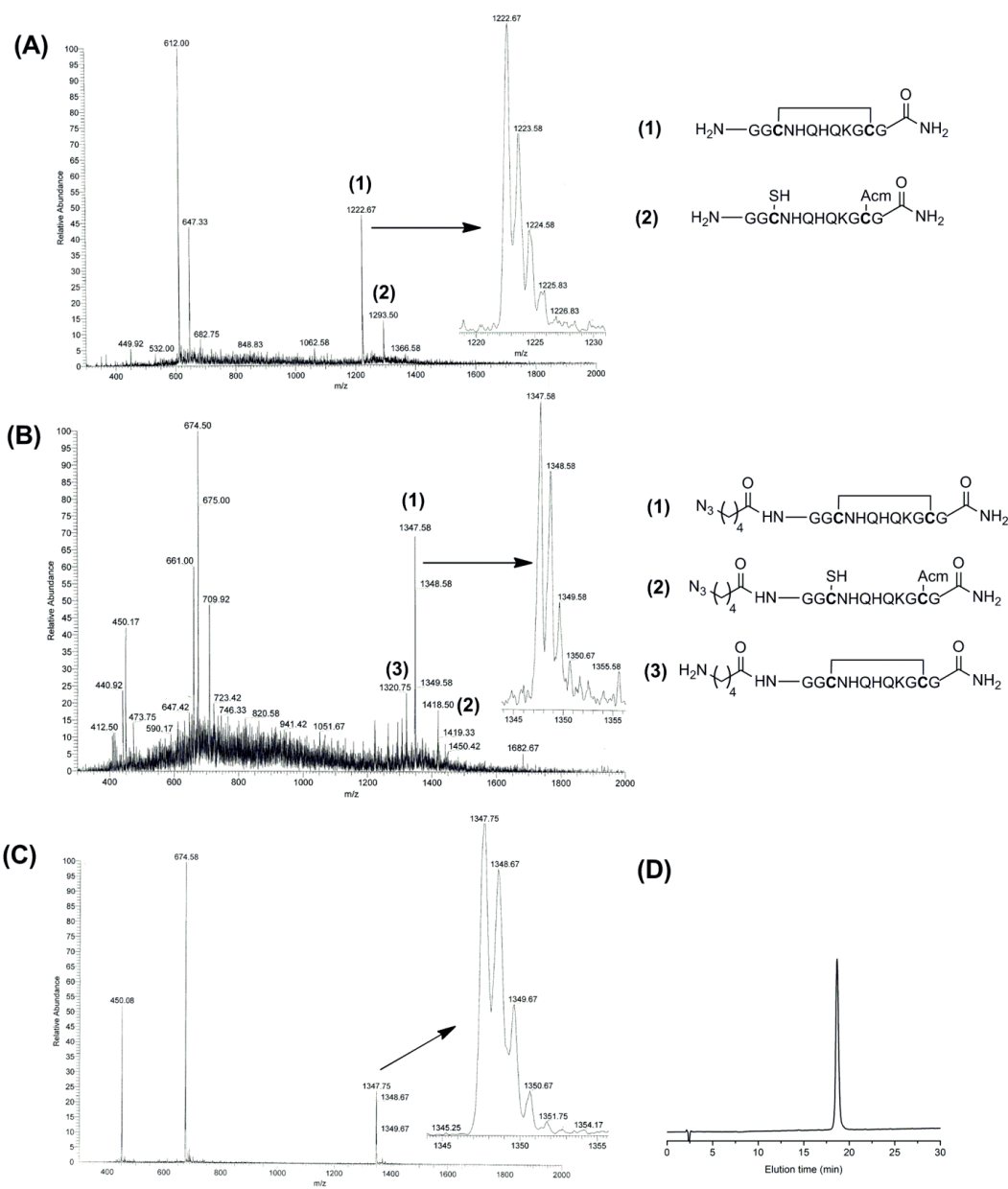
Figure S2. (A) ESI-MS spectrum of crude **Pep1** after Tl(CF₃COO)₃ mediated oxidation. (B) ESI-MS spectrum of crude **Pep1** after N-terminal azide functionalization. (C) ESI-MS spectrum and (D) HPLC elution chromatogram of pure **Pep1**.
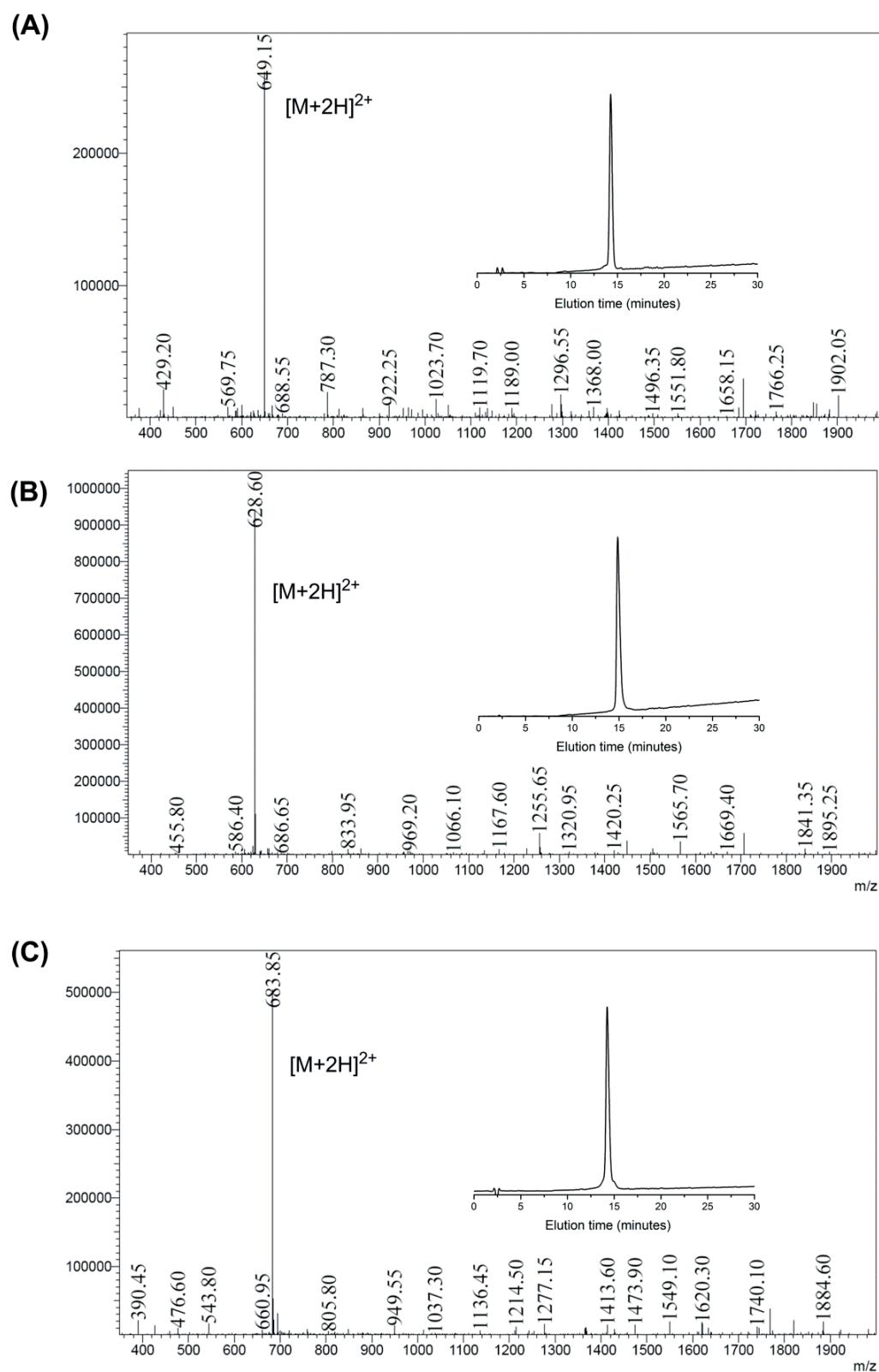
Figure S3. HPLC elution profiles and corresponding ESI-MS spectra of purified cyclic peptide disulfides (A) **Pep2,** (B) **Pep3** and (C) **Pep4**.
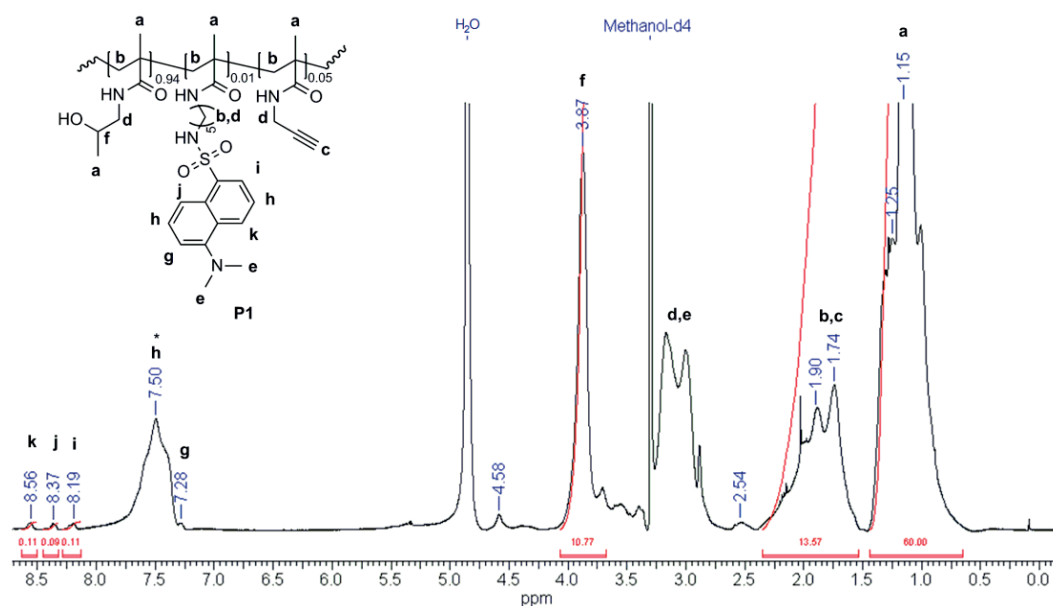
Figure S4. ^{1}H-NMR spectrum of **P1** in methanol-d$_4$. * = 1 H peaks associated with the hydrogen of the amide groups.
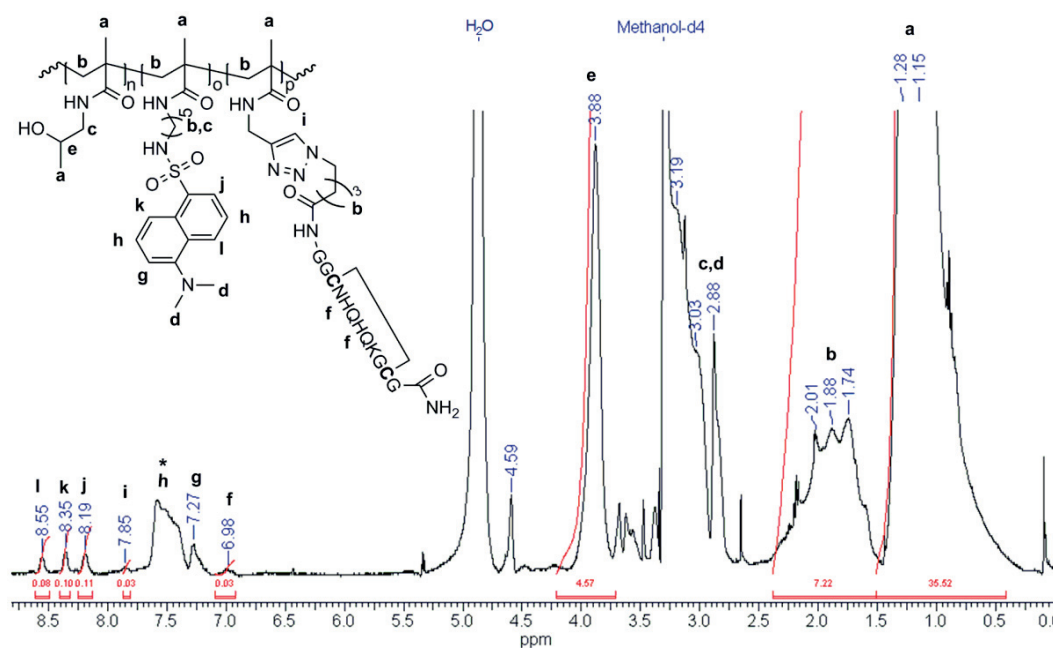
Figure S5. ^{1}H-NMR spectrum of copolymer obtained using CuAAC condition **C5 (PC5)** in methanol-d$_4$. * = 1H peaks associated with the hydrogen of the amide groups.
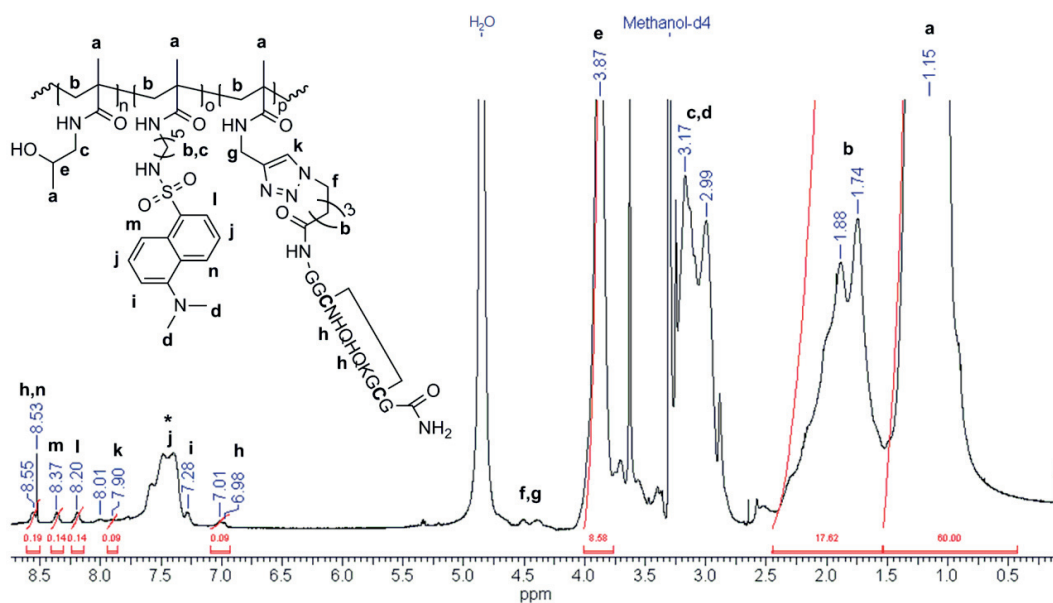
Figure S6. ^{1}H-NMR spectrum of **PPep1a** in methanol-d_4. * = 1H peaks associated with the hydrogen of the amide groups.
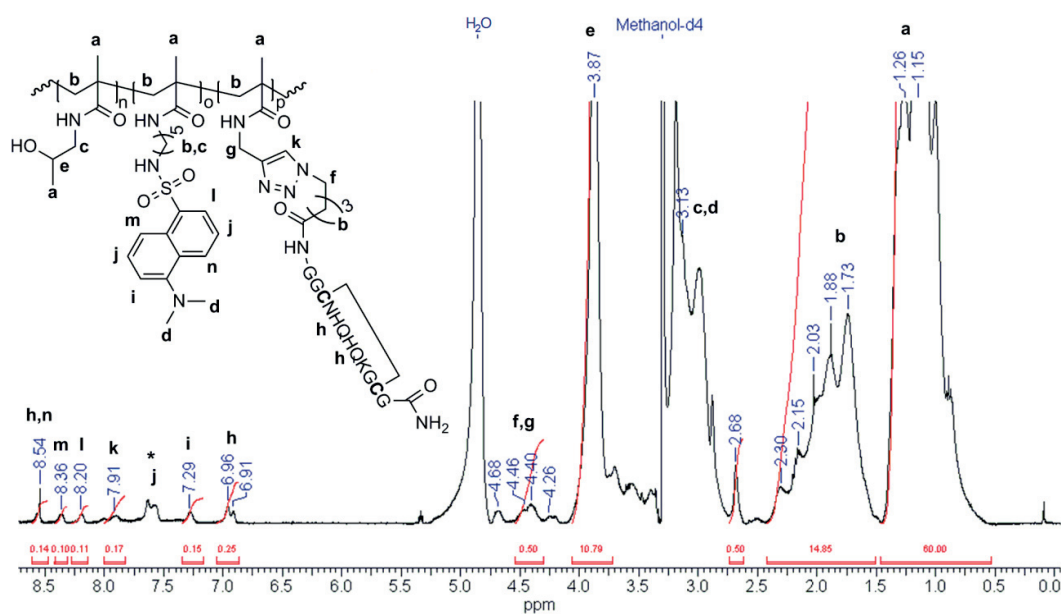

Figure S7. ^{1}H-NMR spectrum of **PPep1b** in methanol-d_4. * = 1H peaks associated with the hydrogen of the amide groups.
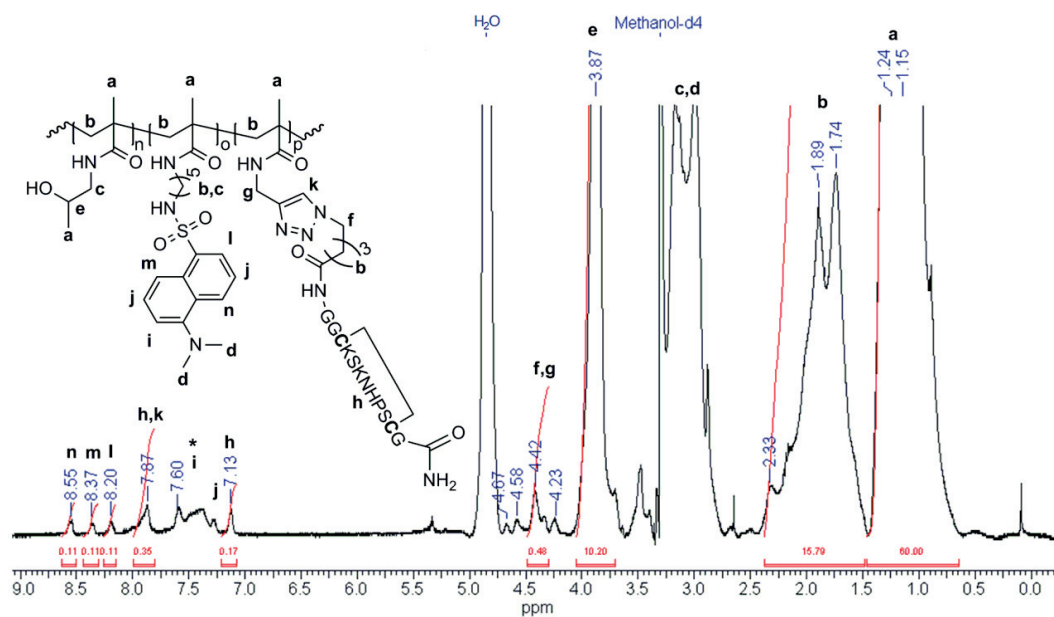
Figure S8. ^{1}H-NMR spectrum of **PPep2** in methanol-d_4. * = 1H peaks associated with the hydrogen of the amide groups.
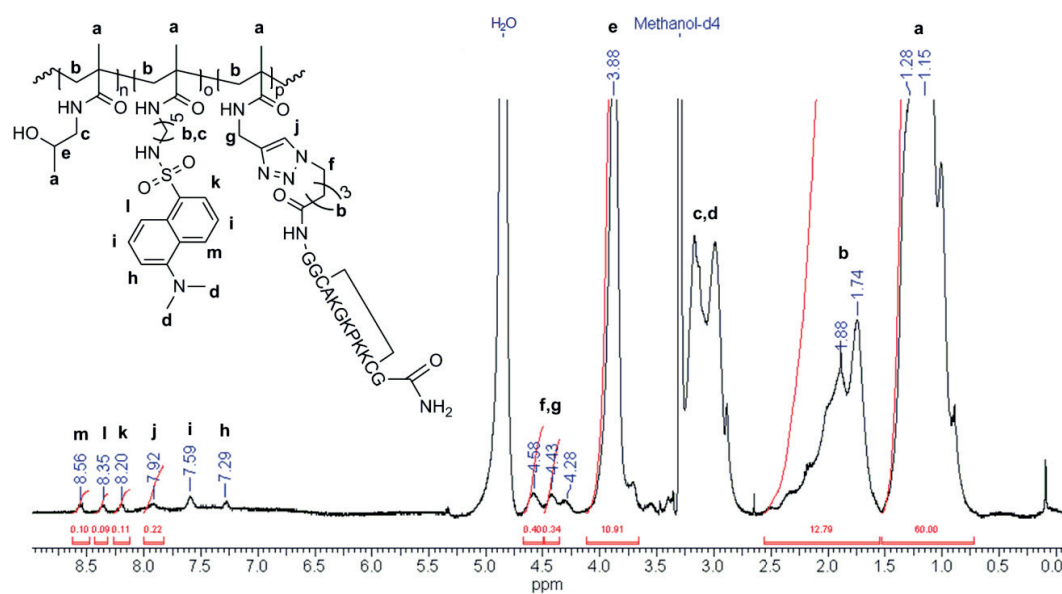

Figure S9. ^{1}H-NMR spectrum of **PPep3** in methanol-d_4.

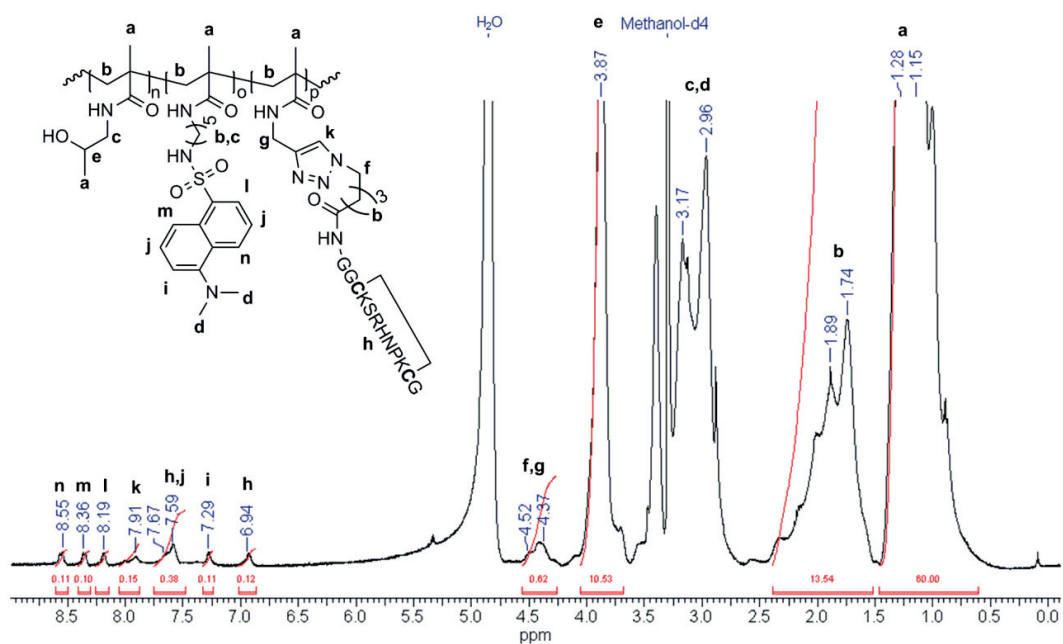**Figure S10.** ^{1}H-NMR spectrum of **PPep4** in methanol-d$_4$.

3. Peptide-Enhanced Selective Surface Deposition of Polymer Based Fragrance Delivery Systems on Cotton[1]

3.1. Introduction

Fragrances are highly volatile compounds that have a pleasant odor. The high volatility of these compounds, however, necessitates the design of systems that allow their long-term storage prior to the application as well as their controlled release particularly in the aqueous media to the target of interest.[1-3] Polymers are attractive delivery systems that can be used to store and provide controlled release of these volatile compounds. Polymeric fragrance delivery systems can be subdivided into two categories. The first strategy, so called polymeric profragrances, is based on the delivery of the fragrance upon its chemical release from a polymer backbone in the presence of external stimuli at ambient conditions.[4-7] In the second strategy, fragrances are physically encapsulated in a variety of polymeric carriers, such as triblock copolymers,[8-9] amphiphilic multi-arm star block copolymers,[10,11] core-shell type vesicles prepared via miniemulsion polymerization[12-16] and nanocapsules obtained via nanoprecipitation.[17]

In addition to providing a robust environment that prevents evaporation and degradation upon storage as well as to allow a sustained release of fragrance molecules, another important characteristic of polymeric fragrance delivery systems is their deposition on the target of interest, such as *e.g.* cotton under laundry wash conditions. Even though this is a critical step in the application of many fragrance containing products, only very little work has been done that has touched on enhancing the substrate deposition of polymer based fragrance delivery systems. For instance, Berthier and coworkers improved the deposition of poly(maleic acid)-based polymeric profragrances onto cotton fabric under softener medium by increasing the hydrophobicity of the polymers with the incorporation of long alkyl chains or Jeffamine groups.[7,18] This

---

enhanced deposition upon increased polymer hydrophobicity, however, did not directly result in higher fragrance release from cotton surfaces, as it was also found in the same work that these polymeric profragrances incorporating hydrophilic poly(ethylene glycol) (PEG) side chain groups allows higher fragrance release compared to hydrophobic ones.[7] Furthermore, this strategy may not be applicable to the fragrance carriers, as their surface functionalization with hydrophobic groups may lead to aggregation in aqueous media. Therefore, a novel strategy that is both applicable to polymeric profragrances and fragrance carriers and allows at the same time their enhanced deposition without compromising the fragrance release is highly desirable.

Phage display is a powerful tool for the identification of peptide sequences that selectively recognize the target of interest.[19-21] Although phage display was primarily used for the identification of biological substrate binders, its scope was highly expanded in the last decade, such that it was employed to isolate short peptides recognizing inorganic crystals,[22-24] carbon-based materials[25,26] as well as "soft matter" surfaces as desbribed in Chapter 1.[27-30] More relevantly, it was utilized to identify cellulose binding peptides,[31-33] the primary constituent of cotton fabric, which is one of the surfaces that enhanced fragrance deposition is desired. For instance, Kumar and coworkers reported the improved deposition of protein constructs containing a phage display identified cellulose-binding peptide onto cotton under laundry detergent conditions.[34] However, the high cost of the preparation of a purely protein-based material combined with the further difficulty of incorporating fragrances by chemical or physical means may prevent these constructs to be feasible as potential delivery systems.

This Chapter aims to explore the feasibility of short peptide sequences identified by phage display to enable selective surface deposition of fragrance delivery systems to cotton under fabric softening conditions. From that point, this Chapter can be subdivided into three parts which were illustrated in **Scheme 1**. In the first part, the identification of cotton fabric binding cyclic peptide disulfides (CXC's) via phage display in a fabric softener medium will be reported. In the second part, the synthesis of peptide-poly(*N*-(2-hydroxypropyl)methacrylamide) (PHPMA) conjugates, which can serve as a model polymeric profragrance platform, will be demonstrated. Since the identified CXC's did not contain any lysine residues, in contrast to the strategy illustrated in Chapter 2, a direct post-polymerization aminolysis of a poly(pentafluorophenyl methacrylate) (PPFMA)
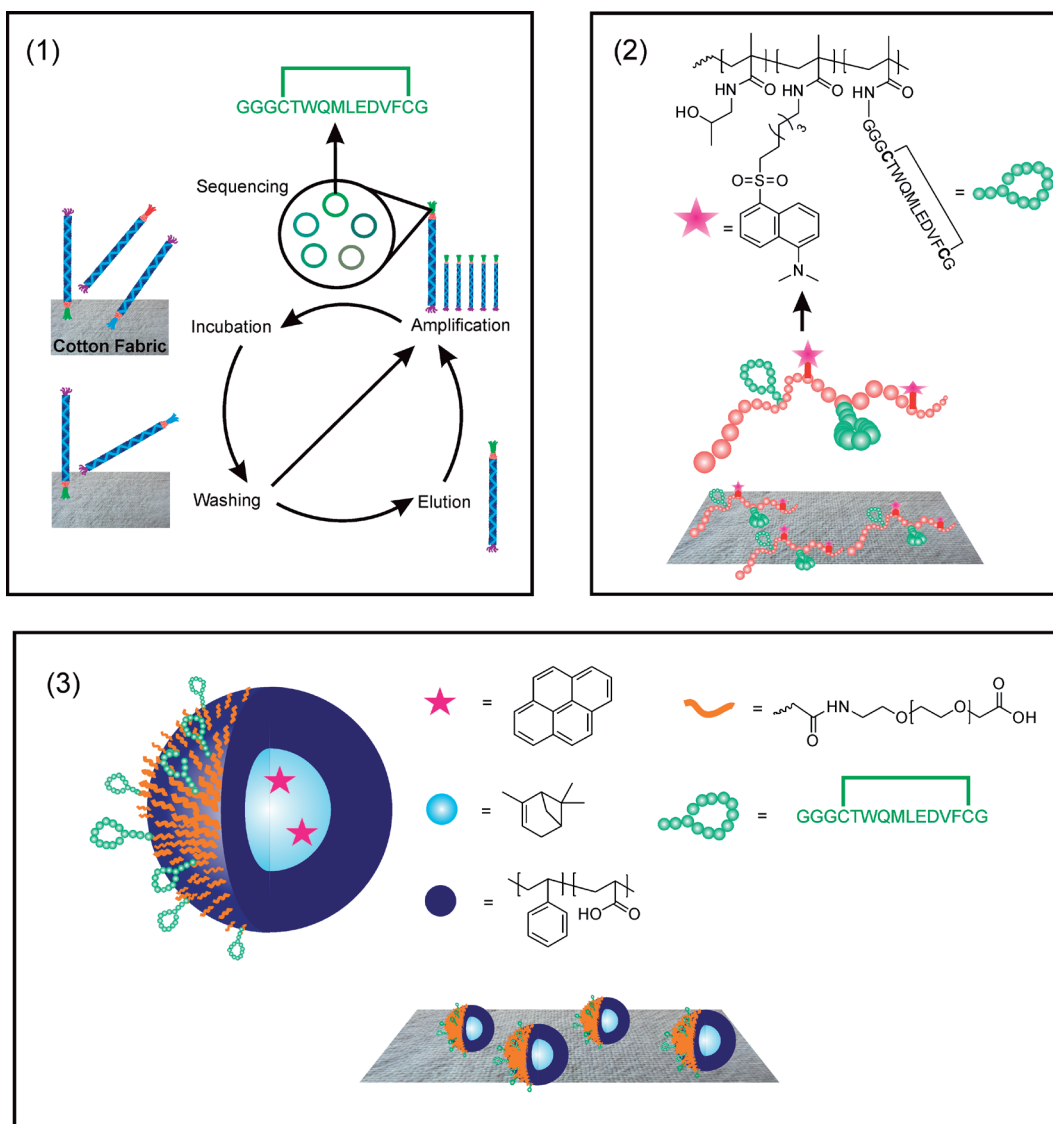
Scheme 1. Overall strategy for the preparation of polymeric fragrance delivery systems that selectively bind to cotton under fabric softening conditions. (1) Identification of cotton fabric binding peptides via phage display. (2) Preparation of cyclic peptide disulfide-PHPMA conjugates as model polymeric profragrance systems. (3) Preparation of fragrance loaded, peptide-nanoparticle hybrids via miniemulsion polymerization.

precursor with the N-terminal amine groups of CXC should be possible. It will be shown via fluorescence intensity measurements that small amounts of peptide incorporation improve the deposition of peptide-PHPMA conjugates on cotton 2-3 fold compared to a polymer that does not contain any peptide. In the last part, the synthesis of α-pinene loaded poly(styrene-*co*-acrylic acid) (PS-*co*-PAA) nanoparticles via miniemulsion

polymerization will be reported as a model polymeric fragrance carrier. Successive chemical functionalization of the surface COOH groups of this particle with a bifunctional poly(ethylene glycol) (NH$_2$-PEG-COOH) and the cotton-binding peptide will be demonstrated to enhance the deposition of these particles 2-fold onto cotton under softener conditions. Furthermore, dynamic headspace measurements will reveal higher α-pinene release from the cotton surfaces treated with the peptide functionalized nanoparticles compared to non-functionalized PS-*co*-PAA. From these aspects, this Chapter aims to pave the way for a new class of "smart" fragrance delivery systems that selectively recognize the target of interest under desired application conditions.

3.2. Experimental Section

Materials. The fabric softener emulsion used for the phage display, phage ELISA and the fluorescence intensity measurements was prepared by adding 1.8 g of a mixture containing 82.9 w/w% H$_2$O, 16.5 w/w% Stepantex® VL 90A and 0.6 w/w% CaCl$_2$ (10%) to 600 mL of a 50 mM sodium acetate buffer (pH 3.8). For dynamic headspace sampling experiments, a fabric softener emulsion was prepared by adding 1.8 g of the mixture mentioned above to 600 mL of deionized water. An EMPA (Eidgenössische Materialprüfanstalt) test cotton No: 221 was used as the model cotton fabric in all of the experiments. Affinity selections were carried using a combinatorial phage library displaying 9-mer cyclic peptide disulfides (C9C). These phage libraries were a gift from Christian Heinis group and their construction was described in a previous publication.[35]

All chemicals were used as received unless otherwise described. The synthesis of pentafluorophenyl methacrylate (PFMA),[36] reversible addition-fragmentation chain transfer (RAFT) polymerization of PFMA[37] as well as the removal of the dithioester end-groups of the synthesized PPFMA polymer[38] was performed according to previously described protocols. Triethylamine (TEA), styrene and acrylic acid were freshly distilled before use. Chloramphenicol was received from BioChimica. Tween® 20, bovine serum albumin (BSA), 1-amino-2-propanol (93.0%), dansyl cadaverine (> 97.0%), TEA (97.0%), piperidine (99.0%), thioanisole (≥ 99.0%), dimethyl sulfoxide (DMSO) (99.5%), trifluoroacetic acid (TFA) (99.0%) *N*-methyl-2-pyrrolidone (NMP) (≥ 98.0%), *N,N*-diisopropylethylamine (DIEA) (98.0%), phenol (≥ 99.0%), 1,2-ethanedithiol (≥ 99.0%), sodium dodecyl sulfate (SDS) (≥ 99.0%), hexadecane (HD) (99.0%), 2,2-

azobisisobutryonitrile (99.0%) (AIBN), pyrene (99.0%), α-pinene (98.0%), 2-(N-morpholino)ethanesulfanoic acid (MES) hydrate (99.5%), 2-mercaptoethanol (≥ 99.0%), *N*-(3-dimethylaminopropyl)-*N*′-ethylcarbodiimide hydrochloride (EDC) (≥ 98%), *N*-hydroxysulfosuccinimide sodium salt (Sulfo-NHS) (95%) and poly(ethylene glycol) 2-aminoethyl ether acetic acid (M_n = 5000 g/mol) (NH$_2$-PEG-COOH) were received from Sigma Aldrich. ULTRA-TMB ELISA solution was received from Thermo Scientific. Anti-M13-HRP monoclonal antibody was received from Abcam. All amino acids as well as Oxyma Pure were received from Iris Biotech GMBH. *N,N,N′,N′*-Tetramethyl-*O*-(1H-benzotriazol-1-yl)uronium hexafluorophosphate (HBTU) (98%) was received from Fluorochem.

Methods.

Absorbance and fluorescence intensity measurements were performed with a Tecan Infinite Pro 200 reader. Peptides were synthesized via Fmoc solid phase peptide synthesis (SPPS) using a CEM Liberty automated microwave synthesizer. High pressure liquid chromatography (HPLC) was performed using a Shimadzu Prominence system containing LC-20AP pumps, a FRC-10A fraction collector, a CTD-20AC column oven and a SPD-M20A diode array detector coupled to a LCMS-2020 liquid chromatography mass spectrometer. The peptides were characterized using an analytical Grace Vydac 218TP54 C18 column and purified using Grace Vydac 218TP15 preparative column. ^{1}H-NMR spectra were recorded on a Bruker (ARX-400) 400 MHz spectrometer at room temperature using a relaxation time (t_1) of 10 seconds. Chemical shifts are reported relative to the residual proton signal of the solvent. Size exclusion chromatography (SEC) was performed on a Waters Alliance GPCV 2000 system equipped with refractive index (RI) detector. Separation was carried out at 60 °C with TSK-Gel Alpha 3000 + 4000 columns using DMF + 1gL^{-1} LiBr as eluent and a flow rate of 0.6 mL min^{-1}. Molecular weights were determined relative to narrow polydispersity poly(methyl methacrylate) (PMMA) standards using the RI detector. Results were calculated with the Empower Pro multidetection GPC software (V. 5.00). Particle size and zeta potential measurements were performed using a Malvern Zetasizer Nano SZ analyzer by diluting 1 – 10 μL of the nanoparticle dispersions in 1 mL of a 10 mM NaCl solution. The measurements were performed using a single scattering angle of 173° at 25 °C. Cryogenic transmission electron microscopy (Cryo-TEM) imaging was carried as follows: An EM-grid from Agar Scientific UK, with holey carbon film was held in tweezers and 4-5 μL of particle

solution was applied on the grid. The tweezers were mounted to an automatic plunge freezing apparatus from Vitrobot, FEI, Netherlands to control humidity and temperature. After blotting, the grid was immersed into a small metal container with liquid ethane that is cooled from outside by liquid nitrogen. The speed of cooling was such that the ice crystals did not have the time to form. Observations were made at -170°C in a Tecnai F 20 microscope from FEI, Netherlands operating at 200 kV equipped with a cryo-specimen holder Gatan 626 (Warrendale, PA). Digital images were recorded with an Eagle (FEI) camera that has a resolution of 4098 X 4098 pixels. Carboxylic acid surface concentration on the nanoparticles were determined via conductometric titration using a Hach 44600 conductivity meter similar to the protocol described by Musyanovych and coworkers.[39] Briefly, first an excess of 1 N NaOH was added to 10 mL nanoparticle dispersions with a solid content (SC) of 1 w/w% to bring the pH of the solution to 12. After 10 minutes of stirring, the solutions were titrated with the addition of 50 μL, 0.1 N HCl at each step until the pH of the solution was less than 3. The conductivity and the pH of the solutions were measured at each titration step. The concentration of carboxylic acid groups per gram of particle was calculated using the amount of consumed HCl, which was obtained from the conductivity curves. The number of –COOH groups per particle and per nm^2 of particle surface were calculated using the equations described by Musyanovych *et al*.[39] These calculations were provided in Supporting Information.

Procedures.

Identification of cotton-binding peptides under fabric softening conditions via phage display. Combinatorial C9C phage library was produced via the proliferation of chloramphenicol resistant *E.coli.* TG1 cell lines having an optical density (OD) of 0.1 in 500 mL 2YT media containing 0.1 mg/mL chloramphenicol for 16 hours at 30 °C. Next, the bacteria pellet was precipitated by centrifugation and the supernatant, which contained the phages, was mixed with 190 mL of a 2.5 M NaCl solution containing 20 w/w% polyethylene glycol (PEG). The phages were isolated by centrifugation and subsequently resuspended in 8 mL fabric softener emulsion. The concentration of the input phages was approximately 2 x 10^{12} plaque forming units (pfu)/mL in the beginning of each round of selection.

Prior to incubation, cotton fabric samples (7.5 mm x 7.5 mm) were prewashed once with isopropanol, three times with MilliQ water and air dried. After that, cotton fabric

samples were incubated with 8 mL fabric softener emulsions containing the phages for 20 minutes at room temperature with gentle agitation in falcon tubes. Then cotton fabric samples were removed from the falcon tubes, inserted into new tubes, and washed 8 times either with 10 mL tris buffered saline solution (TBS) (pH 7.4) containing 0.1 v/v% Tween® 20 at each round of selection (**Condition 1**) or the TBS buffer containing 0.1, 0.2, 0.3, 0.4 and 0.5 v/v% Tween® 20 in the 1st, 2nd, 3rd, 4th and 5th rounds of selection (**Condition 2**), respectively, to remove the weakly bound phages. The cotton samples were further washed twice more with 10 mL TBS solution that did not contain any Tween® 20, removed from the falcon tubes and dried. Each washing step was performed for 5 minutes with gentle agitation and the samples were transferred into new falcon tubes for four different times throughout the 10 washing steps in order to minimize the selection of background binders associated with the polystyrene tube.

The infection of the phages was also carried out using two different conditions. In the first condition (**Condition a**), cotton bound phages were first eluted with 2 mL, 50 mM glycine.HCl buffer (pH 2.2) for 5 minutes and the eluted phage solution was immediately neutralized with 1 mL 1M TBS buffer (pH 8.0). This solution was then added to 30 mL 2YT media containing fresh TG1 cells having an OD of 0.4 and the infection was carried out for 90 minutes at 37 °C. In the second condition, (**Condition b**) cotton fabric samples containing the strongly bound phages were directly inserted into 30 mL 2YT media containing fresh TG1 cells after the washing step, and the infection was similarly carried out for 90 minutes at 37 °C. Following infection, the solutions were centrifuged, the supernatants were discarded, the bacterial pellets were resuspended in 1 mL 2YT and subsequently plated into chloramphenicol containing agar plates. The plates were incubated overnight at 37 °C and scraped off for the recovery of the infected bacteria. Aliquots of solutions were taken following the infection step to determine the output phage titers after each selection round. In total, 4 independent affinity selections were carried up to the 5th round. These selection experiments are referred to **1a**, **1b**, **2a** and **2b** depending on the washing (**Condition 1** and **2**) and infection (**Condition a** and **b**) steps performed. These conditions and the evolution of the output phage titers with respect to number of selection rounds are summarized in **Table S1** and **Figure S1**. Individual colonies of phage infected TG1 cells were picked from the 3rd, 4th and 5th rounds of selection from each of the 4 conditions, their plasmids were extracted using a QIAGEN spin Miniprep kit and these plasmids were sent to sequencing analysis.

Phage ELISA. The individual phages that were identified as potentially affine cotton fabric binders and the combinatorial C9C phage library were produced similar to the protocol described in the previous section. The phages were resuspended in 2 mL fabric softener emulsion and the initial concentrations of the phages were calculated from the average of three independent phage titrations.

Before incubation, a 96-well polystyrene plate was blocked with 500 μL of a phosphate-buffered saline solution (pH 7.4) containing 0.1% Tween® 20 (PBST 0.1%) and 2% BSA for 30 minutes. Next, the wells were washed three times with 500 μL MilliQ H_2O and air dried. Prewashed cotton fabric samples (0.5 cm x 0.5 cm, mass = 10-12 mg) were introduced to the wells and 250 μL fabric softener emulsions having phage concentrations ranged from 2 x 10^9 to 5 x 10^{12} pfu/mL were added. Phage ELISA experiments were carried out by using both the individual phages that have been identified as potentially affine binders as well as with the combinatorial phage library, in which the latter was used as a reference. In addition to these experiments, blank measurements were also performed by incubating the cotton fabric samples with fabric softener that does not contain any phage. Incubations were carried out for one hour and the cotton fabric samples were washed three times with 250 μL PBST 0.1% (pH 7.4) and one more time with PBS (pH 7.4) (Washing cycle). Another blocking step was performed by introducing 250 μL PBST 0.1% containing 2% BSA and the residual BSA was washed off by subsequently performing another washing cycle. Following the second washing cycle, the samples were incubated with 250 μL PBST 0.1% buffer containing 2% BSA as well as 1/5000 dilution of a 40 μg/mL stock solution of Anti-M13-HRP antibody for one hour and another washing cycle was subsequently performed to remove the unbound antibody. The cotton fabric samples were dried and transferred into a new 96-well plate. 125 μL of an ULTRA-TMB solution were added to these wells, which led to the evolution of a colorimetric response. The evolution of the colorimetric response was quenched by adding 125 μL of 2 M H_2SO_4 after 15 minutes. 200 μL fractions of the quenched solutions were transferred into a new 96-well plate and the absorbance in the wells was measured at 450 nm. The normalized absorbances associated with the amount of cotton bound phage were calculated by taking the difference between the absorbance values obtained from the sample and the blank measurements. All of the phage ELISA experiments were performed three times in triplicates. The apparent binding strengths of the phages were calculated using Serizawa's method by fitting the normalized absorbance as a function of phage concentration by using a Langmuir-type adsorption model.[28]

Synthesis of cyclo(GGGCTWQMLEDVFCG-amide) (Pep1). Solid phase peptide synthesis (SPPS) was carried at a scale of 0.25 mmol using Rink-amide resin (0.352 g) with a loading capacity of 0.71 mmol/g. Deprotection of Fmoc groups, coupling with the amino acid and washing was performed before and after the incorporation of each amino acid to the sequence. A two-step Fmoc deprotection was perfomed using 40 W microwave for 30 seconds and 54 W microwave power for 6 minutes (T = 75 °C), respectively with a 5 mL DMF/piperidine = 4:1 solution containing 0.1 M Oxyma pure. Coupling of the amino acids was carried out by the subsequent addition of 0.2 M amino acids in 5 mL DMF, 0.5 M of HBTU and Oxyma-Pure in 2 mL of DMF (activator) and 2 M of DIEA in 1 mL NMP (activator base) for 6 minutes using a microwave power of 24 W (T = 60 °C). Washing of the resin before and after the addition of each amino acid was performed using 10 mL DMF. Following SPPS, the resin was transferred to a reaction vessel and washed succesively with 50 mL of DMF, DCM, MeOH and DCM and dried under a flow of N_2. Peptide cleavage was carried out by treating the resin-bound peptide for a period of 3 hours with a 5 mL cleavage cocktail composed of TFA/phenol/H_2O/thioanisole/EDT 90:2.5:2.5:2.5:2.5 v/v%. The crude, linear peptide was washed and precipitated four times with cold diethyl ether, dissolved in 3:2 H_2O/AcN (v/v%) and lyophilized without further purification. After lyophilization, a 1 mg/mL solution of the linear peptide in a 0.01 M PBS buffer (pH 7.4) containing 2 v/v% of DMSO was prepared and the oxidation was carried for 16 hours at room temperature with rigorous stirring. Following the oxidation, the mixture was directly lyophilized. The cyclic peptide was then purified using preparative HPLC using gradient from 5% AcN/100% H_2O (0.1% TFA) to 60% AcN/40% H_2O (0.1% TFA) for 21 minutes with a flow rate of 20 mL/min. Pure fractions were collected and lyophilized. Purity ≥ 95% (HPLC), ESI-MS: ([M+H]$^+$ found: 1600.75 m/z, [M+H]$^+$ th: 1600.86 m/z). HPLC elution profile and the ESI-MS spectrum of the pure peptide are provided in **Figure S2**.

Synthesis of Pep1-PHPMA conjugates. The synthesis of PHPMA conjugates that contain **Pep1** and dansyl cadeverine was carried out via a three step post-polymerization modification starting from a reactive PPFMA precursor (**Scheme 2**). Four different polymer conjugates were prepared, where in the first three, 3, 5 and 7 mol% of **Pep1** were introduced to the reaction mixture with respect to starting pentafluorophenyl ester (PFMA) groups. These polymers are referred to **PPep1a, PPep1b** and **PPep1c**,

respectively. The fourth conjugate did not contain **Pep1** but only dansyl cadaverine, which was used as a control conjugate in fluorescence intensity measurements (**PC**).
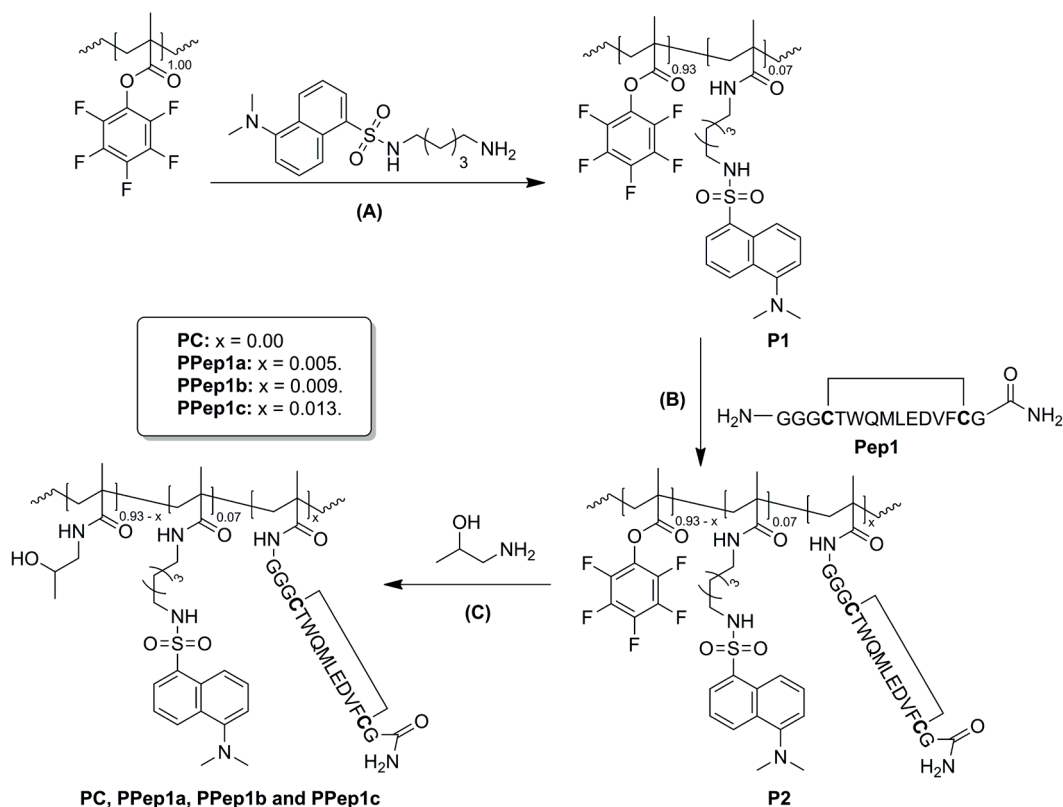
Scheme 2. Schematic illustration of the synthesis of **Pep1**-PHPMA conjugates. (A) 400 mg of PPFMA (1.584 mmol PFMA groups) and 37.24 mg of dansyl cadaverine (0.07 equiv.) in 20 mL DMF/TEA 9:1, 24 hours, room temperature. (B) **P1** (0.396 mmol starting PFMA groups) and 19.02, 31.70 or 44.38 mg of **Pep1** (0.03, 0.05 or 0.07 equiv. of starting PFMA groups) in 5 mL DMF/TEA 9:1, 24 hours, room temperature. (C) **P2** (0.396 mmol starting PFMA groups) and 61.14 μL of 1-amino-2-propanol (2 equiv. of starting PFMA groups) in 5 mL DMF/TEA 5:1, 4 days, room temperature.

The synthesis is as follows: 400 mg of PPFMA ($M_{n,NMR}$ = 42000 g/mol and M_w/M_n = 1.20 - 1.584 mmol PFMA groups) were dissolved in a mixture containing 12 mL anhydrous DMF and 2 mL freshly distilled TEA in a round bottom flask under N_2. Next, 37.24 mg (0.111 mmol, 7 mol% of PFMA groups) of dansyl cadaverine was dissolved in 6 mL of anhydrous DMF in a separate flask and added to the reaction mixture under N_2. The reaction was carried out for 24 hours at room temperature under stirring. After that,

the mixture was divided into four fractions having equal volumes and 19.02, 31.70 and 44.38 mg of **Pep1** (3, 5 and 7 mol% of starting PFMA groups) was added to three of the mixtures. No **Pep1** was added to the fourth mixture. The reactions were allowed to continue for an additional 24 hours at room temperature under N_2 with stirring. In the final step, 61.14 μL (0.792 mmol, 2 equiv. of the starting PFMA groups) of 1-amino-2-propanol, 3 mL of DMF and 1 mL of TEA were added to each of the mixtures under a flow of N_2 and the reactions continued for four additional days at room temperature under N_2 with stirring. Finally, the conjugates were precipitated/washed with Et_2O and DMF three times, centrifuged and dried overnight in reduced vacuum at room temperature. The conjugates were dissolved in H_2O/MeOH 9:1 v/v% and dialyzed against H_2O/MeOH 9:1 v/v% using a Spectra/Por dialysis membrane having a MWCO 6000-8000 g/mol for three days and lyophilized. White fluffy solids were obtained. Yields: 55-65%. ^{1}H-NMR spectra of the conjugates in methanol-d_4 with the assignment of the signals are provided in **Figure S3.**

Surface deposition of Pep1-PHPMA conjugates. Prewashed cotton samples (0.5 cm x 0.5 cm, mass = 10 - 12 mg) were inserted into the wells of a 96-well plate. Next, 250 μL of a fabric softener emulsion containing 0.01 to 0.2 mg/mL of **Pep1**-PHPMA conjugates was introduced to the wells. In parallel, same solutions were also introduced to the wells that did not contain any cotton fabric (blank measurements). The incubation was carried out for one hour at room temperature with gentle agitation. Following the incubation, 100 μL of the solutions were transferred into a new 96-well plate. The solutions were diluted 3-fold with fabric softener emulsion and the fluorescence intensities of the solutions (FI_{cotton}) were recorded at $\lambda_{em} = 504$ nm using $\lambda_{ex} = 335$ nm. Separately, the fluorescence intensity of the solutions introduced to the wells that do not contain any cotton (FI_{blank}) were also diluted 3-fold in a new 96-well plate and measured. The difference between the fluorescence intensities of FI_{blank} and FI_{cotton} yielded the amount of conjugate deposited ($FI_{deposited}$). Finally, the $FI_{deposited}$ values were normalized to one with respect to the FI_{blank} values recorded in the measurements that contain the highest concentration of **Pep1**-PHPMA conjugates (0.2 mg/mL). All measurements were performed in triplicates on three independent cotton substrates.

Synthesis of PS-*co*-PAA nanoparticles via miniemulsion polymerization. PS-co-PAA nanoparticles were prepared via miniemulsion polymerization, following a protocol similar to that reported by Musyanovych and coworkers.[39] In a round bottom flask, 24 mg SDS (83 μmol) was dissolved in 8 mL MilliQ water under N_2 in an ice bath with stirring. Next, 2 gr of organic phase composed of 29.3 mg AIBN (183 μmol), 83.0 mg hexadecane (365 μmol) and the appropriate amounts of styrene, acrylic acid, α-pinene and pyrene was prepared in another flask under N_2 at 0 °C. These amounts were summarized at **Table 3**. The organic phase was added to the aqueous phase and the mixture was preemulsifed by stirring at 2000 rpm at 0 °C and under N_2 for 1 hour. The mixture was then sonicated for 10 min. at 0 °C in a Bandelin Sonorex sonic bath (140 W, 35 kHz) to prepare the miniemulsion and subsequently heated to 72 °C for 5 hours for the polymerization. Monomer conversions were calculated by ^{1}H-NMR analysis of an aliquot taken immediately after the reaction in THF-d_8. Following the polymerization, the latexes that did not contain any α-pinene were first cleaned via centrifugation and redispersion cycles in MilliQ water. The α-pinene containing nanoparticles in contrast could not be centrifuged. These latexes were purified via extensive dialysis against H_2O using a Spectra/Por Float-A-Lyzer® G2 dialysis device with a MWCO of 300000 g/mol for one week. The removal of the unreacted monomers was verified by ^{1}H-NMR analysis of an aliquot taken after the dialysis in THF-d_8. The calculation of the encapsulation efficiency of α-pinene ($\varepsilon_{\alpha\text{-pinene}}$), solid contents of the dispersions (SC_{ly} and SC_{NMR}) and the monomer conversions are provided in the Supporting Information. ^{1}H-NMR spectra of the dispersions in THF-d_8, as well as results of particle size and zeta potential measurements and pH and conductometric titration curves are provided in **Figure S4-S7.**

Surface functionalization of PS-*co*-PAA nanoparticles. Following the optimization of the styrene, acrylic acid, α-pinene and pyrene amounts, (particle **A2P1F2**), cotton binding **Pep1** was attached to the surface of the particles with or without the presence of PEG linker. The overall strategy was illustrated in **Scheme 3**.

A2P1F2-Pep1: 720 μL of a dispersion of **A2P1F2** having a SC of 13.9 w/w% in MilliQ water (750 μM of surface COOH groups in 10 mL solution) was introduced into an Eppendorf tube. Next, 500 μL of solution containing 20 mM EDC (1 mM in 10 mL, 10 equiv. with respect to **Pep1**) in 0.05 M MES buffer (pH 6.0) and 750 μL of solution containing 20 mM Sulfo-NHS (1.5 mM in 10 mL, 15 equiv. with respect to **Pep1**) in 0.05 M MES buffer (pH 6.0) was added to the tube and the final volume of the solution was

adjusted to 10 mL by adding 8.03 mL of 0.05 M MES buffer. The activation of the surface COOH groups was allowed to continue for 30 minutes at room temperature with agitation. Next, unreacted EDC and Sulfo-NHS were removed from the dispersions via tangential flow filtration using Spectrum Labs polyethersulfone hollow fiber having a MWCO of 300000 g/mol. The final volume of the filtrate was adjusted to 5 mL in MilliQ water and 5 mL of solution containing 200 μM **Pep1** (100 μM in 10 mL) in 0.1 M PBS buffer (pH 7.5) was added. The final solid content of the dispersion was 1 w/w%. The reaction was allowed to continue for 2.5 hours at room temperature with agitation. The solutions were recovered and dialyzed against a Spectra/Por Spectra/Por Float-A-Lyzer® G2 dialysis device with a MWCO of 300000 g/mol for one day.
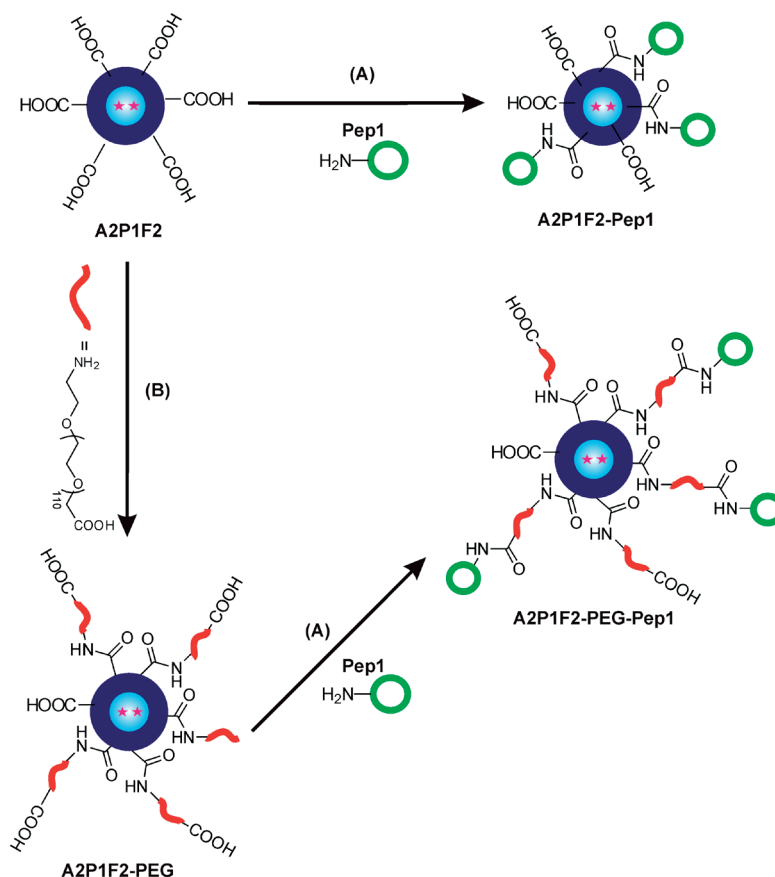
Scheme 3. Functionalization of **A2P1F2** surfaces with **Pep1** with or without the presence of a PEG linker.

A2P1F2-PEG: PEGylation of **A2P1F2** surface was carried using 1.25 equivalents of NH$_2$-PEG-COOH with respect to surface COOH groups and the synthesized particles was

named as **A2P1F2-PEG**. Briefly, 1.44 mL of dispersion of **A2P1F2** having a solid content of 13.9 w/w% in MilliQ water (1.5 mM of surface COOH groups in 10 mL solution) was introduced into an Eppendorf tube. Next, 400 μL of a solution containing 100 mM EDC (4 mM in 10 mL, 2.7 equiv. with respect to surface COOH groups) in 0.05 M MES buffer (pH 6.0) and 600 μL of a solution containing 100 mM Sulfo-NHS (6 mM in 10 mL, 4 equiv. with respect to surface COOH groups) in 0.05 M MES buffer (pH 6.0) was added to the tube and the final volume of the solution was adjusted to 5 mL by adding 2.56 mL of 0.05 M MES buffer. The activation of surface COOH groups was allowed to continue for 30 minutes at room temperature under agitation. Next, 28 μL (20 mM) 2-mercaptoethanol was added to the mixture to quench the further activation of COOH groups. After 10 minutes, 5 mL of a solution containing 4 mM NH_2-PEG-COOH (2 mM in 10 mL, 1.25 equiv. with respect to surface COOH groups) in 0.1 M PBS buffer was added to the reaction mixture. The final solid contents of the dispersions were 2 w/w%. The reactions were allowed to continue for 2.5 hours at room temperature with agitation. The solutions were recovered and dialyzed against a Spectra/Por Spectra/Por Float-A-Lyzer® G2 dialysis device with a MWCO of 300000 g/mol for one day.

A2P1F2-PEG-Pep1: The synthesis of this particle was carried using the identical procedure as described for the preparation of **A2P1F2-Pep1** and therefore will not be described in detail. The only difference was the solid content of the **A2P1F2-PEG** (2 w/w%) used in this reaction compared to **A2P1F2** (13.9 w/w%), and therefore, the amounts of EDC, sulfo-NHS and **Pep1** added to the reaction mixture were adjusted to keep the same stoichiometric ratios between the reagents. The final solid content of the dispersion was 0.5 w/w%.

Surface deposition of PS-*co*-PAA nanoparticles. Prewashed cotton samples (0.5 cm x 0.5 cm, mass = 10 - 12 mg) were inserted into wells of a 96-well plate. Next, 250 μL of fabric a softener emulsion containing 0.002 to 0.2 mg/mL of nanoparticles were introduced to the wells. In parallel, same solutions were also introduced to the wells that did not contain any cotton fabric (blank measurements) The incubation was carried out for one hour at room temperature with gentle agitation. Following the incubation, 100 μL of the solutions were transferred into a new 96-well plate. The solutions were diluted 3-fold with fabric softener emulsion, and the fluorescence intensities of the solutions (FI_{cotton}) were recorded at λ_{em} = 386 nm using λ_{ex} = 264 nm. Separately, the fluorescence intensity of the solutions introduced to the wells that do not contain any cotton (FI_{blank}) were also diluted 3-fold in a new 96-well plate and measured. The difference between the

fluorescence intensities of FI_{blank} and FI_{cotton} yielded the amount of conjugate deposited ($FI_{deposited}$). Finally, the $FI_{deposited}$ values were normalized to one with respect to the FI_{blank} values recorded in the measurements that contain the highest concentration of nanoparticles (0.2 mg/mL). All measurements were performed in triplicates on at least two independent cotton substrates.

Dynamic headspace sampling. Two prewashed cotton fabric samples (12 cm x 12 cm, mass = 3.00 – 3.30 g) were washed in a beaker with 60 mL of a fabric softener emulsion containing nanoparticle dispersions (0.072 mg/mL) and 8.7 mg of encapsulated α-pinene. An additional experiment was also carried by washing the cotton fabric samples with 600 mL of a fabric softener emulsion containing 8.7 mg of free α-pinene. The cotton samples were gently agitated for three minutes, then allowed to stand for two more minutes, and finally removed from the beakers and wrung out by hand until the mass of the wet cotton fabric samples was approximately 7.0 g. The samples were line dried for 4 hours at room temperature and inserted into a headspace cell (Volume = 160 mL) that is thermostatted at 25°C.

The following steps were performed similar to the protocol described by Trachsel *et al.*[40] A 200 mL/min air flow that was filtered through activated charcoal and bubbled through a saturated NaCl solution, which allows to keep the humidity constant at 75%, was aspirated through the headspace cell. α-pinene evaporated from the surface of the cotton fabric samples was first collected using a waste Tenax® cartridge in the first 30 minutes in order to allow the equilibration of the system. Afterwards, the waste cartridge was replaced by the sample Tenax® cartridge and the evaporated α-pinene was collected for 15 minutes (4.5 hours after washing). Evaporated α-pinene was collected two more times for 15 minute periods 5.5 and 6.5 hours after washing, respectively, using new sample Tenax® cartridges. Each experiment was carried two times using two different cotton fabric samples (duplicates). The sample cartridges were thermally desorbed on a Perkin Elmer TurboMatrix ATD desorber coupled to an Agilent Technolgies 7890 A gas chromatograph (GC) equipped with an HP-1 capillary column (30 m, i.d. 0.32 mm, film thickness 0.25 μm). The GC analysis was performed using a one-step gradient from 70 °C to 200 °C at 20 °C/min. Headspace concentrations of α-pinene were obtained via external standard calibrations using 5 different α-pinene concentrations between 3.9×10^{-2} to 1.0×10^{-5} M in acetone. 2 μL of these solutions were injected into sample Tenax® cartridges and immediately desorbed and subsequently analyzed using the same protocol described

above. Plotting the α-pinene concentrations in ng/L as a function of GC peak areas yielded a straight line with a correlation coefficient (R^2) of 0.9997.

3.3. Results and Discussion

3.3.1. Identification of cotton binding peptides via phage display.

The first step towards the construction of fragrance delivery systems that selectively deposit onto cotton fabric under fabric softening conditions was the identification of cotton fabric binding peptides using phage display. These peptides can be, in theory, used to enhance the deposition of any fragrance delivery system onto cotton under softener conditions. This enhanced deposition would then allow to release higher amounts of fragrance from the cotton surface. Alternatively, the grafting of these peptides onto fragrance delivery systems would permit reducing the amount of delivery system while delivering the same amount of fragrance as compared to delivery systems that are not functionalized with the peptide.

In order to identify cotton fabric binding peptides, a combinatorial phage library displaying a randomized 9-mer cyclic peptide disulfide (C9C) was employed. A cyclic library was chosen rather than a linear one, as it was previously shown that the phage libraries displaying conformationally constrained cyclic sequences can allow the identification of binders with greater affinities as compared to linear, flexible sequences.[41,42] Furthermore, incubation of the phage library with the cotton fabric was carried out in fabric softening conditions rather than in standard buffers (*i.e.* 0.1 M PBS, pH 7.4) in order to identify binders that can be directly used under realistic application conditions, as it was already demonstrated that the use of different incubation media may lead to the isolation of entirely different sequences.[43]

Four different phage display experiments were performed in parallel by either varying the stringency of the washing step (**Conditions 1** and **2**) or by carrying out the infection step with or without eluting the cotton fabric bound phages following the washing (**Conditions a** and **b**). These four experiments were named as **1a**, **1b**, **2a** and **2b** depending on the washing and elution steps performed and they are summarized in **Table S1**. Each of these experiments was carried up to the 5th round. The enrichment of the phage library towards the cotton fabric with respect to the number of selection rounds

was monitored by counting the output phage titers in all of the experiments. **Figure S1** shows that in each of these experiments, output phage titers gradually increased to 10^8-10^9 pfu/mL after the 5th round from 10^4-10^6 pfu/mL after the 1st round of selection, suggesting 10^3-10^5 fold enrichments of the starting phage library towards cotton fabric. Higher output phage titers were obtained when cotton bound phages were not eluted following the washing step (**Conditions 1b** and **2b**). On the other hand, the stringency of the washing conditions did not significantly affect the evolution of the output phage titers.

Table 1. List of potentially affine cotton fabric binding peptides identified by phage display, their frequency in the sequencing analysis as well as their apparent binding strength (K_{app}) and maximum relative affinity (RA_{max}), which were calculated from phage ELISA experiments.

Sequence ID.	Sequence	Frequency / Total frequency	K_{app} / 10^{10} M^{-1}	RA_{max}
Seq1	**C** T W Q M L E D V F **C**	5/96	11.4	1.88
Seq2	**C** Q S I M G L L H Y **C**	29/96	7.2	1.59
Seq3	**C** Q A G W G P L H Y **C**	1/96	6.2	1.34
Seq4	**C** A K R W G P L H Y **C**	1/96	5.3	1.62
Seq5	**C** S V L Y G Q L H F **C**	1/96	4.7	1.31
Seq6	**C** Q N I M G L L H Y **C**	1/96	1.2	1.82
Seq7	**C** K V W V G Q L H V **C**	1/96	-	-
Seq8	**C** S S L W G E L H I **C**	1/96	-	-
Seq9	**C** Q G F Y G A L H L **C**	1/96	-	-

Random colonies were picked from the 3rd, 4th and 5th round of selection and they were sent to sequencing analysis. **Table 1** shows that out of 96 sequenced colonies, 29 of them had the sequence **CQSIMGLLHYC** (**Seq2**). The selection of this sequence did not seem to depend on the phage display experiment carried out, as it was selected in each of the four independent experiments**.** Furthermore, seven other colonies shared consensus with this sequence such that the 5th, 7th and 8th amino acids were G, H and Y, respectively, in all of these sequences. Another sequence (**CTWQMLEDVFC** – **Seq1**), which did not share any consensus with other sequences, was also detected 5 times. This sequence was only observed in the experiments in which the cotton fabric bound phage was eluted prior to infection (Experiments **1a** and **2a**). These results suggest that the phage display experiments carried out on cotton fabric under softener conditions successfully led to the enrichment of the phage library towards cotton and allowed the isolation of potentially affine cotton binding sequences. One common feature of the selected sequences was that

they were primarily composed of non-charged amino acids and therefore it is possible to speculate that peptide-cotton fabric interactions are dominated by hydrogen bonding and Van der Waals forces.

The next step was to verify the relative affinities and the apparent binding strengths of the isolated sequences via phage ELISA. Phage ELISA was carried by using the individual colonies that were selected as potentially affine cotton fabric binders and also the combinatorial phage library, which served as a control. Furthermore, phage ELISA of a sequence isolated from the 3rd round of selection (**C**HPQVGYYPG**C**), which was speculated to be a "nuisance" sequence, was also performed. This sequence is referred to **SeqN**. Relative affinities of the individual phage clones were reported with respect to the phage ELISA signal of the library. The calculation of the relative affinities and the apparent binding strengths were performed by using Serizawa's method.[28]
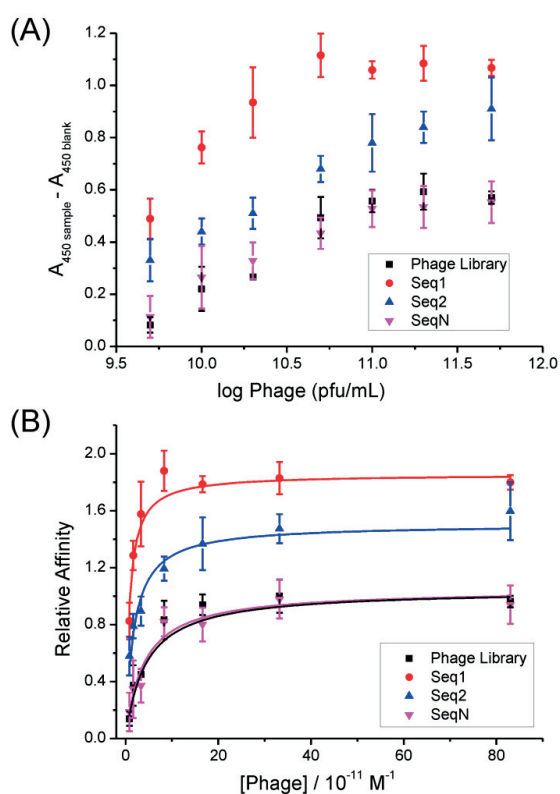

Figure 1. Evolution of the (A) colorimetric response and the (B) relative affinity as a function of phage concentration in the phage ELISA experiments of **Seq1**, **Seq2**, **SeqN** and the combinatorial phage library. The error bars represent the standard deviation of 9 independent measurements.

Figure 1A shows the normalized phage ELISA signal of **Seq1**, **Seq2**, **SeqN** and the phage library and **Figure 1B** illustrates the calculated relative affinities as a function of phage concentration with the corresponding Langmuir adsorption fittings. Phage ELISA experiments revealed that **Seq1**, which did not share any consensus with the other isolated sequences, was the strongest cotton fabric binder under softener conditions with a maximum relative affinity (RA_{max}) of 1.9. **Seq2**, which was the most frequently selected sequence in the phage display experiments, did not bind to cotton fabric as much as **Seq1** as it had a RA_{max} of 1.6. On the other hand, the Langmuir adsorption fit of **SeqN** did not differ from that of the phage library, which indicates that it was not a selective cotton fabric binder. **Table 1** summarizes the RA_{max} and the apparent binding strengths of the isolated sequences. Phage ELISA results of all of the investigated sequences were provided in **Figure S8.** These phage ELISA experiments provided further evidence that the phage display has successfully led to the isolation of cotton fabric binding peptide sequences, which can be used to construct fragrance delivery systems that recognizes and selectively deposits onto cotton fabric under fabric softening conditions.

3.3.2. Cotton binding Pep1-PHPMA conjugates as a model polymeric profragrance platform

3.3.2.1. Design strategy and the synthesis of the conjugates.

Following the identification of **Seq1** as the strongest cotton fabric binding peptide via phage display, the next step was to explore whether the incorporation of this sequence would enhance the deposition of such a system on cotton. These linear polymers in fact can be utilized as polymeric profragrance platforms with the additional incorporation of fragrance molecules that can be released in the presence of external stimuli, such as pH, light and temperature.[4,6,7] In order to achieve this, poly(*N*-(2-hydroxypropyl) methacrylamide) (PHPMA) was selected as the polymer platform owing to its biocompatibility, solubility in aqueous media as well as the possibility to prepare multifunctional copolymers starting from a reactive active ester precursor, such as poly(pentafluorophenyl methacrylate) (PPFMA).[37,44] This route has already been explored to prepare peptide-polymer conjugates[45-47] and therefore, it is an attractive model system as peptide functionalized polymeric profragrances.

Prior to the preparation of the **Pep1**-PHPMA conjugates, the first step was the synthesis of the cotton binding peptide via standard F-moc based SPPS. A GGG sequence was added to the N-terminal of **Seq1** as a flexible linker and a single glycine was incorporated to its C-terminal to prevent the racemization of the peptide during synthesis.[48] Following the cleavage of the crude, linear peptide, the cyclic peptide was obtained via DMSO mediated oxidation. The resulting peptide (cyclo(NH$_2$-GGG**C**TWQMLEDVF**C**G-amide)) was named **Pep1**. The HPLC elution profile and the ESI-MS spectrum of pure **Pep1** were provided in **Figure S2.**

Table 2. Summary of the characterization and the extent of cotton fabric deposition of **Pep1**-PHPMA conjugates. In addition to **Pep1**, each of the reported PHPMA conjugates also incorporate 7 mol% of dansyl cadaverine groups.

Polymer name	Pep1 [a]		SEC analysis[b]			Fluorescence intensity measurements	
	Feed (mol%)	Incorporated (mol%)	M_w (g/mol)	M_n (g/mol)	PDI	Extent of polymer deposition (%)	Relative deposition with respect to **PC**
PHPMA	-	-	43200	30700	1.41	-	-
PC	-	-	42200	30000	1.40	12.6 ± 2.5	-
PPep1a	3.0	0.5	40200	27400	1.47	24.2 ± 4.4	1.92 ± 0.35
PPep1b	5.0	0.9	38400	25200	1.53	31.4 ± 3.1	2.49 ± 0.25
PPep1c	7.0	1.3	36600	23900	1.53	35.7 ± 4.8	2.83 ± 0.38

[a] Calculated from the ^{1}H-NMR spectra of the conjugates in methanol-d$_4$.
[b] Calculated by SEC analysis of the conjugates in DMF.

A three step post-polymerization modification was employed for the preparation of water soluble **Pep1-PHPMA** conjugates containing different amounts of **Pep1** (**Scheme 2**). These conjugates were named as **PPep1a**, **PPep1b** and **PPep1c** and contained 0.5, 0.9 and 1.3 mol% of **Pep1**, respectively. Furthermore, a fixed amount of fluorescent dansyl cadaverine (7 mol% with respect to starting PFMA groups) was incorporated to these polymers. The extent of **Pep1** incorporation was calculated from the ^{1}H-NMR peak integral ratios associated with the imidazole ring of the histidine at 7.01-7.09 ppm and the average of the three aromatic proton integrals of dansyl groups between 8.17-8.54 ppm by assuming the absence of PFMA hydrolysis. A fourth conjugate that did not contain any **Pep1** but only 7 mol% dansyl cadaverine was also synthesized (**PC**), and it served as the control conjugate in the fluorescence intensity measurements. **Figure S3** provides the ^{1}H-NMR spectra of these four conjugates in methanol-d$_4$ with the complete assignment of the

signals. SEC analysis of these conjugates in DMF revealed a monomodal distribution, indicating the absence of cross-linking side reactions during post-polymerization modification. **Table 2** summarizes the characterization of the **Pep1**-PHPMA conjugates. It is worth mentioning that the increased **Pep1** incorporation resulted in lower measured molecular weights of PHPMA conjugates in SEC analysis. This was presumed to arise from the hydrophobic nature of the peptide, which led to a decrease in the hydrodynamic volume of the conjugates in a polar organic solvent such as DMF.

3.3.2.2. Deposition of Pep1-PHPMA conjugates.

In the next step, **Pep1**-PHPMA conjugates were deposited on cotton under fabric softening conditions (0.01-0.02 mg/mL), and the extent of deposition was assessed via fluorescence intensity measurements. **Figure 2A** shows the normalized fluorescence intensity associated with the amount of deposited conjugate onto cotton fabric as a function of conjugate concentration for each of the four polymers. The average deposition (%) of the conjugates over a concentration range of 0.01-0.2 mg/mL was calculated from the slope of the linear curve fittings. These measurements demonstrated the improved deposition of PHPMA conjugates with increased **Pep1** incorporation, such that 0.5 (**PPep1a**) 0.9 (**PPep1b**) and 1.3 (**PPep1c**) mol% of polymer bound peptide led to 25.2, 31.4 and 35.7% deposition of **Pep1**-PHPMA conjugates, respectively. On the other hand, the PHPMA conjugate that did not contain any **Pep1** (**PC**) only deposited at 12.6%. These results indicate that the **Pep1** incorporation onto PHPMA conjugates led to 2-3 fold enhancements of the deposition to the cotton fabric under softener conditions (**Table 2**). Additionally, the cotton fabric samples incubated with 0.2 mg/mL of polymer conjugates were removed from the wells, dried and excited under a 8 W fluorescent lamp operating at λ_{ex} = 335 nm in order to visualize the deposition of the **Pep1**-PHPMA conjugates with increased peptide incorporation (**Figure 2B**). These results suggest that the **Pep1** promotes the deposition of PHPMA copolymers onto cotton fabric, and it can be of use to construct potential polymeric profragrance systems that selectively bind to cotton surfaces and subsequently release the fragrances.
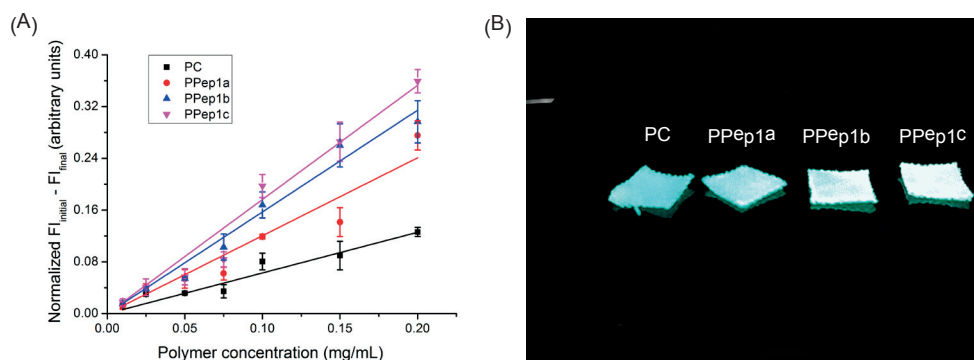
Figure 2. (A) Normalized fluorescence intensity associated with the cotton fabric deposited **Pep1**-PHPMA conjugates as a function of polymer concentration. Error bars represent the standard deviation of 9 measurements. (B) Cotton fabric samples excited at 365 nm with an 8 W fluorescent lamp following their exposure to 0.2 mg/mL of **Pep1**-PHPMA conjugates.

3.3.3. Cotton binding PS-*co*-PAA nanoparticles as a model polymeric fragrance carrier.

3.3.3.1. Design strategy of the nanoparticles.

Following the demonstration that the incorporation of **Pep1** into linear PHPMA conjugates enhanced their deposition on cotton, the final step was to explore whether this peptide would also be of use to improve the deposition of other polymeric fragrance carriers onto cotton fabric. Miniemulsion polymerization is an attractive strategy to prepare polymeric fragrance carriers for a variety of reasons. First, it has already been used to prepare nanoparticles that effectively encapsulate hydrophobic fragrances in their core and provide long term storage and subsequently release of these volatile compounds.[12-16] Second, these nanoparticles are often stabilized by surfactants such as SDS, and thus are highly dispersed in aqueous media, which is critical for fragrance delivery to cotton under laundry wash conditions. Furthermore, functional monomers such as acrylic acid, 2-aminoethyl methacrylate and many others[49] are compatible with miniemulsion polymerization and they can be copolymerized with a main monomer to yield nanoparticles having surface functional groups (*i.e.* COOH, NH$_2$ groups). These groups can be used to attach **Pep1** to the particle surfaces.

3.3.3.2. Synthesis of α-pinene loaded PS-*co*-PAA nanoparticles

To obtain peptide functionalized polymeric fragrance carriers, first the miniemulsion copolymerization of styrene and acrylic acid using AIBN as the initiator, hexadecane (HD) as the superhydrophobe and SDS as the surfactant was carried out.[39] α-Pinene and pyrene were chosen as the model fragrance and the fluorescent dye, respectively, as they were already demonstrated to be compatible with miniemulsion polymerization.[14,50] The styrene, acrylic acid, α-pinene and pyrene composition of the nanoparticles was optimized following several experiments, which were summarized in **Table 3**. First, nanoparticles were prepared by varying the styrene to acrylic acid feed ratio without using any α-pinene and pyrene (**AO-A2**). A styrene to acrylic acid feed ratio of 10:1 led to 97 mol% of styrene and 62 mol% of acrylic acid conversion (**A2** in **Table 3**). These conversions were calculated from ^{1}H-NMR analysis of an aliquot taken immediately after the polymerization in THF-d_8 (**Figure S4A-S4C**). The synthesized nanoparticles had a narrow size distribution (PDI = 0.031) with an average diameter of 136 nm as evidenced by DLS analysis and contained 2.07×10^5 surface COOH groups per particle according to conductometric titration experiments (**A2** in **Table 4**). The DLS size distribution data and the conductometic titration curves of the particles were provided in Figure **S5** and **S7**. Cryo-TEM images of **A2** further verified the relatively monodisperse nature of the synthesized nanoparticles (**Figure 3A**) and the imaging analysis revealed an average particle diameter of 121 nm.

Table 3. Characterization of α-pinene and pyrene loaded PS-*co*-PAA nanoparticles prepared by miniemulsion polymerization.

Particle name	Feeds				Conversions[a]		Coagulum (w/w%)[b]	$\varepsilon_{\alpha\text{-}pinene}$ (%)	SC_{NMR} (w%)[a]	SC_{ly} (w%)[b]
	$f_{styrene}$ (w/w%)	f_{AA} (w/w%)	$f_{\alpha\text{-}pinene}$ (w/w%)	f_{pyrene}* (w/w%)	$p_{styrene}$ (mol%)	P_{AA} (mol%)				
A0	100	0	0	0	100	-	0	-	20.0	19.7
A1	95	5	0	0	100	57	1.4	-	19.2	19.2
A2	90	10	0	0	98	62	6.3	-	18.0	17.4
A2P1	72	8	20	0	96	60	0	78	14.7	16.1
A2P1F1	72	8	20	2	97	44	4	63	14.0	16.1
A2P1F2	72	8	20	1	95	45	0	86	13.9	16.0
A2P2	54	6	40	0	57	3	6.8	48	6.2	8.1

[a] Calculated from the ^{1}H-NMR of an aliquot of the reaction mixture taken immediately after the polymerization in THF-d_8.

[b] Calculated gravimetrically.

* Weight fraction of pyrene = mass of pyrene added / (mass of styrene + comonomer + fragrance).
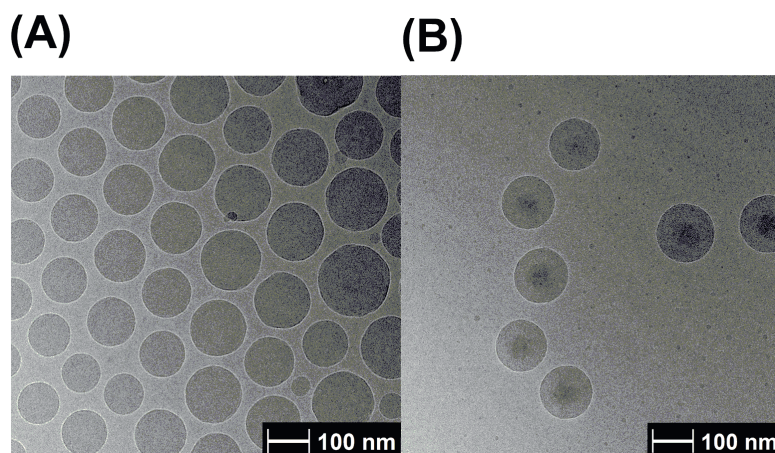
Figure 3. Cryo-TEM images of (A) **A2** and (B) **A2P1F2** nanoparticles.

In the second step, 20 or 40 w/w% of α-pinene was introduced to the organic phase by keeping the styrene to acrylic acid feed ratio at 10:1 (**A2P1** and **A2P2**). **Table 3** shows that 40 w/w% of α-pinene (**A2P2**) significantly decreased the styrene conversion, almost completely inhibited the acrylic acid polymerization and only led to 48% encapsulation ($\varepsilon_{\alpha\text{-pinene}}$) of the fragrance as evidenced from ^{1}H-NMR analysis in THF-d_8 (**Figure S4E**). Furthermore, conductometric titration of **A2P2** did not reveal any surface COOH groups (**Figure S7**) further providing evidence that 40 w/w% of α-pinene has inhibited the polymerization of acrylic acid. Therefore, 20 w/w% of α-pinene was kept constant in later experiments as it still allowed quantitative conversion of styrene, 60 mol% conversion of acrylic acid and the $\varepsilon_{\alpha\text{-pinene}}$ of **A2P1** was 78%. Conductometic titration, however, revealed a decreased surface COOH concentration for **A2P1** (1.33 $(\text{nm}^2)^{-1}$) as compared to **A2** (2.07 $(\text{nm}^2)^{-1}$) (**Table 4** and **Figure S7**).

The final step of the optimization was carried out by additionally adding either 1 or 2 w/w% of pyrene with respect to the organic phase (**A2P1F2** and **A2P1F1**, respectively). **Table 4** and **Figure S5** shows that 2 w/w% of pyrene yielded nanoparticles with a bimodal size distribution. In order to circumvent this, the pyrene content was reduced to 1 w/w% with respect to the organic phase (**A2P1F2),** which afforded monodisperse nanoparticles with an average diameter of 145 nm as evidenced by DLS analysis (**Figure S5**). These particles have also effectively encapsulated the fragrance as ^{1}H-NMR analysis revealed an $\varepsilon_{\alpha\text{-pinene}}$ value of 86% (**Figure S4G**). Furthermore, Cryo-TEM images clearly showed the core-shell type morphology of **A2P1F2**, which provides visual evidence for

the successful encapsulation of α-pinene in the core of these particles (**Figure 3**). On the other hand, the surface COOH concentration of **A2P1F2** (1.14 $(nm^2)^{-1}$) was even smaller compared to that of **A2P1** (1.33 $(nm^2)^{-1}$). This was due to the fact that the acrylic acid conversion was decreased from 60 to 45 mol% with the addition of 1 w/w% pyrene (**Table 4**). This COOH concentration, however, was considered to be still sufficient to functionalize the particle surface with **Pep1.** Following these optimization steps, **A2P1F2** was chosen as the model polymeric fragrance carrier and subsequently functionalized with **Pep1.**

Table 4. DLS and conductometic titration analyses of α-pinene and pyrene loaded PS-*co*-PAA nanoparticles.

Particle name	DLS data[a]		Number of surface -COOH groups per[b]	
	z-average (nm)	PDI	particle	nm^2
A0	131	0.013	-	-
A1	119	0.042	8.30×10^4	1.87
A2	136	0.031	2.07×10^5	3.56
A2P1	127	0.043	6.74×10^4	1.33
A2P1F1	104 * 366 *	0.220	N.A.	N.A.
A2P1F2	145	0.098	7.53×10^4	1.14
A2P2	178	0.140	0	0

[a] Measured in 10 mM NaCl solution.

[b] Determined via conductometric titration.

* A multimodal size distribution was observed.

3.3.3.3. Peptide functionalization of nanoparticle surfaces.

Prior to the functionalization of **A2P1F2** surfaces with **Pep1**, first the feasibility of the peptide incorporation onto the particle surfaces was explored. This was achieved by measuring the fluorescence intensity associated with surface bound peptide following the EDC/Sulfo-NHS reaction between C-terminal dansylated GGG**C**QSIMGLLHY**C**G (**Pep2D**) and **A2P1**. The synthesis of **Pep2D** as well as the EDC/Sulfo-NHS coupling protocol was summarized in Supporting Information (**Scheme S1**) and its HPLC elution profile and the ESI-MS spectrum was provided in **Figure S9**. Since the purification of C-terminal dansylated **Pep1** could not be achieved, this model particle surface functionalization was carried out with the peptide that was found to be the second most

affine to cotton fabric surfaces. **Figure S10** shows the fluorescence emission spectra of 100 μM of free **Pep2D** and **A2P1-Pep2D** when 100 μM of the peptide was used in the reaction. Although these emission spectra verified the presence of surface bound **Pep2D**, its surface concentration could not be calculated owing to the significant enhancement of the dansyl group fluorescence following the attachment of the peptide to the particle surface. This can be attributed to the interactions between the SDS groups that are present in the particle surface and the dansyl groups, which was previously demonstrated to enhance the fluorescence of dansyl derivatives by Cao *et al*.[51]

In the next step, the surface of **A2P1F2** nanoparticles was functionalized with **Pep1** either with or without the presence of a NH$_2$-PEG-COOH linker. The functionalization was achieved via one or two-step EDC/Sulfo-NHS coupling reaction between surface COOH and peptide and/or PEG NH$_2$ groups (**Scheme 3**). The direct functionalization of **A2P1F2** surface COOH groups with **Pep1** resulted in no significant change in the zeta-potential of the particles, which were named as **A2P1F2-Pep1** (**Table 5 – Figure S6**). In the second strategy, a PEG linker was first introduced to **A2P1F2** surfaces in order to circumvent the macroscopic aggregation of the particles in softener media, which was observed during the fluorescence intensity measurements of non-PEGylated particles. This aggregation is presumed to take place due to the attractive electrostatic interactions between the negatively charged sulfate groups of SDS and the cationic surfactant present in the softener formulation. Therefore a PEG layer was introduced to the particles in order to stabilize them sterically in fabric softener medium by shielding these electrostatic interactions. Furthermore, since SDS is known to be a strong peptide chelator,[51] which can cause a change in the conformation and thus the affinity of the peptide, it would be beneficial to separate the peptide and SDS groups with a PEG spacer.

The PEGylation of **A2P1F2** nanoparticles led to a decrease in zeta-potential from -68 to -49 mV, indicating partial shielding of the SDS groups, while the average size of the particles was slightly increased from 145 to 148 nm (**Table 5, Figure S5-56**). This particle was named as **A2P1F2-PEG**, and it was found to be stable under fabric softening conditions unlike non-PEGylated ones. In the final step, **Pep1** was incorporated to **A2P1F2-PEG** and this incorporation yielded an average particle size of 172 nm with an increased particle size distribution from 0.096 to 0.190, which suggests partial aggregation of the particles (**A2P1F2-PEG-Pep1 – Table 5**). This partial aggregation was further supported by a decrease in the zeta potential from -49 to -27 mV, which indicates significantly decreased electrostatic stabilization of these particles. However,

the dispersion of **A2P1F2-PEG-Pep1** particles in fabric softener emulsion did not result with the formation of macroscopic aggregates. Therefore, **A2P1F2-PEG-Pep1** can be used as a model carrier system to assess the influence of **Pep1** to the deposition of these nanoparticles onto cotton via fluorescence intensity measurements in the next step.

3.3.3.4. Deposition of PS-*co*-PAA nanoparticles.

Following the optimization of the peptide functionalized nanoparticles as model polymeric fragrance carriers, fabric softener emulsions containing particles varying from 0.001 to 0.02 w/w% (0.01 to 0.2 mg/mL) were exposed to cotton fabric to assess the extent of deposition of these particles onto cotton via fluorescence intensity measurements. **Figure 4A** shows the normalized fluorescence intensity associated with the amount of deposited particles onto cotton fabric as a function of particle solid contents (SC). The average deposition (%) of the particles was calculated from the slope of the linear curve fittings. These results show that the **Pep1** incorporation enhanced the deposition of both PEGylated and non-PEGylated particles. Furthermore, the stabilization of the particles in softener conditions as well as the separation of the surface SDS groups and the peptide via PEGylation further improved the deposition to 13.0% for **A2P1F2-PEG-Pep1** compared to 10.2% for the **A2P1F2-Pep1**. The extent of the deposition of the particles was summarized in **Table 5**. These results indicate that successive PEGylation and **Pep1** incorporation improve the deposition of **A2P1F2** nanoparticles by two-fold, and verify the feasibility of using **Pep1** to enhance the surface deposition of polymeric fragrance carriers.

Table 5. DLS, fluorescence intensity and dynamic headspace concentrations of PEG and/or **Pep1** functionalized nanoparticles.

Particle name	DLS data[a]			Fluorescence intensity measurements		Dynamic headspace measurements	
	z-average (nm)	PDI	ζ (mV)	Deposition (%)	Relative deposition w. r. t. to **A2P1F2**	[α-pinene] released after 90 min. of sampling (ng/L)	[α-pinene]relative w. r. t. **A2P1F2** after 90 min. sampling (ng/L)
A2P1F2	145	0.098	-68	7.1 ± 0.9	-	3.9 ± 0.4	-
A2P1F2-Pep1	139	0.083	-71	10.2 ± 2.6[*]	1.44 ± 0.37[*]	6.7 ± 0.7	1.71 ± 0.18
A2P1F2-PEG	148	0.096	-49	6.6 ± 0.4	0.93 ± 0.06	5.6 ± 0.8	1.44 ± 0.20
A2P1F2-PEG-Pep1	172	0.190	-27	13.0 ± 1.8	1.97 ± 0.27	8.5 ± 0.4	2.18 ± 0.10

[a] Measured in 10 mM NaCl solution.

* This particle partially aggregated in fabric softener emulsion after 1 hours of incubation.

3.3.3.5. Dynamic headspace sampling of fragrance evaporation from PS-*co*-PAA nanoparticles.

In a final effort to elucidate whether the **Pep1**-mediated improved deposition of these particles resulted in an increased α-pinene release from cotton fabric surfaces, dynamic headspace sampling measurements were carried out. In order to achieve this, cotton fabric samples were treated with particle dispersions containing a fixed amount of α-pinene (8.7 mg) under fabric softening conditions and subsequently wrung out and dried for four hours prior to headspace sampling. Apart from the nanoparticles, 8.7 mg of non-encapsulated α-pinene was also used as a reference to explore the influence of fragrance encapsulation on its release from cotton fabric surfaces. **Figure 4b** shows the headspace concentrations of α-pinene that was released from the cotton fabric surfaces after a sampling time of 30, 90 and 150 minutes. First, these results show that the encapsulation of α-pinene in **A2P1F2** already increased the fragrance deposition and release from the cotton surface. Furthermore, the **Pep1** mediated enhanced deposition of particles also led to a further increase in the fragrance release from cotton fabric surfaces, such that approximately 2.2-fold higher α-pinene release was detected for **A2P1F2-PEG-Pep1** as compared to **A2P1F2**. **Table 4** summarizes the α-pinene headspace concentrations after a sampling time of 90 minutes. In summary, these headspace sampling and fluorescence intensity measurements illustrate that **Pep1** can also be used to engineer polymeric fragrance carriers that selectively deposits onto cotton fabric under softener conditions.
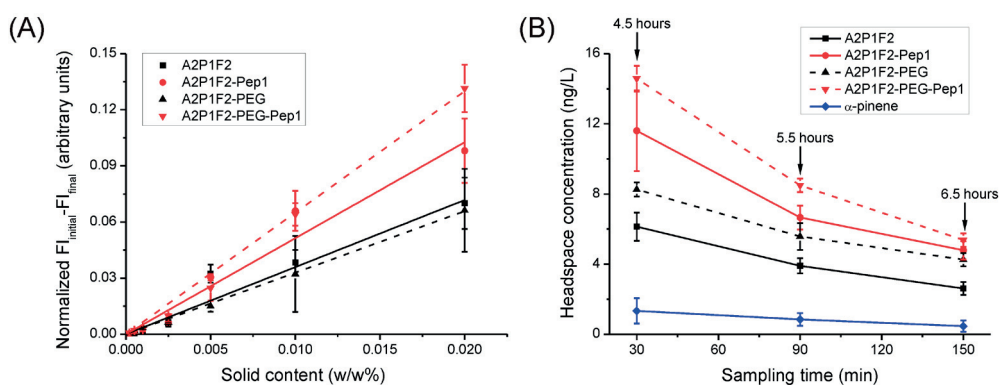
Figure 4. (A) Normalized fluorescence intensity associated with the cotton fabric deposited nanoparticles as a function of particle solid content of the dispersions. Error bars represent the standard deviation of 6 measurements. (B) Headspace concentrations of α-pinene as a function of sampling time following the exposure of the cotton fabric

samples to nanoparticles and free α-pinene. The arrows indicate the time after the incubation of the cotton fabric with the particle dispersions. Error bars represent the standard deviation of 4 measurements.

3.4. Conclusions

Phage display identified peptides can open new avenues to engineer materials having superior properties compared to the conventional ones. In this work, a cotton fabric binding peptide was identified by phage display and subsequently used to enhance the deposition of model fragrance delivery systems based on linear polymers and nanoparticles onto cotton under fabric softening conditions. While linear PHPMA copolymers and PS-*co*-PAA nanoparticles were used as model polymeric fragrance delivery systems in the scope of this work, it can be envisioned that this phage display identified peptide can theoretically enable the selective surface deposition of any system onto cotton under softening conditions.

3.5. References

(1)   Quellet C.; Schudel, M.; Ringgenberg, R. *Chimia* **2001**, *55*, 421-428.

(2)   Friberg, S. E. *Adv. Colloid Interface Sci.* **1998**, *75*, 181-214.

(3)   Bauer, K.; Garbe, D.; Surburg, H. ed. John Wiley & Sons, *Common fragrance and flavor materials: preparation, properties and uses.* John Wiley & Sons, 2008.

(4)   Herrmann, A. *Angew. Chem. Int. Edit.* **2007**, *46*, 5836-5863.

(5)   Berthier, D.; Trachsel, A.; Fehr, C.; Ouali, L.; Herrmann, A. *Helv. Chim. Acta* **2005**, *88*, 3089-3108.

(6)   Morinaga, M.; Morikawa, H.; Wang, Y.; Sudo, A.; Endo, T. *Macromolecules* **2009**, *42*, 2229-2235.

(7)   Berthier, D. L.; Paret, N.; Trachsel, A.; Herrmann, A. *Bioconjugate Chem.* **2010**, *21*, 2000-2012.

(8)   Suzuki, K.; Saito, Y.; Tokuoka, Y.; Abe, M.; Sato, T. *J. Am. Chem. Oil Soc.* **1997**, *74*, 55-59.

(9)   Berthier, D. L.; Schmidt, I.; Fieber, W.; Schatz, C.; Furrer, A.; Wong, K.; Lecommandoux, S. *Langmuir* **2010**, *26*, 7953-7961.

(10)   Kreutzer, G.; Ternat, C.; Nguyen, T. Q.; Plummer, C. J. G.; Månson, J.-A. E.; Castelletto, V.; Hamley, I. W.; Sun, F.; Sheiko, S. S.; Herrmann, A.; et al. *Macromolecules* **2006**, *39*, 4507-4516.

(11)   Ternat, C.; Ouali, L.; Sommer, H.; Fieber, W.; Velazco, M. I.; Plummer, C. J. G.; Kreutzer, G.; Klok, H.-A.; Månson, J.-A. E.; Herrmann, A. *Macromolecules* **2008**, *41*, 7079-7089.

(12)   Theisinger, S.; Schoeller, K.; Osborn, B.; Sarkar, M.; Landfester, K. *Macromol. Chem. Phys.* **2009**, *210,* 411-420.

(13)   Jing, H.; Weijun, D.; Liqin, L.; Zuobing, X. *J. Appl. Polym. Sci.* **2014**, *131*, 40182-40188.

(14)   Hofmeister, I.; Landfester, K.; Taden, A. *Macromolecules* **2014**, *47*, 5768-5773.

(15)   Hofmeister,I.; Landfester,K.; Taden,A. *Angew. Chem. Int. Edit.* **2015**,*54*,327-330.

(16)   Popadyuk, N.; Popadyuk, A.; Kohut, A.; Voronov, A. *Int. J. Cosmetic Sci.* **2015**, 1-9.

(17)   Hosseinkhani, B.; Callewaert, C.; Vanbeveren, N.; Boon, N. *New Biotechnol.* **2015**, *32*, 40-46.

(18)   Berthier, D.; Paret, N.; Trachsel, A.; Fieber, W.; Herrmann, A. *Polymers* **2013**, *5*, 234-253.

(19)   Smith, G. P.; Petrenko, V. A. *Chem. Rev.* **1997**, *97*, 391-410.

(20)   Cortese, R.; Felici, F.; Galfre, G.; Luzzago, A.; Monaci, P.; Nicosia, A. *Trends Biotechnol.* **1994**, *12*, 262-267.

(21)   Rodi, D. J.; Makowski, L. *Curr. Opin. Biotechnol.* **1999**, *10*, 87-93.

(22)   Sarikaya, M.; Tamerler, C.; Jen, A. K. Y.; Schulten, K.; Baneyx, F. *Nat. Mater.* **2003**, *2*, 577-585.

(23)   Artzy Schnirman, A.; Zahavi, E.; Yeger, H.; Rosenfeld, R.; Benhar, I.; Y. Reiter,Y.; Sivan, U. *Nano Lett.* **2006**, *6*, 1870-1874.

(24)   Chen, H.; Su, X.; Neoh, K.-G.; Choe, W.-S. *Anal. Chem.* **2006**, *78*, 4872-4879.

(25)   Wang, S.; Humphreys, E. S.; Chung, S.-Y.; Delduco, D. F.; Lustig, S. R.; Wang, H.; Parker, K. N.; Rizzo, N. W.; Subramoney, S.; Chiang, Y.-M.; Jagota, A. *Nat. Mater.* **2003**, *2*, 196-200.

(26)   Cui, Y.; Kim, S. N.; Jones, S. E.; Wissler, L. L.; Naik, R. R.; McAlpine, M. C. *Nano Lett.* **2010**, *10*, 4559-4565.

(27)   Sanghvi, A. B.; Miller, K. P. H.; Belcher, A. M.; Schmidt, C. E. *Nat. Mater.* **2005**, *4*, 496-502.

(28)   Serizawa, T.; Sawada, T.; Matsuno, H.; Matsubara, T.; Sato, T. *J. Am. Chem. Soc.* **2005**, *127*, 13780-13781.

(29)   Serizawa, T.; Sawada, T.; Matsuno, H. *Langmuir*, **2007**, *23*, 11127-11133.

(30)   Günay, K. A.; Klok, H.-A. *Bioconjugate Chem.* **2015**, *26*, 2002-2015.

(31)   Serizawa, T.; Iida, K.; Matsuno, H.; Kurita, K. *Chem. Lett.* **2007**, *36*, 988-989.

(32)   Qi, M.; O'Brien, J. P.; Yang, J. J. *Biopolymers* **2008**, *90*, 28-36.

(33)   Guo, J.; Catchmark, J. M.; Mohamed, M. N. A.; Benesi, A. J.; Tien, M.; Kao, T. H.; Watts, H. D.; Kubicki, J. D. *Biomacromolecules* **2013**, *14*, 1795-1805.

(34)   Kumar, M.; Sanford, K. J.; Cuevas, W. P.; Du, M.; Collier, K. D.; Chow, N. *Biomacromolecules* **2006**, *7*, 2543-2551.

(35)   Heinis, C.; Rutherford, T.; Freund, S.; Winter, G. *Nat. Chem. Biol.* **2009**, *5*, 502-507.

(36)   Eberhardt, M.; Théato, P. *Macromol. Rapid Commun.* **2005**, *26*, 1488-1493.

(37)   Gibson, M. I.; Fröhlich, E.; Klok, H.-A. *J. Polym. Sci. Polym. Chem.* **2009**, *47*, 4332-4345.

(38)   Perrier, S.; Takolpuckdee, P.; Mars, C. A. *Macromolecules* **2005**, *38*, 2033-2036.

(39)   Musyanovych, A.; Rossmanith, R.; Tontsch, C.; Landfester, K. *Langmuir*, **2007**, *23*, 5367-5376.

(40)   Trachsel, A.; Chapuis, C.; Herrmann, A. *Flavour Frarance J.* **2013**, *28*, 280-293.

(41)   Koivunen, E.; Wang, B.; Ruoslahti, E. *Nat. Biotechnol.* **1995**, *13*, 265-270.

(42)   Giebel, L. B.; Cass, R.; Milligan, D. L.; Young, D.; Arze, R.; Johnson, C.; *Biochemistry* **1995**, *34*, 15430-15435.

(43)   Goldman, E. R.; Pazirandeh, M. P.; Charles, P. T.; Balighian, E. D.; Anderson, G. P. *Anal. Chim. Acta* **2002**, *457*, 13-19.

(44)   Mohr, N.; Barz, M.; Forst, R.; Zentel, R. *Macromol. Rapid Commun.* **2014**, *35*, 1522-1527.

(45)   Singha, N. K.; Gibson, M. I.; Koiry, B. P.; Danial, M.; Klok, H.-A. *Biomacromolecules* **2011**, *12*, 2908-2913.

(46)   Danial, M.; Root, M. J.; Klok, H.-A. *Biomacromolecules*, **2012**, *13*, 1438-1447.

(47)   Nuhn, L.; Hartmann, S.; Palitzsch, B.; Gerlitzki, B.; Schmitt, E.; Zentel, R.; Kunz, H. *Angew. Chem. Int. Ed.* **2013**, *52*, 10652-10656.

(48)   Grandas, A.; Jorba, X.; Giralt, E.; Pedroso, E. *Int. J. Pept. Protein Res.* **1989**, *33*, 386-390.

(49)   Crespy, D.; Landfester, K. *Beilstein J. Org. Chem.* **2010**, *6*, 1132-1148.

(50)   Tamai, T.; Watanabe, M.; Maeda, H.; Mizuno, K. *J. Polym. Sci. Polym. Chem.* **2008**, *46*, 1470-1475.

(51)   Cao, J.; Ding, L.; Hu, W.; Chen, X.; Chen, X.; Fang, Y. *Langmuir* **2014**, *30*, 15364-15372.

(52)   Reynolds, J. A.; Tanford, C. *Proc. Natl. Acad. Sci. U. S. A.* **1970**, *66*, 1002-1007.

3.6.   Supporting Information

Table S1. Overview of the different affinity selection experiments that were performed in order to identify cotton fabric binding peptide sequences.

		Washing	
		0.1% Tween 20 in each round (**1**)	0.1, 0.2, 0.3, 0.4 and 0.5% Tween in 1st, 2nd, 3rd, 4th and 5th round, respectively (**2**)
Infection	Cotton bound phage eluted with Glycine.HCl, pH 2.2 (**a**)	**1a**	**2a**
	Phage bound cotton directly immersed into infection media (**b**)	**1b**	**2b**
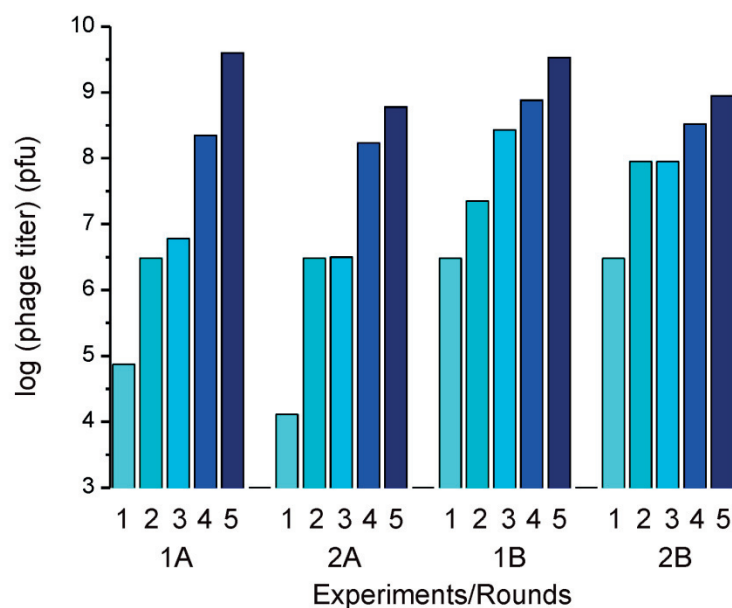
Figure S1. Evolution of the output phage titers with respect to number of rounds in each of the four affinity selection experiments.

(A)

(B)
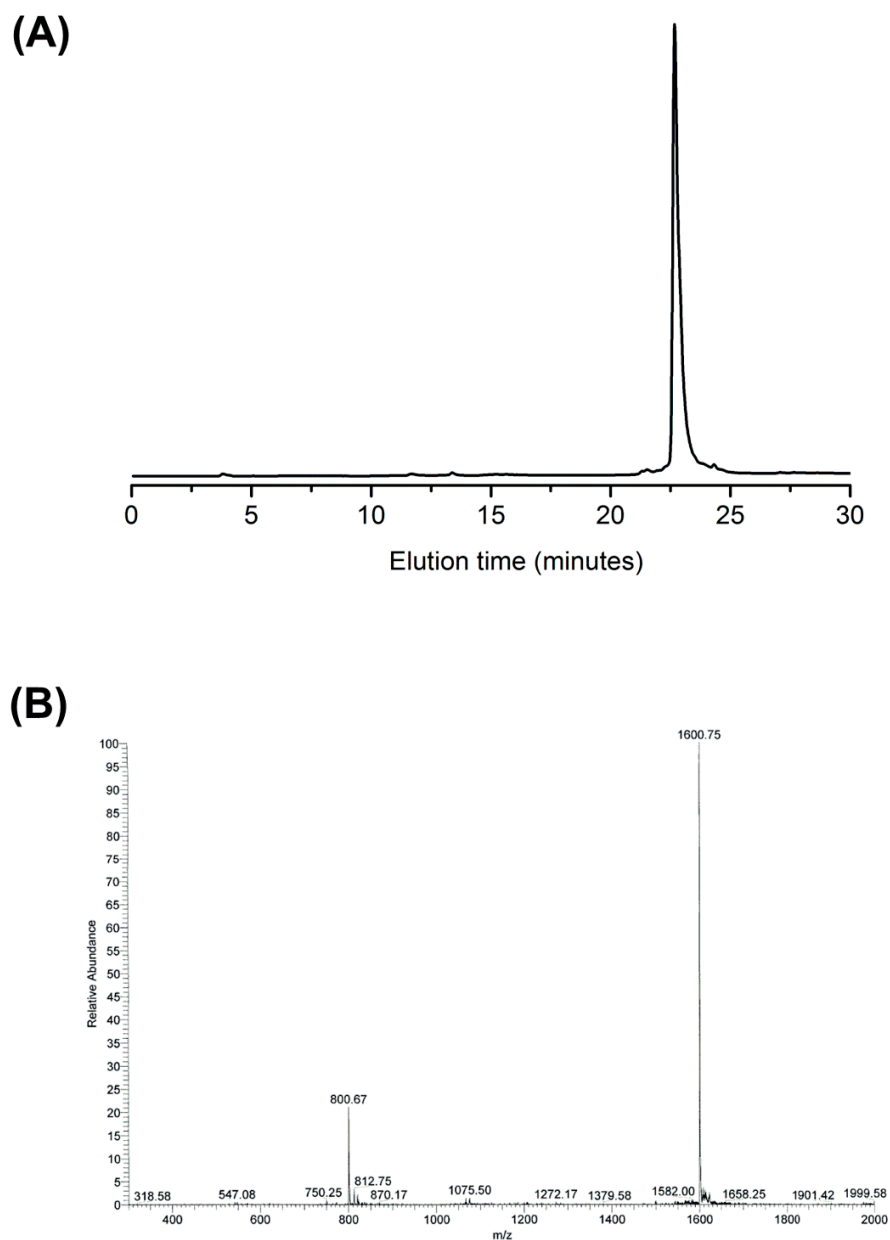
Figure S2. (A) HPLC elution profile (B) and the ESI-MS spectrum of **Pep1**.
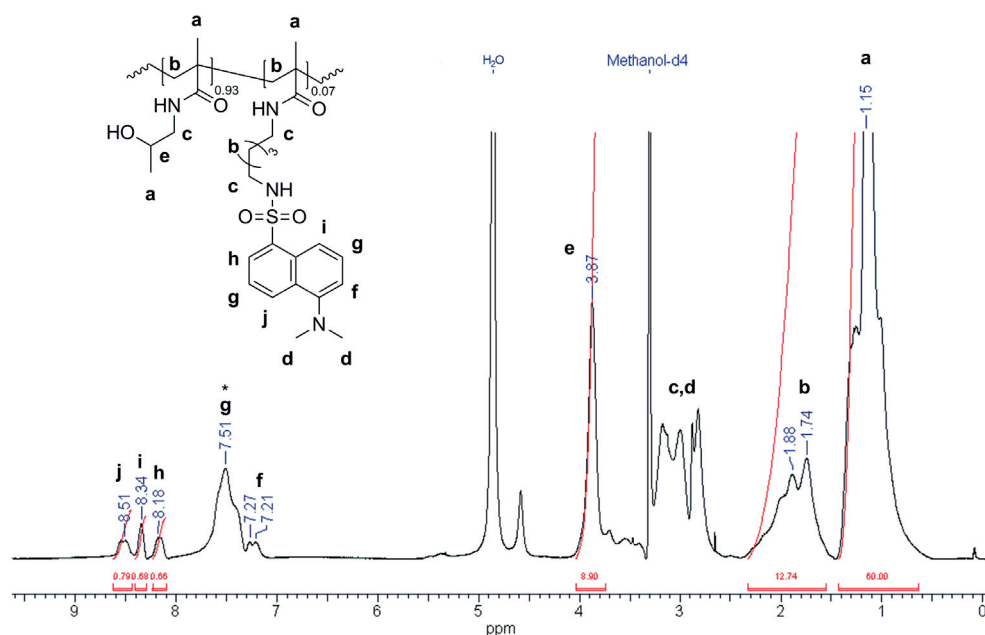
Figure S3A. ^{1}H-NMR spectrum of **PC** in methanol-d$_4$. * = ^{1}H-NMR signal associated with amide groups.
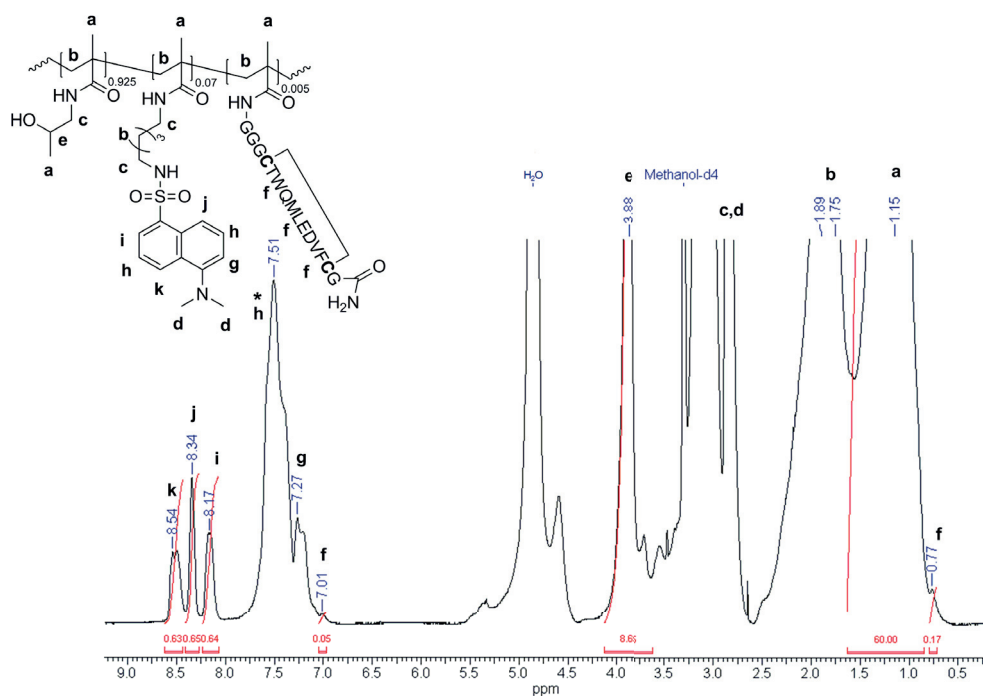
Figure S3B. ^{1}H-NMR spectrum of **PPep1a** in methanol-d$_4$. * = ^{1}H-NMR signal associated with amide groups.
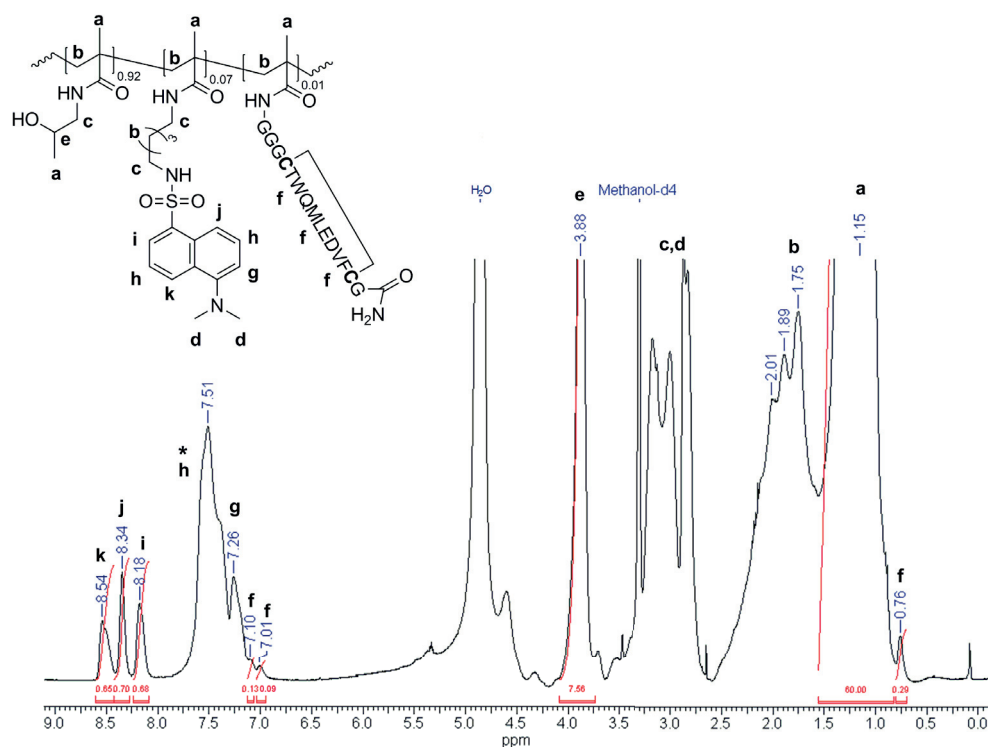
Figure S3C. ^{1}H-NMR spectrum of **PPep1b** in methanol-d_4. * = ^{1}H-NMR signal associated with amide groups.
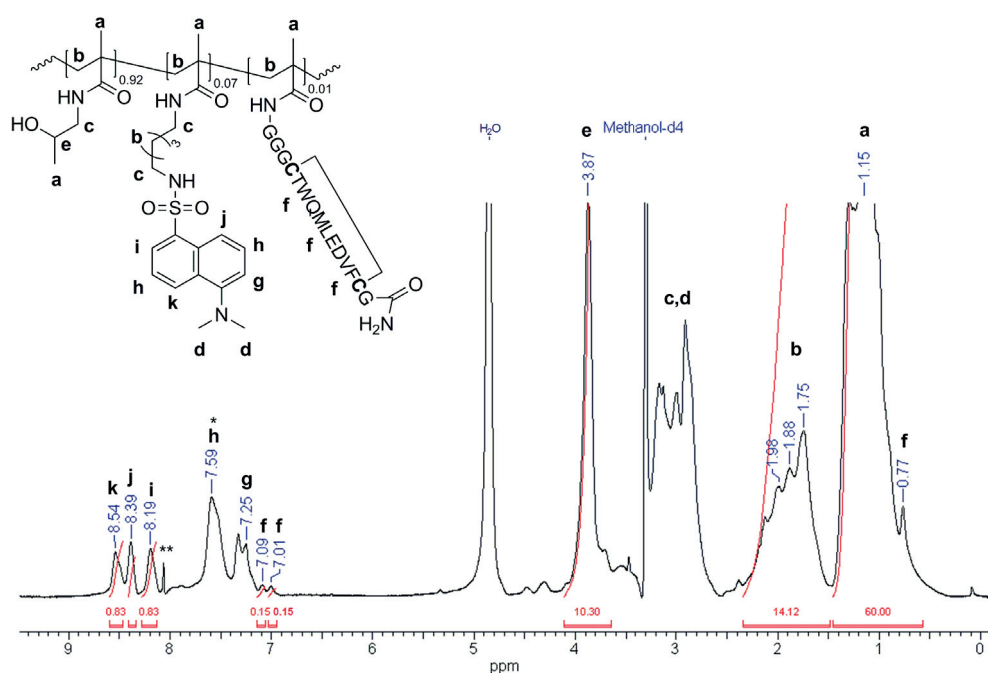
Figure S3D. ^{1}H-NMR spectrum of **PPep1c** in methanol-d_4. * = ^{1}H-NMR signal associated with amide groups. ** = Residual DMF solvent peak.

Calculation of the monomer conversions, α-pinene encapsulation efficiency, solid content and surface –COOH concentration of nanoparticles.

1 – Styrene conversion: $p_{styrene} = \dfrac{\dfrac{A_{PS_{rxn}-7.09ppm}}{3}}{\dfrac{A_{PS_{rxn}-7.09ppm}}{3} + \dfrac{A_{st_{rxn}-7.39ppm}}{2}} \times 100\%$

where, $\dfrac{A_{PS_{rxn}-7.09ppm}}{3}$ indicates the ^{1}H-NMR integral of PS signal at 7.09 ppm in the aliquot taken immediately after the polymerization, and $\dfrac{A_{st_{rxn}-7.39ppm}}{2}$ denotes the ^{1}H-NMR integral of unreacted styrene signal at 7.39 ppm in the aliquot taken immediately after the polymerization.

2 - Acrylic acid (AA) conversion: $p_{AA} = 1 - \left[\dfrac{\dfrac{A_{AA_{rxn}-6.06ppm}}{\dfrac{A_{PS_{rxn}-7.09ppm}}{3} + \dfrac{A_{st_{rxn}-7.39ppm}}{2}}}{n_{AA}/n_{st}} \right] \times 100\%$

where, $A_{AA_{rxn}-6.06ppm}$ indicates the ^{1}H-NMR integral of unreacted AA signal at 6.06 ppm in the aliquot taken immediately after the polymerization and n_{AA} and n_{st} denotes the molar feed of acrylic acid and styrene, respectively.

3 - Encapsulation efficiency (ε$_{α\text{-pinene}}$) = $\dfrac{\dfrac{A_{\alpha-pinene_{di}-5.18ppm}}{A_{PS_{di}-7.09\ ppm}}}{\dfrac{A_{\alpha-pinene_{rxn}-5.18\ ppm} - \dfrac{A_{st_{rxn}-7.39ppm}}{2}}{A_{PS_{rxn}-7.09\ ppm}}} \times 100\%$

where, $A_{\alpha-pinene_{di}-5.18ppm}$ and $A_{PS_{di}-7.09\ ppm}$ indicates the ^{1}H-NMR integrals of α-pinene and PS signals at 5.18 and 7.09 ppm, respectively, in the aliquots taken after a week of dialysis and $A_{\alpha-pinene_{rxn}-5.18\ ppm}$ denotes the ^{1}H-NMR integral of α-pinene signal at 5.18 ppm in the aliquot taken immediately after the polymerization. This calculation is based on the assumption that the amount of PS in the dispersion does not change during the dialysis.

4 – Solid content (SC) of nanoparticles:

a) Gravimetric solid content (SC$_{ly}$): $SC_{ly} = \frac{m_{ly}}{1\,g}$, which indicates the solid mass when 1 g of a dispersion is lyophilized.

b) Solid content according to ^{1}H-NMR (SC$_{NMR}$):

$$SC_{NMR} = 20 \times (p_{styrene} \times w_{f\,styrene} + p_{AA} \times w_{f\,AA} - w_{f\,coagulum}) \%$$

where, 20 is the weight fraction (w/w%) of the organic phase, $w_{f\,styrene}$ and $w_{f\,AA}$ are the weight fractions of styrene and acrylic acid, respectively, in the organic phase, and $w_{f\,coagulum}$ is the weight fraction of coagulum with respect to the organic phase.

5 – Surface COOH groups of nanoparticles: The calculation of COOH groups per particle and their surface density were calculated using the equations described by Musyanovych *et al.*[1]

$$COOH\ groups/1\ g\ polymer = \frac{V_{HCl} \times M_{HCl} \times N_A}{SC}$$

where, the V_{HCl} and M_{HCl} are the consumed volume of HCl in conductometric titration experiments, N_A is the Avogadro's number and SC is the solid content of the dispersion used in titration experiments.

$$COOH\ groups/particle = COOH\ groups/1\ g\ polymer \times \frac{3 \times \pi \times r^3 \times \rho}{4}$$

where, r is the number average radius of the particles calculated from DLS data and ρ is the density of polystyrene nanoparticles (1.045 gr/cm^3). Eventually,

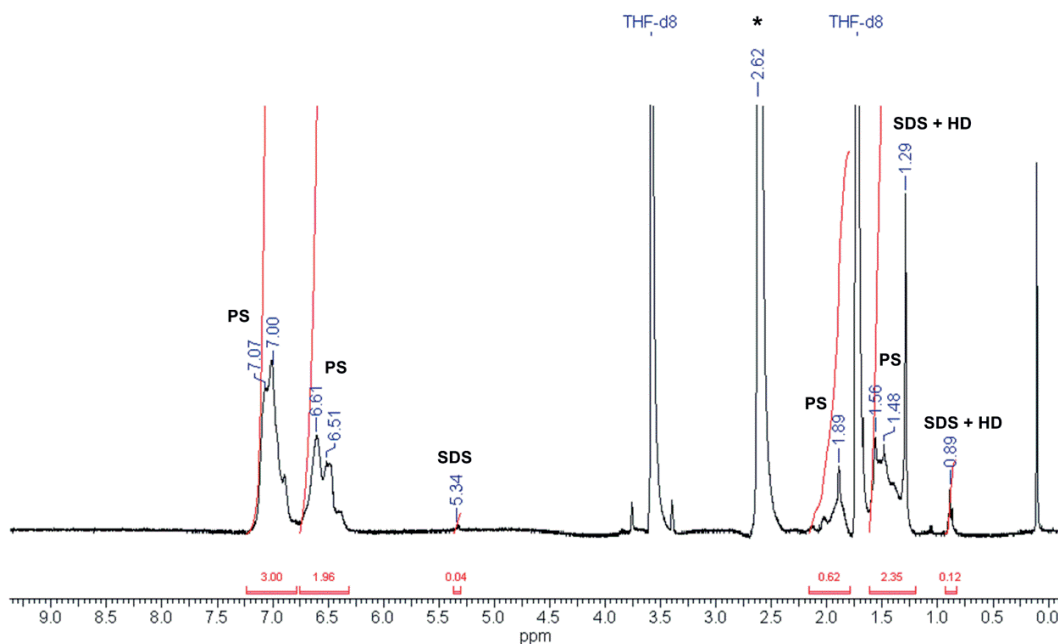$$COOH\ groups/nm^2 = \frac{COOH\ groups/particle}{4 \times \pi \times r^2}$$

Figure S4A. ^{1}H-NMR spectrum of **A0** dispersion taken immediately after the polymerization in THF-d$_8$. * = Water solvent peak.
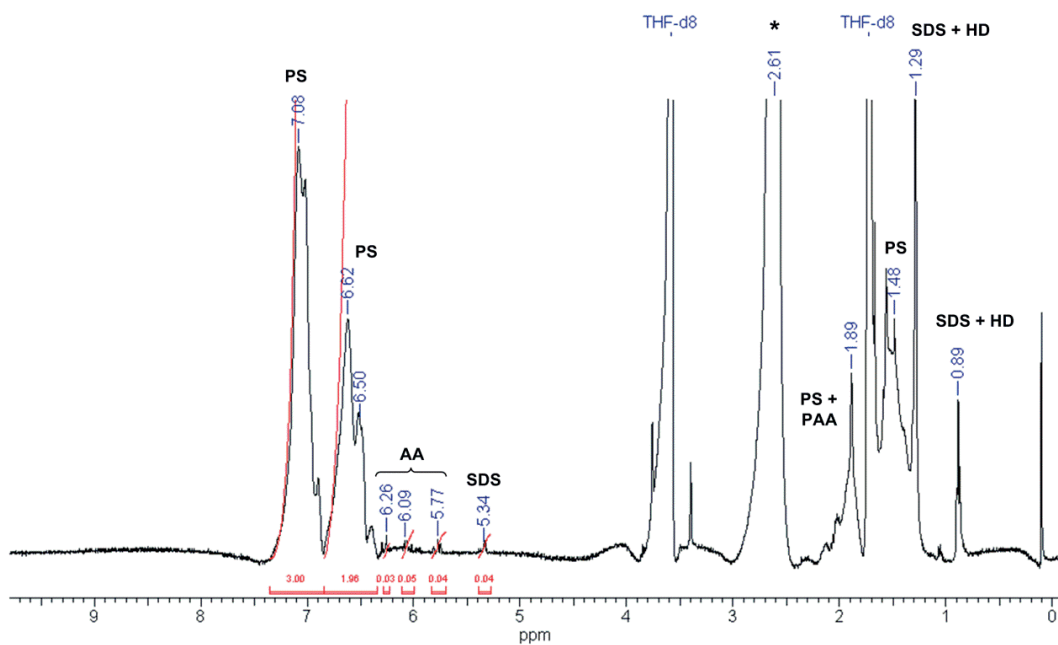

Figure S4B. ^{1}H-NMR spectrum of **A1** dispersion taken immediately after the polymerization in THF-d$_8$. * = Water solvent peak.
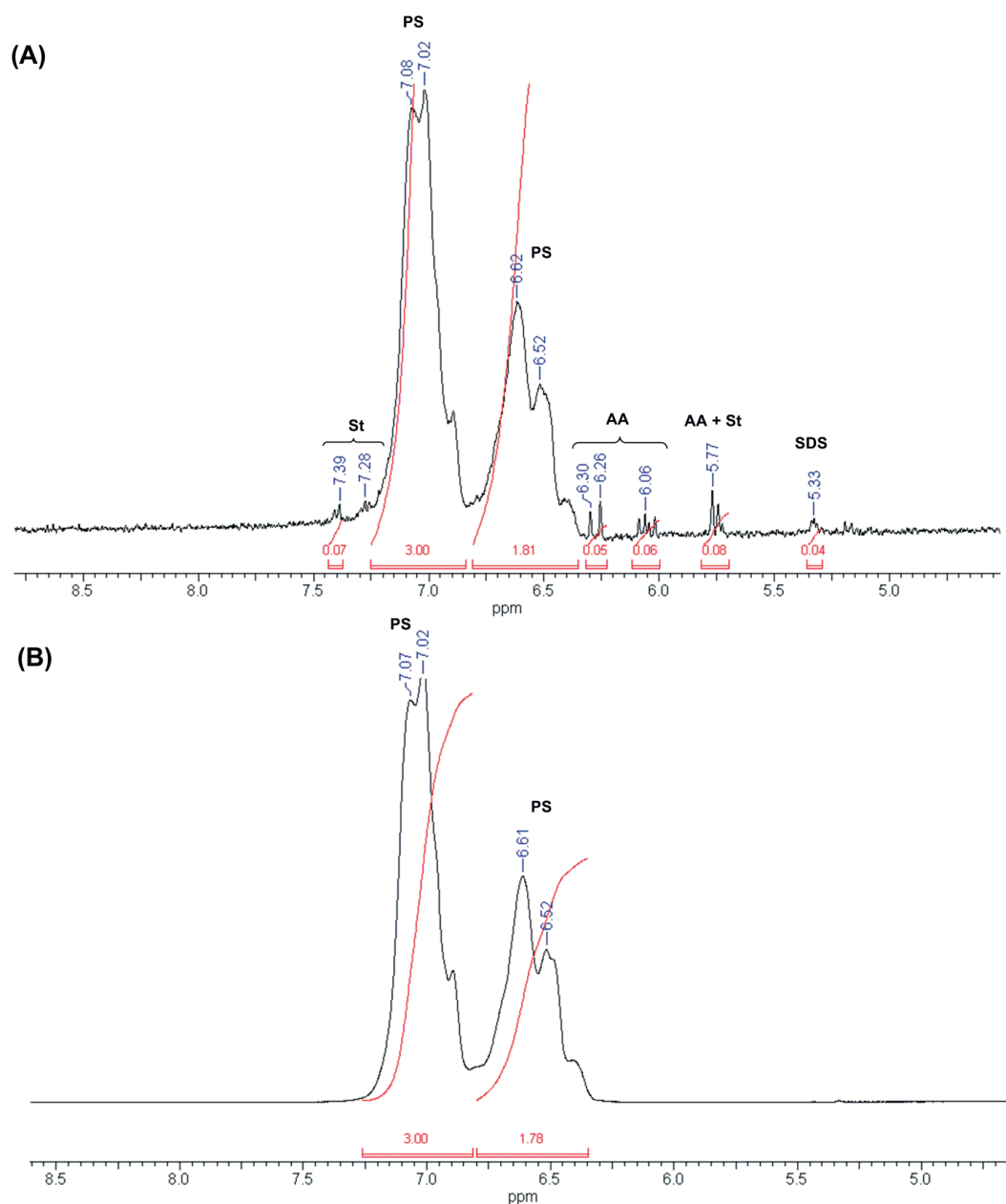
Figure S4C. ^{1}H-NMR spectrum of **A2** dispersions (A) taken immediately after the polymerization and (B) after a week of dialysis, in THF-d$_8$ between 5-9 ppm.
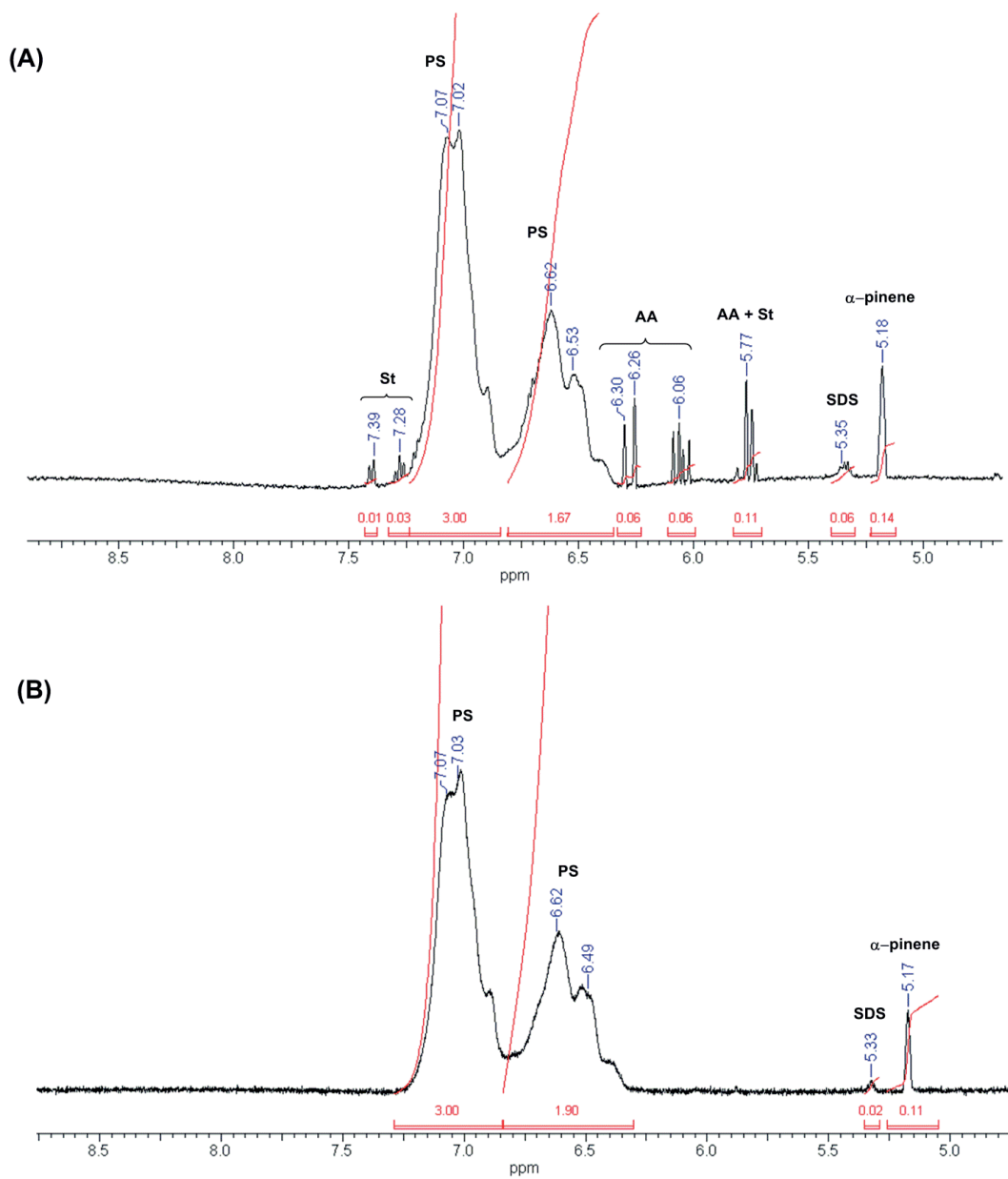
Figure S4D. ^{1}H-NMR spectrum of **A2P1** dispersions (A) taken immediately after the polymerization and (B) after a week of dialysis, in THF-d$_8$ between 5-9 ppm.
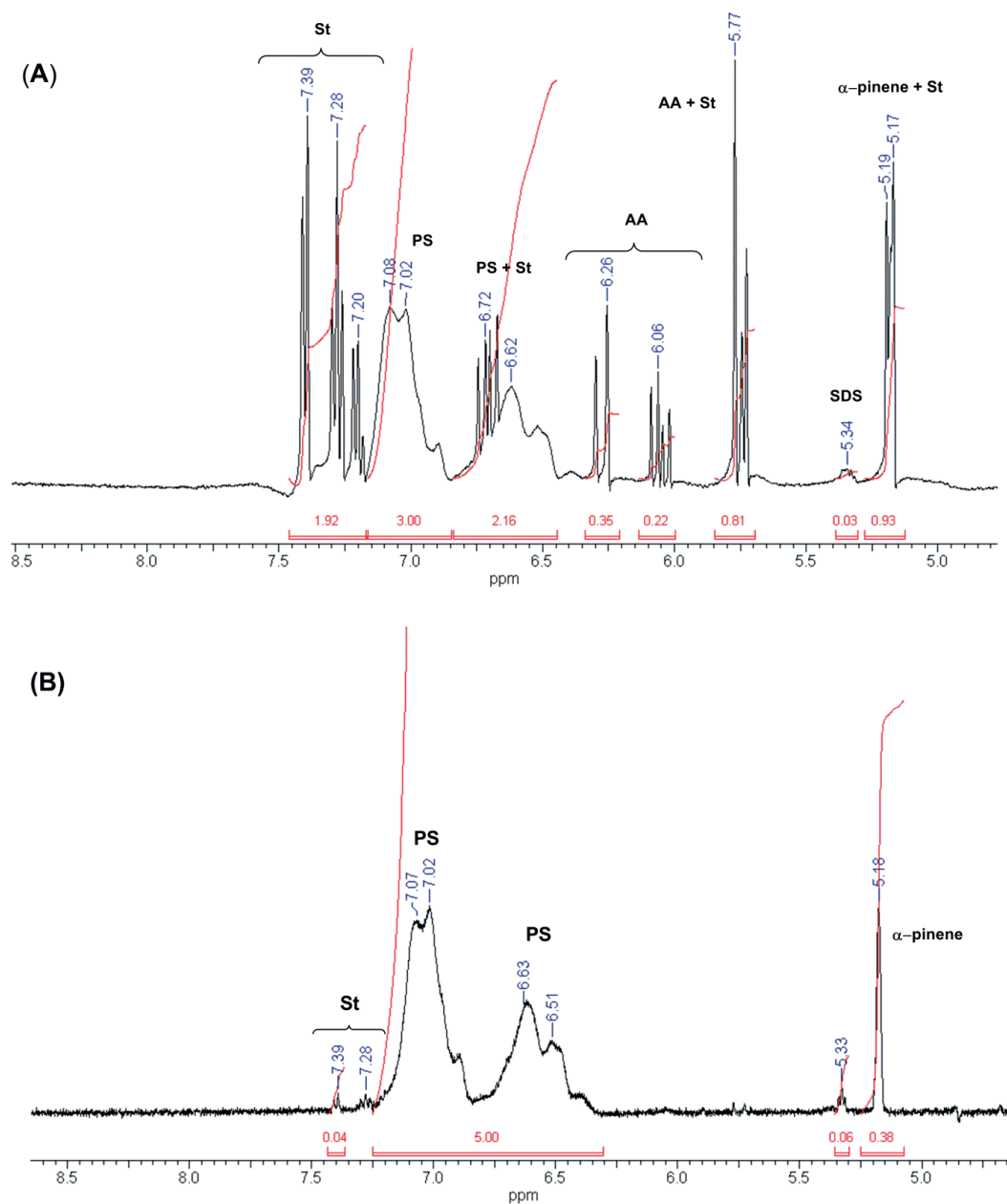
Figure S4E. ¹H-NMR spectrum of **A2P2** dispersions (A) taken immediately after the polymerization and (B) after a week of dialysis, in THF-d$_8$ between 5-9 ppm. Residual styrene (2 mol%) was observed after a week of dialysis.
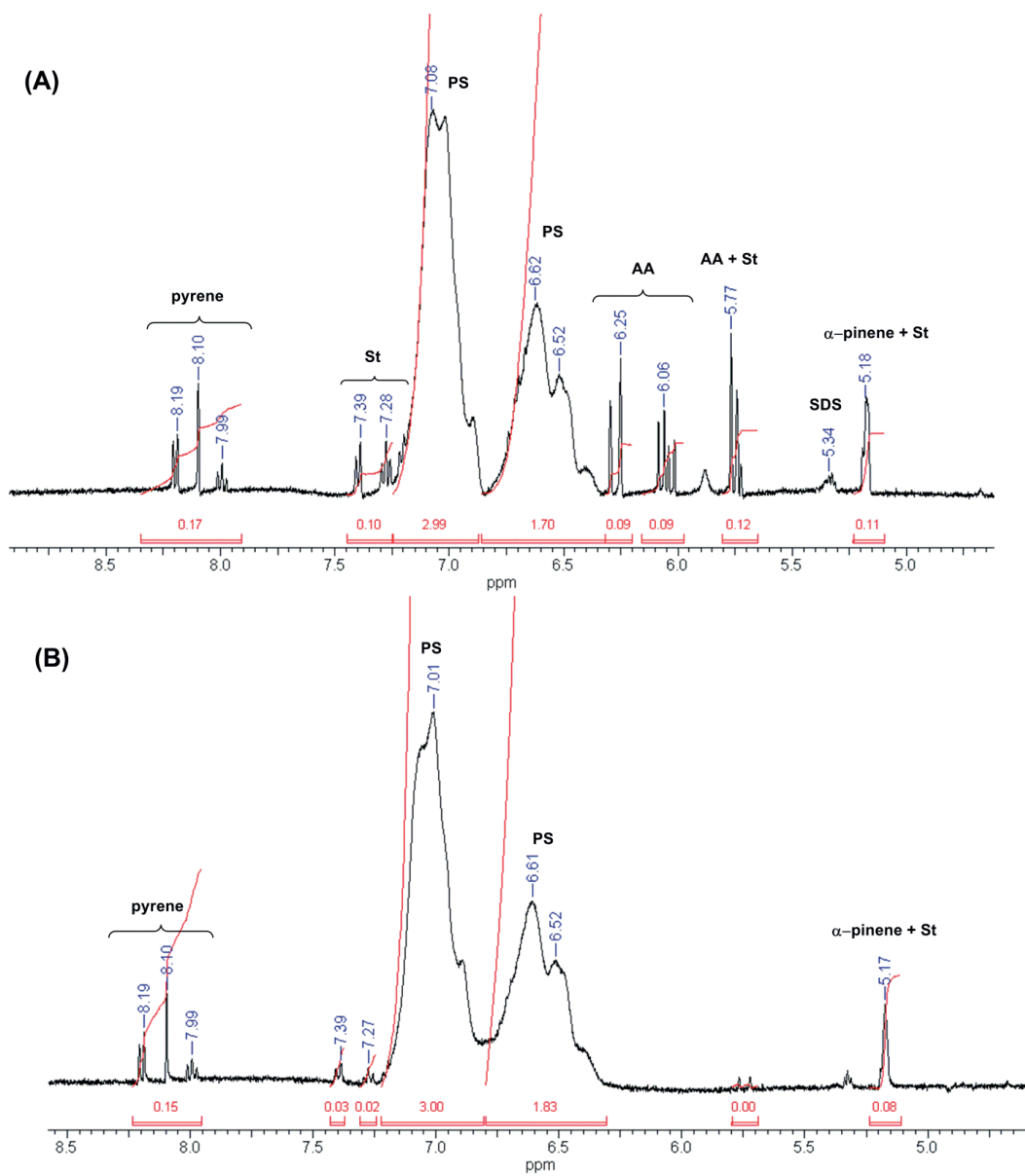
Figure S4F. ^{1}H-NMR spectrum of **A2P1F1** dispersions (A) taken immediately after the polymerization and (B) after a week of dialysis, in THF-d_8 between 5-9 ppm. Residual styrene (1 mol%) was observed after a week of dialysis.
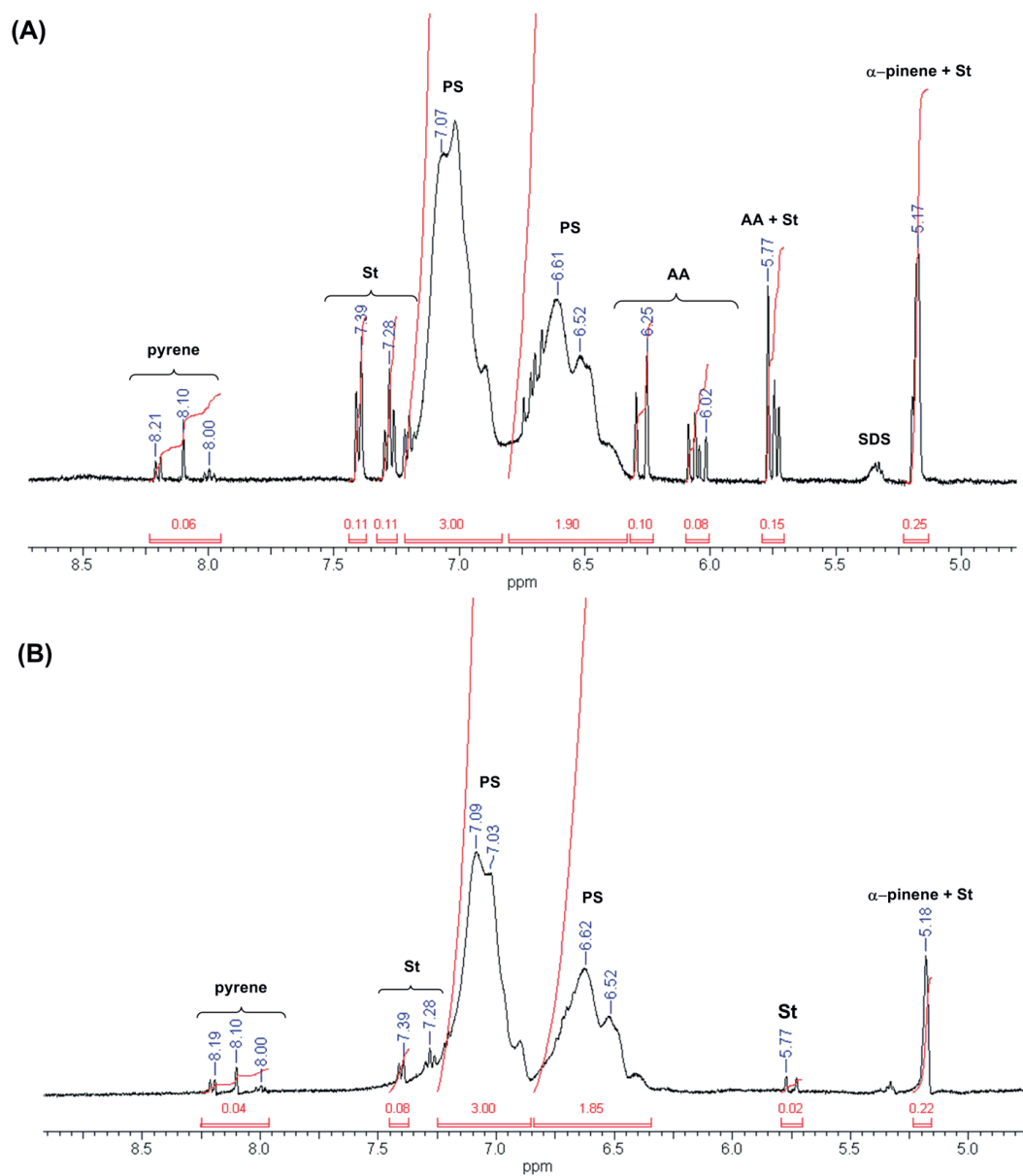
(A)

(B)

Figure S4G. ^{1}H-NMR spectrum of **A2P1F2** dispersions (A) taken immediately after the polymerization and (B) after a week of dialysis, in THF-d$_8$ between 5-9 ppm. Residual styrene (2-3 mol%) was observed after a week of dialysis.
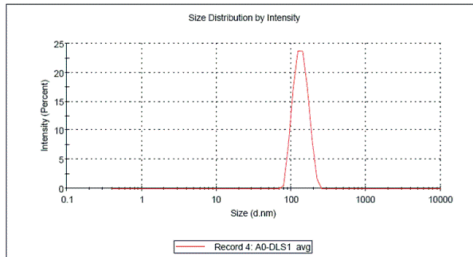
AO

Z-Average (d.nm): 131.1	Peak 1:	136.3	100.0	29.72
PdI: 0.013	Peak 2:	0.000	0.0	0.000
Intercept: 0.947	Peak 3:	0.000	0.0	0.000
Result quality Good			

A1

Z-Average (d.nm): 118.9	Peak 1:	125.6	100.0	30.37
PdI: 0.042	Peak 2:	0.000	0.0	0.000
Intercept: 0.946	Peak 3:	0.000	0.0	0.000
Result quality Good			
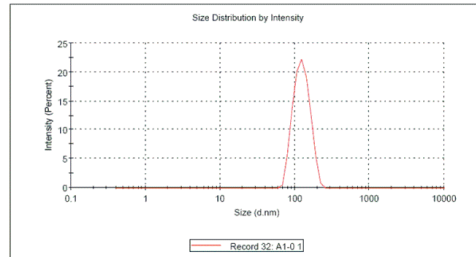
A2

Z-Average (d.nm): 135.5	Peak 1:	142.4	100.0	33.32
PdI: 0.031	Peak 2:	0.000	0.0	0.000
Intercept: 0.934	Peak 3:	0.000	0.0	0.000
Result quality Good			
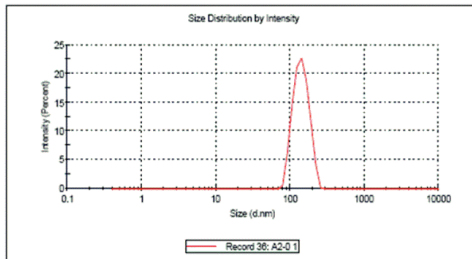
A2P1

Z-Average (d.nm): 127.3	Peak 1:	135.1	100.0	34.48
PdI: 0.043	Peak 2:	0.000	0.0	0.000
Intercept: 0.957	Peak 3:	0.000	0.0	0.000
Result quality Good			
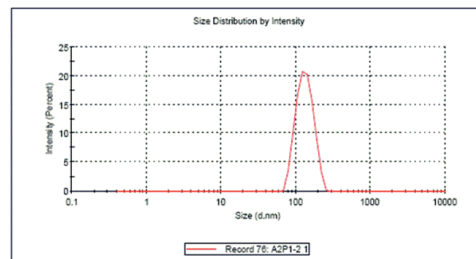
A2P2

Z-Average (d.nm): 178.1	Peak 1:	201.2	100.0	77.69
PdI: 0.140	Peak 2:	0.000	0.0	0.000
Intercept: 0.941	Peak 3:	0.000	0.0	0.000
Result quality Good			
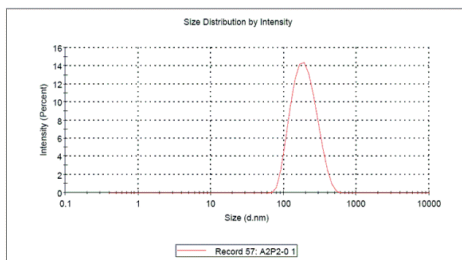
A2P1F1

Z-Average (d.nm): 119.1	Peak 1:	103.6	76.6	26.37
PdI: 0.220	Peak 2:	366.5	23.4	58.37
Intercept: 0.926	Peak 3:	0.000	0.0	0.000
Result quality Good			

111

A2P1F2

Z-Average (d.nm): 145.0	Peak 1:	160.9	100.0	53.56
PdI: 0.098	Peak 2:	0.000	0.0	0.000
Intercept: 0.927	Peak 3:	0.000	0.0	0.000
Result quality Good			

A2P1F2-PEG

Z-Average (d.nm): 147.9	Peak 1:	160.8	100.0	47.18
PdI: 0.079	Peak 2:	0.000	0.0	0.000
Intercept: 0.937	Peak 3:	0.000	0.0	0.000
Result quality Good			

A2P1F2-PEG-Pep1

Z-Average (d.nm): 171.9	Peak 1:	188.4	99.5	69.84
PdI: 0.190	Peak 2:	5185	0.5	482.8
Intercept: 0.935	Peak 3:	0.000	0.0	0.000
Result quality Good			

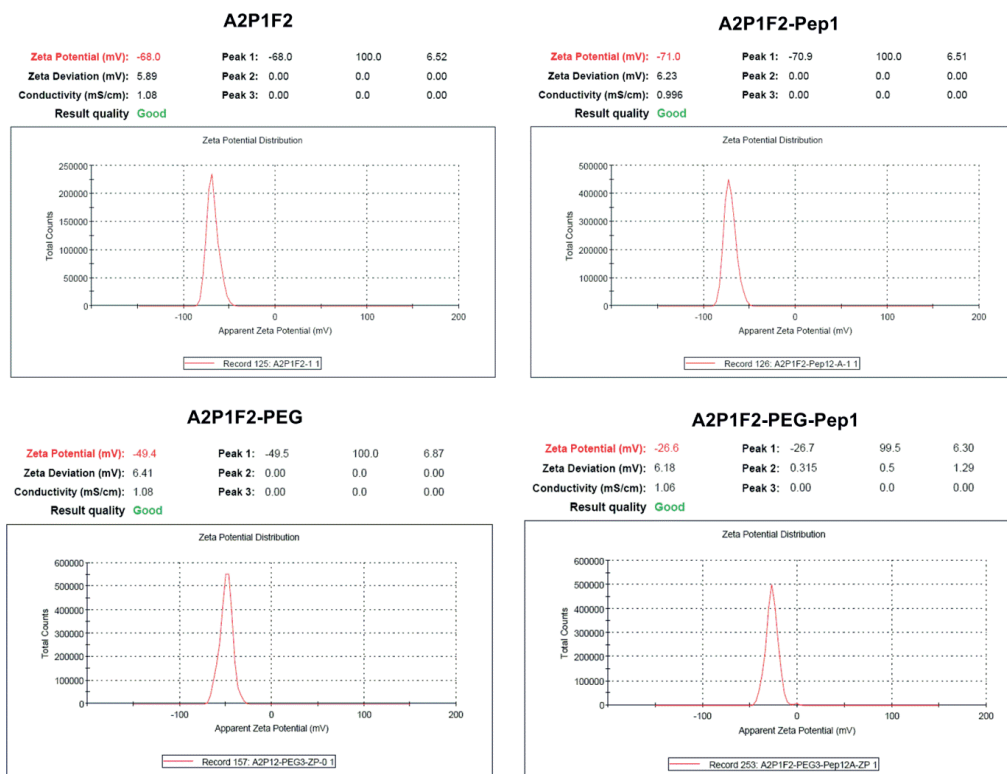**Figure S5.** DLS size measurements of nanoparticles.

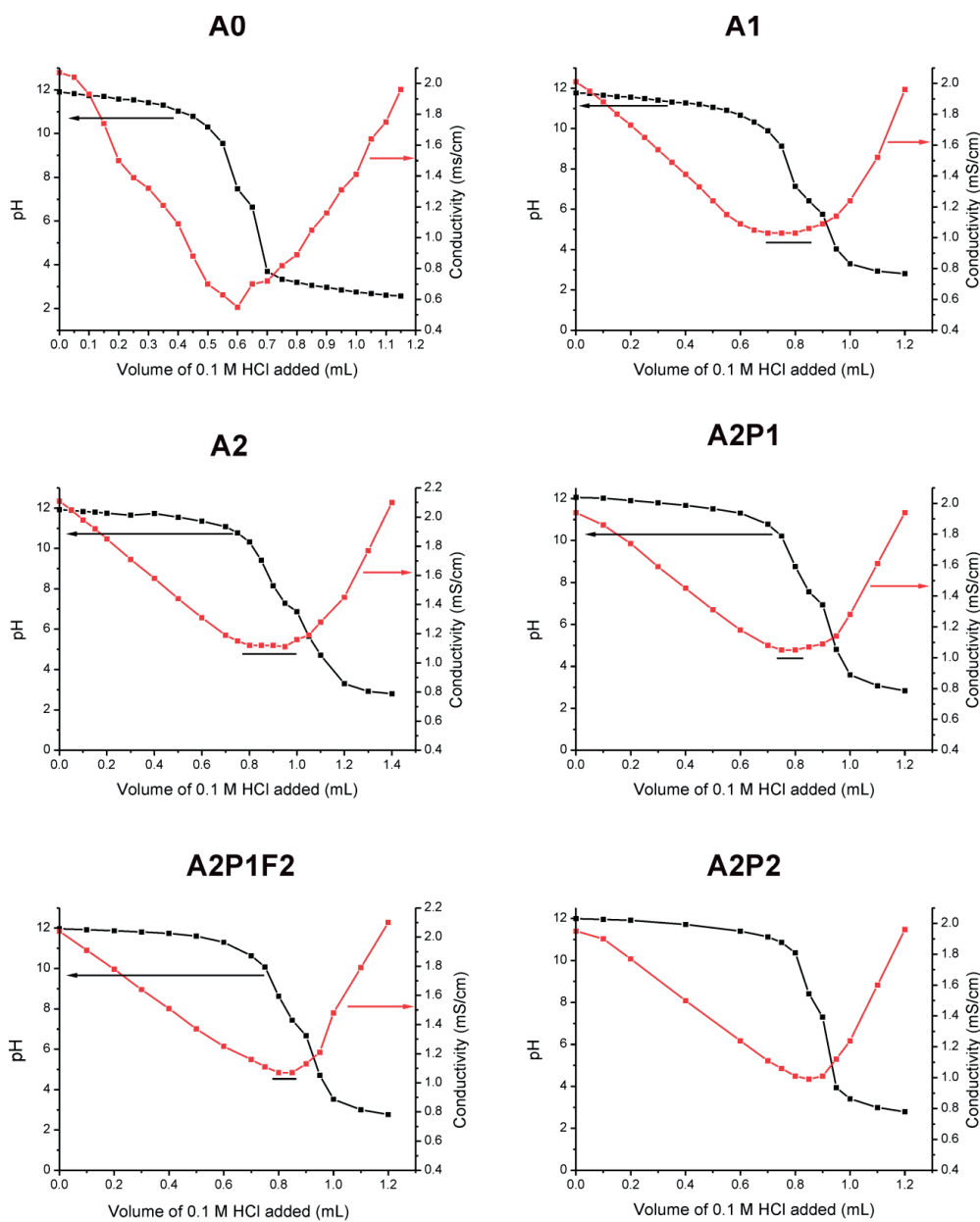**Figure S6.** Zeta-potential measurements of surface functionalized nanoparticles.

Figure S7. pH and conductometric titration curves of nanoparticle dispersions. The straight line at the bottom of the saddle region represents the volume of the 0.1 M HCl solution that is consumed to titrate surface COOH groups of the nanoparticles.
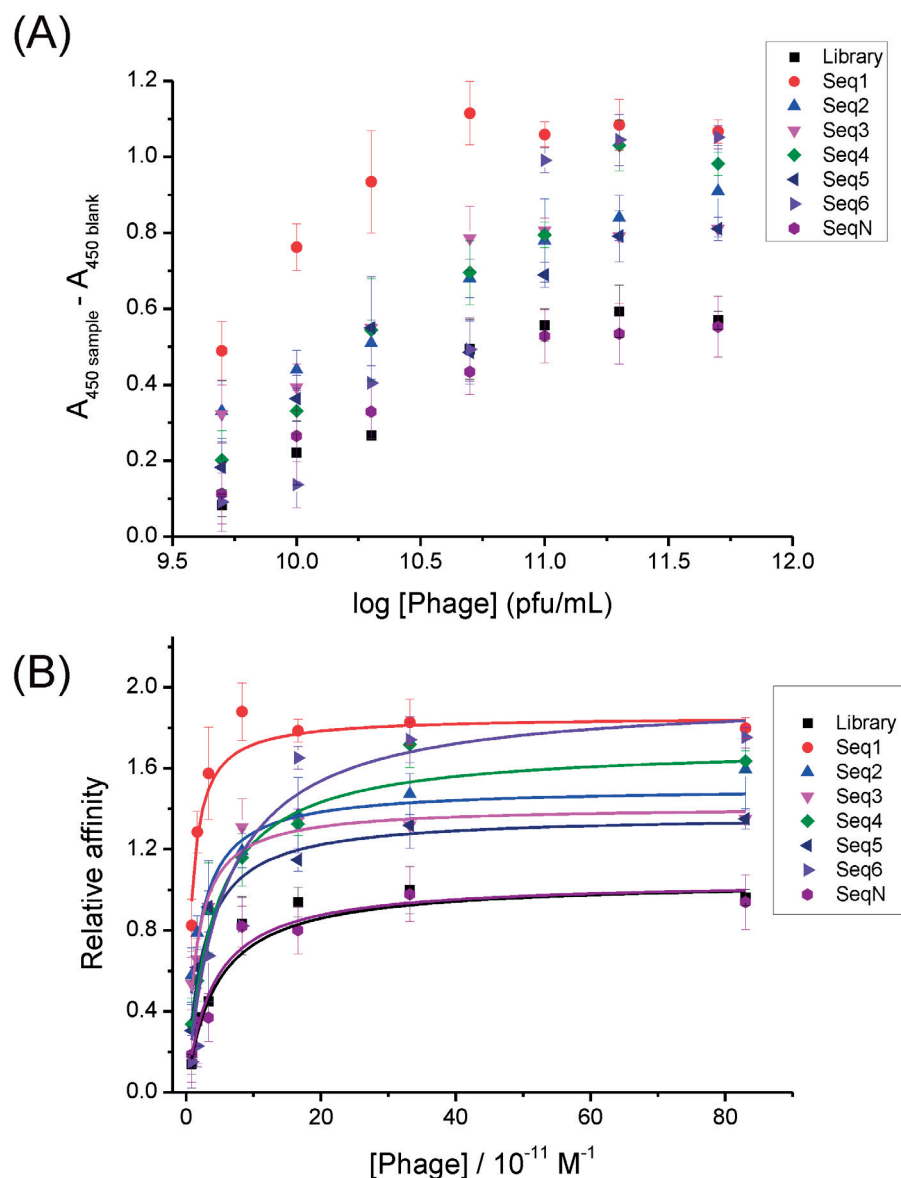
Figure S8. (A) Evolution of the colorimetric response and the (B) relative affinity as a function of phage concentration in the phage ELISA experiments of potentially affine sequences as well as of combinatorial phage library. The error bars represent the standard deviation of 9 independent measurements.

Synthesis of cyclo(GGGCQSIMGLLHYCG-dansyl) (Pep2D).

Synthesis of C-terminal dansylated **Pep2** (**Pep2D**) was achieved by using a protocol similar to that described by Feldborg *et al.*[2] and that is briefly summarized in **Scheme S1.**
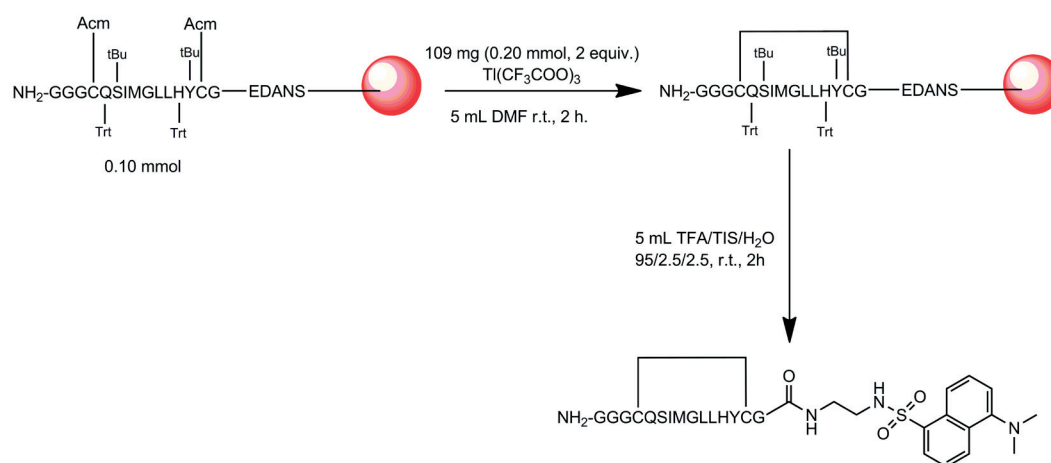
Scheme S1. Schematic illustration of the synthesis of **Pep2D**.

Solid phase peptide synthesis (SPPS) was carried out at a scale of 0.10 mmol using Dansyl Novatag[TM] resin (Merck Millipore) (0.227 g) with a loading capacity of 0.44 mmol/g. Deprotection of Fmoc groups, coupling with the amino acid and washing was performed identical to the protocol described for the synthesis of **Pep1**. Following the SPPS, the resin was transferred to a reaction vessel, consecutively washed with 50 mL DMF, DCM, MeOH and DCM and dried under a flow of N_2. Next, the reaction vessel that contained the resin was flushed with N_2 for 15 minutes. The resin was first resuspended in 2.5 mL of anhydrous DMF and then 2.5 mL of DMF solution containing 109 mg of thallium(III) trifluoroacetate ($Tl(CF_3COO)_3$) (TCI, $\geq$ 95%) was added. ($Tl(CF_3COO)_3$) allows the one-step removal of acetamidomethyl (Acm) protecting groups of cysteine and subsequent intramolecular disulfide bond formation.[3] The reaction was allowed to continue for 2 hours at room temperature with agitation under N_2. Following the $Tl(CF_3COO)_3$ mediated oxidation, the resin was washed 5 times with 50 mL of DMF and once more with 50 mL DCM and dried under a flow of N_2. Cleavage of the peptide was achieved with the addition of 5 mL of a solution containing TFA/TIS/H_2O 95:2.5:2.5 v/v% to the reaction vessel. The cleavage was allowed to continue for 2 hours at room temperature with agitation. The crude peptide was washed with repetitive centrifugation

and resuspension in cold diethylether for 4 times, dissolved in H_2O/AcN 3:2 v/v% solution and lyophilized. The crude peptide was purified via HPLC using a gradient from 5% AcN/100% H_2O (0.05% TFA) to 60% AcN/40% H_2O (0.05% TFA) for 30 minutes with a flow rate of 20 mL/min. Purity $\geq$ 85% (HPLC). ESI-MS: ([M+2H]$^{2+}$ found: 885.20 m/z, [M+2H]$^{2+}$ th.: 885.30 m/z).
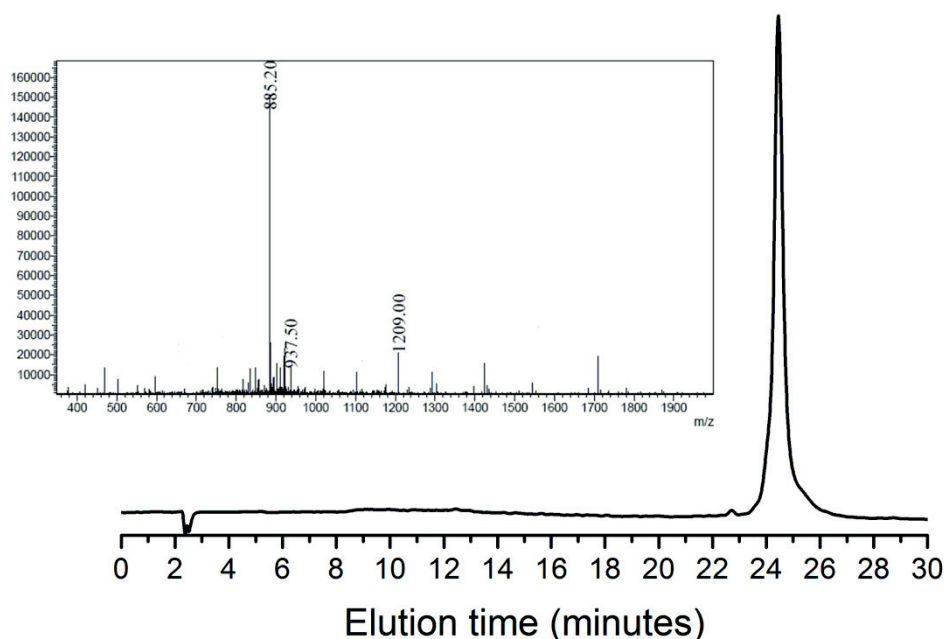

Figure S9. HPLC elution profile and ESI-MS spectrum of **Pep2D.**

Surface functionalization of A2P1 with Pep2D.

The functionalization of **A2P1** surfaces with **Pep2D** was achieved using 1 w/w% **A2P1** dispersion, 100 μM **Pep2D**, 1 mM EDC and 1.5 mM Sulfo-NHS and carried out by using the protocol described for the functionalization of **A2P1F2** surfaces with **Pep1** and therefore, will not be described in detail. The synthesized nanoparticles (**A2P1-Pep2D**) were dialyzed against MilliQ H_2O for 1 day using a Spectra/Por Spectra/Por Float-A-Lyzer® G2 dialysis device with a MWCO of 300000 g/mol prior to fluorescence intensity measurements. Fluorescence emission spectra of 100 μM **Pep2D** and **A2P1-Pep2D**, when 100 μM of **Pep2D** was used in the reaction, was recorded in 10 mM PBS buffer (pH 7.4) with λ_{ex} = 335 nm.
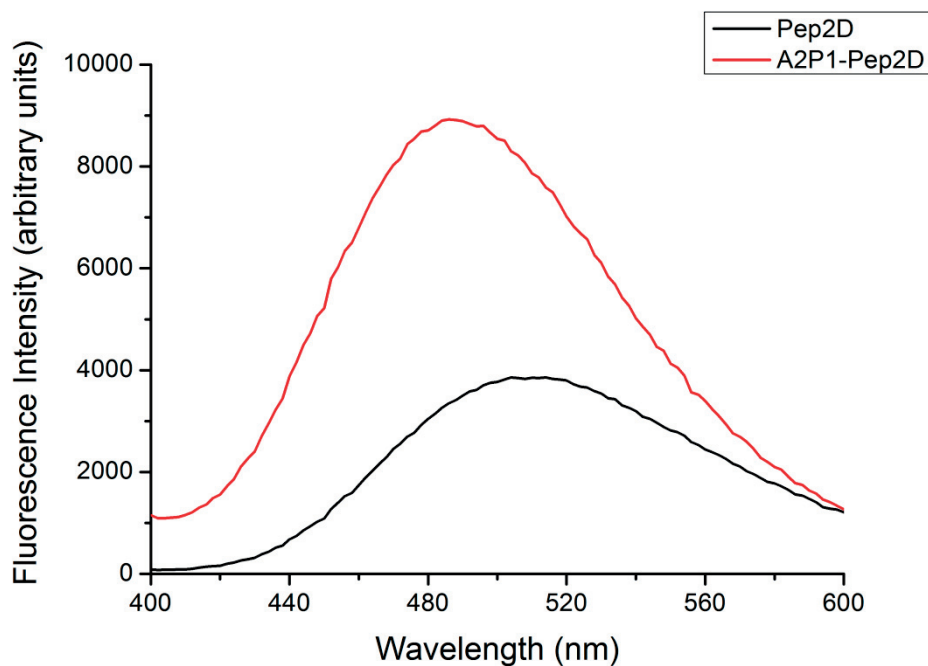
Figure S10. Fluorescence emission spectra of 100 μM **Pep2D** and **A2P1-Pep2D**, when 100 μM of **Pep2D** was used in the reaction, in 0.01 M PBS, pH 7.4. The excitation wavelength was 335 nm.

References for Supporting Information:

(1)   Musyanovych, A.; Rossmanith, R.; Tontsch, C.; Landfester, K. *Langmuir*, **2007**, *23*, 5367-5376.

(2)   Feldborg, L. N.; Jølck, R. I.; Andresen, T. L. *Bioconjugate Chem.* **2012**, *23*, 2444-2450.

(3)   Fujii, N.; Otaka, A.; Funakoshi, S.; Bessho, K.; Watanabe, T.; Akaji, K.; Yajima, H. *Chem. Pharm. Bull.* **1987**, *35*, 2339-2347.

4. Human Hair Targeting Polymeric Fragrance Delivery Systems using Phage Display Identified Peptides[2]

4.1. Introduction

Various considerations should be taken into account to design fragrance delivery systems that can effectively deposit from a personal care product onto the surface of interest such as hair, and subsequently provide a long lasting perception of these volatiles by controlling the rate of their release from these surfaces. First of all, fragrances are highly volatile compounds that have a pleasant odor and that easily evaporate during application.[1,3] Second, many of the fragrances, such as aldehydes, are prone to oxidation under ambient conditions, which can rapidly lead to a loss of their activity and furthermore the degradation products can act as contact allergens.[4,5] These challenges can be overcome by using polymers as fragrance delivery systems, as these systems can allow the long term storage of the fragrances, prevent their degradation and control the rate of their release.[6,10] Two different general strategies have been explored for the preparation of polymeric fragrance delivery systems. The first strategy is based on the covalent grafting of fragrances onto polymers using labile bonds that can be cleaved in the presence of external stimuli, such as pH, temperature and light.[7,8] These systems are referred to polymeric profragrances. The second strategy relies on the encapsulation of fragrances in polymeric carriers.[9,10]

While many of these polymeric delivery systems primarily aim to address the issues related with the volatility, stability and the controlled release of fragrances, it is also highly desirable to enhance the deposition of these systems onto the surface of interest.

---

[2] This Chapter will be submitted as the following paper: "Human Hair Targeting Polymeric Fragrance Delivery Systems using Phage Display Identified Peptides", K.A. Günay, D. L. Berthier, H. A. Jerri, D. Benczédi, A. Herrmann and H.-A. Klok.

To optimize the olfactive impact and benefits of fragrance delivery systems, deposition and substantivity after rinsing must be maximized. Fragrances are among the most expensive materials formulated into many consumer products and while encapsulation protects the core and controls the release of the precious and volatile oil payload, surface functionalization strategies must be used to improve the affinity of the delivery systems for the targeted substrate. Maximization of surface deposition will minimize the loss of unadhered fragrance oil payloads which are otherwise washed down the drain. In particular, the efficient deposition of fragrances and fragrance delivery systems from a shampoo medium onto hair is a challenging task. This challenge can be briefly summarized as follows: The primary function of a shampoo is to cleanse the hair surface[11-13] by removing hydrophobic molecules such as various non-covalently bound lipids[14] and dust particles. The removal of these hydrophobic molecules is typically achieved using anionic surfactants, as they can effectively entrap these molecules by forming micelles. These micelles can be easily rinsed off with water owing to the electrostatic repulsion between the anionic tail of these surfactants and the hair surfaces.[15] Since most of the fragrances are also hydrophobic, they predominantly localize inside the micelles rather than in the aqueous phase.[16] Consequently, they are rinsed off together with these surfactants. The ability to deposit actives and film-forming polymers onto hair for palliative, conditioning and styling effects is well established,[17-22] but the mechanisms driving delivery of insoluble microparticles and microcapsules onto hair from rinse-off personal cleansing systems still require further development. Current proposed deposition mechanisms include ionic interactions, general adhesion, specific adhesion and the commonly accepted mechanism of coacervate precipitation upon dilution of complex cleanser formulations.[23-25]

Phage display, which is a powerful in vitro selection technique that allows the isolation of substrate selective, highly affine short peptide binders,[26-28] may offer an alternative solution to identify binding motives useful to selectively deposit fragrance delivery systems onto hair under shampoo conditions as it has also found use for the isolation of short peptide binders to cosmetically relevant substrates such as cotton,[29,30] skin,[31] and hair.[32] Using phage display, O'Brien *et al.* have identified hair-binding peptides which remain on the hair surface after shampoo treatment, following their incubation either in standard tris-buffered saline (TBS) solutions or hair conditioner formulations.[32] These peptides can be useful as a deposition aid for conditioning agents and hair colorants. Although these peptides remained bound after the shampoo treatment, this does not

necessarily indicate that they are selectively deposited onto hair under shampoo conditions, owing to the different nature of shampoo (anionic) and conditioning (cationic) media, which can affect the nature and the strength of hair-peptide interactions at a molecular scale. In one interesting example, Verrips and coworkers have performed antibody phage display in a shampoo medium to identify llama single-domain antibody fragments (VHHs) that bind to the *Malassezia furfur* cell surface protein (Malf1), which is one of the fungi associated with dandruff formation.[33] While the binding strengths of antibodies having conformationally constrained binding sites are typically higher to the target of interest as compared to short, flexible peptide sequences, their higher production cost combined with lower stability[34] may limit their use as a deposition aid for fragrance delivery systems.

This Chapter will report the use of phage display identified peptides to construct potential hair-targeting polymeric fragrance delivery systems (**Scheme 1**). The first part will describe the identification of hair binding cyclic peptide disulfides (CXC) via phage display under shampoo conditions. In the second part, the CXC-poly(*N*-(2-hydroxypropyl methacrylamide) (PHPMA) conjugates that were synthesized in Chapter 2 will be used as a model hair targeting polymeric profragrance platform. Fluorescence intensity measurements will reveal that the incorporation of small amounts of these phage display identified peptides enhances the deposition of these polymers 3.5-5.0 fold onto hair under shampoo conditions. In the final section, the influence of the stringency of the shampoo medium and the steric hindrance in the terminal positions of the hair binding peptide towards hair recognition will be investigated using fluorescently tagged peptides.

The goal of this work was to move beyond formulation parameters and passive deposition mechanisms, and instead enable the selective surface deposition of fragrance delivery systems onto hair via phage display identified peptides. The general approach chosen in this work can be subdivided into three parts as illustrated in **Scheme 1.** The first part will describe the identification of hair binding cyclic peptide disulfides via phage display under shampoo conditions. In the second part, these peptides will be used to construct peptide-poly(*N*-(2-hydroxypropyl)methacrylamide) (PHPMA) conjugates. Fluorescence intensity measurements reveal that the incorporation of small amounts of these phage display identified peptides enhances the deposition of these polymers 3.5-5.0 fold onto hair under shampoo conditions. In the third part, first the synthesis of peptide functionalized polyurethane/urea-type core-shell microcapsules containing a model perfume will be demonstrated. The peptide functionalization of these microcapsules will

result in approximately a 10-fold enhancement of their deposition according to HPLC measurements. Finally, the amount of fragrance release from peptide functionalized microcapsules will be shown to be significantly higher than that of non-functionalized control microcapsules as a result of increased deposition via dynamic headspace sampling measurements.
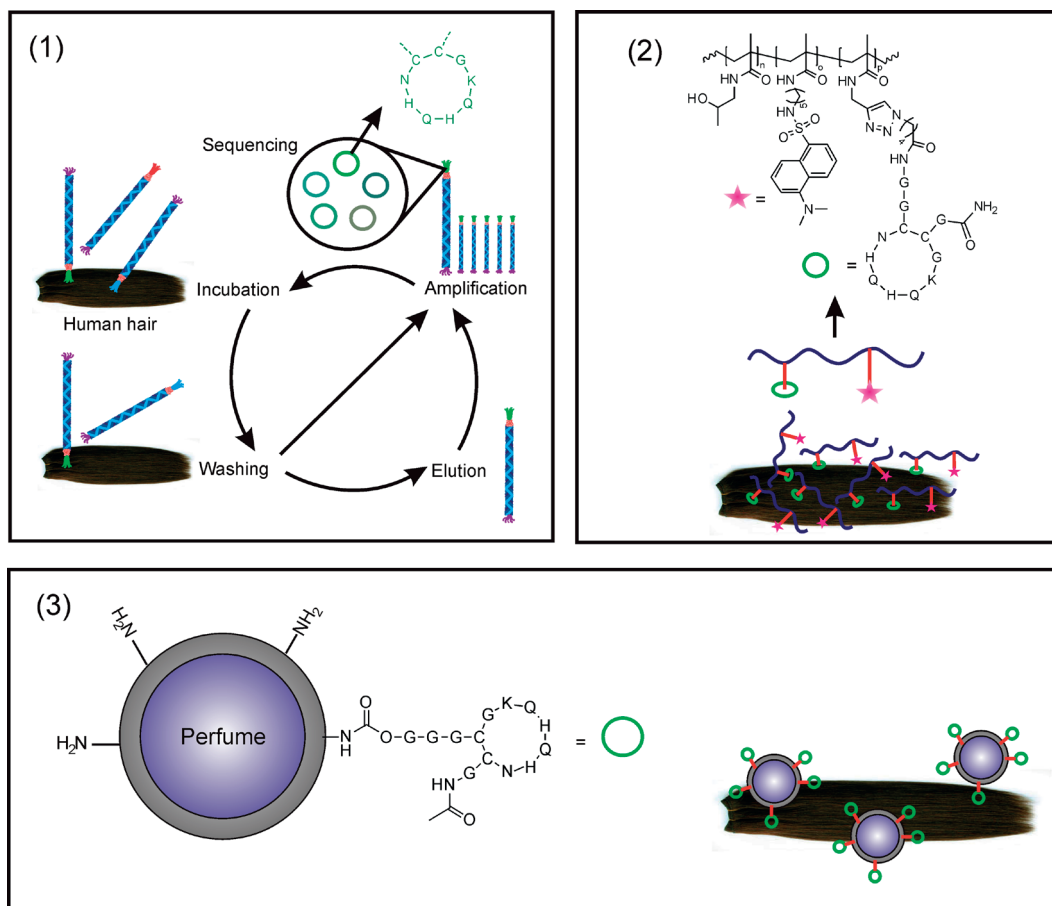
Scheme 1. Overview of the preparation of potential fragrance delivery systems using phage display identified peptides. (1) Identification of hair binding peptide ligands via phage display under shampoo conditions. (2) Preparation of peptide-PHPMA conjugates as hair binding model polymeric profragrances. (3) Functionalization of core-shell microcapsules containing a model perfume.

4.2. Results and Discussion

4.2.1. Identification and characterization of hair binding peptides.

The first part of this work will elucidate the feasibility of phage display experiments under shampoo conditions to identify hair binding peptides. Although these peptides will be used to enhance the deposition of only the fragrance delivery systems in the next parts, it is worth noting that their use can be expanded to selectively deposit other benefit agents, i.e. conditioners and anti-dandruff agents, onto hair from shampoo formulations. A detailed phage display protocol that allowed the identification of hair binding peptides is provided in the Supporting Information.

The identification of hair binding peptide sequences was carried using a combinatorial phage library that displays 7-mer cyclic peptide disulfides (C7C). A cyclic peptide library was utilized rather than a linear one as it is known that conformationally constrained libraries often led to the isolation of peptide binders with higher affinity compared to their linear counterparts.[35,36] Two independent phage display experiments were performed in parallel up to the 5th round by using two different washing conditions. Briefly, the washing step was performed either by keeping the surfactant (Tween® 20) concentration constant at 0.1 w/w% (**Condition 1**) or by gradually increasing it from 0.1 to 0.5 w/w%, which enhanced the washing stringency (**Condition 2**), as a function of selection rounds. These two experiments were named as **Experiment 1** and **2**, depending on the washing step performed. Output phage titers were measured after each round of selection in these experiments in order to determine the enrichment of the phage library towards the hair samples. **Figure S1** shows that while the output phage titers were in the range of $\sim 10^6$ pfu/mL in the first round, they gradually increased to 1-5 x 10^8 pfu/mL up to the 4th round of selection in both experiments, suggesting a 10^2-10^3 fold enrichment of the phage library towards hair. On the other hand, in the 5th selection round, a slight decrease in the output phage titers in **Experiment 2** was observed, illustrating the effect of the increased stringency of the washing step towards the enrichment of the phage libraries. Owing to this decrease in the output phage titers in the 5th round, the affinity selection experiments were not continued for a 6th round. Subsequently, individual clones from the 4th and 5th round of selection were sent to sequencing analysis.

Table 1. List of hair binding peptides identified by phage display, their frequency in the sequencing analysis, net charge at pH 6.0 as well as their apparent binding strength (K_{app}) and maximum relative affinity (RA_{max}), which were calculated from phage ELISA experiments.

Sequence ID.	Sequence	Frequency / Total frequency	Net charge at pH 6.0	K_{app} / 10^{10} M^{-1}	RA_{max}
Pep1	**C** N H Q H Q K G **C**	10/32	+ 3.09	108	37.23
Pep2	**C** K S K N H P S **C**	5/32	+ 3.53	21.0	18.44
Pep3	**C** Q N A H Q K G **C**	4/32	+ 1.54	2.4	4.18
Pep4	**C** Q S H K N N K **C**	2/32	+ 3.53	N.A.	N.A.
Pep5	**C** G H N K N K D **C**	2/32	+ 2.54	N.A.	N.A.
Pep6	**C** H D K Q S K K **C**	2/32	+ 3.54	N.A.	N.A

Table 1 shows the list of potentially affine hair binding sequences as well as their observed frequency in the sequencing analysis. These sequences shared in common that they were primarily composed of cationic (lysine (K), histidine (H)) and polar (asparagine (N), glutamine (Q), serine (S)) amino acids with a net charge between +1.5 to +3.5 at the pH of the shampoo formulation used (6.0). As the hair surface is known to have a net negative charge,[15] these results indicate that the recognition of the hair surface with these peptides predominantly relies on the electrostatic interactions. It is worth mentioning that these sequences did not share any consensus motif, which is frequently observed after the affinity selection experiments that were carried out to identify binders, for example, to proteins having specific binding pockets. The absence of a consensus motif among these hair binders can therefore be attributed to the absence of any specific binding pockets on the hair surfaces, if observed at a molecular level.

In the next step, phage enzyme-linked immunosorbent assay (ELISA) experiments were performed in order to determine the binding strengths as well as the relative deposition (affinity) of three of the most frequently selected sequences (**Pep1-Pep3**, **Table 1**) compared to the phage library. The phage ELISA protocol is provided in the Supporting Information. **Figure 1** shows that the ELISA experiment of two of these sequences, **Pep1** (**C**NHQHQKG**C**) and **Pep2** (**C**KSKNHPS**C**) yielded a colorimetric signal that was 37 and 18-fold higher, respectively, than that of the phage library, which was used as a control. **Pep3** (**C**QNAHQKG**C**) also showed selectivity towards the hair surfaces, but to a lower extent (RA_{max} = 4.18). This exceptionally high relative deposition of **Pep1** and **Pep2** can be primarily attributed to the capability of these sequences to selectively

recognize the hair surfaces, but also partly to the very little deposition of the phage library under shampoo conditions. **Figure 1A** shows that the evolution of the colorimetric response as a function of phage concentration in the ELISA experiment carried out using the phage library saturates at very small absorbance values. This residual colorimetric response of the phage library, which can be considered as a non-specific control, also provides evidence about the challenging nature of efficiently depositing benefit agents, such as fragrance delivery systems without the use of deposition aids onto hair under shampoo conditions. Similarly, the exceptionally high relative deposition of **Pep1** and **Pep2** highlights the potential of using peptides as a deposition aid under these conditions. To conclude this section, these results demonstrate that phage display is a suitable technique even under shampoo conditions, which is a very stringent medium, and it allows the identification of high affinity peptide sequences for hair surfaces.
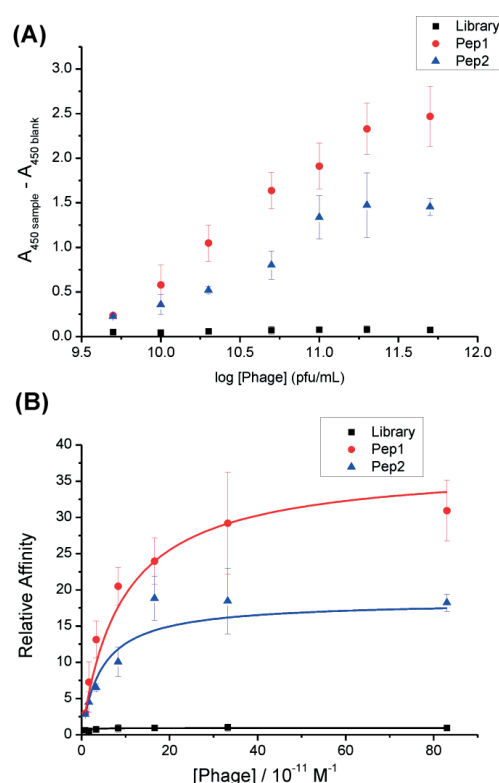

Figure 1. (A) Evolution of the colorimetric response and (B) the relative affinity as a function of phage concentration in the phage ELISA assay of **Pep1, Pep2** and the combinatorial phage library. The error bars represents the standard deviation of 9 independent measurements.

4.2.2. Peptide-PHPMA conjugates as model polymeric profragrances.

Following the successful identification of hair-binding peptides under shampoo conditions, the next step was to assess the feasibility of using them to enhance the deposition of linear polymers onto hair. These polymers can be in fact further designed as a polymeric profragrance platform by incorporating fragrance molecules via a labile linker that can be cleaved with external stimuli, such as pH, temperature and light.[7,8] To allow the incorporation of the isolated peptides onto both the model polymeric profragrance and the microcapsules, the cyclic peptide sequence **Pep1** (**Table 1**) was functionalized either with N-terminal azide (**N₃-Pep1**), N-terminal amine (**NH₂-Pep1**) and C-terminal carboxylic acid (**Pep1-COOH**) groups prior to the synthesis of the fragrance delivery systems. Furthermore, an N-terminal azide functionalized **Pep2** (**N₃-Pep2**) was also synthesized and used in the preparation of model polymeric profragrances. The structures of these peptides are shown in **Scheme 2**. The preparation of azide functionalized peptides is reported in the Supporting Information. HPLC elution profiles as well as the ESI-MS spectra of the peptides are provided in **Figure S2.**
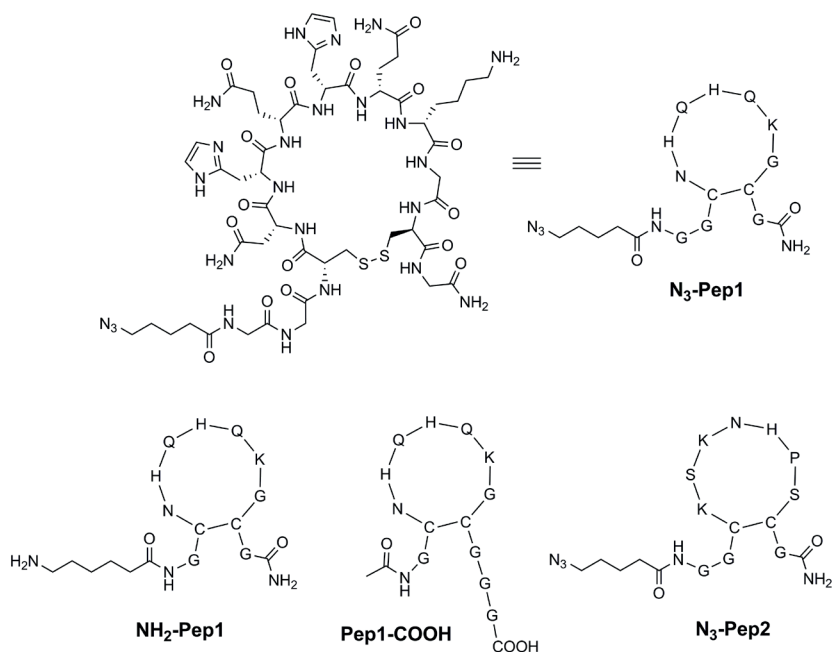
Scheme 2. Full and abbreviated structures of **Pep1** functionalized with (A) N-terminal azide (**N₃-Pep1**) and (B) C-terminal carboxylic acid (**Pep1-COOH**) as well as (C) **Pep2** with N-terminal azide groups (**N₃-Pep2**) to allow grafting of cyclic peptide sequences **Pep1** or **Pep2** onto model polymeric profragrances or core-shell microcapsules.
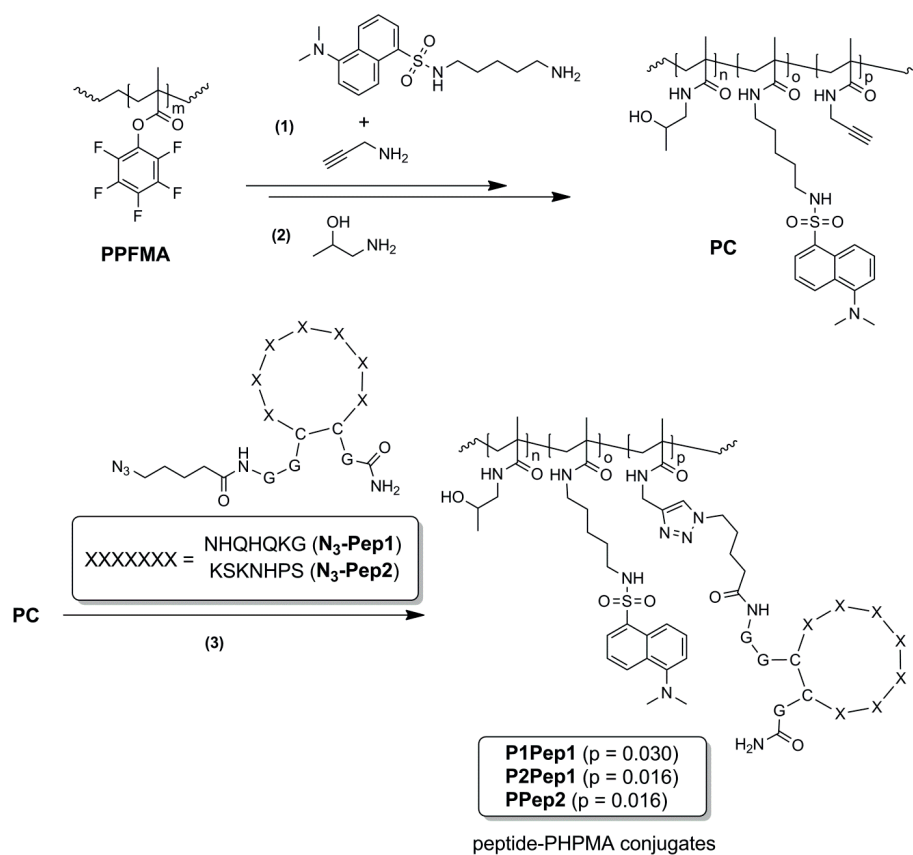
Scheme 3. Schematic illustration of the synthesis of peptide-PHPMA conjugates **P1Pep1**, **P2Pep1** and **PPep2**.[37]

In order to obtain a peptide functionalized model polymeric profragrance platform, a three-step post-polymerization modification of a poly(pentafluorophenyl methacrylate) (PPFMA) active ester precursor to yield water soluble peptide-PHPMA conjugates **P1Pep1**, **P2Pep1** and **PPep2** was performed (**Scheme 3** and Supporting Information).[37] Briefly, the post-polymerization modification strategy first involved a two-step active ester aminolysis of pentafluorophenyl ester groups with 5 mol% of propargylamine and 1 mol% of dansyl cadaverine in the first step followed by the quantitative modification of the remaining active ester groups into *N*-(2-hydroxypropyl)methacrylamide (HPMA) units to yield a water soluble polymer in the second step (**PC**). Dansyl groups were introduced in order to determine the deposition of these polymers onto hair via fluorescence intensity measurements. In the final step, N-terminal azide functionalized hair binding cyclic peptide disulfides (**N₃-Pep1** and **N₃-Pep2**) were incorporated using the propargylamine units via copper-catalyzed azide/alkyne cycloaddition (CuAAC) reaction using the protocol described by Finn and coworkers.[38] In total, three peptide-PHPMA

conjugates were prepared in which the first two incorporated 0.3 (**P1Pep1**) and 1.6 (**P2Pep1**) mol% of **N$_3$-Pep1**, respectively, in order to assess the influence of the extent of peptide incorporation to the deposition of polymer conjugates. The third conjugate was designed to incorporate 1.6 mol% of **N$_3$-Pep2** (**PPep2**), which can be used to compare the capability of **Pep1** and **Pep2** to promote the binding of these polymers onto hair surfaces. The extent of peptide incorporation to these conjugates was summarized in **Table 2**.

Table 2. The degree of peptide incorporation onto PHPMA conjugates and their extent of deposition onto hair under shampoo conditions.

Polymer name	Peptide		Fluorescence intensity measurements	
	Peptide sequence	Incorporation (mol%)[a]	Extent of polymer deposition (%)	Relative deposition with respect to **P1**
PC	-	-	1.4 ± 1.5	-
P1Pep1	**C**NHQHQKG**C**	0.3	5.0 ± 0.5	3.6 ± 1.1
P2Pep1	**C**NHQHQKG**C**	1.6	7.4 ± 1.6	5.3 ± 1.1
PPep2	**C**KSKNHPS**C**	1.6	6.7 ± 1.4	4.8 ± 1.1

[a] Calculated from ^{1}H-NMR analysis of the conjugates in methanol-d$_4$.

 Fluorescence intensity measurements were carried out in the next step to assess the deposition of these three peptide-PHPMA conjugates onto hair under shampoo conditions. The measurements were also performed using a fourth conjugate that did not contain any peptide (**PC**), which was used as a control. The experimental protocol of the fluorescence intensity measurements is provided in the Supporting Information. **Figure 2** shows the extent of polymer deposition when 0.2 mg/mL of these conjugates were applied to 10 mg of hair in a shampoo formulation. The results indicate that while the deposition of **PC** was only 1.5%, 0.3 mol% incorporation of **N$_3$-Pep1** (**P1Pep1**) already led to a 3.5-fold enhancement of the deposition of the peptide-PHPMA conjugates (5.0%). When the **N$_3$-Pep1** content was 1.6 mol% (**P2Pep1**), the deposition of the conjugates further increased to 7.4%. These results show that the incorporation of **Pep1** enhanced the deposition of the peptide-PHPMA polymers onto hair, and its extent can be tuned with the amount of **Pep1** incorporated into these polymers. Fluorescence intensity measurements revealed that **Pep2** can also be used as an effective hair deposition aid as its incorporation improved the deposition of the peptide-PHPMA polymers by 4.8-fold (6.7%) (**PPep2**). This value was statistically not significantly different from the deposition of **P2Pep1** according to a two-sided Student's t-test that compares the means

of two independent measurements (p = 0.37). The extent of deposition of these four peptide-PHPMA conjugates is summarized in **Table 2**, and the fluorescence intensity measurements carried out using a polymer concentration range between 0.01 to 0.2 mg/mL are illustrated in **Figure S3**. In summary, these results show that the incorporation of both peptide sequences **Pep1** and **Pep2** enhanced the deposition of linear polymers onto hair in a shampoo medium, and therefore, they can be used to prepare potential polymeric profragrances that selectively target human hair.
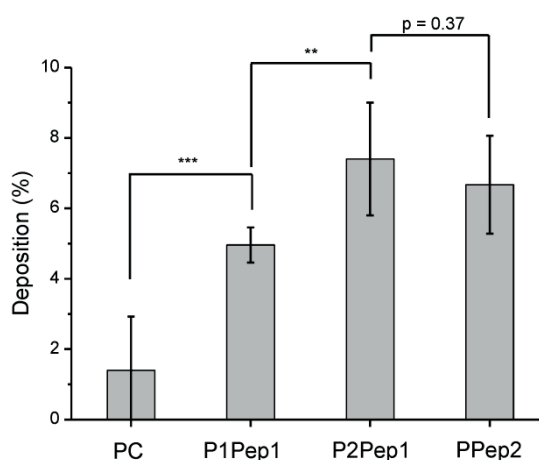

Figure 2. The extent of deposition of peptide-PHPMA conjugates. The reported depositions were measured following the incubation of 0.2 mg/mL of the polymers to 10 mg of hair. Error bars represent the standard deviation of 9 independent measurements. *** and ** represent a p value smaller than 0.001 and 0.01, respectively, in a two-sided Student's t-test that compares the means of two independent measurements. The difference between the extent of deposition of **P2Pep1** and **PPep2** was not statistically significant (p = 0.37).

4.2.3. Deposition of dansylated peptides.

In the previous section, the preparation of the peptide-PHPMA conjugates was achieved via the incorporation of the peptides from their N-termini to the polymer backbone. This conjugation strategy, however, may result in a loss of peptide activity if the binding domains of these peptides are in close proximity to the N-terminus, because these domains may not be well accessible after the conjugation of **N$_3$-Pep1** and/or **N$_3$-Pep2** to the PHPMA copolymers. This section, therefore, aims to compare the effect of

steric hindrance either in N or C-termini of **Pep1** towards its ability to bind onto hair surfaces. Furthermore, the influence of the stringency of the shampoo medium as a limiting factor for the deposition of these peptides will also be investigated.

Dansyl-Pep1   **Pep1-Dansyl**   **Dansyl-Pepx**
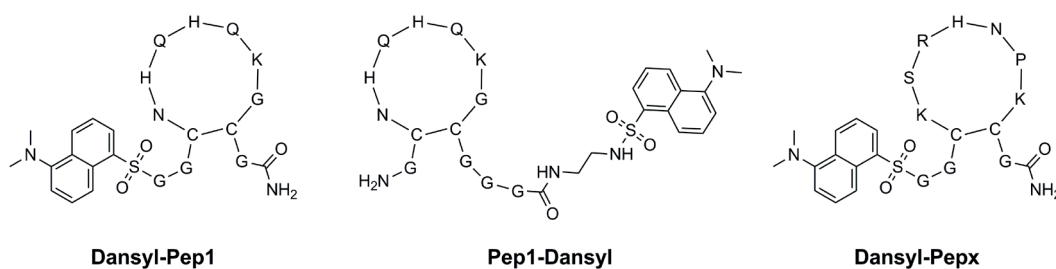
Scheme 4. Structures of dansylated cyclic peptide disulfides **Dansyl-Pep1**, **Pep1-Dansyl** and **Dansyl-Pepx**.

The influence of the steric hindrance in close proximity to the terminal groups as well as the soil-removing properties of the shampoo medium towards the binding of **Pep1** was assessed by comparing the extent of deposition of N- and C- terminal dansylated **Pep1** both in a shampoo formulation and in a 50 mM citrate buffer at pH 6.0. The only difference between the shampoo and the citrate buffer was the presence of surfactants in the former medium, whereas both the pH and buffer strength were identical. The N- and C-terminal dansylated **Pep1** variants are named as **Dansyl-Pep1** and **Pep1-Dansyl**, respectively (**Scheme 4**). Furthermore, an N-terminal dansylated variant of a randomized cyclic peptide (**Dansyl-Pepx**), a highly cationic peptide that shares sequence similarity with **Pep2** was used as a control in these experiments. The preparation of these peptides is explained in detail in the Supporting Information, and the HPLC elution profiles as well as the corresponding ESI-MS spectra of these three peptides are provided in **Figure S2**.

Figure 3 and **Figure S4** shows the extent of hair deposition when 15 μM of these peptides were exposed to 10 mg of hair both in shampoo and citrate buffer. First of all, these results demonstrate the selective binding of **Pep1** towards hair as both the N- and C-terminal dansylated **Pep1** deposited 3-5 times higher than **Dansyl-Pepx** from the shampoo and the citrate buffer. Second, it is evident from these experiments that the presence of surfactants in the shampoo formulation significantly limits the extent of **Pep1** deposition, irrespective from the terminal location of the incorporated dansyl groups.

Third, the comparison of N- and C-terminal dansylated **Pep1** first revealed that while **Pep1-Dansyl** deposited slightly higher (5.4%) than **Dansyl-Pep1** (4.2%) under shampoo conditions, this difference was not found to be statistically significant (p = 0.27). On the other hand, the extent of deposition of **Pep1-Dansyl** (26.7%) was more than two-fold as compared to **Dansyl-Pep1** (12.9%) in the citrate buffer. **Table 3** summarizes the extent of hair deposition of these three peptides both under shampoo and citrate buffer conditions. These results suggest that although the difference between the deposition for **Pep1-Dansyl** and **Dansyl-Pep1** was not significant in the shampoo medium, owing to the significant difference observed in the citrate buffer, the binding domain of **Pep1** is in closer proximity to the N-terminus. In the light of these findings, **Pep1** will be attached from its C-terminus to the surface of the polymeric fragrance carriers in order to potentially increase the deposition of these particles in the next step.
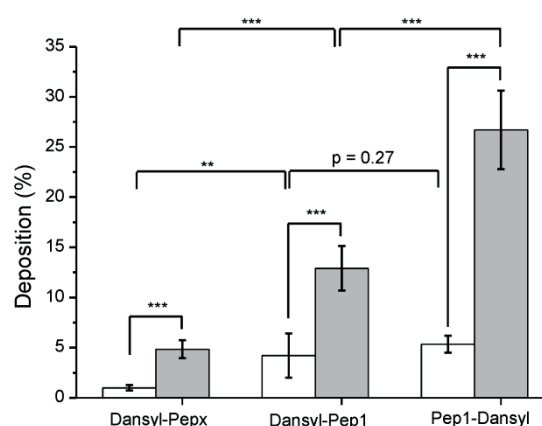
Figure 3. The extent of deposition of dansylated peptides onto hair from a shampoo formulation (white bars) and from a 50 mm citrate buffer at pH 6.0 (grey bars). Error bars represent the standard deviation of 6 independent measurements. *** and ** represent a p value smaller than 0.001 and 0.01, respectively, in a two-sided Student's t-test that compares the means of two independent measurements. The difference between the extent of deposition of **Dansyl-Pep1** and **Pep1-Dansyl** was not statistically significant under shampoo conditions (p = 0.27).

Table 3. The extent of deposition of 15 μM of dansylated peptides onto 10 mg hair in a shampoo formulation and a 50 mM citrate buffer solution.

| Peptide name	Peptide sequence	Deposition (%)	
		Under shampoo conditions	In 50 mM citrate buffer, pH 6.0
Dansyl-Pepx	**C**KSRHNPK**C**	1.0 ± 0.3	4.8 ± 0.4
Dansyl-Pep1	**C**NHQHQKG**C**	4.2 ± 2.2	12.9 ± 2.2
Pep1-Dansyl	**C**NHQHQKG**C**	5.4 ± 0.9	26.7 ± 3.9

4.2.4. Peptide-functionalized polyurethane/urea core-shell microcapsules as model fragrance carriers.

4.2.4.1. Synthesis of peptide-functionalized polyurethane/urea core-shell microcapsules.

Polyurethane/urea capsules have been prepared by interfacial polymerization between a water-soluble amino compound and an oil-soluble isocyanate, wherein the water-soluble monomer diffuses through the interface and burgeoning membrane to crosslink the oil-soluble monomer in the oil phase.[39,40] Guanidine carbonate and and Takenate® D-110N (**Scheme S1**) are used as the water-soluble amine and the oil-soluble isocyanate co-monomer, respectively. Isocyanate co-monomer was solubilized in a model perfume to be encapsulated consisted of a mixture of Romascone®, Verdox®, Dorisyl, Salicynile® and Cyclosal at an equivalent weight ratio (**Scheme 5**) as well as 10 w/w% of Uvinul® A+ as a UV-tracer for the deposition measurements. The interfacial polymerization yielded polyurea core-shell microcapsules with an average diameter of 10 μM. These capsules are referred to **C0**.

Since the hair deposition of C-terminal dansylated **Pep1** was found to be higher than the N-terminal dansylated variant in the previous section, surface grafting of **Pep1** was achieved by using 1-ethyl-3-(3-(dimethylamino)propyl)carbodiimide (EDC) / *N*-hydroxysuccinimide (NHS) coupling reaction between the surface amino groups of **C0** and a C-terminal carboxylic acid functionalized **Pep1** (**Pep1-COOH**) in the next step. Surface amino groups in **C0** microcapsules resulted from the hydrolysis of the residual isocyanate groups or the unreacted guanidine groups. To this end, two different **Pep1** grafted microcapsules were prepared by either using 1 or 10 w/w% of **Pep1-COOH** with respect to the mass of **C0** during the EDC/NHS coupling reaction. These capsules are

referred to **C1** and **C2**, respectively. The aqueous phases of the microcapsules dispersions (**C1** and **C2**) were analyzed by HPLC to detect and quantify the free peptide. Almost quantitative conversions were achieved for the grafting in both cases (**Figure S5**). Furthermore, successful surface grafting of highly cationic **Pep1-COOH** was indirectly determined from zeta-potential measurements, which increased from -2.2 to 10.1 mV at pH 3 in deionized water following 10 w/w% incorporation of the peptide (**C2 - Table S1**). The similar trend was also observed in 1 mM KCl solution, but the difference between the zeta-potential of **C0** and **C2** was reduced.
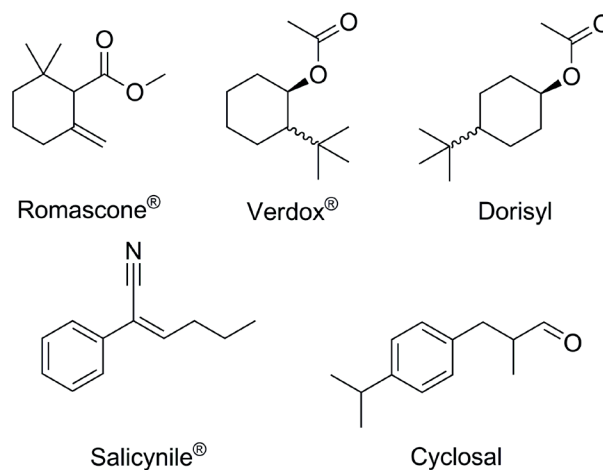
Scheme 5. Chemical structures of the ingredients of the model perfume.

4.2.4.2. Deposition of polyurethane/urea core-shell microcapsules on hair.

A quantitative deposition test method was established and implemented to probe the grafting efficiency of the targeting peptides on the surface of microcapsules **C1** and **C2** and consequent affinity of functionalized microcapsules for hair. To determine the deposition efficiency following conjugation of **Pep1-COOH**, a reproducible deposition test protocol was followed using a model cleanser formulation containing anionic surfactant (sodium lauryl ether sulfate (SLES), 12 w/w%), amphoteric surfactant (cocamidopropyl betaine (CAPB), 3 w/w%) and a conditioning film-forming polymer, Polyquaternium 7 (Salcare® SC-60, 0.5 w/w%) and subsequently the pH of the solution was adjusted 5.5. The protocol for the microcapsule deposition experiments were provided in the Supporting Information.
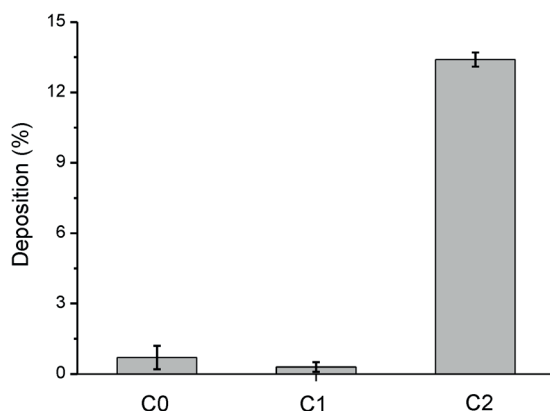
Figure 4. Average percentage of oil deposited onto hair from a microcapsule-loaded model cleanser formulation after rinsing. The average percentage of oil deposited from peptide-functionalized microcapsule **C1** and **C2**, generated using different peptides, grafting sequences and surface grafting densities is benchmarked against the unmodified control capsules, **C0**.

Figure 4 shows the extent of deposition of **C0**, **C1** and **C2** microcapsules onto hair under model cleanser formulation. First of all, these results show that 1 w/w% of **Pep1-COOH** grafting (**C1**) did not enhance the deposition of microcapsules. However, when the **Pep1-COOH** content of the capsules was increased to 10 w/w%, almost a 20-fold enhancement in deposition was achieved, such that while only 0.7% of **C0** deposited only hair, this value was 13.4% for **C2** (**Table 4**). The extent of deposition of the microcapsules is summarized in **Table 4**. These results show that **Pep1** can be used to significantly enhance the deposition of fragrance loaded microcapsules onto hair, however, only after relatively high grafting of the peptide onto the surface of the microcapsules. This enhancement at high grafting density can be attributed to the multivalency of the **Pep1** on the capsule surfaces, as multivalency effects were previously shown to significantly improve the binding strength of peptide-grafted nanoparticles.[41,42]

Table 4. Average amount of deposition and standard deviations of core-shell microcapsules **C0**, **C1** and **C2** on hair from a model cleanser formulation after rinsing under real-life application conditions.

Capsule	Amount of grafted peptide (w/w%)	Average deposition (%)	Relative deposition with respect to **C0**
C0	---	0.7 ± 0.5	---
C1	1	0.3 ± 0.2	0.4
C2	10	13.4 ± 0.3	19.1

4.2.4.3. Release of the model fragrance from core-shell microcapsules on hair.

After the demonstration that the grafting of **Pep1-COOH** to the surface of core-shell microcapsules significantly increased their deposition on hair under realistic shampoo cleansing application conditions, the final step was to investigate whether this improved deposition also resulted in increased headspace concentrations of the model perfume released from the capsules on the hair surface. Dispersions of microcapsules **C0** and **C2** were thus added to the model cleanser to contain the same total amount of model perfume in the final formulation. Hair samples were then washed with the model cleanser under the same conditions described for the deposition measurements. The uncut hair samples were then line-dried and the evaporation of the ingredients of the model fragrance analyzed by dynamic headspace analysis after 6 and 24 hours. The protocol for the headspace measurements were provided in the Supporting Information.

Table 5. Dynamic headspace concentrations and standard deviations for the release of the different ingredients of the model perfume encapsulated in **C0** or **C2** on hair from a shampoo cleanser application after line-drying for 6 and 24 hours.

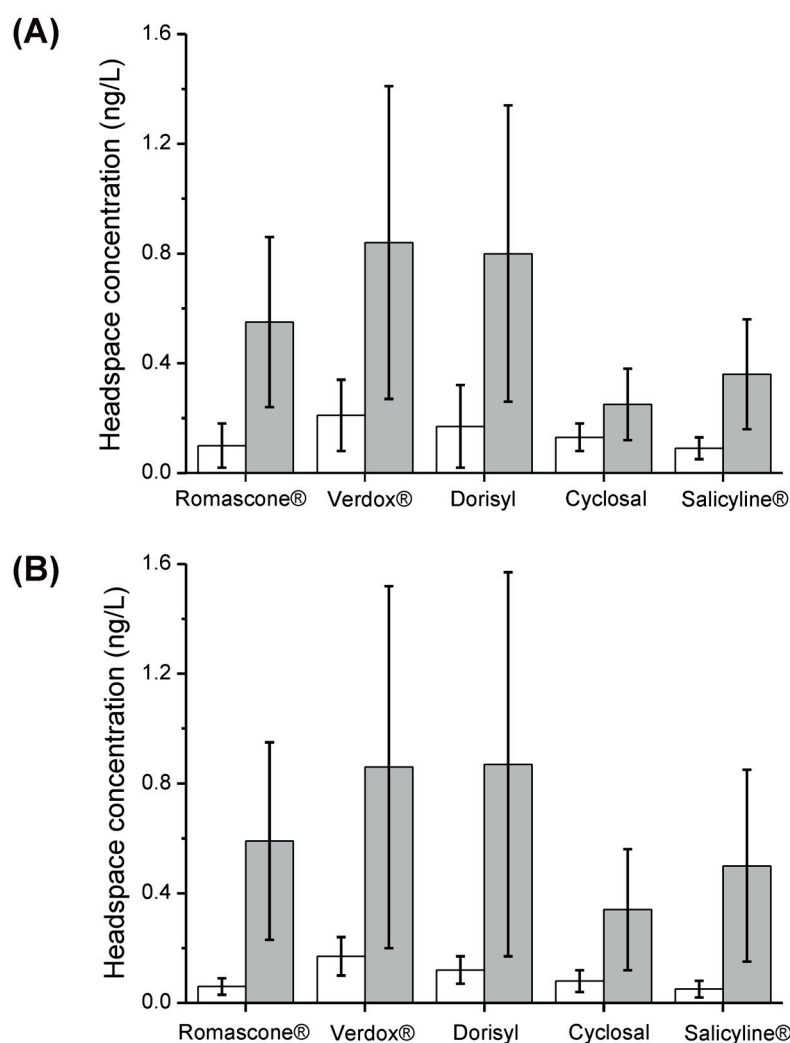| Capsule name	Drying time (h)	Romascone® ($ng\ L^{-1}$)	Verdox® ($ng\ L^{-1}$)	Dorisyl ($ng\ L^{-1}$)	Cyclosal ($ng\ L^{-1}$)	Salicynile® ($ng\ L^{-1}$)
C0	6	0.10 ± 0.08	0.21 ± 0.13	0.17 ± 0.15	0.13 ± 0.05	0.09 ± 0.04
C2	6	0.55 ± 0.31	0.84 ± 0.57	0.80 ± 0.54	0.25 ± 0.13	0.36 ± 0.20
C0	24	0.06 ± 0.03	0.17 ± 0.07	0.12 ± 0.05	0.08 ± 0.04	0.05 ± 0.03
C2	24	0.59 ± 0.36	0.86 ± 0.66	0.87 ± 0.70	0.34 ± 0.22	0.50 ± 0.35

Figure 5. Headspace concentrations measured for the different ingredients of the model perfume released from microcapsules **C0** (white bars) and **C1** (grey bars) on hair after a shampoo application and drying for (A) 6 hours and (B) 24 hours. Error bars represent the standard deviation of 2 measurements.

Figure 5 shows significantly increased fragrance release from the hair surfaces treated with **C2** microcapsules compared to **C0** both after 6 and 24 hours. Furthermore, while the headspace concentrations of the fragrances released from **C0** decreased with increasing drying time, those released from **C2** remained constant or even slightly increased with time. The relatively large standard deviations were attributed to the fact that the measurements were performed under realistic application conditions, in which several

physiochemical parameters such as ambient temperature and relative humidity during drying, and amongst many others, and not strictly controlled.[43] **Table 5** summarizes the headspace concentrations for the release of each of the fragrance in the perfume composition encapsulated in **C0** or **C2** after 6 and 24 hours. These data demonstrate that our approach to increase the deposition of polymeric fragrance carriers onto hair by using a selective cyclic peptide tag indeed allowed improving the performance of fragrance delivery under realistic rinse-off shampoo cleansing conditions. Enhanced deposition of these fragrance delivery systems usually translates directly to improved olfactive intensity and hence more effective delivery technologies. An order of magnitude improvement in adhesion and retention was thus expected to lead to appreciable improvements in the sensorial impact of the functionalized microcapsules.

4.3. Conclusions

Phage display identified peptides offer a solution to tackle the modest deposition of fragrance delivery systems onto hair under shampoo formulations. As a proof-of-concept, first, the feasibility of identifying hair binding peptide ligands under highly stringent shampoo medium was demonstrated. In the next step, hair binding peptide ligands were incorporated into PHPMA conjugates and the peptide incorporation was found to enhance the deposition of these polymers onto hair surfaces with a factor of 3.5 to 5. As a final example, polyurethane/urea core-shell type microcapsules containing a model perfume was synthesized and subsequently functionalized with the hair-binding peptide. 10 w/w% grafting of the peptide was found to increase the deposition of the capsules onto hair approximately with a factor of 20. This enhanced deposition led to higher release of the model perfume from the hair surfaces even after 24 hours under realistic application conditions as evidenced by dynamic headspace measurements.

4.4. References

(1)   Surburg, H.; Panten, J. *Common fragrance and flavor materials: preparation, properties and uses*, 6th Ed., Wiley-VCH, Weinheim, **2016**.

(2)   Ohloff, G.; Pickenhagen, W.; Kraft, P. *Scent and chemistry*, Wiley-VCH, Weinheim, **2011**.

(3)   *Flavours and fragrances – chemistry, bioprocessing and sustainability*, Berger, R. G. (Ed.), Springer Verlag, Berlin, **2007**.

(4)   Hagvall, L.; Bäcktorp, C.; Svensson, S.; Nyman, G.; Börje, A.; Karlberg, A.-T. *Chem. Res. Toxicol.*, **2007**, *20*, 807-814.

(5)   Marteau, C.; Ruyffelaere, F.; Aubry, J. M.; Penverne, C.; Favier D.; Nardello-Rataj, V. *Tetrahedron*, **2013**, *69*, 2268-2275.

(6)   Park, S.-J.; Arshady, R. *Microspheres, Microcapsules Liposomes*, **2003**, *6*, 157-198.

(7)   Herrmann, A. *Angew. Chem. Int. Ed.*, **2007**, *46*, 5836-5863.

(8)   Herrmann, A. *Chem. Unserer Zeit*, **2015**, *49*, 36-47.

(9)   Patravale, V. B.; Mandawgade, S. D. *Int. J. Cosmetic Sci.,* **2008**, *30*, 19-33.

(10)   Zhu, G.; Xiao, Z.; Zhou, R.; Yi, F. *Adv. Mater. Res.*, **2012**, *535-537*, 440-445.

(11)   Breuer, M. M. *J. Soc. Cosmet. Chem.*, **1981**, *32*, 437-458.

(12)   Glassman, R. *Drug Cosmet. Ind.*, **1997**, *160*, 50-58.

(13)   Deeksha; Malviya, R.; Sharma, P. K.; *Recent Pat. Inflammation Allergy Drug Discovery*, **2014**, *8*, 48-58.

(14)   Shaw, D. A. *Int. J. Cosmet. Sci.*, **1979**, *1*, 317-328.

(15)   Bhushan, B. *Biophysics of human hair: structural, nanomechanical, and nanotribological studies*, Springer, Berlin, New York, **2010**.

(16)   Fischer, E.; Fieber, W.; Navarro, C.; Sommer, H.; Benczédi, D.; Velazco, M.; Schönhoff, M. *J. Surfactants Deterg.*, **2009**, *12*, 73-84.

(17)   Drovetskaya, T. V.; Diantonio, E. F.; Kreeger, R. L.; Amos, J. L.; Frank, D. P. *J. Cosmet Sci.*, **2007**, *58*, 421-434.

(18)   Berthiaume, M. D.; Jachowicz, J. *J. Colloid Interface Sci.*, **1991**, *141*, 299-315.

(19)   Oshimura, E.; Abe, H.; Oota, R. *J. Cosmet. Sci.*, **2007**, *58*, 347-357.

(20)   Salvador, A.; Chisvert, A.; del Cañizo Gómez, C. in *Analysis of cosmetic products*, A. Salvador and A. Chisvert (Eds.), Elsevier, Amsterdam, **2007**, 332-339.

(21)   Nazir, H.; Li, P.; Wang, L.; Lian, G.; Zhu, S.; Ma, G. *J. Colloid Interface Sci.*, **2011**, *364*, 56-64.

(22)   Nazir, H.; Wang, L.; Lian, G.; Zhu, S.; Zhang, Y.; Liu, Y.; Ma, G. *Colloids Surf., B*, **2012**, *100*, 42-49.

(23)   *Interaction of surfactants with polymers and proteins*, Goddard, E. D.; Ananthapadmanabhan, K. P. (Eds.), Chapter 4, CRC Press, Boca Raton, **1993**.

(24)   Lochhead, R. Y.; Huisinga, L. R.; Waller, T. *Cosmet. Toiletries*, **2006**, *121* (3), 75-82.

(25)   Kalantar, T. H.; Tucker, C. J.; Zalusky, A. S.; Boomgaard, T. A.; Wilson, B. E.; Ladika, M.; Jordan, S. L.; Li, W. K.; Zhang, X.; Goh, C. G. *J. Cosmet. Sci.*, **2007**, *58*, 375-384.

(26)   Cortese, R.; Felici, F.; Galfre, G.; Luzzago, A.; Monaci, P.; Nicosia, A. *Trends Biotechnol.*, **1994**, *12*, 262-267.

(27)   Smith, G. P.; Petrenko, V. A. *Chem. Rev.*, **1997**, *97*, 391-410.

(28)   Rodi, D. J.; Makowski, L. *Curr. Opin. Biotechnol.*, **1999**, *10*, 87-93.

(29)   Kumar, M.; Sanford, K. J.; Cuevas, W. A.; Du, M.; Collier, K. D.; Chow, N. *Biomacromolecules*, **2006**, *7*, 2543-2551.

(30)   O'Brien, J. P.; Yang, J. (to E. I. Du Pont De Nemours & Co.), *Peptide-based diblock and triblock dispersants and diblock polymers,* US Pat. Appl. Publ. US 2005/054752, **2005**.

(31)   Wang, H.; Wu , Y.; O'Brien, J. P. (to E. I. Du Pont De Nemours & Co.), *Method for identifying skin care composition-resistant skin-binding peptides,* US Pat. Appl. Publ. US 2006/0199206, **2006**.

(32)   O'Brien, J. P.; Wang, H.; Wilkins, A. E.; Wu , Y. (to E. I. Du Pont De Nemours & Co.), *Method for identifying shampoo-resistant hair-binding peptides and hair benefit agents therefrom*, US Pat.Appl. Publ. US 2006/0073111, **2006**.

(33)   Dolk, E.; van der Vaart, M.; Lutje Hulsik, D.; Vriend, G.; Haard, H.; Spinelli, S.; Cambillau, C.; Frenken, L.; Verrips, T. *Appl. Environ. Microbiol.*, **2005**, *71*, 442-450.

(34)   Ladner, R. C.; Sato, A. K.; Gorzelany, J.; de Souza, M. *Drug Discov. Today*, **2004**, *9*, 525-529.

(35)   Giebel, L. B.; Cass, R.; Milligan, D. L.; Young, D.; Arze, R.; Johnson, C. *Biochemistry*, **1995**, *34*, 15430-15435.

(36)   Koivunen, E.; Wang, B.; Ruoslahti, E. *Nat. Biotechnol.*, **1995**, *13*, 265-270.

(37)   Günay, K. A.; Klok, H.-A. *Polym. Chem.*, **2016**, *7*, 970-978.

(38)   Hong, V.; Presolski, S. I.; Ma, C.; Finn, M. G. *Angew. Chem. Int. Ed.*, **2009**, *48*, 9879-9883.

(39)   Yoshizawa, H.; Kamio, E.; Hirabayashi, N.; Jacobson, J.; Kitamura, Y. *J. Microencapsulation*, **2004**, *21*, 241-249.

(40)   Hong, K.; Park, S. *J. Appl. Polym. Sci.*, **2000**, *78*, 894-898.

(41)   Montet, X.; Funovics, M.; Montet-Abou, K.; Weissleder, R.; Josephson, L. *J. Med. Chem.*, **2006**, *49*, 6087-6093.

(42)   Gray, B. P.; Li, S. Brown, K. C. *Bioconjugate Chem.*, **2013**, *24*, 85-96.

(43)   Buchs, B.; Godin, G.; Trachsel, A.; de Saint-Laumer, J.-Y.; Lehn, J.-M. Herrmann, A. *Eur. J. Org. Chem.*, **2011**, 681-695.

4.5. Supporting Information – Experimental Section

Materials. All chemicals were used as received unless otherwise described. Synthesis of pentafluorophenyl methacrylate (PFMA) monomer,[1] reversible addition-fragmentation chain transfer (RAFT) polymerization of PFMA[2] as well as the removal of the dithioester end-groups of the synthesized PPFMA polymer[3] were performed according to previously described protocols. Chloramphenicol was received from BioChimica. Tween[®] 20, bovine serum albumin (BSA), 1-amino-2-propanol (93.0%), dansyl cadaverine (> 97.0%), propargylamine (97%), triethylamine (TEA) (97.0%), piperidine (99.0%), trifluoroacetic acid (TFA) (99.0%) *N*-methyl-2-pyrrolidone (NMP) (98.0%), *N,N*-diisopropylethylamine (DIEA) (98.0%), triisopropylsilane (TIS) (99%), tris(3-hydroxypropyltriazolylmethyl)amine (THPTA) (95%), aminoguanidine hydrochloride (99%), guanidine carbonate (99%), $CuSO_4 \cdot 5H_2O$ (97%), sodium ascorbate (Na_{Asc}) (98%), dansyl chloride (98%) and 1-ethyl-3-(3-(dimethylamino)propyl)carbodiimide (EDC) (97%) were received from Sigma Aldrich. *N*-hydroxysuccinimide (NHS) was obtained from Alfa Aesar. ULTRA-TMB ELISA solution was received from Thermo Scientific. Anti-M13-HRP monoclonal antibody was received from Abcam. All Fmoc-amino acids except S-acetaminomethyl (Acm) protected cysteine (Fmoc-Cys(Acm)), Oxyma-Pure and F-moc Rink Amide resin were received from Iris Biotech. Fmoc-Cys(Acm) (99%) and 5-azidopentanoic acid (5-AzPOH) (97%) were obtained from Bachem. *N,N,N′,N′*-Tetramethyl-*O*-(1H-benzotriazol-1-yl)uronium hexafluorophosphate (HBTU) (98%) was received from Fluorochem. Thallium trifluoroacetate ($Tl(CF_3COO)_3$) (97%) was obtained from TCI. Texapon[®] N70 NA and Salcare[®] SC 60 were obtained from BASF. Mirataine[®] BET C-30 was obtained from Solvia. Takenate[®] D-110N was obtained from Mitsui Chemicals. Poly(vinyl alcohol) KC506 was obtained from Kuraray. Acetonitrile (AcN) (HPLC grade) was obtained from VWR international. Dansyl Novatag resin was received from Merck Millipore. Tenax[®] TA (poly(2,6-diphenyl-*p*-phenylene oxide), 35-60 Mesh) was obtained from Agilent Technologies. Cartridges used for headspace sampling were filled with 100 mg of the polymer. Cyclic peptide disulfide **Pep1-COOH** (95.0%) was received from ChinaPeptides.

A model shampoo formulation for the phage display experiments was prepared by adding sodium lauryl ether sulfate (SLES, Texapon[®] N70 NA, 12.0 g) and cocamidopropylbetaine (CAPB, Mirataine[®] BET C-30, 3.0 g) to a citrate buffer (50 mM, 1 L). The final pH was adjusted to 6.0. For the testing of functionalized microcapsules, a

model cleanser was formulated with SLES (17.2 g), CAPB (10.0 g), Salcare$^®$ SC 60 (1 w/w% in water, 50.0 g) and deionized water (22.8 g), which was meant to be a simplification of typical shampoo and shower gel cleansing formulations. The pH was adjusted with a citric acid solution (50%) to 5.5. Net untreated brown Caucasian hair swatches (0.5 g, 10 cm) with an average diameter of 0.4 mm were purchased from International Hair Importers and used as received. Affinity selections were carried using a combinatorial phage library displaying 9-mer cyclic peptide disulfides (C9C). These phage libraries were a gift from Prof. Christian Heinis and their construction was described in a previous publication.[4]

The synthesis of N-terminal azide functionalized hair binding peptides (**Pep1** and **Pep2**) and the peptide-PHPMA conjugates (**P1Pep1**, **P2Pep1** and **PPep2**) were already reported in Chapter 2, and therefore they will not be described here in detail. Similarly, the synthesis of C-terminal dansylated peptide (**Pep1-Dansyl**) will not be explained herein as it was carried out using the identical protocol reported for the preparation of **Pep2D** in the Supporting Information of **Chapter 3**.

Methods. Fluorescence intensity and absorbance measurements were performed with a Tecan Infinite Pro 200 reader. Synthesis of the peptides was carried using Fmoc SPPS using a CEM Liberty automated microwave synthesizer. HPLC was performed using a Shimadzu Prominence system containing LC-20AP pumps, FRC-10A fraction collector, CTD-20AC column oven and SPD-M20A diode array detector coupled to a LCMS-2020 liquid chromatography mass spectrometer. The peptides were characterized using an analytical Grace Vydac 218TP54 C18 column and purified using Grace Vydac 218TP15 preparative column. ^{1}H-NMR spectra were recorded on a Bruker (ARX-400) 400 MHz spectrometer at room temperature using a relaxation time (t$_1$) of 10 seconds. Chemical shifts were reported relative to the residual proton signal of the solvent. The solid content and amount of model fragrance encapsulated into core-shell microcapsule dispersions were assessed by thermogravimetric analysis on a TGA/SDTA851e instrument (Mettler-Toledo) equipped with a microbalance having an accuracy of 1 μg and a 35 mL oven.[5] Samples (ca. 12 mg) were introduced into an aluminium oxide crucible (70 μL) and their mass was measured as a function of temperature and time under a constant flow of nitrogen (20 mL/min). Measurements were carried out at temperatures from 25°C to 50°C, at a rate of 5°C/min, then at 50°C for four hours. Stable core-shell microcapsules afforded plateau corresponding to the mass of solid in the dispersion.

Procedures.

Identification of hair binding peptides under shampoo conditions by phage display. A combinatorial C7C phage library was produced via the incubation of chloramphenicol resistant *E. coli* TG1 cell lines (OD = 0.4) in a 2YT medium (500 mL, containing 0.1 mg/mL of chloramphenicol) at 30 °C. After 16 hours, the bacteria pellet was precipitated by centrifugation and the supernatant that contains the phages was mixed with 190 mL of an aqueous solution of NaCl (2.5 M) containing 20 w/w% of polyethylene glycol (PEG). The phages were isolated by centrifugation and subsequently resuspended in the model shampoo formulation (8 mL). The concentration of the input phages was approximately 2 x 10^{12} plaque forming units (pfu) at the beginning of the each round of selection.

Knotted hair samples (9-11 mg) were prewashed once with H$_2$O/isopropanol 16:1 v/v% and three more times with MilliQ water and allowed to dry for 2 hours prior to their incubation with the phage solution. Then, the hair samples were exposed to the model shampoo formulation (8 mL) containing the phages for 20 minutes at 37 °C with gentle agitation in falcon tubes. The hair samples were then removed from the falcon tubes, inserted into new tubes, and washed 8 times either with a tris buffered saline solution (TBS, 10 mL, pH 7.4) that contained 0.1 v/v% of Tween® 20 at each round of selection (**Condition 1**) or with the TBS buffer containing 0.1, 0.2, 0.3, 0.4 and 0.5 v/v% of Tween® 20 in the 1st, 2nd, 3rd, 4th and 5th rounds of selection (**Condition 2**), respectively, to remove the weakly bound phages. Hair samples were washed twice more with the TBS solution (10 mL) that did not contain any Tween® 20, removed from the falcon tubes and dried. Each washing step was carried for 5 minutes with gentle agitation and the samples were transferred into new falcon tubes for four different times throughout the 10 washing steps in order to minimize the selection of background binders associated with the polystyrene tube.

Following the washing, the infection step was performed by directly immersing the hair samples into the 2YT medium (30 mL) containing fresh TG1 with an OD of 0.4. The infection was allowed to continue for 90 minutes at 37 °C. Then, the solutions were centrifuged, the supernatants were discarded, the bacterial pellets were resuspended in 2YT (1 mL) and subsequently plated into chloramphenicol containing agar plates. The plates were incubated overnight at 37 °C and scraped off for the recovery of the infected bacteria. Aliquots of these solutions were also taken and plated into agar plates following the infection step to determine the output phage titers after each selection round. In total,

2 independent affinity selection experiments were carried up to the 5th round, which were named as **C1** and **C2** depending on the performed washing step **1** and **2**, respectively. The evolution of the output phage titers with respect to number of selection rounds in these experiments is summarized in **Figure S1**. Individual colonies of phage infected TG1 cells were picked from the 3rd, 4th and 5th rounds of selection from these 2 experiments, their plasmids were extracted using a QIAGEN spin Miniprep kit and these plasmids were subsequently sent to sequencing analysis.
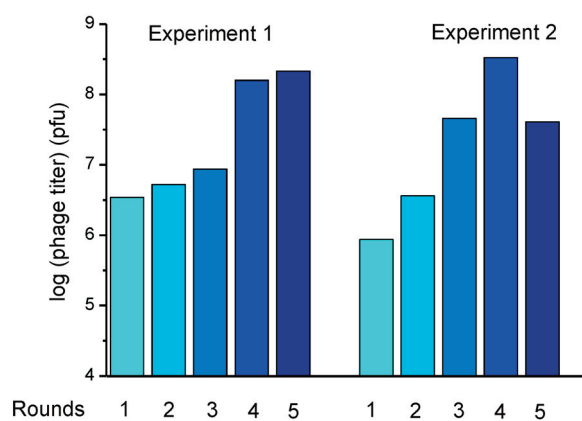

Figure S1. Evolution of the output phage titers with respect to number of rounds in affinity selection experiments **1** and **2**.

Phage ELISA. The individual phages, which were identified as potentially affine hair binders and the combinatorial C7C phage library were produced similar to the protocol described in the previous section. The phages were re-suspended in the model shampoo formulation (2 mL) and the initial concentrations (input titer) of the phages were calculated from the average of three independent phage titrations.

Before incubation, the surfaces of 1.5 mL polystyrene Eppendorf tubes were blocked with PBS buffer (500 μL, pH 7.4) containing 0.1 w/w% of Tween® 20 (PBST 0.1%) and 2 w/w% of BSA for 30 minutes. Then, the tubes were washed with MilliQ H_2O (3 x 500 μL) and air dried. Prewashed hair samples (mass = 9-11 mg) were introduced to the wells and the model shampoo formulation (250 μL) containing varying phage concentrations between 2 x 10^9 to 5 x 10^{12} pfu/mL was added. Phage ELISA experiments were carried out by using both the individual phages that have been identified as potentially affine binders as well as with the combinatorial phage library, which were used as a reference.

In addition to these experiments, blank measurements were also performed by incubating the hair samples with the model shampoo that does not contain any phage. Incubations were carried out for one hour at 37 °C and the hair samples were subsequently washed three times with PBST 0.1% (250 μL, pH 7.4) and one more time with PBS (pH 7.4) (Washing cycle). Another blocking step was performed by introducing PBST 0.1% (250 μL) containing 2 w/w% of BSA and the residual BSA was washed off by subsequently performing another washing cycle. In the next step, the samples were incubated with PBST 0.1% buffer (250 μL) containing 2 w/w% of BSA and 1/5000 dilution of a 40 μg/mL stock solution of Anti-M13-HRP antibody for one hour and another washing cycle was performed to remove the unbound antibody. The hair samples were allowed to dry and subsequently transferred into new Eppendorf tubes. An ULTRA-TMB solution (250 μL) was added to these wells in order to initiate the colorimetric response. The evolution of the colorimetric response was quenched by adding H_2SO_4 (2 M, 250 μL) after 15 minutes. Fractions of the quenched solutions (200 μL) were transferred into a 96-well plate and the absorbance in the wells was measured at 450 nm. The normalized absorbances associated with the amount of hair bound phage were calculated by taking the difference between the absorbance values obtained from the sample and the blank measurements. All of the phage ELISA experiments were performed three times. The apparent binding strengths of the phages were calculated using Serizawa's method by fitting the normalized absorbance as a function of phage concentration according to a Langmuir-type adsorption model.[6]

Synthesis of N-terminal dansylated peptides (Dansyl-Pep1 and Dansyl-Pepx). The on-resin construction, thallium(III) trifluoroacetate mediated intramolecular cyclization as well as the cleavage of these peptides was carried using the protocol reported for the synthesis of **Pep1** in Chapter 2, and therefore will not be described herein in detail. The only difference in the synthesis of these peptides was the incorporation of an N-terminal dansyl group following the intramolecular cyclization rather than 5-azidopentanoic acid, which was used during the preparation of **Pep1**.
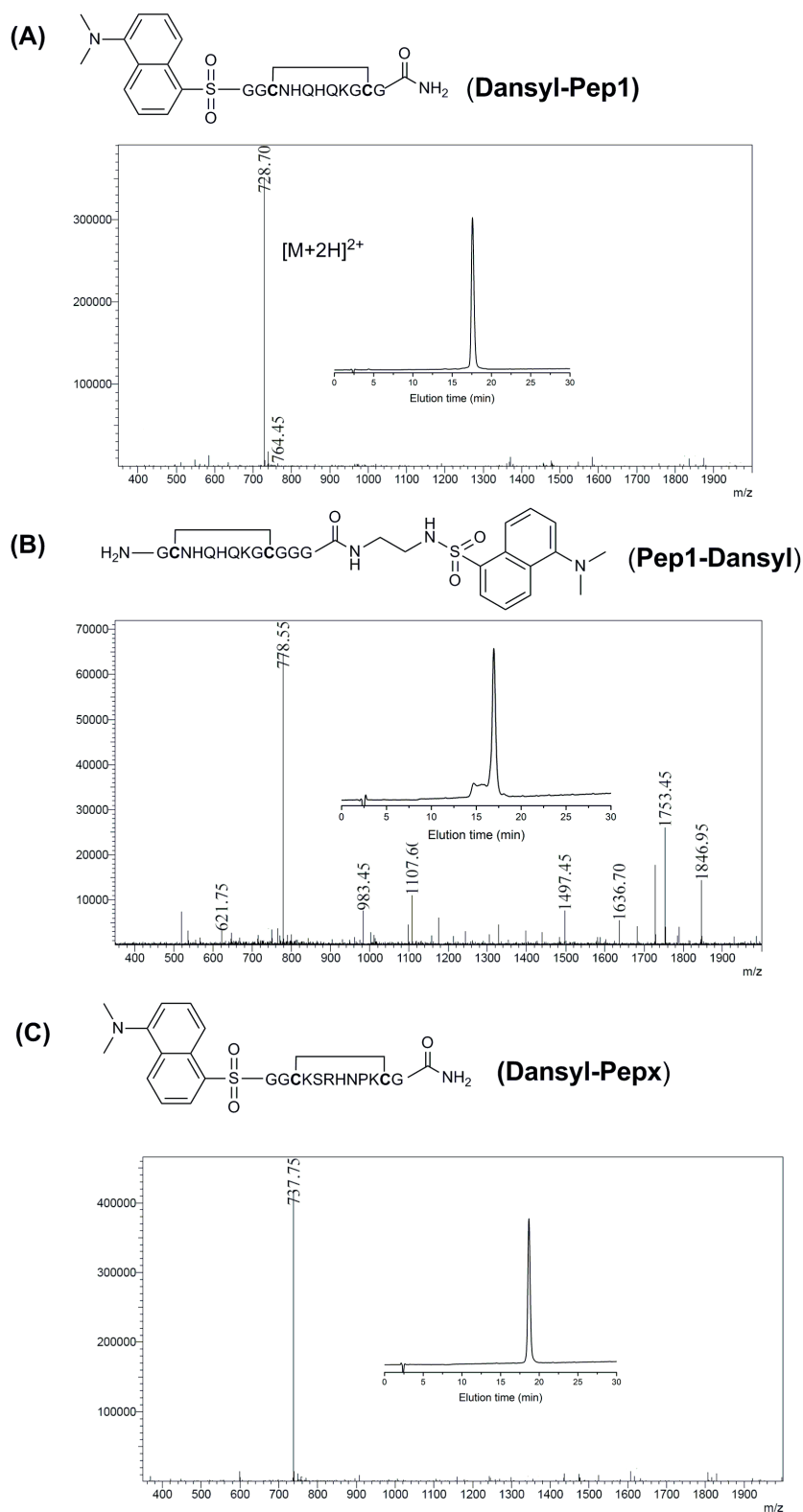
Figure S2. HPLC elution profiles and the ESI-MS spectra of (A) **Dansyl-Pep1**, (B) **Pep1-Dansyl** and (C) **Dansyl-Pepx**.

Briefly, incorporation of N-terminal dansyl groups was achieved as follows: 269 mg dansyl chloride (1.00 mmol, 4 equiv. with respect to Rink-amide bound intramolecularly cyclized peptide) was dissolved in 5 mL anhydrous DMF in a round bottom flask and subsequently 348 µL N,N-diisopropylethylamine (DIEA) (2.00 mmol, 8 equiv. with respect to the resin bound peptide) was added under a flow of N_2. In parallel, the resin that contains the intramolecularly cyclized peptide was swollen in 5 mL anhydrous DMF in a reaction vessel. After that, the mixture that contains the dansyl chloride and DIEA was transferred to the reaction vessel via a cannula under a flow of N_2. The reaction was allowed to continue for 2 hours at room temperature with gentle agitation. In the final step, the resin bound peptides were washed 3 times with 50 mL DMF and once more with 50 mL DCM and dried. The cleavage and HPLC purification of the peptides was carried using the protocol described for the synthesis of **Pep1** in Chapter 2 in the subsequent steps. **Figure S2** provides the analytical HPLC elution profiles as well as the corresponding ESI-MS spectra of the N and C-terminal dansylated peptides.

Surface deposition measurements of peptide-PHPMA conjugates and dansylated peptides. The protocol of the fluorescence intensity measurements was identical both for the peptide-PHPMA conjugates and the dansylated peptides except for two differences: First, while the concentration range of the peptide-polymer conjugates were between 0.01 to 0.2 mg/mL in these experiments, 0.5 to 15.0 µM of the peptides were incubated with hair samples to assess their extent of depositions. Secondly, apart from shampoo conditions, the extent of deposition of peptides onto hair was also assessed at 50 mM citrate buffer at pH 6.0 without the presence of SLES and CAPB in order to determine the influence of the stringency of the shampoo medium to the binding of the peptides.

Briefly, prewashed hair samples (mass = 9-11 mg) were inserted into 1.5 mL polystyrene Eppendorf tubes. Then, 500 µL of a model shampoo formulation or citrate buffer solution containing varying concentrations of peptide-PHPMA conjugates or dansylated peptides were introduced to the tubes. In parallel, same solutions were also introduced to the tubes that did not contain any hair (Blank measurements). The incubation was carried for one hour at 37 °C with gentle agitation. Following the incubation, 100 µL of the solutions were transferred into a 96-well plate. The solutions were diluted 3-fold with model shampoo formulation or citrate buffer solution, and the fluorescence intensities of the samples (FI_{hair}) were recorded at $\lambda_{em} = 530$ nm using $\lambda_{ex} = 335$ nm. Separately, the fluorescence intensity of the solutions introduced to the wells that

do not contain any cotton (FI_{blank}) were also diluted 3-fold in a new 96-well plate and measured. The difference between the fluorescence intensities of FI_{blank} and FI_{hair} yielded the amount of conjugate deposited ($FI_{deposited}$). Finally, the $FI_{deposited}$ values were normalized to one with respect to the FI_{blank} values recorded in the measurements that contain the highest concentration of peptide-PHPMA conjugates (0.2 mg/mL) or the dansylated peptides (15 µM). Fluorescence intensity measurements of peptide-polymer conjugates were performed three times in triplicates, whereas the measurements carried using dansylated peptides were repeated two times in triplicates. **Figure S3 and S4** provides the results of the fluorescence intensity measurements that is carried out using the entire polymer and peptide concentration range, respectively.
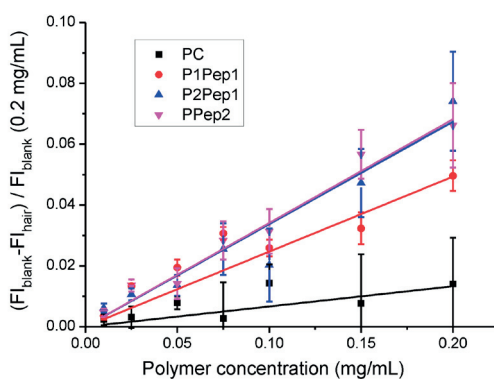

Figure S3. Normalized fluorescence intensity (FI) associated with the amount of hair deposited peptide-PHPMA conjugates as a function of polymer concentration. Error bars represent the standard deviation of 9 independent measurements.
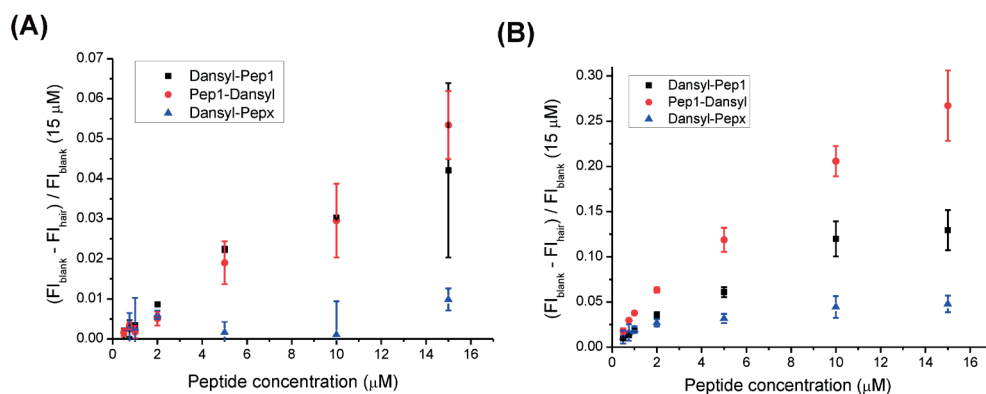

Figure S4. Normalized fluorescence intensity (FI) associated with the amount of hair deposited peptides as a function of peptide concentration under (A) shampoo and (B) 50 mM citrate buffer solutions. Error bars represent the standard deviation of 6 independent measurements.

Preparation of dispersions of polyurethane/urea core-shell microcapsules (C0). In a beaker, a mixture of a model perfume (consisting of Romascone®, Verdox®, Dorysil, Salicynile® and Cyclosal, 5.00 g each for a total of 20.00 g), a UV-tracer (Uvinul A+, 2.00 g) and an isocyanate (Takenate® D-110N, 5.10 g, 12 mmol NCO, **Scheme S1**) was added to an aqueous solution (49.00 g) of poly(vinyl alcohol) KC506 (2.00 g) in water (100.00 g) and stirred with an Ultra-Turrax at 24000 rpm for 4 minutes. The pH of the resulting emulsion was adjusted to about 10.5-11.0 with a solution of sodium hydroxide (30 w/w %). The emulsion was then transferred into a Schmizo reactor (250 mL) equipped with an anchor and a mechanical stirrer and stirred at 350 rpm. A solution of an amine (guanidine carbonate, 0.90 g, 20 mmol NH_2) in water (5.00 g) was added dropwise at room temperature during 1 hour. The reaction mixture was then heated to 70°C during 1 hour and kept at the same temperature for 2 hours to afford **C0** (average diameter: 10 μm, solid content: 45.7 w/w%, amount of encapsulated model perfume in the dispersion: 37.0 w/w%, in the capsule: 80.9 w/w%.
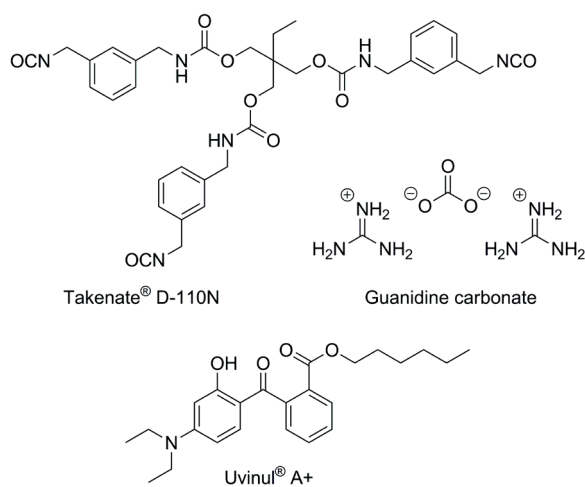
Scheme S1. Structures of Takenate® D-110N and guanidine carbonate used for the preparation of polyurethane/urea core-shell microcapsules and of Uvinul® A+ serving as a UV-tracer for the hair deposition measurements.

Preparation of dispersions of polyurethane/urea core-shell microcapsules C1 and C2. Microcapsules **C0** were washed by decanting the capsule dispersion and removing the aqueous phase. The resulting dispersion was diluted with water (20 mL) twice, and

the aqueous phase removed each time. Finally a washed dispersion of **C0** containing 33.2 w/w% of capsules was obtained (as shown by thermogravimetry).

The washed dispersion of capsules **C0** (5.80 g) was placed in a Schmizo reactor (250 mL), equipped with an anchor and a mechanical stirrer, and diluted with water (80 g) at pH 10.50. Then, a solution of cyclic peptide **Pep1-COOH** (0.04 g =1 w/w%), EDC (0.029 g), NHS (0.017 g) in water (14 g) prepared in a beaker at pH 5.02 was added, and the reaction mixture stirred at room temperature for 24 hours to afford a white dispersion. The obtained dispersion was decanted and the aqueous phase removed to afford **C1** (solid content: 20.5 w/w%, amount of encapsulated model perfume in the dispersion: 16.6 w/w%). HPLC elution profile of the residual aqueous phase of **C1** dispersion did not reveal the presence of **Pep1-COOH**, which indicates quantitative incorporation of the peptide onto the surface of the capsules (**Figure S5**).

Similarly, the washed dispersion of **C0** (2.60 g), diluted with water (7.50 g) at pH 9.00, was modified as described above using cyclic peptide **Pep1-COOH** (0.17 g = 10 w/w%), EDC (0.13 g), NHS (0.07 g) to afford **C2** as a white dispersion (solid content: 20.9 w/w%, amount of encapsulated model perfume: 16.9 w/w%). HPLC elution profile of the aqueous phase of **C2** dispersion revealed the presence of residual **Pep1-COOH**, which indicates that the majority of the peptide was incorporated onto the surface of the capsules (**Figure S5**).

Table S1. Zeta potentials for **C0** and **C2** in pH-adjusted DI water or 1 mM KCl solution to probe surface charge as a function of solution pH. Determination of a positive surface potential for **C2** at low pH confirmed the grafting efficacy and availability of positively-charged side chains which may drive deposition onto hair and are sufficiently protonated at low pH.

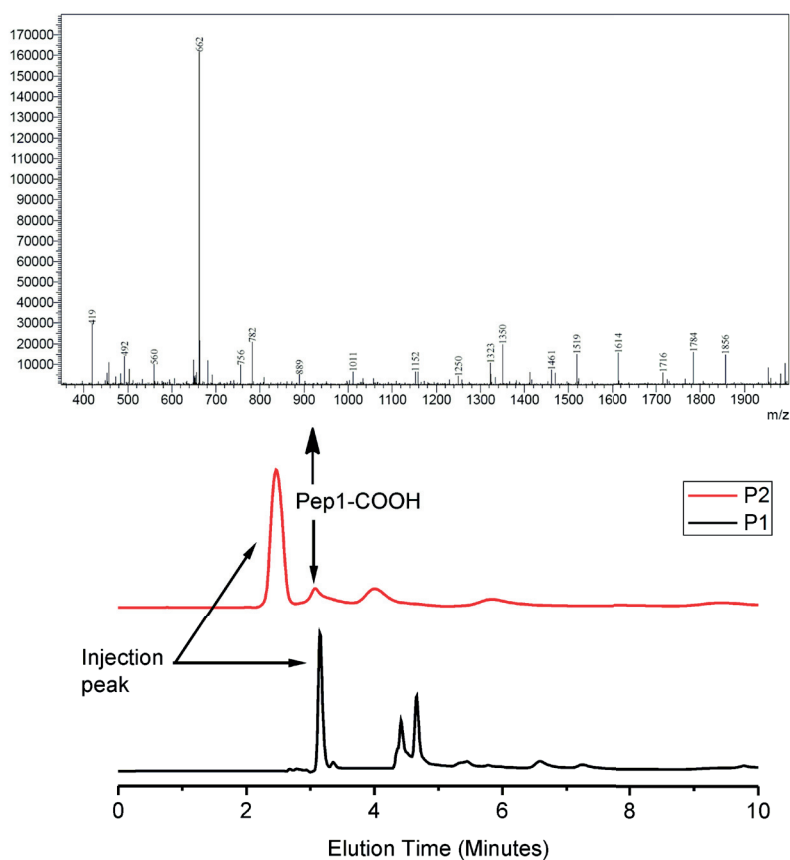| Capsule	Zeta potentials in pH adjusted DI water (mV)	
	pH 3	pH 9
C0	-2.2	-14.6
C2	10.1	-12.2
	Zeta potentials in pH adjusted 1 mM KCl solution (mV)	
	pH 3	pH 9
C0	-0.8	-2.2
C2	1.2	-1.7

Figure S5. HPLC elution profiles of the residual aqueous phase of **C1** and **C2** dispersions and the ESI-MS spectrum of the peak that is associated with residual **Pep1-COOH**.

Deposition of core-shell microcapsules on hair. Core-shell microcapsules were deposited onto human hair swatches from a shampoo cleanser application using the following test protocol (**Figure S6**). (a) Hair swatches (0.5 g) were wetted with warm tap water (39°C) and (b) gently squeezed out. (c) The capsule-loaded (0.5 w/w%) model cleanser formulation (0.1 mL) was then applied and the surfactant mixture was distributed with (d) 5-10 horizontal and (e) 5-10 vertical passes. As a reference, an aliquot of each formulation applied to hair was loaded into a scintillation vial to serve as the 100% deposition control. (f) The hair swatch was then rinsed with tap water (100 mL), and the excess water was gently squeezed out. (g) For the quantification of the functionalized microcapsule deposition, the hair swatch was then cut into a pre-weighed 20 mL scintillation vial.
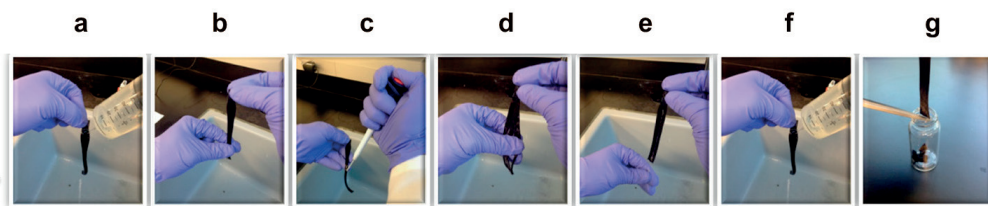
Figure S6. Protocol for the deposition of core-shell microcapsules on hair from a model cleanser formulation.

Core-shell microcapsules **C0**, **C1**, and **C2** containing the model perfume and a UV-tracer were deposited onto hair swatches according to the protocol described above. The process illustrated in **Figure S6** was repeated in triplicate and then the vials containing the cut hair were dried in a vacuum oven, weighed to determine the mass of the hair in the vials, and finally prepared for solvent extraction of the tracer using 200 proof ethanol (4 mL) under sonication for 1 hour. Controls were also prepared in triplicate by adding the model cleanser formulation (0.1 mL) containing microcapsules to an empty vial. Controls facilitate determination of tracer extraction efficiency and applied oil mass (100% deposition). After sonication, the samples were filtered through a 0.45 µm PTFE filter and the extracted tracer masses for the applied and control samples were determined by HPLC using a UV detector. The percentage of oil mass deposited onto hair swatches after rinsing was then calculated.

Dynamic headspace analysis. Dispersions of polyurethane/urea core-shell microcapsules **C0** (0.13 g) or **C2** (0.39 g) were added to the model cleanser formulation to make up for 10.01 g and to contain the same amount (0.48 w/w%) of model perfume in the final formulation. The samples were manually shaken for 10 minutes. The core-shell microcapsules with the model perfume were then deposited onto the hair swatches following the protocol described above (steps (a)-(f), **Figure S6**). The uncut hair swatches were line-dried for 3.5 hours (210 minutes) and analyzed by dynamic headspace sampling.

For the dynamic headspace measurements one of the hair swatches was placed in a homemade headspace sampling cell (inner volume ca. 160 mL), which was thermostatted at 25°C. A constant air flow (ca. 200 mL min^{-1}, which was filtered through activated charcoal and bubbled through a saturated solution of NaCl to ensure a constant humidity of the air of ca. 75%) was aspirated through the headspace sampling cell.[7,8] To equilibrate

the system, the volatiles evaporating from the hair surface were adsorbed onto a waste Tenax® cartridge for 130 minutes. Then a clean Tenax® cartridge was placed in the system, and the volatiles were collected over a period of 20 minutes. The end of the sampling corresponded to a total of 6 hours of drying. The hair swatch was then placed back for line-drying and re-analyzed 24 hours later (end of sampling) as described above (equilibrating for 130 minutes with a waste cartridge and sampling for 20 minutes on a clean cartridge). The waste cartridges were discarded and the clean cartridges thermally desorbed on a Perkin Elmer TurboMatrix 350 desorber coupled to an Agilent Technologies 7890A gas chromatograph equipped with a HP-1 capillary column (30 m, i.d. 0.25 mm, film 0.25 µm) and coupled to an Agilent Technologies 5975C inert MSD mass spectrometer. The volatiles were analyzed using a temperature gradient starting at 100°C for 1 minute, then going to 220°C at 10°C/minute. Headspace concentrations (in ng/L air) were obtained by external standard calibration using five different concentrations of the model perfume to be released in ethanol. Each calibration solution was injected onto a clean Tenax® cartridge, which was desorbed and analyzed under the same conditions. The results obtained for the release of the different ingredients of the model perfume are summarized in **Table 5**.

References for Supporting Information:

(1)   Eberhardt, M.; Théato, P. *Macromol. Rapid Commun.*, **2005**, *26*, 1488-1493.

(2)   Gibson, M. I.; Fröhlich, E.; Klok, H.-A. *J. Polym. Sci. Polym. Chem.*, **2009**, *47*, 4332-4345.

(3)   Perrier, S.; Takolpuckdee, P.; Mars, C. A. *Macromolecules*, **2005**, *38*, 2033-2036.

(4)   Heinis, C.; Rutherford, T.; Freund, S.; Winter, G. *Nat. Chem. Biol.*, **2009**, *5*, 502-507.

(5)   Berthier, D. L.; Schmidt, I.; Fieber, W.; Schatz, C.; Furrer, A.; Wong, K.; Lecommandoux, S. *Langmuir*, **2010**, *26*, 7953-7961.

(6)   Serizawa, T.; Sawada, T.; Matsuno, H.; Matsubara, T.; Sato, T. *J. Am. Chem. Soc.*, **2005**, *127*, 13780-13781.

(7)   Buchs, B.; Godin, G.; Trachsel, A.; de Saint-Laumer, J.-Y.; Lehn, J.-M.; Herrmann, A. *Eur. J. Org. Chem.*, **2011**, 681-695.

(8)   Trachsel, A.; Chapuis, C.; Herrmann, A. *Flavour Fragrance J.*, **2013**, *28*, 280.

5. Conclusions and Perspectives

The potential avenues that involve the use of hybrid systems composed of a biomolecular domain such as a peptide and a synthetic element such as a polymer is rapidly expanding. In this Thesis, the feasibility of phage display identified peptide ligands to enhance the deposition of polymeric fragrance delivery systems both onto cotton fabric and human hair under relevant washing conditions is demonstrated. While the peptides serve as the recognition domains that promote the selective surface deposition of these polymer based materials, polymers prevent the premature evaporation and the degradation of fragrances, which contributes to the long lasting perception of these volatile chemicals.

Following an introduction to the phage display technique and its applicability to identify soft matter binding peptide ligands in **Chapter 1**, a general synthetic strategy that proceeds at mild reaction conditions without the requirement of peptide protecting groups to prepare peptide-polymer conjugates was illustrated in **Chapter 2**. The synthetic strategy was based on a three step post-polymerization modification of an active ester PPFMA precursor with alkyne and dansyl containing amines in the first step and with 1-amino-2-propanol in the second step to yield a water soluble PHPMA intermediate. In the final step, azide functionalized cyclic peptide disulfides (CXC) were incorporated into this intermediate via copper catalyzed azide/alkyne cycloaddition (CuAAC) reaction to yield peptide-PHPMA conjugates. The use of a biorthogonal reaction such as CuAAC was necessary, as the peptides contained multiple amine groups and a disulfide bond, which prevented the use of amine and thiol-based chemistries to prepare well-defined peptide-polymer conjugates. These conjugates were later used as model hair-binding polymeric profragrances in **Chapter 4**.

Chapter 3 presented the preparation of two different polymer based fragrance delivery systems that can selectively deposit onto cotton under fabric softening conditions upon the incorporation of cotton binding peptide ligands identified by phage display. These systems were linear PHPMA conjugates and α-pinene loaded poly(styrene-*co*-acrylic acid) (PS-*co*-PAA) nanoparticles. The incorporaton of the strongest cotton binding peptide was found to enhance the deposition of these systems 200-300% as evidenced by fluorescence intensity measurements. Furthermore, α-pinene release from the cotton surfaces incubated with the fragrance loaded nanoparticles were found to be in correlation

with the extent of their deposition via headspace measurements. As a summary, the incorporation of the phage display identified peptide to the PS-*co*-PAA nanoparticles was found to enhance both their deposition and fragrance release at the same time, which could not be achieved by the physiochemical optimization of existing fragrance delivery systems.

In a second example, the overall concept presented in **Chapter 3** was applied to prepare potential hair binding fragrance delivery systems under shampoo conditions in **Chapter 4**. This is a more challenging study as compared to the work shown in **Chapter 3**, as the deposition of fragrance delivery systems is required during the shampoo wash, in which its primary function is to remove, for example, fats and dirt from the hair surfaces. Furthermore, hair is a very heterogenous substrate at a molecular level. As a result of this heterogeneity, there was the risk that it may not have contained adequate number of identical surface binding sites that could be recognized by specific peptide sequences during phage display experiments. **Chapter 4**, however, demonstrated the feasibility of identifying substrate selective peptide ligands to hair surfaces under shampoo conditions using phage display. Following the successful identification of the hair binding peptides, the peptide-PHPMA conjugates that were prepared in **Chapter 2** were utilized as model hair-binding polymeric profragrances. The incorporation of these peptides was found to enhance the deposition of PHPMA polymers 3-4 fold onto hair surfaces via fluorescence intensity measurements. In a final effort, the influence of the steric hindrance in the peptide terminal regions as well as the stringency of the shampoo medium towards the deposition was assessed using N- or C-terminal dansylated variants of the strongest hair binding peptide. These findings can be used during the design of the hair binding polymeric fragrance carriers in the future steps.

It is worth mentioning that the general strategy presented in this Thesis is not limited to fragrance delivery systems. The deposition of various other benefit agents, such as conditioners, softeners, anti-dandruff agents, anti-bacterials, amongst many others can be enhanced using these peptide ligands. Furthermore, following the identification of appropriate peptide binders, the scope of this strategy can be expanded to other cosmetically relevant substrates, such as skin, nail and tooth.

The final words will be on the potential steps that can be taken to further improve the deposition of fragrance delivery systems using this general strategy. This is crucial from a commercial standpoint as peptides are quite expensive, whereas fabric softener and shampoos are relatively cheap formulations. The commercial viability of this strategy,

therefore, would only be possible with the development of peptide "tags" that are even more selective than the ones that were used in the scope of this Thesis. For example, this can be achieved using multivalent peptide constructs that mimicks the presentation of the peptide ligands on the phage, rather than the monovalent ligands that were used in this work. This multivalency, so called the "avidity" effects were found to enhance the binding strengts of peptide ligands 2-3 orders of magnitude as illustrated in **Chapter 1**. Similarly, tandem repeats, which are composed of multiple repetitions of the binding sequences that are linked to one another, can yield ligands with higher binding strengths. Finally, in the scope of this thesis, the influence of each amino acid towards the binding of the identified peptides onto cotton and hair was not investigated. This investigation may reveal small motifs composed of 3-4 amino acids that can also effectively recognize these substrates without compromising the binding stregths. The use of smaller motifs would also result with decreased cost of peptide per batch of fragrance delivery systems.

.Curriculum vitae

Kemal Arda Günay

École Polytechnique Fédérale de Lausanne (EPFL) / STI / IMX
/ LP / MXD 131, Station 12, 1015, Lausanne Switzerland
+41 78 876 23 84
kemalardagunay@gmail.com

EDUCATION

2011 – 2016   **Ph. D. in Laboratory of Polymers**
EPFL, Switzerland.

2009 – 2011   **M. Sc. in Materials Science and Engineering**
EPFL, Switzerland. Grade – 5.53/6.00.

2005 – 2009   **B. Sc. in Materials Science and Engineering**
Minor in Chemistry
Sabanci University, Turkey. GPA – 3.50/4.00.

Ph. D. THESIS

Title   **Bioinspired selective surface deposition of fragrance delivery systems.**

Supervisor   Prof. Harm-Anton Klok

Description   I developed "smart" polymeric fragrance delivery systems that selectively deposits onto cotton fabric under fabric softener and laundry detergent conditions and to hair under shampoo formulations. I performed the work in close collaboration with Firmenich SA. The work was subdivided into three parts:

➢ Identification of cotton and hair-binding peptides using phage display.

➢ Synthesis of linear peptide-polymer conjugates that selectively deposits onto cotton and human hair.

➢ Preparation of novel fragrance loaded nanoparticles.

M. Sc. THESIS

Title   **Synthesis and post-polymerization modification of poly(pentafluorophenyl methacrylate) brushes.**

Supervisor   Prof. Harm-Anton Klok

Description   I developed the controlled synthesis of a reactive polymer brush, which can be used as a precursor for the preparation of diverse, functional surface coatings.

EXPERIENCE

June 2015	**Research Intern**, FIRMENICH SA.
Description	I carried dynamic headspace sampling measurements using fragrance loaded nanoparticles.
2013 – Current	**Research Scholar,** PRESCOUTER, INC.
Description	I provided online consultancy as a global research scholar to leading companies in the field such as **General Cable**, **Afton**, **Bridgestone**, **PepsiCo**, **Nova Chemicals**, **BASF** and **Sun Products**.

SKILLS AND INSTRUMENTS

(Polymer) Chemistry: RAFT polymerization, ATRP, free radical polymerization, miniemulsion polymerization, polycondensation reactions, variety of post-polymerization modification reactions and the synthesis of challenging peptides.

Materials Science: Functional polymers, targeting nanoparticles and polymer brushes.

Biotechnology: Phage display, enzyme-linked immunosorbent assay (ELISA), prokaryotic recombinant protein expression and gel electrophoresis.

Analytical techniques: Atomic force microscopy (AFM), nuclear magnetic resonance spectroscopy (NMR), solid-phase peptide synthesis (SPPS), high pressure liquid chromatography (HPLC), mass spectroscopy (MS), gas chromatography (GC), Fourier transform infrared spectroscopy (FT-IR), thermogravimetric analysis (TGA), differential scanning calorimetry (DSC), size-exclusion chromatography (SEC), dynamic light scattering (DLS) and dynamic headspace sampling.

PUBLICATIONS

1 - **K. A. Günay,** N. Schüwer and H.-A. Klok, "**Synthesis and post-polymerization modification of poly(pentafluorophenyl methacrylate) brushes**", *Polymer Chemistry,* **2012**, 3, 2186-2192.

2 - **K. A. Günay,** P. Théato, and H.-A. Klok, "**History of post-polymerization modification**", *Functional Polymers by Post-Polymerization Modification: Concepts, Guidelines and Applications,* **2013**, 1-44.

3 - **K. A. Günay**, P. Théato and H.-A. Klok, "**Standing on the shoulders of Hermann Staudinger: Post-polymerization modification from past to present**", *Journal of Polymer Science Part A: Polymer Chemistry*, **2013**, 51, 1-28.

4 - **K. A. Günay** and H.-A. Klok, "**Identification of soft matter binding peptide ligands using phage display**", *Bioconjugate* Chemistry, **2015**, 26, 2002-2015.

5 - **K. A. Günay**, H.-A. Klok, "**Synthesis of cyclic peptide disulfide-PHPMA conjugates via sequential active ester aminolysis and CuAAC coupling**" *Just accepted in Polymer Chemistry*.

6- **K. A. Günay**, D. Benczédi, A. Herrmann and H.-A. Klok, "**Peptide-enhanced selective surface deposition of polymer-based fragrance delivery systems**", *Manuscript in preparation*.

7- **K. A. Günay**, D. L. Berthier, H. A. Jerri, D. Benczédi, H.-A. Klok and A. Herrmann "**Human hair targeting polymeric fragrance delivery systems using phage display identified peptides**", *Manuscript in preparation*.

SUPERVISION

Fall 2012-2015 **Teaching Assistant** *for the master's level course "Polymer Chemistry and Macromolecular Engineering" in the Materials Science and Engineering Department in EPFL.*

Spring 2014 **M. Sc. thesis** *of Ms. Szu-Ying Tu, "Influence of the local charges on the alkylation and dealkylation of methionine-containing peptides".*

Fall 2012 **Semester project** *of Ms. Lina Klockare, "Investigating the influence of different surface-initiated ATRP agents to growth kinetics of polymer brushes".*

LANGUAGES

Turkish	**Mother tongue**
English	**Full working proficiency**
French	**Limited working proficiency**